(12)

SDAC-TR-79-5

A STATISTICAL DISCRIMINATION EXPERIMENT FOR EURASIAN EVENTS USING A TWENTY-SEVEN STATION NETWORK

D.W. Rivers, D.H. von Seggern, B.L. Elkins and H.S. Sproules

Seismic Data Analysis Center

Teledyne Geotech, 314 Montgomery Street, Alexandria Virginia 22314

08 JULY, 1980

APPROVED FOR PUBLIC RELEASE; DISTRIBUTION UNLIMITED.

Sponsored by

The Defense Advanced Research Projects Agency (DARPA)

DARPA Order No. 2551

Monitored By

AFTAC/VSC

312 Montgomery Street, Alexandria, Virginia 22314

Disclaimer: Neither the Defense Advanced Research Projects Agency nor the Air Force Technical Applications Center will be responsible for information contained herein which has been supplied by other organizations or contractors, and this document is subject to later revision as may be necessary. The views and conclusions presented are those of the authors and should not be interpreted as necessarily representing the official policies, either expressed or implied, of the Defense Advanced Research Projects Agency, the Air Force Technical Applications Center, or the US Government.

Unclassified

SECURITY CLASSIFICATION OF THIS PAGE *(When Data Entered)*

REPORT DOCUMENTATION PAGE		READ INSTRUCTIONS BEFORE COMPLETING FORM
1. REPORT NUMBER SDAC-TR-79-5	2. GOVT ACCESSION NO. AD-A116 048	3. RECIPIENT'S CATALOG NUMBER
4. TITLE *(and Subtitle)* A STATISTICAL DISCRIMINATION EXPERIMENT FOR EURASIAN EVENTS USING A TWENTY-SEVEN-STATION NETWORK		5. TYPE OF REPORT & PERIOD COVERED Technical 6. PERFORMING ORG. REPORT NUMBER
7. AUTHOR(s) D. W. Rivers H. S. Sproules D. H. von Seggern B. L. Elkins		8. CONTRACT OR GRANT NUMBER(s) F08606-79-C-0007
9. PERFORMING ORGANIZATION NAME AND ADDRESS Teledyne Geotech 314 Montgomery Street Alexandria, Virginia 22314		10. PROGRAM ELEMENT, PROJECT, TASK AREA & WORK UNIT NUMBERS VT/9709
11. CONTROLLING OFFICE NAME AND ADDRESS Defense Advanced Research Projects Agency Nuclear Monitoring Research Office 1400 Wilson Blvd. Arlington, Virginia 22209		12. REPORT DATE 08 July, 1980 13. NUMBER OF PAGES 189
14. MONITORING AGENCY NAME & ADDRESS *(if different from Controlling Office)* VELA Seismological Center 312 Montgomery Street Alexandria, Virginia 22314		15. SECURITY CLASS. *(of this report)* Unclassified 15a. DECLASSIFICATION/DOWNGRADING SCHEDULE

16. DISTRIBUTION STATEMENT *(of this Report)*

APPROVED FOR PUBLIC RELEASE; DISTRIBUTION UNLIMITED.

17. DISTRIBUTION STATEMENT *(of the abstract entered in Block 20, if different from Report)*

18. SUPPLEMENTARY NOTES

Author's Report Date 11/27/79

19. KEY WORDS *(Continue on reverse side if necessary and identify by block number)*

Seismic Discrimination
Seismic Source Spectrum
M_s : m_b
Signal Complexity
Multivariate Discrimination
Training Set
Eurasia
Tectonic Regions

20. ABSTRACT *(Continue on reverse side if necessary and identify by block number)*

An experiment was performed to test the effectiveness of a multivariate method of analysis for distinguishing earthquakes from explosions. The data base for the experiment consisted of digital recordings made at twenty-seven stations, including four large arrays, of one hundred thirty-three Eurasian events. Spectral magnitudes were measured in three frequency bands of the six phases P, Lg, long-period P, long-period S, LR, and LQ. Complexities of the P-waves were measured in three time windows, and corner frequencies and

DD FORM 1 JAN 73 1473 EDITION OF 1 NOV 65 IS OBSOLETE

Unclassified

SECURITY CLASSIFICATION OF THIS PAGE *(When Data Entered)*

low-frequency spectral levels were computed for the P-wave spectra. When signals could not be detected, spectral magnitudes were measured of noise samples, and these were taken to be detection thresholds. Signal magnitudes and detection thresholds from all the stations were used to find maximum-likelihood estimates of the spectral magnitudes for each event. A "training set" of presumed earthquakes and explosions was used to find discrimination variables by effectively normalizing the network spectral magnitudes to eliminate bias with respect to m_b.

On account of gaps in the data, many different combinations of different numbers of variables were used in the classification of the one hundred thirty-three events. The variables which were applicable to the most events were short-period P-wave spectral ratios. The most effective discriminants were spectral ratios of Love waves to P waves.

The multivariate discrimination resulted in certain misclassifications which were attributable to insufficient data with acceptable signal-to-noise ratios. The misclassification of certain deep earthquakes as explosions may be the result of systematic errors in computing the magnitudes of deep events, or it may reflect actual differences between deep earthquakes and shallow ones. Both deep earthquakes and multiple explosions are prone to misclassification on account of anomalous complexity values. The overlap between the earthquake and explosion populations might have been reduced had magnitude corrections and relative weights been applied to the data from individual stations before network estimates of the magnitudes were computed.

Discriminants involving only short-period data tend to misclassify explosions, but this situation can be rectified (at the expense of increasing the false alarm rate) by assigning more weight to the explosions in the training set. Investigations were made of the influence exerted upon discrimination by both the number and the geographical distribution of events in the training set. Because the earthquakes and the explosions occurred for the most part in regions distant from each other, caution should be taken in applying the results of this experiment to the discrimination of unknown events, expecially those with epicenters in regions not sampled by this data base.

A STATISTICAL DISCRIMINATION EXPERIMENT FOR EURASIAN EVENTS USING A TWENTY-SEVEN-STATION NETWORK

SEISMIC DATA ANALYSIS CENTER REPORT NO.: SDAC-TR-79-5

AFTAC Project Authorization No.:	VELA T/9707/B/ETR
Project Title:	Seismic Data Analysis Center
ARPA Order No.:	2551
Name of Contractor:	TELEDYNE GEOTECH
Contract No.:	F08606-79-C-0007
Date of Contract:	01 October 1979
Amount of Contract:	$279,929
Contract Expiration Date:	30 September 1980
Project Manager:	Robert R. Blandford (703) 836-3882

P. O. Box 334, Alexandria, Virginia 22313

APPROVED FOR PUBLIC RELEASE; DISTRIBUTION UNLIMITED.

ABSTRACT

An experiment was performed to test the effectiveness of a multivariate method of analysis for distinguishing earthquakes from explosions. The data base for the experiment consisted of digital recordings made at twenty-seven stations, including four large arrays, of one hundred thirty-three Eurasian events. Spectral magnitudes were measured in three frequency bands of the six phases P, Lg, long-period P, long-period S, LR, and LQ. Complexities of the P-waves were measured in three time windows, and corner frequencies and low-frequency spectral levels were computed for the P-wave spectra. When signals could not be detected, spectral magnitudes were measured of noise samples, and these were taken to be detection thresholds. Signal magnitudes and detection thresholds from all the stations were used to find maximum-likelihood estimates of the spectral magnitudes for each event. A "training set" of presumed earthquakes and explosions was used to find discrimination variables by effectively normalizing the network spectral magnitudes to eliminate bias with respect to m_b.

On account of gaps in the data, many different combinations of different numbers of variables were used in the classification of the one hundred thirty-three events. The variables which were applicable to the most events were short-period P-wave spectral ratios. The most effective discriminants were spectral ratios of Love waves to P waves.

The multivariate discrimination resulted in certain misclassifications which were attributable to insufficient data with acceptable signal-to-noise ratios. The misclassification of certain deep earthquakes as explosions may be the result of systematic errors in computing the magnitudes of deep events, or it may reflect actual differences between deep earthquakes and shallow ones. Both deep earthquakes and multiple explosions are prone to misclassification on account of anomalous complexity values. The overlap between the earthquake and explosion populations might have been reduced had magnitude corrections and relative weights been applied to the data from individual stations before network estimates of the magnitudes were computed.

Discriminants involving only short-period data tend to misclassify explosions, but this situation can be rectified (at the expense of increasing

the false alarm rate) by assigning more weight to the explosions in the training set. Investigations were made of the influence exerted upon discrimination by both the number and the geographical distribution of events in the training set. Because the earthquakes and the explosions occurred for the most part in regions distant from each other, caution should be taken in applying the results of this experiment to the discrimination of unknown events, especially those with epicenters in regions not sampled by this data base.

TABLE OF CONTENTS

TABLE OF CONTENTS

LIST OF FIGURES

LIST OF FIGURES (continued)

LIST OF TABLES

LIST OF TABLES (Con't)

INTRODUCTION

Although many studies of seismic discrimination have been carried out in the past, they have tended for the most part to concentrate on some single technique, such as $M_s - m_b$ differences. The purpose of the experiment discribed in this report is to develop a systematic technique of discrimination based upon many different potential discriminants. The effectiveness of the multivariate discrimination method is then to be tested by applying it to a large body of data collected for events which encompass a wide range of magnitudes and which occurred in diverse tectonic settings. The utility of the individual discriminants will then be examined in terms of the number of events of the data set to which they may be applied and their power to distinguish between earthquakes and explosions.

The individual discriminants employed in this experiment have been examined in detail in previous reports (von Seggern and Sobel, 1977; Sobel et al, 1977a, 1977b, 1977c; Sobel and von Seggern, 1976, 1978) as they apply to

---

von Seggern, D. H., and P. A. Sobel (1977). Study of selected Kamchatka earthquakes in a seismic discrimination contect, SDAC Report No. TR-76-10, Teledyne, Geotech, Alexandria, Virginia.

Sobel, P. A., D. H. von Seggern, E. I. Sweetser, and D. W. Rivers (1977a). Study of selected events in the Pamirs in a seismic discrimination context, SDAC Report No. TR-77-3, Teledyne Geotech, Alexandria, Virginia.

Sobel, P. A., D. H. von Seggern, E. I. Sweetser, and D. W. Rivers (1977b). Study of selected events in the Baikal Rift Zone in a seismic discrimination context, SDAC Report No. 77-5, Teledyne Geotech, Alexandria, Virginia.

Sobel, P. A., D. H. von Seggern, E. I. Sweetser, and D. W. Rivers (1977c). Study of selected events in the Caucasus in a seismic discrimination context, SDAC Report No. TR-77-6, Teledyne Geotech, Alexandria, Virginia.

Sobel, P. A., and D. H. von Seggern (1976). Study of selected events in the Tien Shan region in a seismic discrimination context, SDAC Report No. TR-76-9, Teledyne Geotech, Alexandria, Virginia.

Sobel, P. A., and D. H. von Seggern (1978). Analysis of selected seismic events from Asia in a seismic discrimination context, SDAC Report No. TR-78-5, Teledyne Geotech, Alexandria, Virginia.

selected regions within Eurasia. Although this experiment was in many ways a logical extension of those earlier reports, it was necessary to a certain extent to sacrifice the constraint of a purely regional study in order to analyze all the chosen events, which occured in many different parts of the Eurasian "Area of Interest" (AI). The multivariate analysis used for this experiment was applied previously to earthquakes and explosions in the Southwestern United States by von Seggern and Rivers (1979). That study analyzed a smaller data base, consisting only of events whose classification was known a priori; in this experiment a known "training set" is used to develop discriminants which may then be applied to the classification of events regarded as unknowns.

---

von Seggern, D. H., and D. W. Rivers (1979). Seismic discrimination of earthquakes and explosions with application to the Southwest United States, SDAC Report No. TR-77-10, Teledyne Geotech, Alexandria, Virginia.

DATA BASE

Records were analyzed for 133 Eurasian events, most of which occurred in the last months of 1977. These events are listed in Table I, along with their epicenters and origin times, which were taken from two separate lists furnished to us. The two sets of epicenters were frequently at variance, with the result that several events were listed by the NEIS as occurring outside the Area of Interest which the data base had been chosen to sample (see Fig. 1). The epicenters must then be regarded as too prone to error to permit discrimination to be carried out on the basis of geography. Had such a geographical discriminant been judged reliable, several events could have been eliminated from further consideration because they were located either outside the political boundaries of the Soviet Union and China or in deep water on either side of the Kuril Islands. Some possible implications of these epicentral differences will be discussed in the section on magnitude calculation. A table of depths for the events will be presented later, when the effect of using such information for discrimination is evaluated.

The previously mentioned Eurasian studies of Sobel and von Seggern showed the importance of tectonic setting upon seismic discrimination. For instance, deep earthquakes occurring on a descending plate behind an island arc are less efficient at generating surface waves than are the shallow earthquakes which occur in front of the island arc at the trench. Teleseismic P-waves from a region characterized by a low-velocity zone in the upper mantle are more strongly attenuated at high frequencies than are signals from regions without such a zone. Strike-slip and dip-slip motions along faults differ in the efficiency with which they generate surface waves. These and other differences between earthquakes in different regions tend to make more difficult the problems of distinguishing earthquakes from explosions. The 133 events were therefore separated into groups occurring in ten geographical regions of the AI, as indicated in the last column of Table I. These regions are defined in Table II.

The data used in the experiment were recorded at a network of 27 stations, which are listed in Table III. Only digital data were analyzed. For each event and each station, the records for as many as six phases (short-period P and Lg; long-period P, S, LR, and LQ) were made available for analysis. In practice, fewer records were available because the Lg window was retained

TABLE I : EVENTS INCLUDED IN THE DISCRIMINATION EXPERIMENT

EVENT	DATE	ORIGIN TIME	LATITUDE	LONGITUDE	REGION
1	26 JUL 77	16 59 57.6	69.532 N	90.583 E	14
3	1 NOV 77	3 54 26.0	55.436 N	130.545 E	3
4	1 NOV 77	17 56 42.7	36.581 N	68.745 E	10
6	4 NOV 77	10 51 40.0	23.000 N	101.000 E	6
7	4 NOV 77	23 54 44.7	30.700 N	81.279 E	7
8	5 NOV 77	2 9 38.0	42.900 N	45.300 E	13
9	5 NOV 77	4 6 58.5	36.635 N	69.128 E	10
10	6 NOV 77	13 31 41.1	36.313 N	71.121 E	10
14	30 JUL 77	1 56 58.0	49.777 N	78.163 E	9
16	10 AUG 77	21 59 58.7	50.923 N	110.761 E	4
17	17 AUG 77	4 26 57.7	49.814 N	78.151 E	9
18	20 AUG 77	21 59 58.7	64.223 N	99.577 E	3
19	1 SEP 77	2 59 57.5	73.376 N	54.581 E	14
20	5 SEP 77	3 2 57.8	50.092 N	78.961 E	9
21	10 SEP 77	16 0 3.3	57.294 N	106.240 E	4
22	30 SEP 77	6 59 55.6	47.800 N	48.145 E	12
23	10 NOV 77	4 57 46.0	37.100 N	71.800 E	10
24	10 NOV 77	9 22 58.0	33.000 N	89.000 E	7
25	12 NOV 77	5 9 16.0	38.000 N	91.000 E	6
26	12 NOV 77	12 27 5.3	35.757 N	71.331 E	10
27	13 NOV 77	21 2 29.3	26.471 N	93.114 E	7
28	15 NOV 77	20 20 46.6	38.172 N	74.158 E	10
29	17 NOV 77	4 23 54.0	28.000 N	90.000 E	7
30	18 NOV 77	5 20 11.3	32.693 N	88.388 E	7
31	18 NOV 77	5 33 19.7	32.640 N	88.431 E	7
32	18 NOV 77	11 27 27.6	32.655 N	88.469 E	7
33	9 OCT 77	11 0 0.3	73.626 N	53.158 E	14
34	18 NOV 77	15 10 41.8	32.719 N	88.316 E	7
35	18 NOV 77	17 23 24.4	32.610 N	88.315 E	7
36	16 OCT 77	20 3 35.0	48.400 N	152.900 E	2
37	18 NOV 77	21 55 39.7	60.081 N	143.373 E	3
38	16 OCT 77	15 2 48.8	36.466 N	71.034 E	10
39	18 NOV 77	23 12 49.5	32.698 N	88.422 E	7
41	13 OCT 77	20 38 52.1	37.301 N	78.058 E	10
45	19 NOV 77	11 51 14.2	36.450 N	71.279 E	10
46	20 NOV 77	1 41 23.0	30.600 N	93.300 E	7
47	16 OCT 77	21 5 37.3	49.419 N	155.431 E	2
48	19 OCT 77	5 1 57.0	36.440 N	71.273 E	10
49	19 OCT 77	21 20 41.6	49.349 N	155.632 E	2
50	20 OCT 77	8 18 7.0	56.426 N	164.133 E	1
53	29 OCT 77	3 6 57.7	49.841 N	78.174 E	9
55	26 OCT 77	5 38 52.2	49.000 N	155.800 E	2
56	26 OCT 77	7 11 31.3	46.400 N	153.500 E	2
57	26 OCT 77	13 14 30.9	51.500 N	153.400 E	2
58	27 OCT 77	7 20 28.9	53.500 N	160.000 E	1
59	28 OCT 77	21 15 1.9	39.569 N	73.406 E	8
60	29 OCT 77	4 14 56.5	47.000 N	152.300 E	2
61	29 OCT 77	6 26 40.6	40.283 N	63.455 E	11
62	29 OCT 77	10 33 56.7	47.137 N	153.158 E	2
63	30 OCT 77	21 38 38.5	45.528 N	145.988 E	3
64	31 OCT 77	9 40 38.5	55.962 N	162.786 E	1
65	20 NOV 77	11 1 22.0	56.800 N	108.500 E	4
66	20 NOV 77	18 55 28.0	39.900 N	73.900 E	8
67	20 NOV 77	20 57 33.1	37.419 N	71.824 E	10
68	20 NOV 77	23 40 35.9	32.395 N	87.765 E	7
69	21 NOV 77	19 43 33.7	36.663 N	71.206 E	10
70	22 NOV 77	0 8 3.7	36.257 N	70.729 E	10
72	22 NOV 77	6 56 14.2	36.478 N	71.236 E	10
73	22 NOV 77	11 33 45.0	43.000 N	89.000 E	8
74	22 NOV 77	19 16 12.0	40.000 N	75.000 E	8
75	23 NOV 77	10 28 7.0	34.000 N	83.000 E	7
76	26 NOV 77	15 44 41.0	37.000 N	71.000 E	10
77	26 NOV 77	22 46 52.2	39.465 N	117.938 E	5
78	27 NOV 77	2 9 7.0	28.000 N	90.000 E	7
79	27 NOV 77	3 57 0.0	50.000 N	79.000 E	9
80	28 NOV 77	9 2 26.0	43.200 N	47.600 E	13
81	30 NOV 77	4 6 57.5	49.957 N	78.931 E	9

TABLE I (CONTINUED)

EVENT	DATE	ORIGIN TIME	LATITUDE	LONGITUDE	REGION
143	2 DEC 77	12 57 10.7	52.929 N	159.714 E	1
144	2 DEC 77	16 15 44.9	44.554 N	146.459 E	2
145	3 DEC 77	17 6 21.9	41.932 N	131.124 E	5
146	4 DEC 77	4 13 47.0	56.200 N	163.100 E	1
147	4 DEC 77	11 39 2.8	48.250 N	146.590 E	2
148	5 DEC 77	23 37 37.1	55.669 N	162.211 E	1
149	6 DEC 77	10 52 53.5	41.425 N	69.730 E	8
150	7 DEC 77	2 3 37.0	41.000 N	72.000 E	8
151	7 DEC 77	16 19 33.9	35.651 N	94.518 E	7
152	8 DEC 77	2 2 54.0	52.900 N	89.700 E	9
153	8 DEC 77	6 45 20.0	41.000 N	72.000 E	8
154	8 DEC 77	13 57 4.4	50.425 N	149.808 E	2
155	8 DEC 77	23 37 22.5	36.263 N	70.574 E	10
156	9 DEC 77	4 23 36.0	54.400 N	160.600 E	1
157	10 DEC 77	21 58 51.3	51.379 N	156.590 E	1
158	12 DEC 77	11 6 42.0	51.400 N	157.500 E	1
159	13 DEC 77	6 58 59.0	35.400 N	88.400 E	7
160	13 DEC 77	11 34 20.0	42.300 N	133.200 E	5
161	15 DEC 77	5 15 42.3	36.545 N	71.150 E	10
162	15 DEC 77	15 7 51.8	43.241 N	45.168 E	13
163	15 DEC 77	15 23 30.7	43.643 N	45.372 E	13
164	16 DEC 77	7 11 41.6	43.233 N	146.763 E	2
165	16 DEC 77	9 8 59.7	51.630 N	159.460 E	1
166	16 DEC 77	10 15 27.5	33.305 N	97.560 E	7
167	16 DEC 77	17 55 14.2	36.891 N	59.760 E	11
168	16 DEC 77	23 17 17.7	43.059 N	47.082 E	13
169	18 DEC 77	6 57 33.3	55.278 N	160.561 E	1
170	18 DEC 77	16 47 17.1	39.865 N	77.334 E	8
171	18 DEC 77	19 9 15.7	51.049 N	157.831 E	1
172	18 DEC 77	20 43 5.9	39.733 N	77.696 E	8
173	19 DEC 77	19 12 25.0	39.764 N	77.714 E	8
175	20 DEC 77	7 27 38.9	39.794 N	69.331 E	8
176	20 DEC 77	20 52 10.0	55.200 N	158.200 E	1
177	21 DEC 77	8 30 46.3	41.952 N	47.915 E	13
178	21 DEC 77	16 39 33.0	52.929 N	159.804 E	1
179	21 DEC 77	20 17 13.6	36.196 N	68.667 E	10
180	21 DEC 77	20 40 5.0	52.800 N	159.500 E	1
182	22 DEC 77	15 5 45.1	52.956 N	159.902 E	1
183	22 DEC 77	19 34 5.0	53.100 N	163.400 E	1
184	23 DEC 77	7 31 44.2	44.818 N	32.801 E	13
185	23 DEC 77	9 9 54.1	39.598 N	77.449 E	8
186	24 DEC 77	3 27 52.0	51.200 N	156.900 E	1
187	25 DEC 77	8 33 37.0	50.000 N	91.000 E	9
188	25 DEC 77	17 38 42.0	40.900 N	69.700 E	8
189	26 DEC 77	4 2 57.3	49.881 N	78.141 E	9
190	26 DEC 77	5 15 21.3	39.917 N	71.967 E	7
191	26 DEC 77	23 4 34.0	33.700 N	80.900 E	7
192	27 DEC 77	7 10 11.0	28.000 N	90.000 E	7
193	27 DEC 77	12 31 0.0	54.700 N	161.500 E	1
194	28 DEC 77	15 10 46.0	56.000 N	162.000 E	1
195	31 DEC 77	3 24 38.6	39.181 N	91.100 E	6
264	20 MAR 76	4 3 39.3	50.054 N	77.337 E	9
265	29 MAR 77	3 56 57.7	49.790 N	78.149 E	9
266	19 MAR 78	3 47 0.0	50.000 N	78.000 E	9
267	11 JUN 78	2 57 0.0	50.000 N	79.000 E	9
268	28 JUL 78	2 47 0.0	50.000 N	78.000 E	9
269	9 AUG 78	18 0 0.0	64.000 N	125.000 E	3
270	24 AUG 78	18 0 0.0	66.000 N	112.000 E	4
271	29 AUG 78	2 37 0.0	50.000 N	78.000 E	9
272	5 SEP 78	0 22 0.0	43.000 N	89.000 E	8
273	21 SEP 78	15 0 0.0	66.000 N	86.000 E	14
274	25 APR 75	4 59 57.0	47.500 N	47.500 E	12
275	5 OCT 75	4 27 0.0	50.000 N	78.000 E	9
276	13 DEC 75	4 56 57.3	49.798 N	78.196 E	9
277	19 MAY 76	2 56 57.9	49.856 N	78.007 E	9
278	23 JUL 76	2 32 58.0	49.800 N	78.100 E	9

(U) Figure 1a. Overall view.
Location of events used in the discrimination experiment.

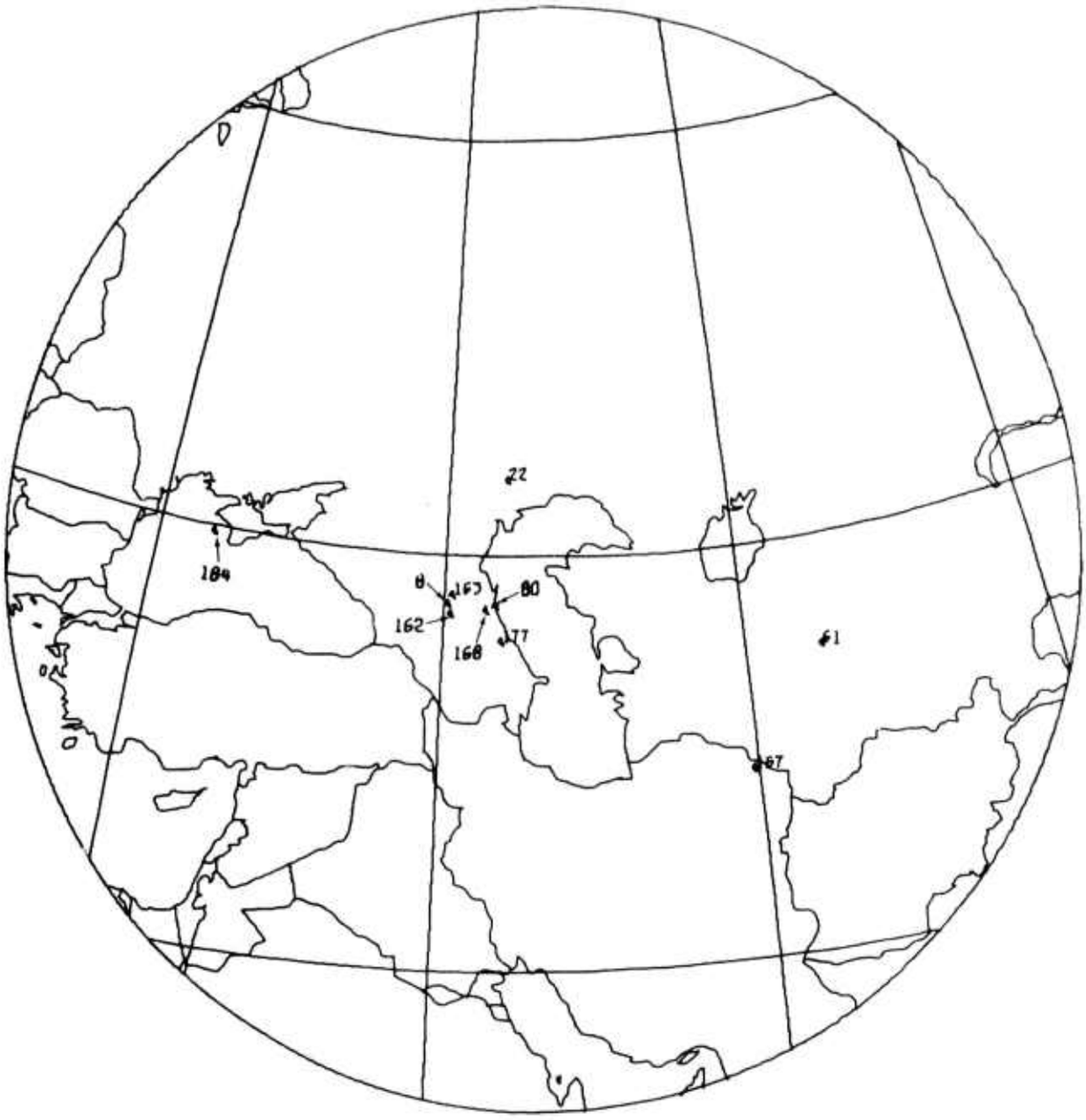

(U) Figure 1b. West Kazakh and Caucasus regions.
Location of events used in the discrimination experiment.

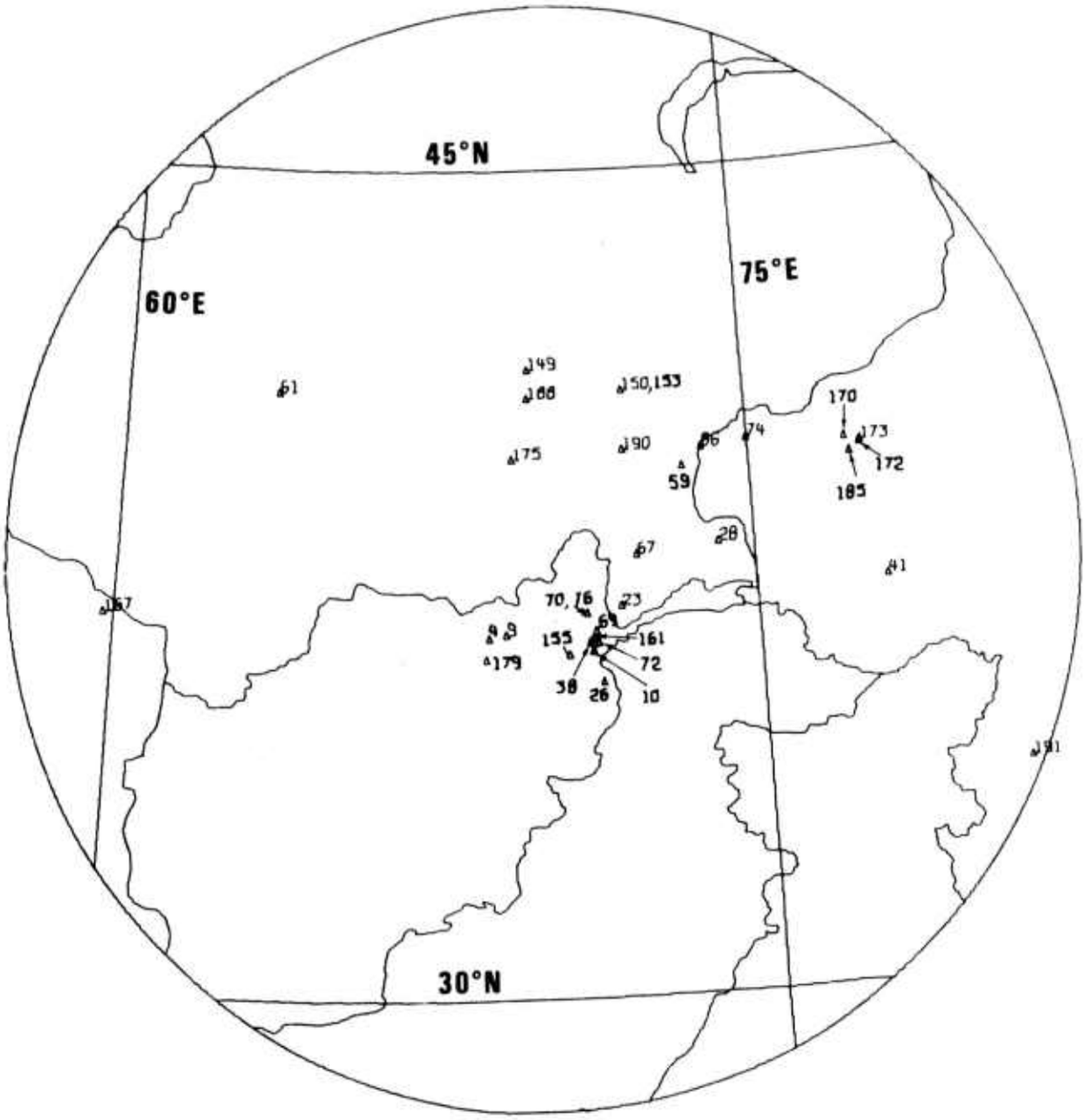

(U) Figure 1c. Tien Shan and Pamirs - Hindu Kush regions.
Location of events used in the discrimination experiment.

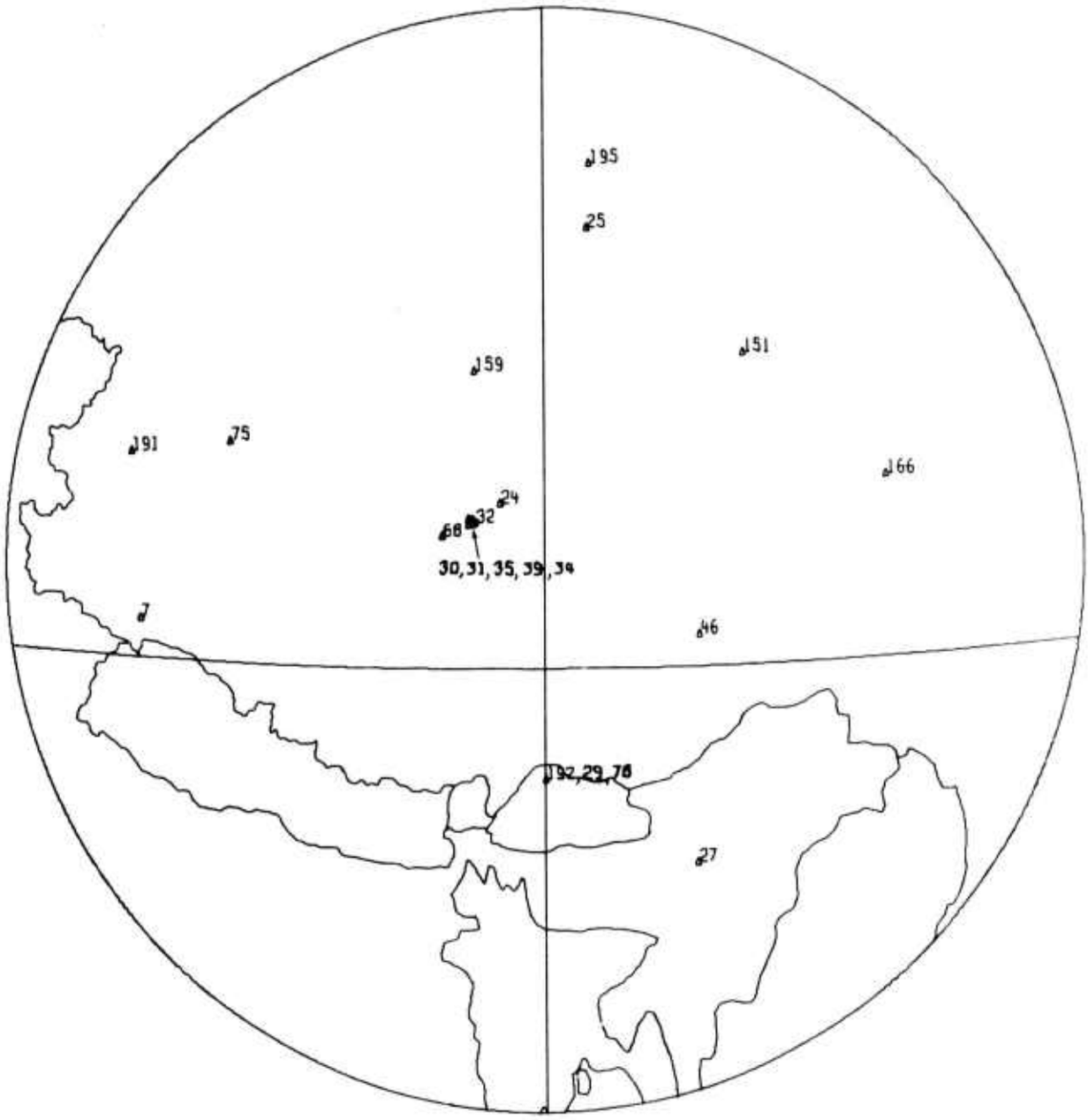

(U) Figure 1d. Tibet region.
Location of events used in the discrimination experiment.

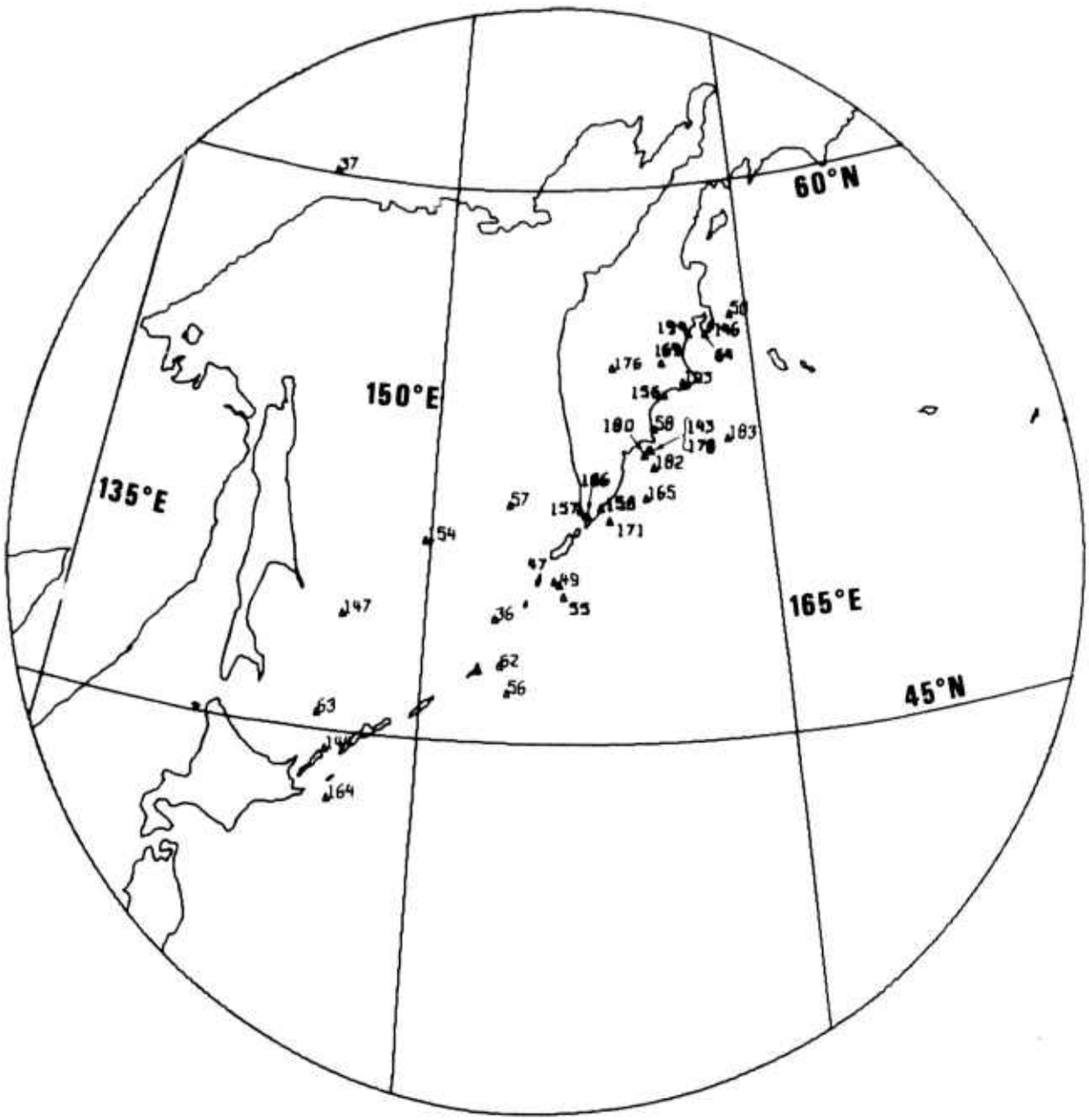

(U) Figure 1e. Kamchatka and Kuril Islands regions.
Location of events used in the discrimination experiment.

TABLE II

(U) Regions within the Eurasian Area of Interest

Number	Name	Events						
1	Kamchatka	50	58	64	143	146	148	156
		157	158	165	169	171	176	178
		180	182	183	186	193	194	
2	Kuril Islands	36	47	49	55	56	57	60
		62	144	147	154	164		
3	Siberia	3	18	37	63	269		
4	Lake Biakal	16	21	65	270			
5	Eastern China	77	145	160				
6	Central China	6	25	195				
7	Tibet	7	24	27	29	30	31	32
		34	35	39	46	68	75	78
		151	159	166	190	191	192	
8	Tien Shan	59	66	73	74	149	150	153
		170	172	173	175	185	188	272
9	East Kazakh	14	17	20	53	79	81	152
		187	189	264	265	266	267	268
		271	275	276	277	278		
10	Pamirs-Hindu Kush	4	9	10	23	26	28	38
		41	45	48	67	69	70	72
		76	155	161	179			
11	Turkmen	61	167					
12	West Kazakh	22	274					
13	Caucasus	8	80	162	163	168	177	184
14	Northwest Russia	1	19	33	273			

TABLE III

Stations Used in the Discrimination Experiment

Alaskan Stations (6):	AT-AK
	BF-AK
	CN-AK
	NJ-AK
	TN-AK
	UC-AK
Special Data Collection System [SDCS] (2):	HN-ME
	RK-ON
Seismic Research Observatories [SRO] (10):	ANMO
	ANTO
	BOCO
	CHTO
	GUMO
	MAIO
	NWAO
	SHIO
	SNZO
	TATO
Alternate Seismic Research Observatories [ASRO] (5):	CTAO
	KAAO
	KONO
	MAJO
	ZOBO
Arrays (4):	ILPA
	KSRS
	LASA
	NORSAR

primarily at KSRS only, and because most of the SRO and ASRO records were of long-period data only. The short-period SRO records consisted mainly of detectable signals, whereas the long-period records were retained of the time window in which a given signal was predicted to arrive, even if no signal could be seen above the noise. The sampling rate for long-period data was one sample per second, and for short-period data, except for NORSAR and LASA, the rate was twenty samples per second. The NORSAR and LASA short-period data, recorded at the rate of ten samples per second, were interpolated to twice that rate when the signals were processed.

Long-period data at NORSAR, ILPA, and KSRS were recorded at seven individual sensors, and LASA data at nine sensors; these were beamformed using the back azimuth for the event being processed and an assumed constant value for the velocity of the wave. The velocities used for beamforming are given in Table IV. In every case the short-period data channel with the largest signal-to-noise ratio was chosen. Short-period data for KSRS and LASA were taken exclusively from the first sensor in the record, providing that channel was not malfunctioning.

The number of data windows processed for each event is shown in Table V. In this table the columns headed "LP" and "LS" refer to long-period P and S, respectively. Many more seismograms were actually available than were processed, but it was decided that certain types of records should be deleted from the data set. Principal among these deleted records were those of body waves for which the epicenter-to-station angular separation Δ exceeded 100°. Deletion of these records insured that no waveforms were distorted due to proximity of the propagation path to the earth's core. No S-waves were processed for which Δ <15°, since no reliable B-factor could be assigned to them and since the long-period S-wave is difficult to separate from surface waves at short distances. On account of the previously mentioned uncertainty in the epicenters of many of the events, magnitudes determined at regional distances were considered unreliable, and thus signals from nearby events were not processed unless their amplitudes could be determined to be consistent with teleseismic measurements. Almost all the records deleted for this reason were actually of noise rather than of signal. (The reason for processing noise records will be explained later). A particular example of disagreement between regional and

TABLE IV

(U) Velocities Used for Beamforming

Phase	Distances	Velocity (km/sec)
P	$\Delta<20°$	$111.2 / (14.80-0.1256 \cdot \Delta)$
P	$\Delta>20°$	$111.2 / (11.14-0.0712 \cdot \Delta)$
S	$\Delta<20°$	$111.2 / (26.98-0.2325 \cdot \Delta)$
S	$\Delta>20°$	$111.2 / (19.48-0.1118 \cdot \Delta)$
LR	all	3.6
LQ	all	3.6

TABLE V
NUMBER OF DATA WINDOWS ANALYZED

EVENT	P	LG	LP	LS	LR	LQ	EVENT	P	LG	LP	LS	LR	LQ
1	14	0	8	8	11	11	144	4	0	10	9	11	11
3	14	1	11	11	13	14	145	11	1	12	11	12	12
4	5	2	9	8	9	10	146	10	1	11	12	13	11
6	7	1	11	10	15	16	147	12	1	11	11	12	12
7	9	0	7	8	12	13	148	6	1	11	8	7	7
8	3	0	8	7	11	12	149	10	2	9	7	12	10
9	12	0	13	10	15	15	150	10	1	12	9	11	12
10	10	2	13	11	12	13	151	11	2	11	11	11	12
14	13	1	11	9	13	13	152	12	2	13	11	13	13
16	7	1	9	8	8	8	153	9	1	13	10	11	12
17	12	1	11	8	12	12	154	11	1	11	12	13	13
18	6	1	7	7	7	7	155	9	2	9	5	10	8
19	10	1	8	8	12	12	156	8	1	12	10	12	12
20	9	1	9	9	9	9	157	10	1	11	12	13	13
21	12	1	9	8	8	11	158	8	1	13	14	15	13
22	6	1	4	2	8	10	159	10	2	12	11	12	12
23	9	1	10	9	10	10	160	11	1	15	13	15	14
24	11	1	11	9	10	12	161	13	2	10	8	11	12
25	11	1	12	12	14	14	162	11	2	10	8	11	11
26	13	1	13	12	14	16	163	12	1	10	8	9	12
27	11	2	9	6	15	17	164	15	1	14	12	14	13
28	5	4	10	8	12	12	165	13	1	13	12	12	11
29	2	2	10	7	13	14	166	14	1	10	11	12	12
30	13	2	12	12	15	13	167	10	1	9	6	10	10
31	15	4	14	12	14	14	168	7	0	10	8	12	11
32	12	1	12	9	13	16	169	14	1	13	12	14	9
33	12	1	9	8	12	12	170	14	2	11	9	12	10
34	6	2	9	8	10	11	171	14	1	14	12	14	14
35	14	2	11	14	15	15	172	11	2	13	11	15	13
36	4	0	10	10	12	13	173	10	3	11	8	13	12
37	12	1	11	12	14	13	175	10	1	11	6	12	12
38	11	1	11	8	8	12	176	6	1	14	12	13	14
39	14	2	14	11	16	15	177	10	2	12	7	10	13
41	5	1	8	7	10	13	178	6	1	10	12	13	13
45	8	1	13	9	13	14	179	6	1	11	8	10	11
46	11	1	12	8	14	14	180	6	1	12	11	14	14
47	14	0	11	13	15	13	182	12	1	13	13	12	14
48	8	1	10	10	10	12	183	12	1	14	13	14	13
49	12	1	9	12	12	10	184	10	1	10	8	10	9
50	14	1	11	12	12	11	185	11	2	10	8	12	12
53	16	1	12	10	10	9	186	4	1	9	9	11	11
55	10	1	10	10	12	10	187	9	2	9	9	10	11
56	2	0	10	10	11	11	188	11	2	8	7	12	12
57	10	1	12	13	13	13	189	11	1	11	9	13	13
58	10	0	13	14	12	11	190	12	3	10	7	13	13
59	7	3	11	9	13	13	191	12	1	9	8	11	11
60	7	0	14	11	12	13	192	8	0	8	8	10	10
61	12	2	10	10	13	14	193	9	2	11	10	9	10
62	13	0	11	11	12	12	194	9	2	12	10	11	10
63	12	1	14	12	14	13	195	12	2	11	11	14	15
64	12	1	13	14	13	13	264	3	1	6	6	5	6
65	12	1	15	15	16	17	265	5	2	6	5	7	8
66	9	1	11	10	14	15	266	13	2	9	10	11	10
67	11	3	8	8	9	11	267	8	1	10	9	11	11
68	14	2	11	10	13	15	268	10	1	9	9	12	12
69	1	2	7	6	9	9	269	14	1	11	12	12	13
70	10	2	12	7	15	14	270	6	1	11	11	11	12
72	10	1	10	10	12	13	271	15	2	10	10	14	12
73	8	2	13	12	14	16	272	7	0	10	10	12	12
74	3	2	8	6	9	9	273	12	1	10	12	14	14
75	9	2	11	9	11	12	274	1	0	0	0	0	0
76	11	2	12	10	12	13	275	0	0	0	0	0	0
77	12	0	13	10	13	13	276	2	0	0	0	1	2
78	8	1	7	7	11	13	277	4	1	6	4	9	7
79	6	2	11	12	13	14	278	4	1	6	5	7	6
80	9	0	8	7	8	10							
81	12	2	11	12	12	13	TOTAL	1275	165	1382	1247	1539	1566
143	13	1	11	12	13	12							

teleseismic magnitudes is that of the high-frequency component of the short-period P-waves. Because the signals from regional events travel only through the crust and not through the mantle, these high frequency components are less attenuated than are those of teleseismic signals. This lack of attenuation introduces a distance-dependent magnitude bias which is a function of both geographical region and frequency, and which therefore cannot be removed by addition of the standard B-factor for P-waves. This problem was especially severe at KAAO (for which many of the AI events are regional), since the spectra of all events close to that station were observed to be nearly flat due to the absence of attenuation, and hence they all appeared very strongly to be explosion-like.

Another reason that certain seismograms were deleted from the data set was that it was believed that the signal may actually have arrived in a time window other than that which was spanned by the seismogram. In some cases, the signal which appeared within the seismogram was believed to be associated with a different event. Other records, which included visually acceptable signals, were deleted because they contained too short a noise sample before the signal arrival to permit accurate measurement of the signal-to-noise ratio [SNR]. Several seismograms were deleted from the data base because the amplitude of both the signal and noise were grossly in error, usually by two or more orders of magnitude, apparently on account of a calibration error. With certain rare exceptions, this problem was confined to HN-ME and RK-ON, the two stations for which calibration data had to be entered into the computer by hand in order to create the digital seismogram tape. Finally, the data set contained nine short-period P windows from GUMO, and they were all deleted because the signal and noise levels were both quite large in every case. A short-period P wave magnitude bias appeared to exist at NORSAR, since the magnitude of almost every event, especially at high frequencies, was noticeably larger there than at almost all the other stations in the network; nevertheless, these signals were all retained. A table listing the relative contribution of each station to the data base will be presented after a description of the discrimination parameters which were measured. Table V shows that after the unusable seismograms were deleted from the data base, no seismograms for event 275 remained. This event was therefore deleted from further consideration.

DISCRIMINATION PARAMETERS

The six phases (short-period P and Lg, long-period P, S, LR, and LQ) which comprised the data for each station and each event were processed to compute twenty-seven parameters, twenty-five of which were to be used for discrimination. These twenty-seven parameters, listed in Table VI, are now described in detail. Whenever no signal could be detected in a given data window, the noise in the window was measured as if it had been a signal, and then it was flagged with a minus sign to denote noise. A total of thirty measurements were actually made on the signals, but the conversion from spectral amplitudes to magnitudes (to be described later) combined the three amplitudes of SH and of SV into three magnitudes for S.

The algorithm for the computation of the P-wave spectral parameters (numbers 4-9 in Table VI) is now presented, and then the time-domain analysis for the complexity and frequency-domain analysis for the spectral amplitudes will be described.

Fitting the Observed Spectrum to a Source Model

Define the modulus of the observed ground displacement spectral density as

$$|A_o(f)| = \left|\int_0^T x(t)e^{-i2\pi ft}dt\right| \tag{1}$$

Details on the actual computation of $|A_o(f)|$ are given in the next section. Hereafter, the bars denoting modulus will be dropped, and the amplitude spectrum is implied throughout. A correction for the instrument response I(f) gives

$$A'_o(f) = A_o(f)/I(f) \tag{2}$$

This spectrum relates to the source spectrum as

$$A'_o(f) = A_s(f)\cdot G(\Delta)\cdot e^{-\pi ft^*}\cdot E(f) \tag{3}$$

where t^* is the attenuation coefficient, $G(\Delta)$ is the divergence term, and E(f)

TABLE VI

Parameters Measured for Each Station and Each Event (Whenever Possible)

Number	Symbol	Explanation	
1	P_1	low-	0.469 - 0.938 Hz
2	P_2	middle- frequency P	1.094 - 1.876
3	P_3	high-	2.031 - 3.438
4	$\Omega_o(-2)$	low-frequency spectral level	
5	$f_c(-2)$	corner frequency	assuming P-wave spectrum decreases as f^{-2}
6	$t^*(-2)$	attenuation coefficient	
7	$\Omega_o(-3)$		
8	$f_c(-3)$	same as 4-6, assuming P-wave spectrum decreases as f^{-3}	
9	$t^*(-3)$		
10	$comp_1$	5-10 sec	
11	$comp_2$	5-15 sec coda interval complexity	
12	$comp_3$	5-30 sec	
13	Lg_1	low-	
14	Lg_2	middle- frequency Lg	
15	Lg_3	high-	
16	LP_1	low-	0.039 - 0.055 Hz
17	LP_2	middle- frequency long-period P	0.063 - 0.086
18	LP_3	high-	0.094 - 0.188
19	LS_1	low-	
20	LS_2	middle- frequency long-period S	
21	LS_3	high-	
22	LR_1	low-	0.016 - 0.031 Hz
23	LR_2	middle- frequency Rayleigh wave (vertical component)	0.039 - 0.053
24	LR_3	high-	0.063 - 0.086
25	LQ_1	low-	
26	LQ_2	middle- frequency Love wave	
27	LQ_3	high-	

is a random error. Taking the logarithm of (3) gives

$$\ln[A_o'(f)] = \ln [A_s(f)\cdot G(\Delta)] - \pi f t^* + \ln[E(f)] \tag{4}$$

It is assumed that the last term is a normally distributed variable with zero mean. A simple source spectral shape is introduced as

$$A_s(f) = \Omega_0 \left(\frac{f_c}{f + f_c}\right)^b \tag{5}$$

where Ω_o is the long-period spectral level at the source. By absorbing the constant $G(\Delta)$ term into Ω_o, the long-period spectral level Ω_o' at the station rather than at the source can be used when (5) is substituted in (4) to give

$$\ln[A_o'(f)] = \ln\Omega_0' + b\cdot\ln\left(\frac{f_c}{f + f_c}\right) - \pi f t^* + \ln[E(f)] \tag{6}$$

The observations $A_o'(f)$ are thus a non-linear combination of the unknown parameters Ω_0', b, f_c, and t* plus a random error term. To simplify the following expression, let

$$Y_i = \ln[A_o'(f)] \tag{7}$$

$$F_i = \ln\Omega_0' + b\cdot\ln\left(\frac{f_c}{f_i + f_o}\right) - \pi f_i t^* \tag{8}$$

$$p_1 = \ln\Omega_0' \tag{9a}$$

$$p_2 = f_c \tag{9b}$$

$$p_3 = b \tag{9c}$$

$$p_4 = -\pi t^* \tag{9d}$$

The iterative least-squares method for fitting non-linear functions will be used. Starting with an initial estimate $p^0 = (p_1^0, p_2^0, p_3^0, p_4^0)$ of the unknown parameters, the function is expanded in a Taylor series about these points:

$$\begin{aligned} F_i = {} & p_1^0 + p_3^0 \ln\left(\frac{p_2^0}{f_i + p_2^0}\right) + p_4^0 f_i \\ & + (p_1 - p_1^0)\left(\frac{dF_i}{dp_1}\right)^0 + (p_2 - p_2^0)\left(\frac{dF_i}{dp_2}\right)^0 \\ & + (p_3 - p_3^0)\left(\frac{dF_i}{dp_3}\right)^0 + (p_4 - p_4^0)\left(\frac{dF_i}{dp_4}\right)^0 \end{aligned} \tag{10}$$

The derivatives are given by

$$\frac{dF_i}{dp_1^0} = 1 \tag{11a}$$

$$\frac{dF_i}{dp_2^0} = \frac{p_3^0 f_i}{p_2^0(f_i + p_2^0)} \tag{11b}$$

$$\frac{dF_i}{dp_3^0} = \ln\left(\frac{p_2^0}{f_i + p_2^0}\right) \tag{11c}$$

$$\frac{dF_i}{dp_4^0} = f_i \tag{11d}$$

Substituting these in (10) gives

$$F_i = F_1^0 + (p_1 - p_1^0) + (p_2 - p_2^0)\frac{p_3^0 f_i}{p_2^0(f_i + p_2^0)} + (p_3 - p_3^0)\ln\left(\frac{p_2^0}{f_i + p_2^0}\right) + (p_4 - p_4^0)f_i \tag{12}$$

Let R_i be the residual between the data and the initial model

$$R_i = Y_i - F_1^0 \tag{13}$$

Since $Y_i = F_i$ plus a random error from the normal density $N(0,\sigma^2)$

$$R_i = F_i - F_1^0 + N(0,\sigma^2) \tag{14}$$

Using (12), the residual becomes

$$R_i = (p_1 - p_1^0) + (p_2 - p_2^0)\frac{p_3 f_i}{p_2^0(f_i + p_2^0)} + (p_3 - p_3^0)\ln\left(\frac{p_2^0}{f_i + p_2^0}\right) + (p_4 - p_4^0)f_i + N(o,\sigma^2) \qquad (15)$$

Equation (13) is termed the "equation of condition." If $\underline{n}$ points in the spectrum are available, the equations of condition can be expressed in matrix form as

$$\begin{bmatrix} W_1 R_1 \\ \cdot \\ \cdot \\ \cdot \\ W_n R_n \end{bmatrix} = \begin{bmatrix} W_1 & W_1 \dfrac{p_3^0 f_1}{p_2^0(f_1 + p_2^0)} & W_1 \cdot \ln\left(\dfrac{p_2^0}{f_1 + p_2^0}\right) & W_1 f_1 \\ \cdot & \cdot & \cdot & \\ \cdot & \cdot & \cdot & \\ \cdot & \cdot & \cdot & \\ W_n & W_n \dfrac{p_3^0 f_n}{p_2^0(f_n + p_2^0)} & W_n \cdot \ln\left(\dfrac{p_2^0}{f_n + p_2^0}\right) & W_n f_n \end{bmatrix} \begin{bmatrix} \Delta p_1 \\ \Delta p_2 \\ \Delta p_3 \\ \Delta p_4 \end{bmatrix} \qquad (16)$$

where arbitrary weights W_i have been entered. Letting the residual vector be R and the coefficient matrix be B, the solution vector $\Delta p = (\Delta p_1, \Delta p_2, \Delta p_3, \Delta p_4)$ is given by

$$\Delta p = (B^T B)^{-1} B^T R \qquad (17)$$

The solutions Δp are added to p^0 to obtain new estimates of the parameters, and the process (13), (16), and (17) is iterated until some convergence criterion is satisfied.

As in all non-linear fitting problems, proper convergence depends on a satisfactory initial estimate of the parameters. These initial estimates must be close to the true parameters in order for the linearization via the Taylor expansion in (10) to be valid. Preliminary work with the spectral fitting

indicated that good initial estimates were not possible in most cases. Therefore, the parameter vector $\underline{p}$ was reduced by assuming a range of values for p_3 and p_4 and solving the non-linear problem for the remaining parameters, which were long-period spectral level and corner frequency, with each set of (p_3, p_4) values. The exponent $\underline{b}(=p_3)$ for decay of the source spectrum was set at either 2 or 3. These are the exponents found in most source model derivations for explosions or earthquakes (von Seggern and Rivers, 1979). The f^{-2} model is favored for explosions and f^{-3} for earthquakes by these authors. The range of t* in p_4 was assumed to be between 0.0 and 1.0, with 0.1 increments. For each combination of t* and b then, the set of equations of condition, reduced from (16), is

$$\begin{bmatrix} W_1 R_1 \\ \cdot \\ \cdot \\ \cdot \\ W_n R_n \end{bmatrix} = \begin{bmatrix} W_1 & W_1 \dfrac{p_3^0 f_1}{p_2^0 (f_i + p_2^0)} \\ \cdot & \cdot \\ \cdot & \cdot \\ \cdot & \cdot \\ W_n & W_n \dfrac{p_3^0 f_n}{p_2^0 (f_n + p_2^0)} \end{bmatrix} \begin{bmatrix} \Delta p_1 \\ \\ \\ \\ \Delta p_2 \end{bmatrix} \tag{18}$$

For each value of $\underline{b}$, the assumed t* which results in the best fit of the data to the model, as determined by the mean-square of the residuals, is taken to be the correct estimate. Note that under the two assumptions b = 2 and b = 3, the t* estimates may differ greatly. For any particular spectrum, convergence was not reached for most of the trial t* values.

An initial estimate of f_c = 1.0 Hz was found to be satisfactory in most test cases and was used throughout in computing the results of this report unless otherwise noted. The initial value of Ω_0' was taken from the average of the spectral points in A_0' (f) between 0.5 and 1.0 Hz for a given signal.

Weighting was done according to the inverse of frequency, that is, $W_i = f_i^{-1}$.

The number of points n of the spectrum which were fit by (18) was variable, being determined by the width of the frequency band lying between the low-and high-frequency cutoffs at which the signal spectrum fell below the level of the noise spectrum. These cutoff frequencies are shown in Figure 2. In order to facilitate the convergence, these cutoffs, and sometimes initial estimates of f_c and Ω_o', were specified for certain signals rather than allowing them to be calculated by the computer. The convergence algorithm was always subjected to the further constraint that 0.2 Hz $\leq f_c \leq$ 5.0 Hz. Plots were made of all spectra so that cases requiring specification of cutoffs and/or initial values could be identified visually.

No spectral fit parameters were assigned to those spectra for which the number of useful points n was less than six or for which no convergence was attained.

Conplexity of the Short-Period P Seismogram

For this computation a window about the short-period P wave, sampled at 20 s/sec, is defined from 10 sec before the P start time to 35 sec after it. A bandpass filter with corner frequencies at 0.5 and 5.0 Hz and rolloffs of 12 db/octave is applied in the time domain. The filter output points are squared and smoothed over 50 points with a rectangular sliding window to produce a smooth envelope trace, and the square roots of the resulting envelope points are then taken. Integration is performed on the final output x (t) through

$$A_j = \sum_{i=1}^{n_j} x_i \qquad j = 1, 5$$

with integrated values defined at n_j = 200, 300, 400, 500 and 900 points (10, 15, 20, 25, and 45 sec) into the window. Define the integrated P-wave signal as

$$S = (A_2 - A_1) - 1/2\ A_1$$

The second term here represents a correction for the noise contribution to the signal amplitude. Now define three coda integrals as

$$C_1 = (A_3 - A_2) - 1/2\ A_1$$

$$C_2 = (A_4 - A_2)/2 - 1/2\ A_1$$

$$C_3 = (A_5 - A_2)/6 - 1/2\ A_1$$

The ratio of coda to signal, or complexity, is

$$C_{p_i} = C_i/S \qquad i = 1, 3$$

for three distinct definitions of coda: 5-10 sec, 5-15 sec, and 5-30 sec after the P arrival time. If the complexity was calculated to be negative, it was interpreted as measuring noise rather than signal coda, and it was set equal to zero so that it would be ignored by further processing.

Spectral Amplitudes for Short-Period P

For the short-period spectra, the folding frequency is 10 Hz since the data are sampled at 20 s/sec. The combination of instrument response and attenuation in the earth will reduce aliasing effects to insignificant levels in nearly all cases.

If a signal is present, the spectrum is computed according to (1) using an FFT algorithm on 6.4 sec (128 points) of data immediately following the starting point of the signal. A noise spectrum is computed on 6.4 sec of data immediately prior to this starting point. The mean of the noise from the start of the available data on the subset tape to the signal start, a window of varying length, is used to compute the mean of the trace. This mean is subtracted from both the noise and the signal window, and a half-cosine bell function is applied to 5% of the data window at both ends before Fourier transformation.

The resulting 65-point spectrum is smoothed once with Hanning weights, and the instrument response is removed according to (2) in order to obtain the ground displacement spectral density in nm-sec. The average spectral density is computed for three bands:

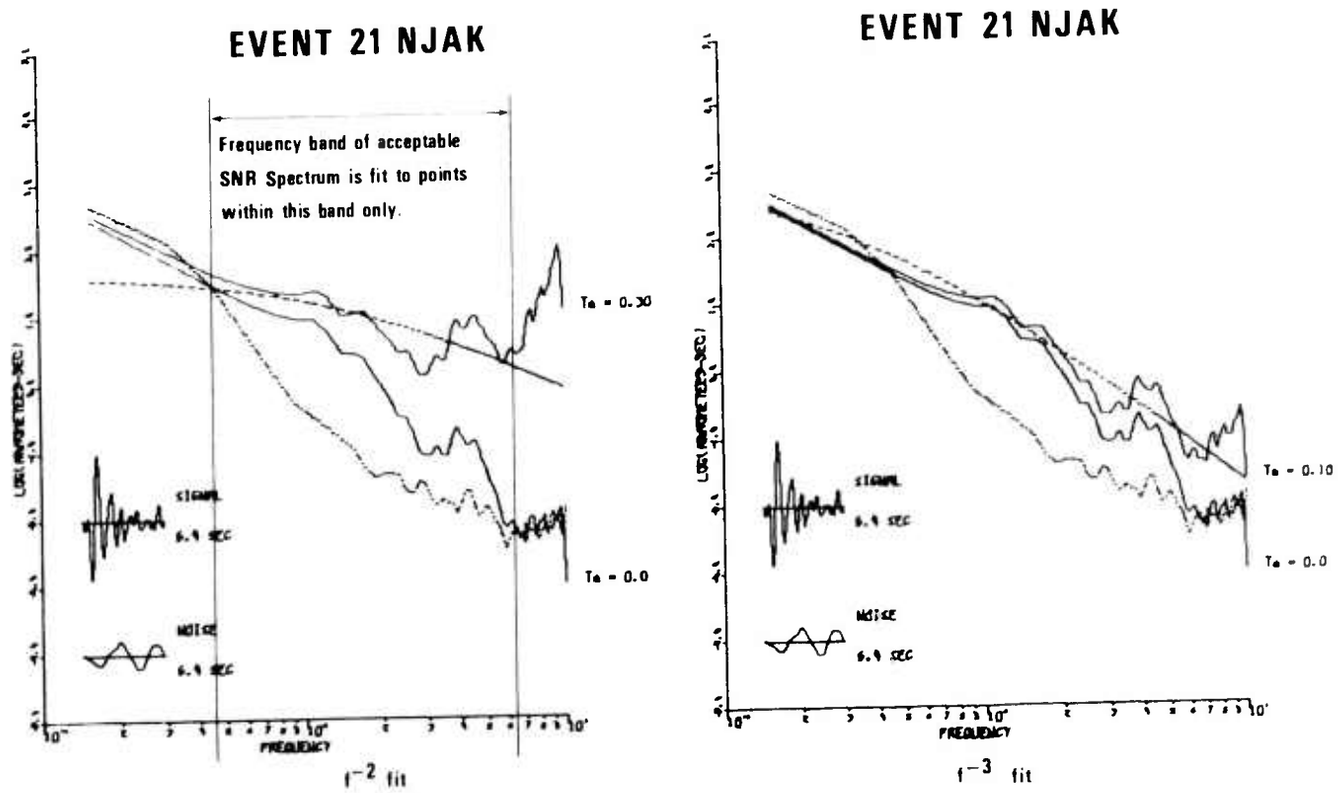

Low-frequency cutoff: 0.45 Hz
High-frequency cutoff: 6.29 Hz
} Selected automatically

Ω_o = 44.215 nm sec

fc = 1.457 Hz

Ω_o = 974.314 nm sec

fc = 0.272 Hz

LEGEND: Dotted line on bottom = noise spectrum

Lower solid line = observed signal spectrum corrected for instrument response but not attenuation

Upper solid line = observed signal spectrum corrected for instrument response and for attenuation

Dashed line = theoretical fit to observed date

Figure 2. Example of the P-wave spectral fit.

0.46875 - 0.9375 Hz (pts. 4-7)
1.09375 - 1.8759 Hz (pts. 8-13)
2.03125 - 3.4375 Hz (pts. 14-23)

The averages in the three signal spectrum bands are compared to those in the three noise spectrum bands; and, for any band where the noise exceeds the signal, the value computed for the signal window is given a negative sign to indicate a noise level estimate. If the trace is judged to have no visible signal and is so flagged for processing, then the program computes only the spectrum for 6.4 sec following the predicted arrival time and automatically appends negative signs to the values for all three spectral bands.

Spectral Amplitudes for Lg

A 25.6 sec (512 point) window for L_g is processed in all cases. The start time of the window is picked such that the energy arriving with a velocity of about 3.5 km/sec is at the start. Mean removal and tapering is done for the P wave. The resulting 257-point spectrum is reduced to 65 points by successive applications of the relation

$$A'(f_i) = \frac{1}{4} A(f_{2i-2}) + \frac{1}{2} A(f_{2i-1}) + \frac{1}{4} A(f_{2i}) \qquad (19)$$

Instrument response is then removed, and three spectral averages are computed over bands identical to those used for the P waves. Flagging of noise values is done in the same manner as for the P wave.

Spectral Amplitudes for Long-Period P and S

Since the long-period data is sampled at 1 s/sec, the folding frequency is .5 Hz. Due to the long-period instrument responses, which all fall off from roughly .05 Hz with slopes of at least 18 db/octave, aliasing is not expected to be significant.

Signal windows for both P and S are the 64 sec (64 points) following the signal start time while noise windows are the 64 sec preceding this time. Mean removal and tapering is done in the same manner as for the short-period P wave. The resulting 33-point spectrum is expanded to 65 points by use of the relations

$$A'(f_i) = A(f_{(i+1)/2}) \qquad i = 1, 3, 5, \ldots \tag{20a}$$

$$A'(f_i) = \frac{1}{2} A(f_{i/2}) + \frac{1}{2} A(f_{i/2+1}) \qquad i = 2, 4, 6, \ldots \tag{20b}$$

Instrument response is removed, and three bands in the long-period body-wave spectra are defined as

.0390625 - .0546875 Hz (pts 6-8)
.0625000 - .0859375 Hz (pts 9-12)
.0937500 - .1875000 Hz (pts 13-25)

Average values of the points in each band are computed. Flagging of noise values is done in the same manner as for short-period P waves.

For the shear wave, the horizontal seismometer components are rotated to give motion perpendicular (SH) and parallel (SV) to the projection of the ray-path on the earth's surface. The SV component was measured on the radial channel only.

Spectral Amplitudes for Rayleigh and Love Waves

Variable windows are set for the Rayleigh and Love waves in the rotated long-period traces by inspection. In general, it was attempted to window the entire dispersed waveforms between periods of 50 to 10 seconds. Due to background noise, such a window could not be well defined in many cases, and the tendency was to overestimate the window length required. A window of noise on the seismogram, equal in length to the LR or LQ window and immediately preceding it, was used for the noise spectral estimate. The trace mean was removed as previously described for the other phases, and again a 5% cosine taper was applied.

The computed spectra for LR and LQ were reduced to 65 points by equation (19), repeated as needed; and the instrument response was removed. The three spectral bands for LR and LQ were

.0156250 - .0312500 Hz (pts 3-5)
.0390625 - .0546875 Hz (pts 6-8)
.0625000 - .0859375 Hz (pts 9-12)

Again, the averages of the spectral amplitudes over the points in each band were used for the three spectral estimates. Noise estimates for when no signal was visible or when the noise spectral estimate exceeded the signal spectral estimates were again indicated by negative signs.

DATA CONTRIBUTION OF EACH STATION

Table VII shows, for each of the twenty-seven discrimination parameters described in the previous section, the total number of observations that were made of that parameter. The listing is separated in order to show the number of instances in which the measurements were of signals and the number of instances in which they were of noise. It can be seen that most of the signal measurements were of the short-period parameters. The contribution of each station to the data base, both of signal and of noise measurements, is shown in Table VIII.

By summing the number of signal and noise observations of short-period P at each station, as given by Table VIII, it is possible to determine not only the total contribution of each station to the data base for that parameter but also the relative effectiveness of each station in detecting the signals. This procedure is illustrated in Table IX. Those stations with a poor detection rate, such as HN-ME and RK-ON, may be readily identified. It is also apparent that the detection rate is frequency-dependent; in particular, P waves at NORSAR have a slightly greater probability of being detected in the high-frequency band than in the middle-frequency band, but at most other stations the middle-frequency band is the more sensitive one. The high SNR at the SRO and ASRO stations leads to large detection probabilities for that network, but it must be noted that the total number of signal and noise observations was, for every station, less than one half of the 133 events.

Comparing the number of observations (signal or noise) of P with the percentage of those which were actually signals, as shown in Table IX, suggests that at many stations seismograms which contained no detectable P signal were systematically excluded from the data base. That the gaps in the data, at least at ANMO, were in fact weak, unobserved signals is shown in Figure 3. This systematic exclusion of weak signals would result in a bias of the data towards larger magnitude estimates for every event. As will subsequently be explained, measurements of the background noise level at those stations which did not

TABLE VII

Total Number of Observations of Each Discrimination Parameter

Refer to Table VI for Explanation of the 27 Parameters

Parameter	Signal	Noise
P_1	556	722
P_2	810	468
P_3	684	594
$\Omega_o(-2)$	654	0
fc(-2)	654	0
t*(-2)	654	0
$\Omega_o(-3)$	654	0
fc(-3)	654	0
t*(-3)	654	0
$comp_1$	466	0
$comp_2$	428	0
$comp_3$	312	0
Lg_1	31	136
Lg_2	25	142
Lg_3	22	145
LP_1	114	1270
LP_2	93	1291
LP_3	71	1313
LS_1	174	1075
LS_2	153	1096
LS_3	127	1122
LR_1	291	1249
LR_2	438	1102
LR_3	320	1220
LQ_1	314	1253
LQ_2	394	1173
LQ_3	290	1277

TABLE VIII

NUMBER OF OBSERVATIONS AT EACH STATION OF EACH DISCRIMINATION PARAMETER.
REFER TO TABLE VI FOR DESCRIPTION OF THE 27 PARAMETERS.

TOTAL OF ALL SIGNAL MEASUREMENTS

	ANMO	ANTO	ATAK	BFAK	BOCO	CHTO	CNAK	CTAO	GUMO	HNME	IB7	KAAO	KONO	KSRS
1 :	28	2	20	41	0	35	43	15	0	4	39	57	0	30
2 :	35	2	32	69	0	36	64	16	0	16	52	62	0	52
3 :	27	2	40	56	0	29	52	14	0	17	38	57	0	47
4 :	31	2	24	56	0	34	54	15	0	12	41	59	0	36
5 :	31	2	24	56	0	34	54	15	0	12	41	58	0	36
6 :	31	2	24	56	0	34	54	15	0	12	41	59	0	36
7 :	31	2	24	56	0	34	54	15	0	12	41	59	0	36
8 :	31	2	24	56	0	33	54	15	0	12	41	59	0	36
9 :	31	2	24	56	0	34	54	15	0	12	41	59	0	36
10 :	14	2	22	49	0	21	53	7	2	4	28	24	0	26
11 :	10	2	22	44	0	21	47	5	2	3	28	24	0	25
12 :	6	2	17	26	0	21	24	1	2	2	14	24	0	27
13 :	0	0	0	0	0	2	0	0	0	0	5	11	0	2
14 :	0	0	0	0	0	2	0	0	0	0	1	11	0	2
15 :	0	0	0	0	0	2	0	0	0	0	2	10	0	0
16 :	2	0	1	8	0	8	0	6	7	0	17	18	0	10
17 :	1	0	0	8	0	7	0	4	6	0	14	14	0	6
18 :	1	0	0	4	0	5	0	0	5	0	11	13	0	6
19 :	7	0	0	11	0	14	0	9	11	2	29	10	0	18
20 :	6	0	0	9	0	13	0	8	9	2	26	7	0	17
21 :	6	0	1	9	0	11	0	8	7	0	22	8	0	13
22 :	22	0	0	14	0	17	0	11	14	3	42	39	0	26
23 :	30	2	1	22	0	24	0	13	20	8	43	43	0	47
24 :	15	1	0	10	0	21	0	3	7	3	35	37	0	45
25 :	16	0	1	14	0	18	0	6	15	6	40	41	0	30
26 :	22	2	2	15	0	25	0	9	18	5	46	44	0	38
27 :	9	1	1	8	0	13	0	3	13	1	37	40	0	35

TABLE VIII (CONTINUED)

TOTAL OF ALL SIGNAL MEASUREMENTS (CONTINUED)

	LAO	MAIO	MAJO	NAO	NJAK	NWAO	RKON	SHIO	SNZO	TATO	TNAK	UCAK	ZOBO
1 :	37	42	8	18	40	2	11	3	0	3	34	44	0
2 :	57	51	9	46	65	4	19	3	0	4	53	63	0
3 :	39	36	9	[illegible]	47	3	18	3	0	1	49	48	0
4 :	43	46	9	42	54	4	19	3	0	3	46	51	0
5 :	43	46	9	42	54	4	19	3	0	3	46	51	0
6 :	43	46	9	42	54	4	19	3	0	3	46	51	0
7 :	43	46	9	42	54	4	19	3	0	3	46	51	0
8 :	42	46	9	42	54	4	19	3	0	3	46	51	0
9 :	43	46	9	42	54	4	19	3	0	3	46	51	0
10 :	23	13	6	37	45	0	10	2	0	2	33	43	0
11 :	25	13	6	36	35	0	8	2	0	2	31	37	0
12 :	21	10	6	32	25	0	7	2	0	2	19	22	0
13 :	0	11	0	0	0	0	0	0	0	0	0	0	0
14 :	0	9	0	0	0	0	0	0	0	0	0	0	0
15 :	0	8	0	0	0	0	0	0	0	0	0	0	0
16 :	6	13	3	4	0	2	1	1	0	7	0	0	0
17 :	4	13	3	4	0	2	0	0	0	7	0	0	0
18 :	3	11	2	3	0	1	1	0	0	5	0	0	0
19 :	5	17	4	6	0	6	3	1	0	21	0	0	0
20 :	5	20	3	6	0	3	2	0	0	17	0	0	0
21 :	5	15	3	3	0	3	0	0	0	13	0	0	0
22 :	10	41	6	11	0	3	2	0	2	21	0	0	7
23 :	19	57	17	30	0	6	5	1	3	37	0	0	10
24 :	12	50	14	26	0	1	3	1	0	32	0	0	4
25 :	11	46	7	15	0	2	0	1	2	38	0	0	5
26 :	15	50	12	25	0	7	2	1	2	44	0	0	9
27 :	10	43	9	21	0	0	1	1	0	34	0	0	5

TABLE VIII (CONTINUED)

TOTAL OF ALL NOISE MEASUREMENTS

	ANMO	ANTO	ATAK	BFAK	BOCO	CHTO	CNAK	CTAO	GUMO	HNME	IR7	KAAO	KONO	KSRS
1 :	9	0	65	54	0	2	50	3	0	46	61	7	0	36
2 :	2	0	53	26	0	1	29	2	0	34	48	2	0	64
3 :	10	0	45	39	0	8	41	4	0	33	62	7	0	69
4 :	0	0	0	0	0	0	0	0	0	0	0	0	0	0
5 :	0	0	0	0	0	0	0	0	0	0	0	0	0	0
6 :	0	0	0	0	0	0	0	0	0	0	0	0	0	0
7 :	0	0	0	0	0	0	0	0	0	0	0	0	0	0
8 :	0	0	0	0	0	0	0	0	0	0	0	0	0	0
9 :	0	0	0	0	0	0	0	0	0	0	0	0	0	0
10 :	0	0	0	0	0	0	0	0	0	0	0	0	0	0
11 :	0	0	0	0	0	0	0	0	0	0	0	0	0	0
12 :	0	0	0	0	0	0	0	0	0	0	0	0	0	0
13 :	0	0	0	2	0	1	0	0	0	0	42	3	0	77
14 :	0	0	0	2	0	1	0	0	0	0	46	3	0	77
15 :	0	0	0	2	0	1	0	0	0	0	45	4	0	79
16 :	65	4	23	74	0	65	0	109	107	35	84	76	2	87
17 :	66	4	24	74	0	66	0	111	108	35	87	80	2	91
18 :	66	4	24	78	0	68	0	115	109	35	90	81	2	91
19 :	53	4	5	72	0	56	0	98	99	32	63	58	2	68
20 :	59	4	5	74	0	57	0	99	101	32	66	61	2	69
21 :	59	4	4	74	0	59	0	99	103	34	70	60	2	73
22 :	96	4	6	59	6	59	0	110	97	37	57	48	2	79
23 :	88	2	5	51	6	52	0	108	91	32	56	44	2	58
24 :	103	3	6	63	6	55	0	118	104	37	64	50	2	60
25 :	95	4	5	61	7	62	0	117	95	31	62	49	2	69
26 :	89	2	4	60	7	55	0	114	92	32	56	46	2	61
27 :	102	3	5	67	7	62	0	120	97	36	65	50	2	64

TABLE VIII (CONTINUED)

TOTAL OF ALL NOISE MEASUREMENTS (CONTINUED)

	LAO	MAIO	MAJO	NAO	NJAK	NWAO	OKON	SHIO	SNZO	TATO	TNAK	UCAK	ZOBO
1 :	52	12	1	67	53	2	38	0	0	3	54	47	0
2 :	32	3	0	39	28	0	30	0	0	2	45	28	0
3 :	50	18	0	33	46	1	31	0	0	5	49	43	0
4 :	0	0	0	0	0	0	0	0	0	0	0	0	0
5 :	0	0	0	0	0	0	0	0	0	0	0	0	0
6 :	0	0	0	0	0	0	0	0	0	0	0	0	0
7 :	0	0	0	0	0	0	0	0	0	0	0	0	0
8 :	0	0	0	0	0	0	0	0	0	0	0	0	0
9 :	0	0	0	0	0	0	0	0	0	0	0	0	0
10 :	0	0	0	0	0	0	0	0	0	0	0	0	0
11 :	0	0	0	0	0	0	0	0	0	0	0	0	0
12 :	0	0	0	0	0	0	0	0	0	0	0	0	0
13 :	0	4	0	7	0	0	0	0	0	0	0	0	0
14 :	0	6	0	7	0	0	0	0	0	0	0	0	0
15 :	0	7	0	7	0	0	0	0	0	0	0	0	0
16 :	74	98	52	80	0	69	35	3	17	111	0	0	0
17 :	76	98	52	80	0	69	36	4	17	111	0	0	0
18 :	77	100	53	81	0	70	35	4	17	113	0	0	0
19 :	76	59	39	69	0	65	36	3	16	97	0	0	0
20 :	76	56	40	69	0	63	37	4	16	101	0	0	0
21 :	76	61	40	72	0	68	39	4	16	105	0	0	0
22 :	60	71	47	76	0	74	43	4	62	97	0	0	55
23 :	51	55	36	57	0	71	40	3	61	81	0	0	52
24 :	58	62	39	61	0	76	42	3	64	86	0	0	58
25 :	70	65	38	73	0	76	39	3	72	78	0	0	80
26 :	66	61	33	62	0	71	37	3	72	72	0	0	76
27 :	71	58	36	67	0	78	38	3	74	82	0	0	80

TABLE IX

Total Observations of P, and How Many Were Signals

	station	P Total Observations	number which were signals P_1	P_2	P_3	percentage which were signals P_1	P_2	P_3
Alaska:	AT-AK	85	20	32	40	24	38	47
	BF-AK	95	41	69	56	43	73	59
	CN-AK	93	43	64	52	46	69	56
	NJ-AK	93	40	65	47	43	70	51
	TN-AK	98	34	53	49	35	54	50
	UC-AK	91	44	63	48	48	69	53
SDCS:	HN-ME	50	4	16	17	8	32	34
	RK-ON	49	11	19	18	22	39	37
Arrays:	ILPA	100	39	52	38	39	52	38
	KSRS	116	30	52	47	26	45	41
	LASA	89	37	57	39	42	64	44
	NORSAR	85	18	46	52	21	54	61
SRO/ASRO:	ANMO	37	28	35	27	76	95	73
	ANTO	2	2	2	2			
	BOCO	0	0	0	0			
	CHTO	37	35	36	29	95	97	78
	CTAO	18	15	16	14			
	GUMO	0	0	0	0			
	KAAO	64	57	62	57	89	97	89
	KONO	0	0	0	0			
	MAIO	54	42	51	36	78	94	67
	MAJO	9	8	9	9			
	NWAO	4	2	4	3			
	SHIO	3	3	3	3			
	SNZO	0	0	0	0			
	TATO	6	3	4	1			
	ZOBO	0	0	0	0			

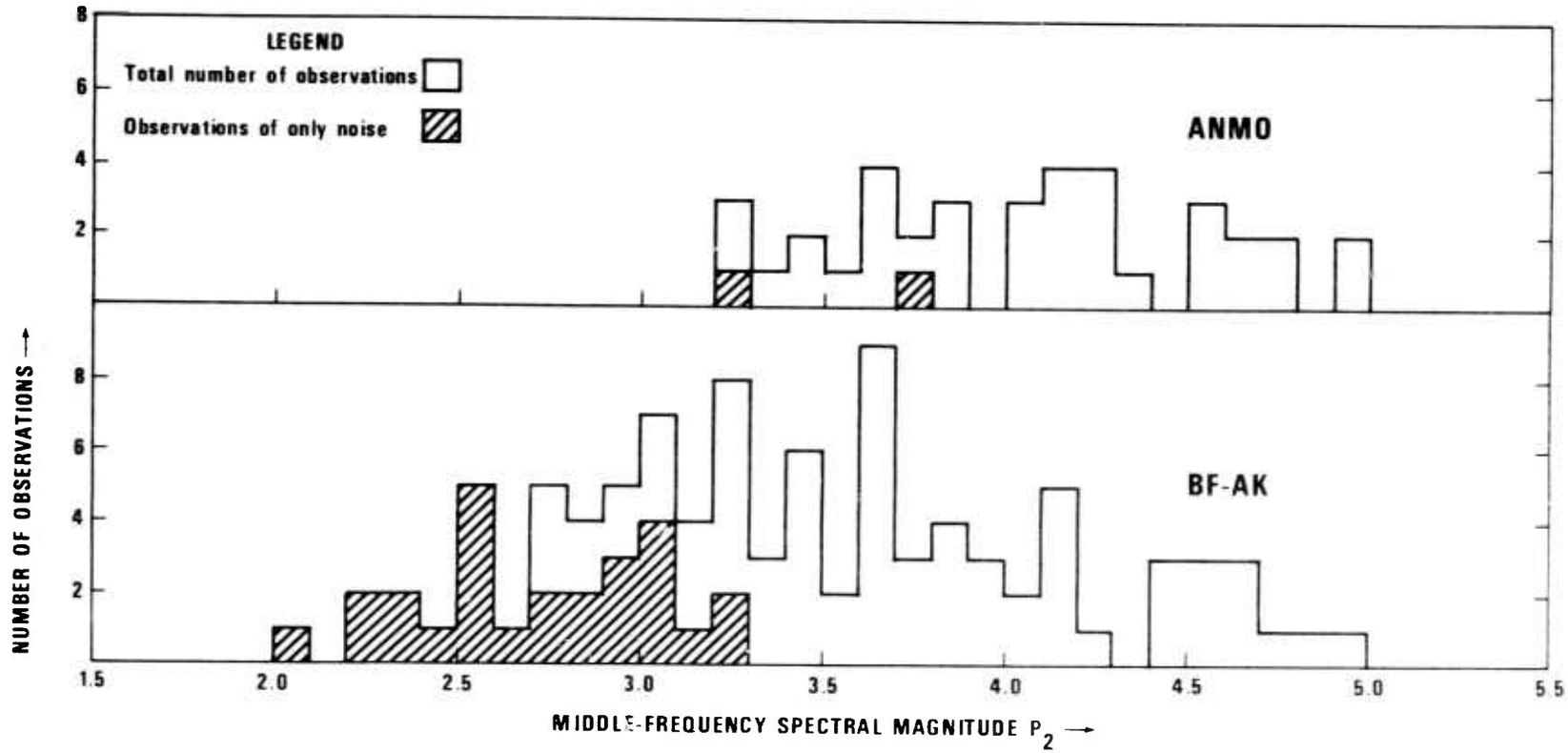

Figure 3. Total number of observations of middle-frequency spectral magnitude P_2 at three stations, and how many were noise.

detect a given signal were used in the maximum-likelihood estimator of Ringdal (1976) in order to minimize the bias which would affect the estimation of the event magnitude of only the signals were used. As a result of the failure in so many instances to include in the data base those seismograms which contained only noise, however, the full power of the maximum-likelihood estimator could not be used. Had the situation which is reflected in Figure 3 been anticipated, the resulting bias in the estimation of the magnitudes of the small events could have been at least partially alleviated by the substitution of average noise levels typical of each station in place of the missing instantaneous measurements of the noise levels at the predicted signal arrival times. Although von Seggern and Rivers (1978) showed that average noise levels can in fact be used effectively in maximum-likelihood magnitude estimations, this procedure was not employed in this experiment.

In contrast to the situation for short-period P, long-period seismograms such as those for LR were included in the SRO data base even if no signal was detected. Table X shows the number of LR seismograms reported from each station and the percentage of seismograms which contained detectable signals. It can be seen that five of the SRO stations reported LR seismograms for more than one hundred events, although signals were detected in only about one third of the cases. It was thus possible to utilize more fully the power of the maximum-likelihood magnitude estimator for LR (and other long-period data) than for short-period P. The LR detection probability is shown in Table X to be frequency-dependent, LR_1 being detected less frequently than LR_2 and LR_3. It is also shown that certain stations, such as ILPA, are more efficient at detecting LR_1 relative to LR_2 than are others, such as KSRS. Finally, Table X shows that

---

Ringdal, F. (1976). Maximum-likelihood estimate of event magnitude, Bull. Seism. Soc. Am., 66, 789.

von Seggern, D. H., and D. W. Rivers (1978). Comments on the use of truncated distribution theory for improved magnitude estimation, Bull. Seism. Soc. Am., 68, 1543.

TABLE X

Total Observations of LR, and How Many Were Signals

	station	LR total Observations	number which were signals			Percentage which were signals		
			LR_1	LR_2	LR_3	LR_1	LR_2	LR_3
Alaska:	AT-AK	6	0	1	0			
	BF-AK	73	14	22	10	19	30	14
SDCS:	HN-ME	40	3	8	3	8	20	8
	RK-ON	45	2	5	3	4	11	7
Arrays:	ILPA	99	42	43	35	42	43	35
	KSRS	105	26	47	45	25	45	43
	LASA	70	10	19	12	14	27	17
	NORSAR	87	11	30	26	13	34	30
SRO/ASRO:	ANMO	118	22	30	15	19	25	13
	ANTO	4	0	2	1			
	BOCO	6	0	0	0			
	CHTO	76	17	24	21	22	32	28
	CTAO	121	11	13	3	9	11	2
	GUMO	111	14	20	7	13	18	6
	KAAO	87	39	43	37	45	49	43
	KONO	2	0	0	0			
	MAIO	112	41	57	50	37	51	45
	MAJO	53	6	17	14	11	32	26
	NWAO	77	3	6	1	4	8	1
	SHIO	4	0	1	1			
	SNZO	64	2	3	0	3	5	0
	TATO	118	21	37	32	18	31	27
	ZOBO	62	7	10	4	11	16	6

the LR data base was heavily influenced by the inclusion of a few certain stations. In particular, it should be noted that LR_2 was detected for more than forty events at only four stations: ILPA, KSRS, KAAO, and MAIO. The detection capability of these stations was due to the beamforming capability of the two arrays and to the proximity of three of the stations to tectonic regions 9 and 10, in which over one fourth of the 133 events occurred. Had these four stations not been included in the data base, the number of detections of LR, and hence the value of the $M_s:m_b$ discriminant, would have been significantly diminished.

CALCULATION OF MAGNITUDES

The amplitude parameters which were described previously were measured for each signal or noise window and then were converted to magnitudes by means of formulas which will now be described. It should be noted that the amplitudes were measured in the frequency domain rather than the time domain (units of nm-sec rather than nm), so the magnitudes are not the same as those which are conventionally calculated from the visual measurement of seismograms. This distinction should create no difficulty, since it is the difference between magnitudes for different parameters and different events, rather than the magnitudes themselves, which is important for discrimination. The same formulas and B-factors are applicable to both the time-domain and frequency-domain magnitudes, since the difference between the two scales should be constant for each parameter.

It has already been mentioned that the small distances between several events and some of the stations used in this report presented certain difficulties for the calculation of magnitudes, and this problem will now be described.

The observed amplitudes of the surface waves LR and LQ were converted to magnitudes by correcting for attenuation and for geometrical spreading of the wavefront (a correction which employs the stationary phase approximation) by means of the formula (cf. Sato, 1967):

$$\text{Magnitude} = \log_{10} (\text{amplitude}) + \log_{10} \left(e^{\gamma r} \sqrt{r \sin (r/Re)} \right) \qquad (21)$$

where r is the epicenter-to-receiver distance in km, Re is the radius of the earth, and γ is a frequency-dependent attenuation coefficient taken from Mitchell et al (1976) and listed in Table XI. The second term on the right-hand side of equation (21) is plotted in Figure 4 as a function of the

---

Sato, R., (1967). Attenuation of seismic waves, J. Phys. Earth, 15, 32.

Mitchell, B. J., L. W. B. Leite, Y. K. Yu, and R. B. Herrmann (1976). Attenuation of Love and Rayleigh waves across the Pacific at periods between 15 and 110 seconds, Bull. Seism. Soc. Am. 66, 1189.

TABLE XI

Constants Used in the Calculation of Spectral Magnitudes

1) LR and LQ Attenuation Coefficients

	band 1	band 2	band 3
frequency (Hz)	0.016-0.031	0.039-0.055	0.062-0.086
γ (km^{-1})	0.0001	0.00015	0.0002

2) Takeoff Angles as a Function of Distance

$i_o = A_4 \cdot \Delta^4 + A_3 \cdot \Delta^3 + A_2 \cdot \Delta^2 + A_1\Delta + A_o$, where

Δ	A_4	A_3	A_2	A_1	A_o
$0.0° \leq \Delta < 9.0°$	0.0	0.0	0.0	-0.055556	47.9
$9.0° \leq \Delta < 11.5°$	0.0	0.0	0.0	-0.24	49.56
$11.5° \leq \Delta < 15.5°$	0.0	0.0	0.0	-0.475	52.2625
$15.5° \leq \Delta < 20.0°$	0.0	0.0	0.0	-1.644444	70.388889
$20.0° \leq \Delta < 30.0°$	-8.9961×10^{-4}	0.088244	-3.1096	45.407	-188.74
$30.0° \leq \Delta < 85.0°$	-1.3478×10^{-6}	3.0859×10^{-4}	-0.025787	0.025787	23.882
$85.0° \leq \Delta < 100.0°$	0.0	-7.8222×10^{-4}	0.22419	-21.429	697.66

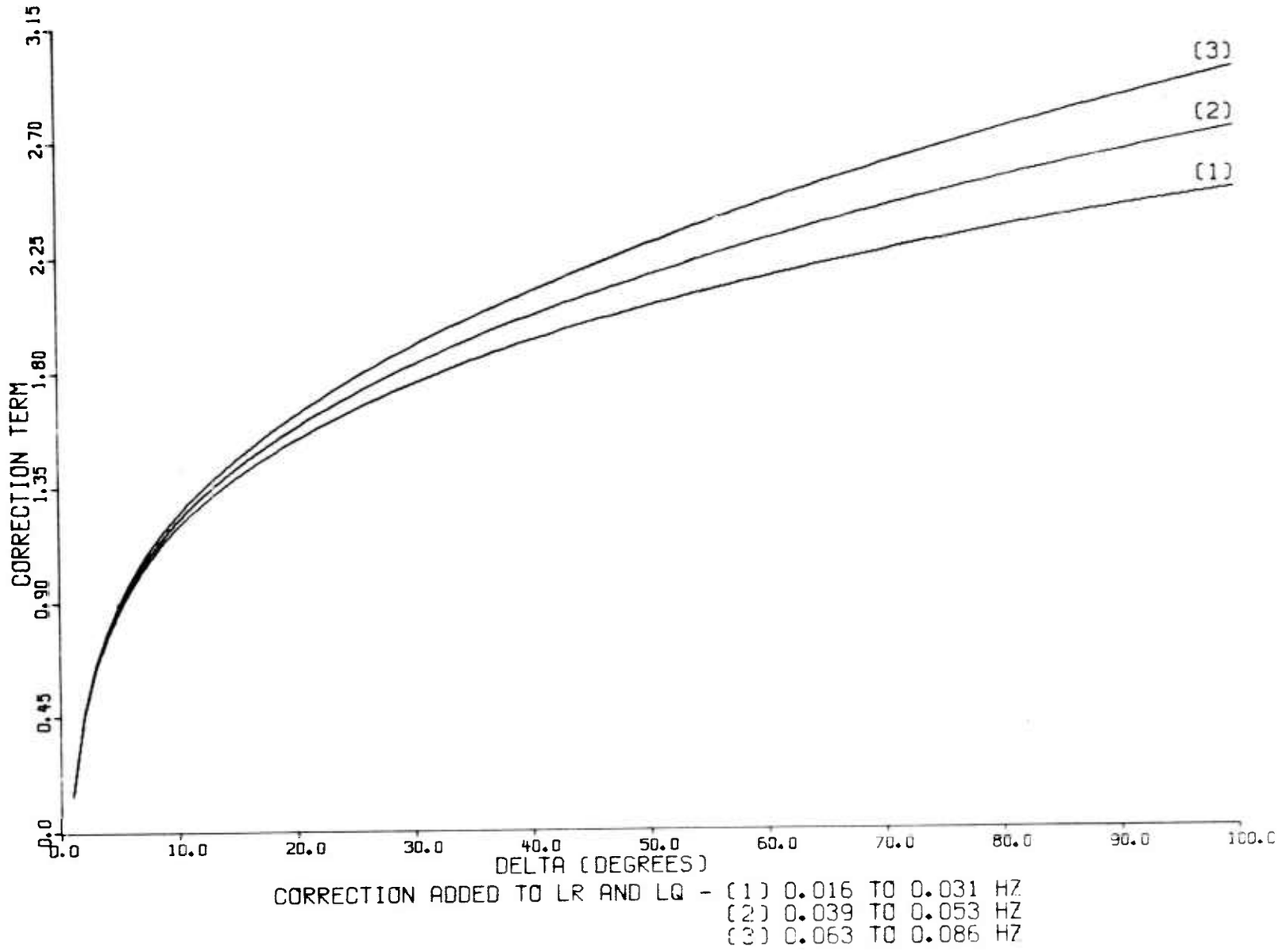

Figure 4. Calculation of Rayleigh-and Love-wave magnitudes.

epicenter-to-receiver angular separation Δ. It is clear from the figure that small changes in the assumed value of Δ are unimportant for teleseismic events, but at distances of less than about 5° they are sufficient to cause substantial fluctuations in the calculated magntiudes. It was on account of this sensitivity to errors in the epicenter location that LR and LQ were in a few cases ignored at small distances if the calculated magnitudes conflicted with those which were measured at teleseimic stations or, much more commonly, if only noise was observed at all stations, in which case no comparison of signal magnitudes could be made.

For Lg, magnitudes were calculated by means of the following formula:

$$\text{Magnitude} = \log_{10} (\text{amplitude}) + \log_{10} r^2. \qquad (22)$$

The distance dependence of this empirical formula, plotted in Figure 5, is stronger than that of equation (21), so epicenter mislocations are problematic at those regional distances at which Lg is ordinarily observed. The data base of Lg detections was insufficient to test the validity of equation (22), and thus it is not known how much error was introduced into the magnitude calculation by the use of this empirical formula. It should be noted that Romney (1959) deduced an amplitude decay proportional to r^{-3} for Lg propagating across the United States.

Body-wave magnitudes were computed from the formula:

$$\text{Magnitude} = \log_{10} (\text{amplitude}) + B(\Delta) \qquad (23)$$

where B is a term which corrects for geometrical spreading of the wavefront and for anelastic attenuation. This "B-factor" is of course dependent upon the depth of the hypocenter, but since all 133 events were to be regarded as possible explosions only B-factors appropriate for surface events were used. For the short-period P-wave magnitudes P_1, P_2, and P_3, B-factors were taken from the study of Veith and Clawson (1972), which used conventional measurements

---

Romney, C. (1959), Amplitudes of seismic body waves from underground nuclear explosions, J. Geophys. Res., 64, 1489.

Veith, K., and G. Clawson (1972). Magnitudes from short-period P-wave data, Bull. Seism. Soc. Am. 62, 435.

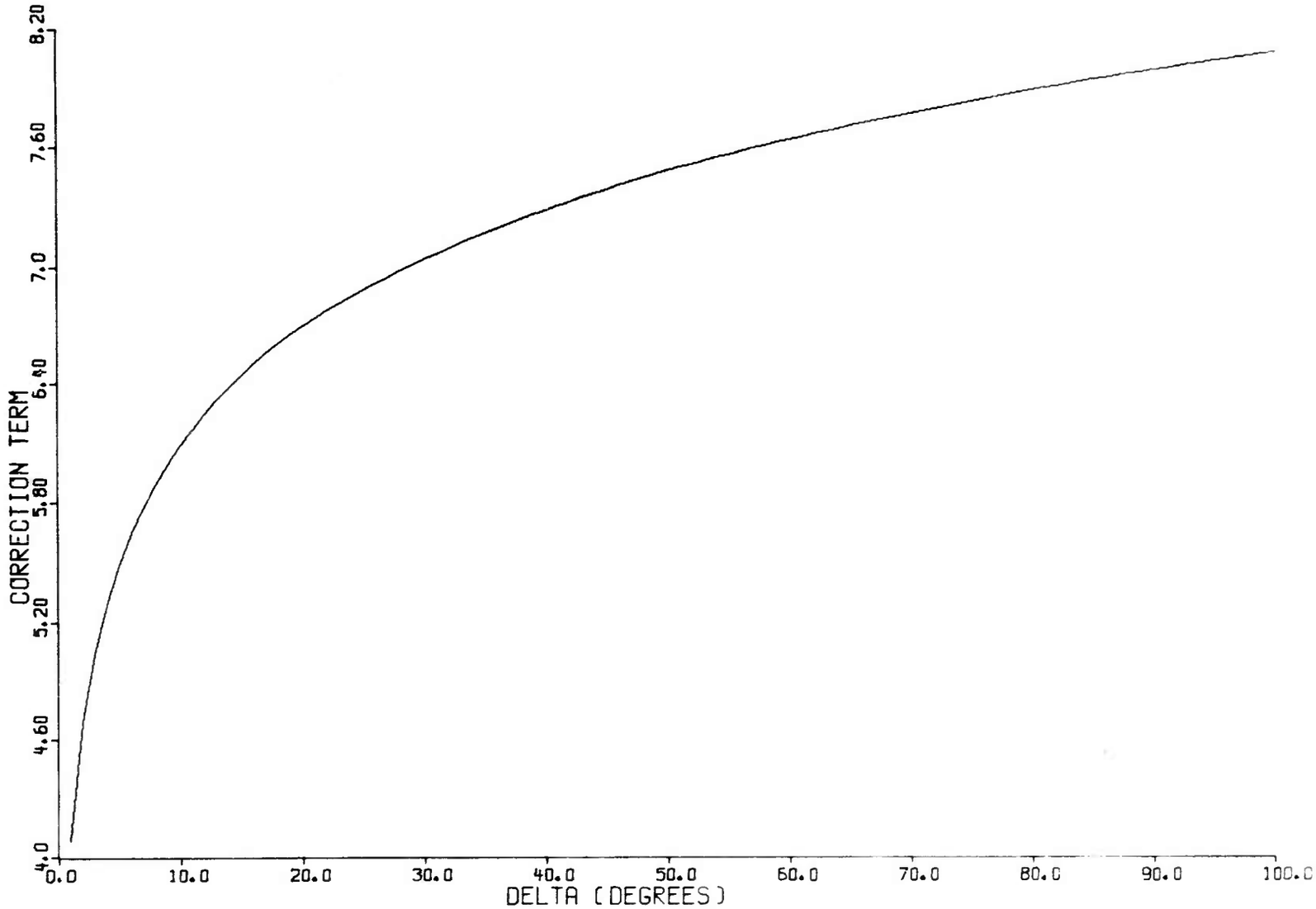

CORRECTION ADDED TO LG - ALL 3 FREQUENCY BANDS

Figure 5. Calculation of Lg magnitudes.

of m_b and hence frequencies in the bands P_1 and P_2. For the long-period P-wave magnitudes LP_1, LP_2, and LP_3, B-factors were taken from the study of Gutenberg and Richter (1956), which used P-waves with frequencies of about 0.25 hz (Gutenberg, 1945). Although this frequency is higher than that of even the high-frequency band LP_3, less frequency-dependent error is introduced into the magnitude calculations by using the Gutenberg-Richter B-factors for the long-period bands than was introduced by using the Veith-Clawson B-factors for all three short-period bands. That this is so may be demonstrated by considering the fact that because geometrical spreading of the wavefront is independent of frequency, the frequency dependence of the shape of the $B(\Delta)$ curve is determined entirely by anelastic attenuation. [A frequency-dependent geometrical spreading effect, namely P-wave diffraction by the earth's core, is unimportant since no measurements were made on body waves for which Δ exceeded 100°]. An assessment of the effect of attenuation may be made by evaluating the quantity $\exp(-\pi f t^*)$ for different frequencies f. This is done in Table XII for an assumed value of 0.5 sec for the attenuation coefficient t^*. It can be seen from the table that the frequency difference between the long-period bands and the values used by Gutenberg and Richter is unimportant. It might appear that B-factors measured at frequencies near one hz are inadequate for the high frequency band P_3, but it will be shown subsequently that the shape of the $B(\Delta)$ curve (as opposed to its absolute level, which may be considered arbitrary) is controlled mainly by geometrical spreading rather than attenuation, so it is not strongly frequency-dependent.

The $B(\Delta)$ curve is shown in Figure 6 for the long-period P magnitudes and in Figure 7 for the short-period P magnitudes. As was the case for surface waves, the P-wave magnitudes are insensitive to small errors in epicenter location if the source-to-receiver separation is teleseismic, but small location errors can lead to substantial errors in the magnitude calculation for smaller distances. This problem is compounded by uncertainties in the $B(\Delta)$ curves

---

Gutenberg, B. (1945). Amplitudes of P, PP and S and magnitudes of shallow earthquakes, Bull. Seism. Soc. Am., 35, 57.

Gutenberg, B., and C. F. Richter (1956). Magnitude and energy of earthquakes, Annali Geofisica, 9, 1.

TABLE XII

Relative Effect of Anelastic Attenuation on P-Wave

Amplitudes at Different Frequencies

Frequency Band	lowest Frequency (hz)	highest Frequency (hz)	mean F (hz)	$e^{-\pi f t^*}\|_{t^*=0.5sec}$
LP_1	0.039	0.055	0.047	0.929
LP_2	0.063	0.086	0.075	0.890
LP_3	0.094	0.188	0.141	0.801
Gutenberg-Richter B(Δ)		(typically)	0.250	0.675
P_1	0.469	0.938	0.704	0.331
P_2	1.094	1.876	1.485	0.331
P_3	2.031	3.438	2.735	0.014
Veith-Clawson B(Δ)		(typically)	1.000	0.208

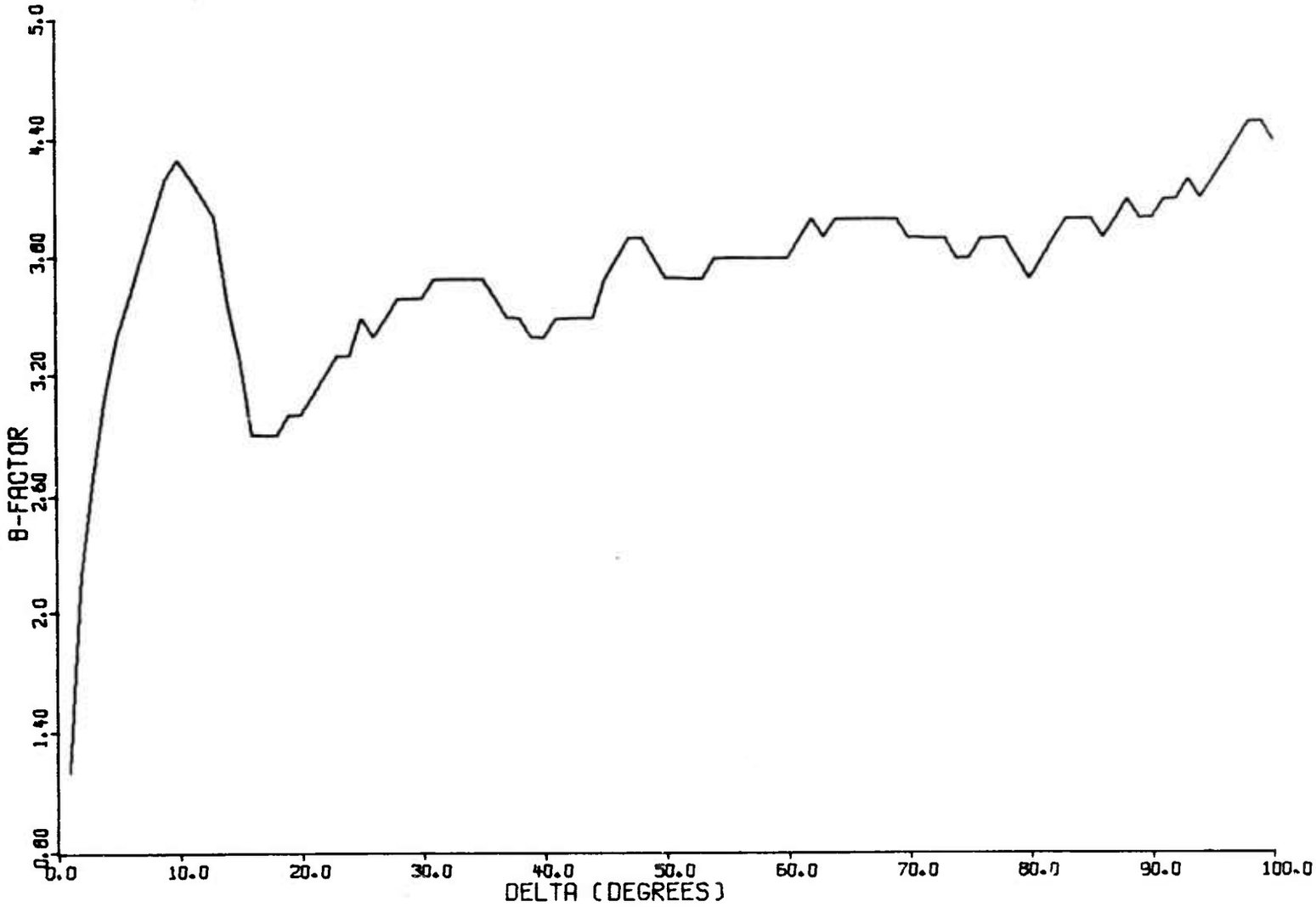

GUTENBERG-RICHTER B-FACTORS FOR LONG-PERIOD P

Figure 6. Calculation of long-period P-wave magnitudes.

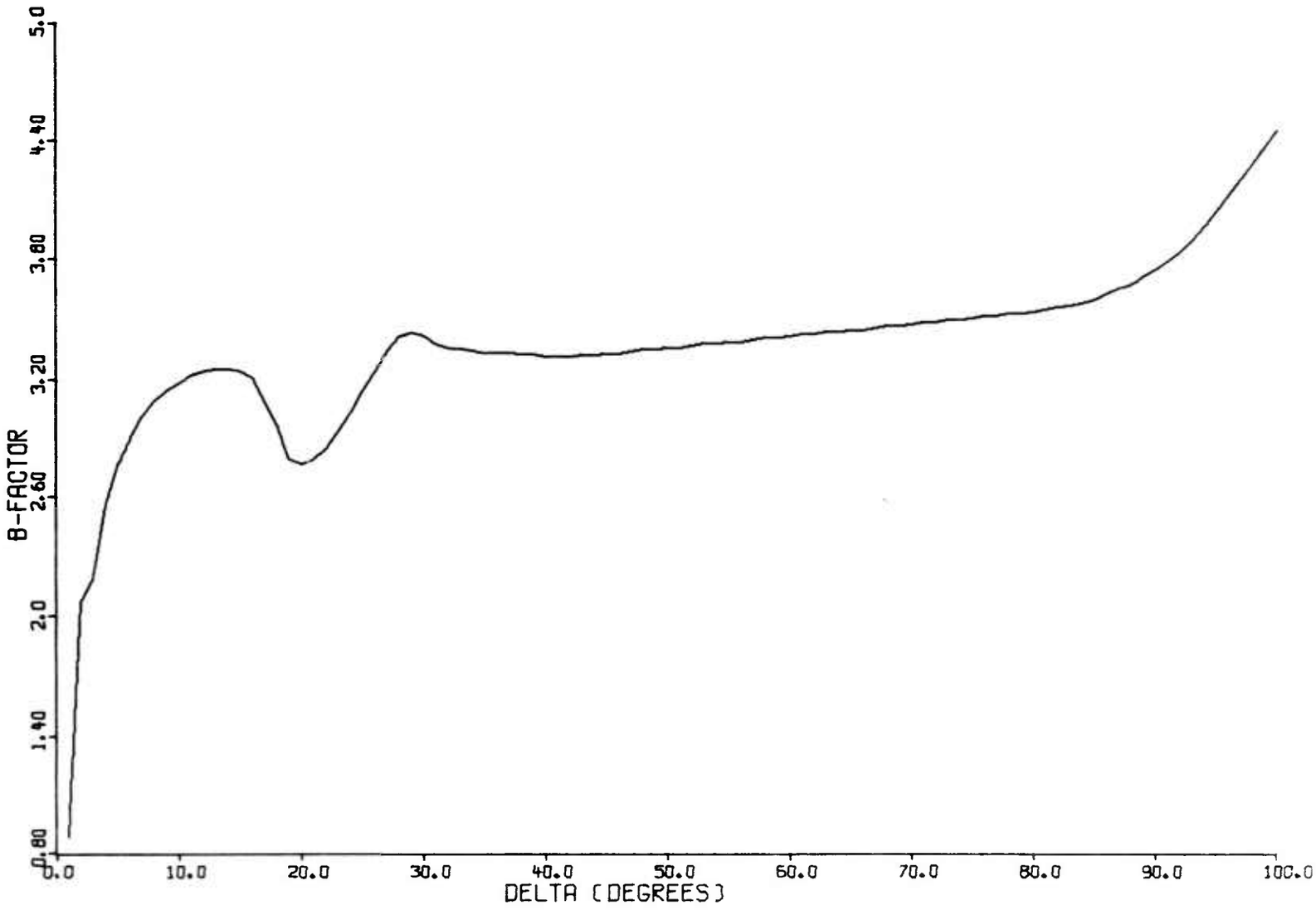

VEITH-CLAWSON B-FACTORS FOR SHORT-PERIOD P

Figure 7. Calculation of short-period P-wave magnitudes.

themselves at distances of less than about 25°. Booth et al (1974) have measured the distance dependence of P-wave amplitudes at frequencies of 1.0 hz and 0.063 hz, and their results show certain differences from the $B(\Delta)$ curves used in this report for the distance range $0° \leq \Delta \leq 25°$. For the 1.0 hz case these differences are less than about 0.3 magnitude units, but for the 0.063 hz case the difference is a whole magnitude at $\Delta = 10°$. Discrepancies between these different determinations of $B(\Delta)$ for a given frequency are probably due to lateral heterogeneity in earth structure, and so they are dependent upon the geographical region in which the (short) source-to-receiver path occurs. As a further complication, triplication of the travel-time curve causes several P phases to arrive close together for small Δ, so at short distances the 60 sec-long window which was used for long-period P contains several different phases which interfere constructively or destructively to produce the spectral amplitude which is measured within that window. A final source of error in the magnitude calculation is introduced by the assumption of zero depth for all events; as can be seen from Figure 9 of Veith and Clawson (1972), the error caused by this assumption is a slowly increasing function of depth for the distance range $30° \leq \Delta \leq 90°$, but at distances of less than about 10° the error increases quite rapidly with depth below the base of the crust. In view of all these different sources of possible error, it is not surprising that the P-wave magnitudes measured at near-regional and regional distances were sometimes in conflict with measurements made at teleseismic distances. In those instances in which such disagreements were found, the observations made at the close-in stations were deleted. Most of the deleted close-in measurements of P, however, were actually measurements of only noise. Such measurements were deleted since the teleseismic observations were also of noise, and no comparison of signal magnitudes could be made.

Booth, D. C., P. D. Marshall, and J. B. Young (1974). Long and short period P-wave amplitudes from earthquakes in the range 0°-114°, Geophys. J. R. Astr. Soc., 39, 523.

An example of the arrival of more than one P phase, in this case for short-period rather than long-period P, is shown in Figure 8. The figure shows the P-wave signature from event 14 as recorded at stations MAIO and KAAO, for which the distances from the epicenter were 19.1° and 16.6°, respectively. It might appear that the seismograms show an earthquake with a small precursor, but in fact event 14 is a presumed explosion. The first arrival at KAAO is due to a ray which penetrates the mantle to a depth of 192 km, and the large motion following it is due to a ray which penetrates to a depth of 428 km. In cases such as this, the 6.4 sec P-wave windows were adjusted to begin at the start of the second arrival, and the 6.4 sec noise window was moved back so that it did not include any of the first P phase. It is interesting to note that at these two SRO stations all single explosions at Semipalatinsk look like multiple events.

It has already been noted that no records of long-period S were analyzed for source-to-receiver separations of less than 15°. The B-factors which were used for S were taken from Gutenberg and Richter (1956). As is shown in Figure 9, the calculated magnitude for S is strongly sensitive to location errors at distances of less than 20°. A further uncertainty in the magnitude is introduced by use of the formula

$$\text{Magnitude} = \frac{1}{2} \log_{10} (SH^2 + SV^2) + B(\Delta) \tag{24}$$

when the amplitudes for both SH and SV exceeded the threshold SNR of 1.5 (or when they were both less than this threshold, in which case the magnitude is a noise level), and use of the formula

$$\text{Magnitude} = \log_{10} (SH) + B(\Delta) \tag{25}$$

when the SH amplitude exceeded the threshold and the SV amplitude did not, or use of the formula

$$\text{Magnitude} = \log_{10} (SV) + B(\Delta) \tag{26}$$

in the opposite case.

A rigorous calculation of the magnitude of the low-frequency spectral level Ω_o can be made by means of the formula

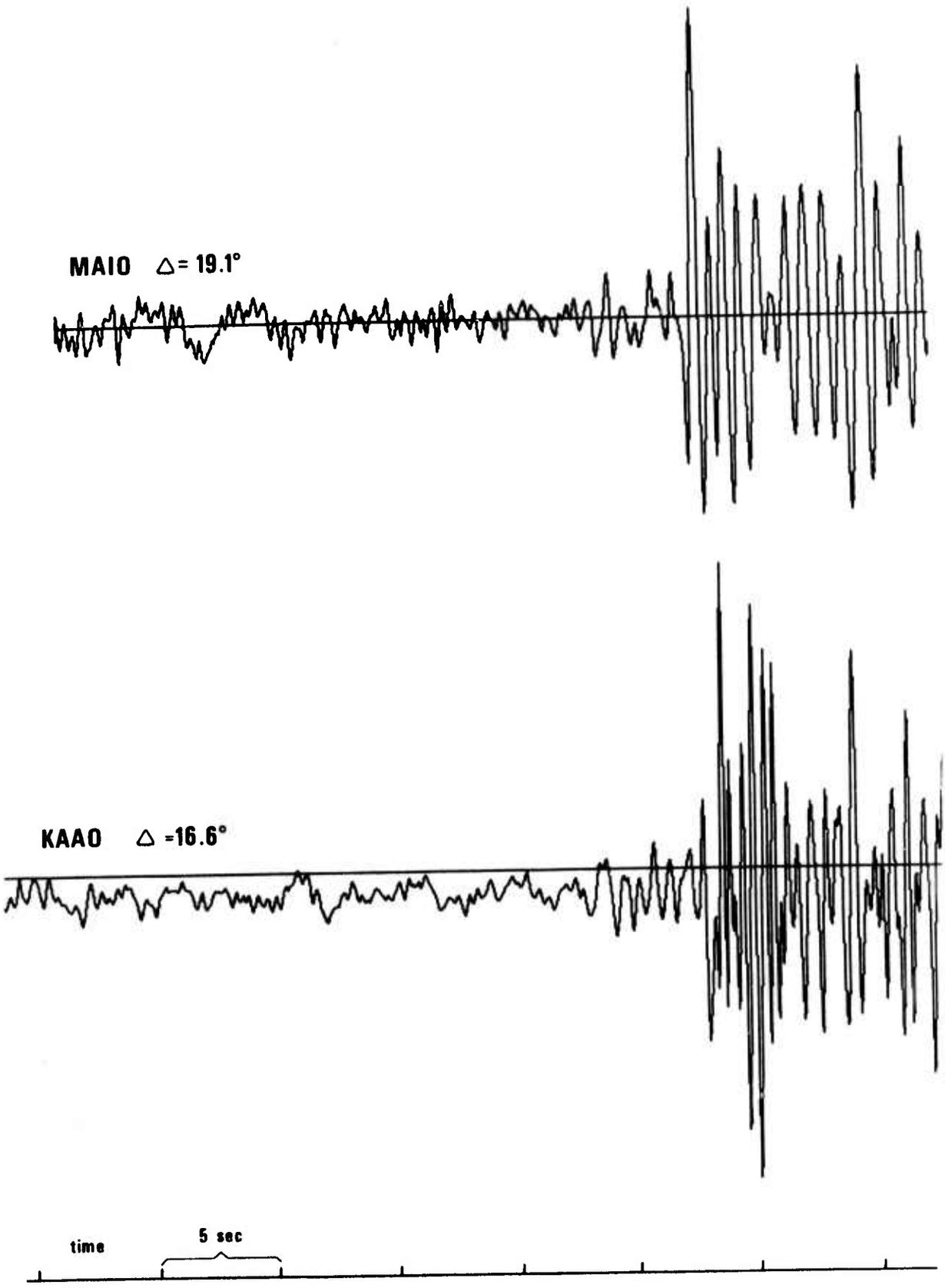

Figure 8. P-wave records at MAIO and KAAO from event 14.

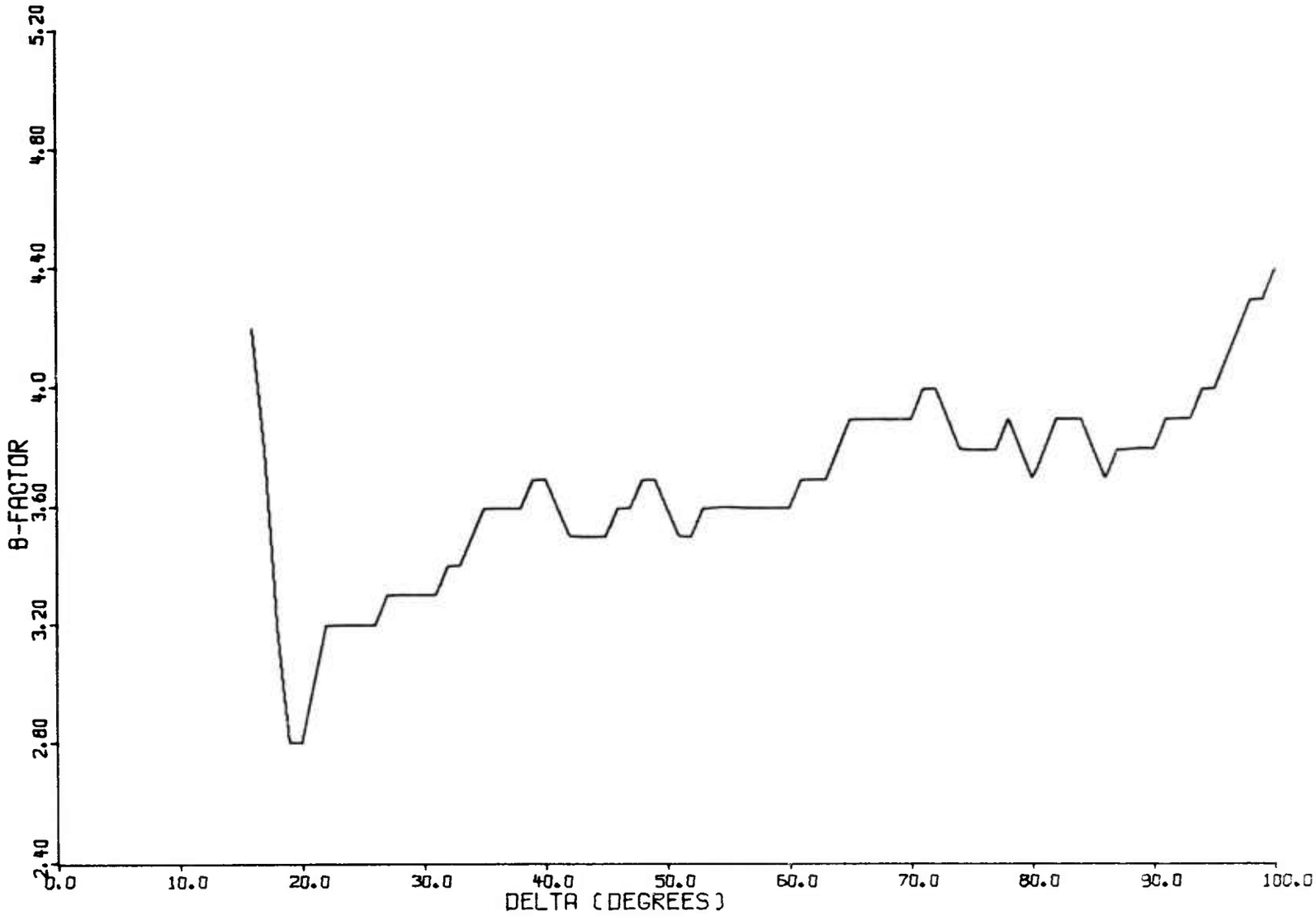

GUTENBERG-RICHTER B-FACTORS FOR LONG-PERIOD S

Figure 9. Calculation of Long-period S-wave magnitudes.

$$\text{Magnitude} = \log_{10} (\text{amplitude}) + \frac{1}{2} \log_{10} \frac{\tan i_o}{\sin \Delta} \frac{d\, i_o}{d\, \Delta} \qquad (27)$$

where the second term on the right-hand side is a correction for the geometrical spreading of the wavefront of the ray which traverses the source-to-receiver angular separation Δ and then emerges at angle i_o with respect to the vertical (Ben-Menahem et al, 1965). Implicit in this formula is the assumption that the source is at zero depth, and hence no distinction is made between angle of incidence at the source and angle of emergence at the receiver. The emergence angle may be computed in terms of a fourth-order polynomial in Δ, as is shown in Table XI. The results of this polynomial computation are illustrated herein as Figure 10. The term $\frac{di_o}{d\Delta}$ which occurs in equation (27) may be obtained simply by taking the slope of the curve in Figure 10, and the results of this procedure are shown in Figure 11. The geometrical spreading correction may then be computed, and it is shown in Figure 12. A comparison of Figures 7 and 12 shows that the shape of the $B(\Delta)$ curve is determined primarily by geometrical spreading, as was asserted previously. The curves in these two figures differ significantly from each other (apart from an irrelevant additive constant) only at distances of less than 20° or greater than 95°. In these same distance ranges the geometrical spreading correction must be regarded as being poorly determined, and it was decided that for this report equation (27) would be approximated by:

$$\text{Magnitude} = \log_{10} (\text{amplitude}) + B(\Delta) \qquad (28)$$

The use of equation (28) might seem to lead to large errors for measurements of Ω_o made at near-regional distances, but in fact no theoretical fit was made to most of the spectra which were observed at such small distances. The reason that the theoretical source spectra could not be computed is that, as has already been noted, the P-wave signals which traversed such short and mostly crustal paths were characterized by quite large amplitudes at high frequencies.

Ben-Menahem, A., S. W. Smith, and T. L. Teng (1965). A procedure for source studies from spectrums of long-period seismic body waves, Bull. Seism. Soc. Am., 55, 203.

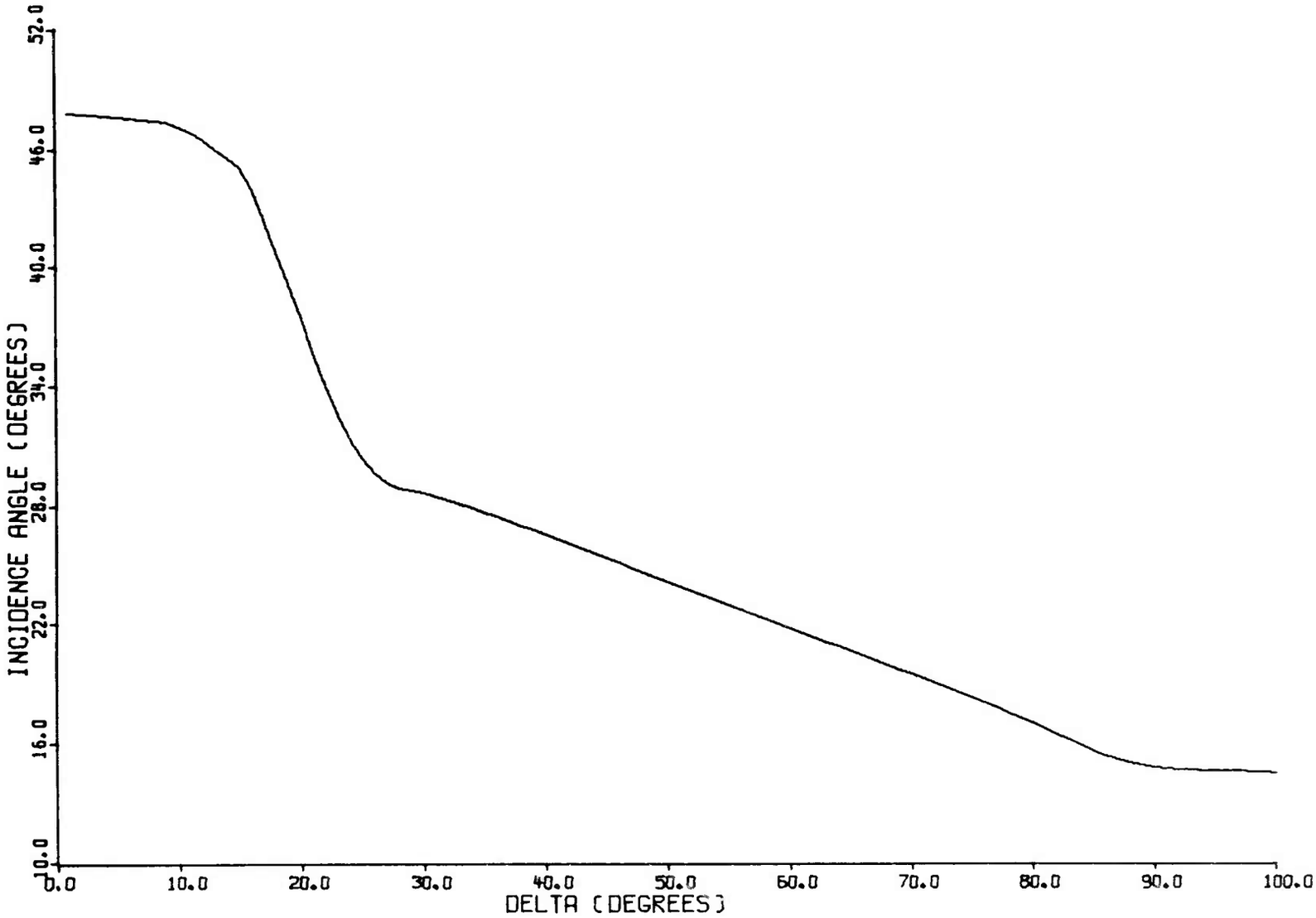

Figure 10. Takeoff angle of a ray as a function of the distance travelled.

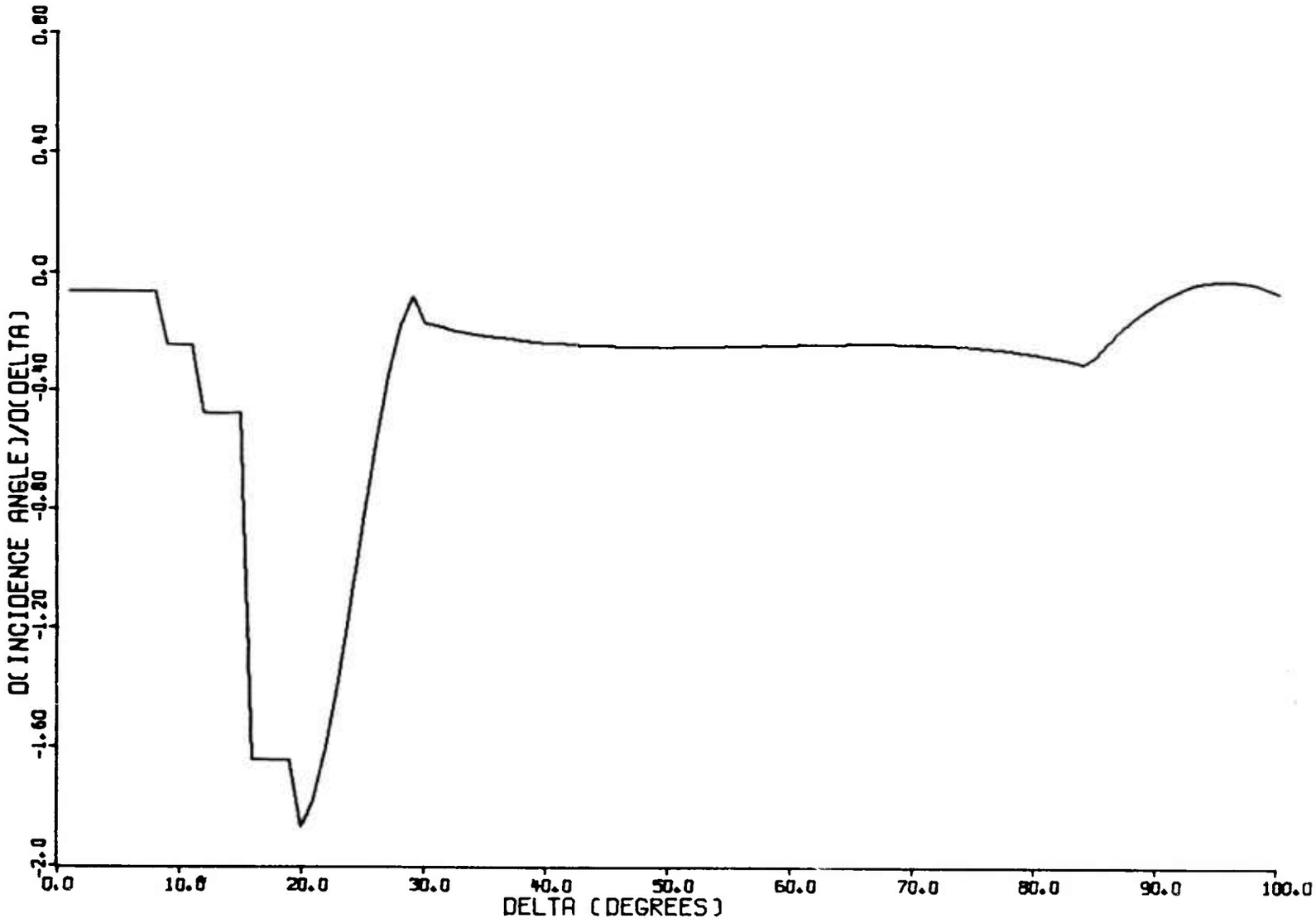

DERIVATIVE OF CURVE OF INCIDENCE ANGLE VERSUS DELTA

Figure 11. First derivative of the curve in Figure 10.

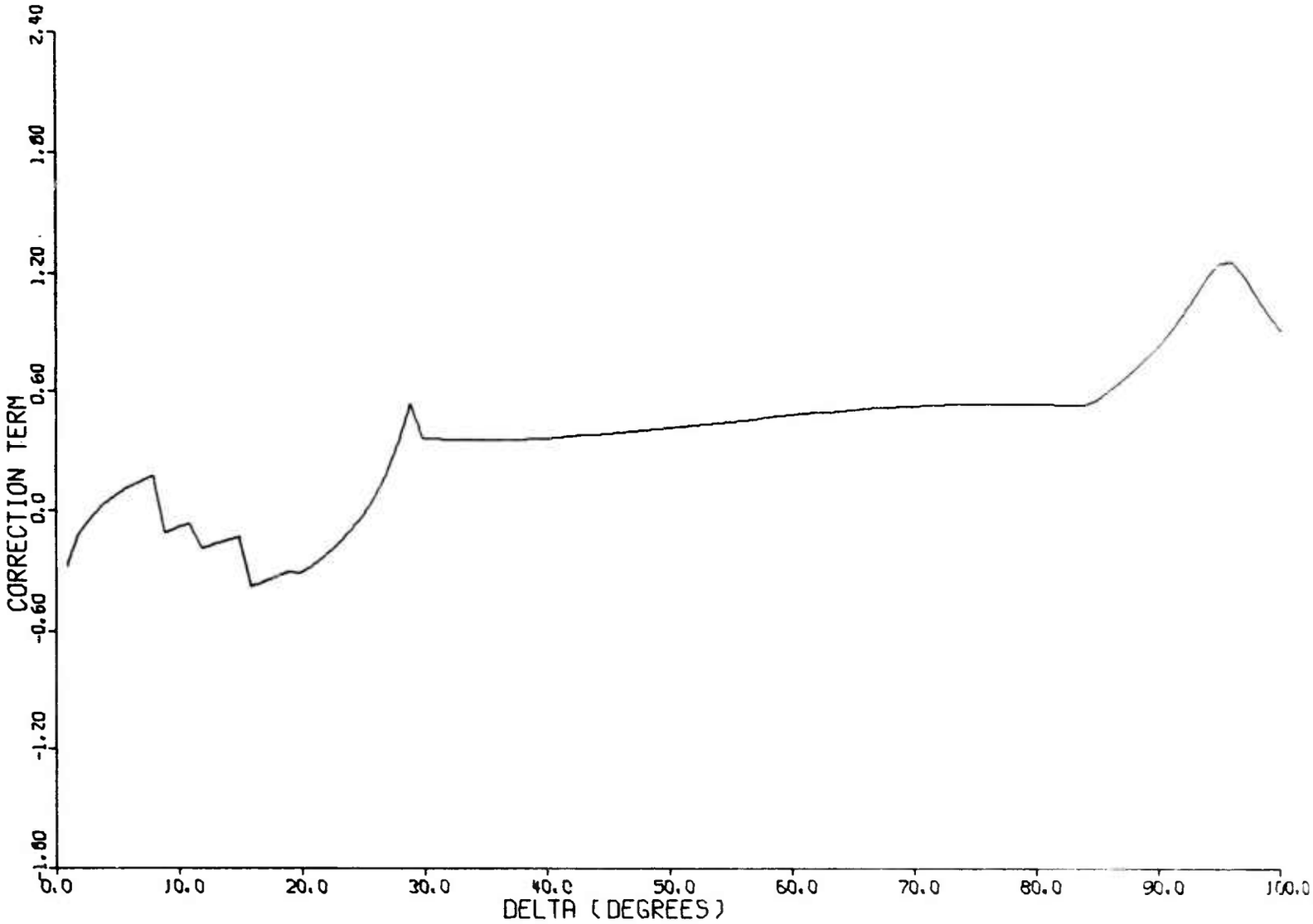

GEOMETRICAL SPREADING CORRECTION TERM ADDED TO LONG-PERIOD LEVEL

Figure 12. Correction to Ω_o for geometrical spreading of the wavefront.

The observed spectra thus appeared nearly flat, and so no suitable corner frequency could be found which yielded a satisfactory source spectrum. Computing the source spectrum was made even more difficult by the imposition of the constraint $t^* \geq 0.1$, so the case of vanishing attenuation could not be treated satisfactorily. As a result, few spectral fits were made at near-regional distances, and the failure of equation 28 to apply at such distances is unimportant. A larger source of error in the magnitude calculation at small distances is the assumption of zero depth for all events. For small distances and even only moderate depths, there is a large difference between the take-off angle i_h and the angle of emergence i_o, so equation (27) fails to describe adequately the geometrical spreading of the wavefront. Even if all the events had occurred at the surface, the correct values of i_o and $\frac{di_o}{d\Delta}$ which should be used for any particular given event are rather uncertain due to local variations in the earth structure and hence in the raypath. A further complication in the determination of $\frac{di_o}{d\Delta}$ for small Δ is the existence of triplications in the travel-time curve which, as was shown in Figure 8, leads to narrowly separated arrivals of rays having different paths and hence different amplitudes (the lesser of which may not be seen at some stations). It was on account of this uncertainty that the approximation given by equation (28) was used in place of equation (27). In theory, a different geometrical spreading correction could be determined for every given source region-to-station path, using values of i_o and $\frac{di_o}{d\Delta}$ (calculated from travel-time residuals) which take into account the effects of local structure. In practice, it might lead to less error in determining Ω_o simply to use only those stations for which $\Delta > 30°$, although for several events only spectra measured at shorter distances are sufficiently noise-free to permit the calculation of the theoretical fit.

"Magnitudes" were created for the corner frequencies by taking the logarithm, since the earthquake-explosion discriminant (to be illustrated later) has the form log (Ω_o) versus log (f_c). The values of the attenuation coefficient t^*, having been used to calculate the P-wave spectral fits, are not to be used further, so no processing is performed upon discrimination parameters numbers 6 and 9.

"Magnitudes" were computed for the complexity variables simply by taking the logarithms of the observed values. During this procedure all complexity

measurements made in certain distance ranges were deleted from the data set. First, no observations were retained for $\Delta<30°$ since in this range the P-wave coda is liable to contain the arrivals of other P phases on account of multipathing. Second, precaution was taken to avoid the inclusion of PcP in the coda by retaining no observations of the short complexity window $comp_1$ for $\Delta>78°$, of $comp_2$ for $\Delta>74°$, and of $comp_3$ for $\Delta>66°$.

It has been mentioned that data records containing only noise and no signal were flagged by means of a minus sign but were otherwise treated as if they had been signals. The data base for each event thus consisted of as many as twenty-seven parameters measured at as many as twenty-seven stations, and eighteen of these parameters could be measurements of either signal or noise. (For noisy P waves, the spectral fit parameters and complexities are set equal to zero). The measurements of noise levels were converted to magnitudes in the same manner as if they had been signals, and they were then assigned a special flag so that they could be distinguished as detection thresholds rather than as actual detections.

For each event, the magnitudes at the individual stations were next combined to give a network estimate of the magnitude for each parameter. For the low-frequency spectral levels, corner frequencies, and complexities this network estimate consisted merely of the arithmetic mean. Network averages of t* are, of course, meaningless, so those two parameters are set equal to zero. For the spectral magnitudes the network estimates were computed using the maximum-likelihood technique of Ringdal (1976). This technique introduces the noise levels into the computation as upper bounds for the magnitudes of undetected signals, thereby eliminating the magnitude bias which would result from the inclusion of only those signals with a large SNR. Because so many observations were of noise rather than of signals, this magnitude bias would have been severe had not the noise measurements been made and the Ringdal method used. There were many cases in which only noise levels and no signals were measured at all the stations for which there were data records. In these cases we have taken Ringdal's formula for the probability of non-detection of an event of a given magnitude by a station with a given noise level and have used it to calculate the likelihood that an event of that magnitude would not have been detected by any of the stations in the network, given the noise

levels. By incrementing the assumed magnitude, we then take as an upper bound for the event magnitude that value for which the likelihood of no detection equals ninety per cent. These upper bounds are flagged as such so that they will be treated separately from the magnitudes which were calculated on the basis of at least one actual detection. In order to carry out this calculation of the upper bounds it is necessary to assume a value of the standard deviation which characterizes random measurements of the magnitude of the parameter in question. We have assumed in all cases a value of 0.40, since this value is typical of time-domain magnitude standard deviations and is at least consistent with the values found for the frequency-domain magnitude in those cases which included detections.

An event-by-event listing of the network estimates of the magnitudes for each parameter is reproduced as Appendix I. It should be noted that the maximum-likelihood estimates were calculated subject to the constraint that the standard deviation of the most likely Gaussian distribution be in the range

$$0.15 \leq \sigma_{lik} \leq 0.63 \tag{29}$$

The number of signal and noise observations used to deduce these values are shown in Appendix II.

DISCRIMINATION VARIABLES

After the deletion of the attenuation coefficients, parameters numbers 6 and 9, there remain twenty-five parameters for which the network-averaged magnitudes for each event are to be used for discrimination. Discrimination which is based upon these magnitudes as raw data, however, can suffer from a magnitude bias and can therefore yield misleading results. One source of this bias is the failure of certain parameters such as M_s to scale with m_b equally for both the earthquake and the explosion populations. Another source of bias is the difference in the magnitude distributions for the two populations, a difference which is illustrated in Figure 13. The criteria for assignation of the events to one or the other of the two populations will be explained subsequently. Asymmetry between the two distributions can lead to spurious "discriminants". As a hypothetical example, consider classical $M_s - m_b$ discrimination as carried out upon a set of events consisting of small explosions and large earthquakes (Figure 14). Depending upon the exact shape of the distribution of the events in the $M_s - m_b$ plane, a straightforward statistical analysis might determine that the two populations of events were best separated by a discriminant line having a nearly horizontal slope. The criterion upon which future events would be classified is that events with large M_s are always earthquakes and events with small M_s are always explosions. Although this hypothetical example is an extreme one, it points out that a magnitude bias can be built into a discriminant function if raw data are used.

The remedy for this bias is to perform discrimination based not on the individual variables M_s and m_b but rather on the single variable $(M_s - m_b)$. In this manner one implicitly imposes the constraint that the M_s versus m_b discriminant line has unit slope. If this line has some (unknown) intercept c on the M_s - axis, all events for which $M_s - m_b > c$ lie above the line $M_s = m_b + c$, and hence they are earthquakes. Similarly, those events for which $M_s - m_b < c$ are explosions. The statistical analysis then consists of finding the M_s - intercept c rather than both the intercept and the slope. Of course one may specify <u>a priori</u> the intercept also (as in the case of the classical relation $M_s = m_b + 1.5$), in which case the variable $(M_s - m_b)$ may be used as a discriminant without reference to any statistical analysis of a given population of earthquakes and explosions.

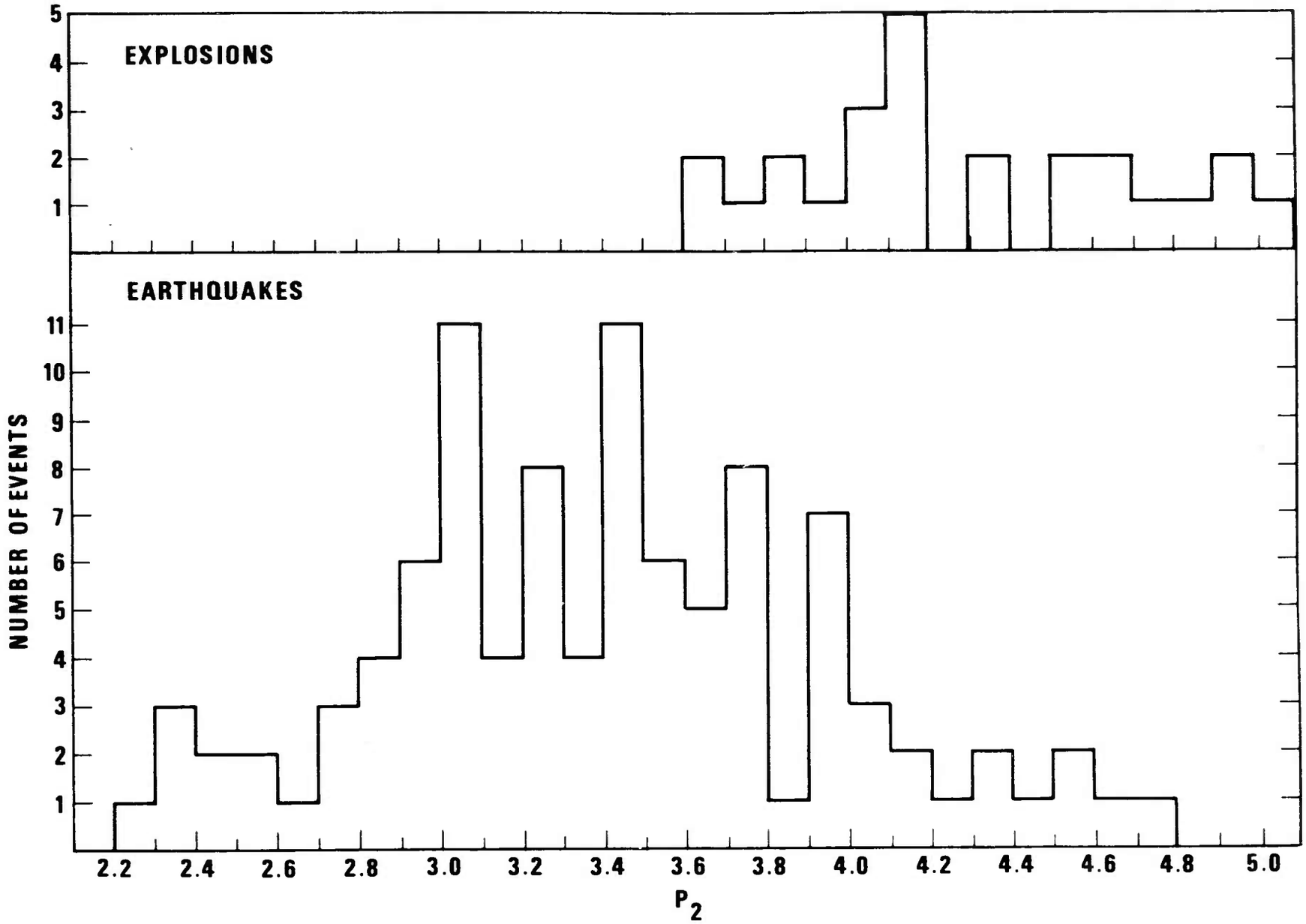

Figure 13. Distribution of middle-frequency P-wave magnitudes P_2 for explosions and earthquakes.

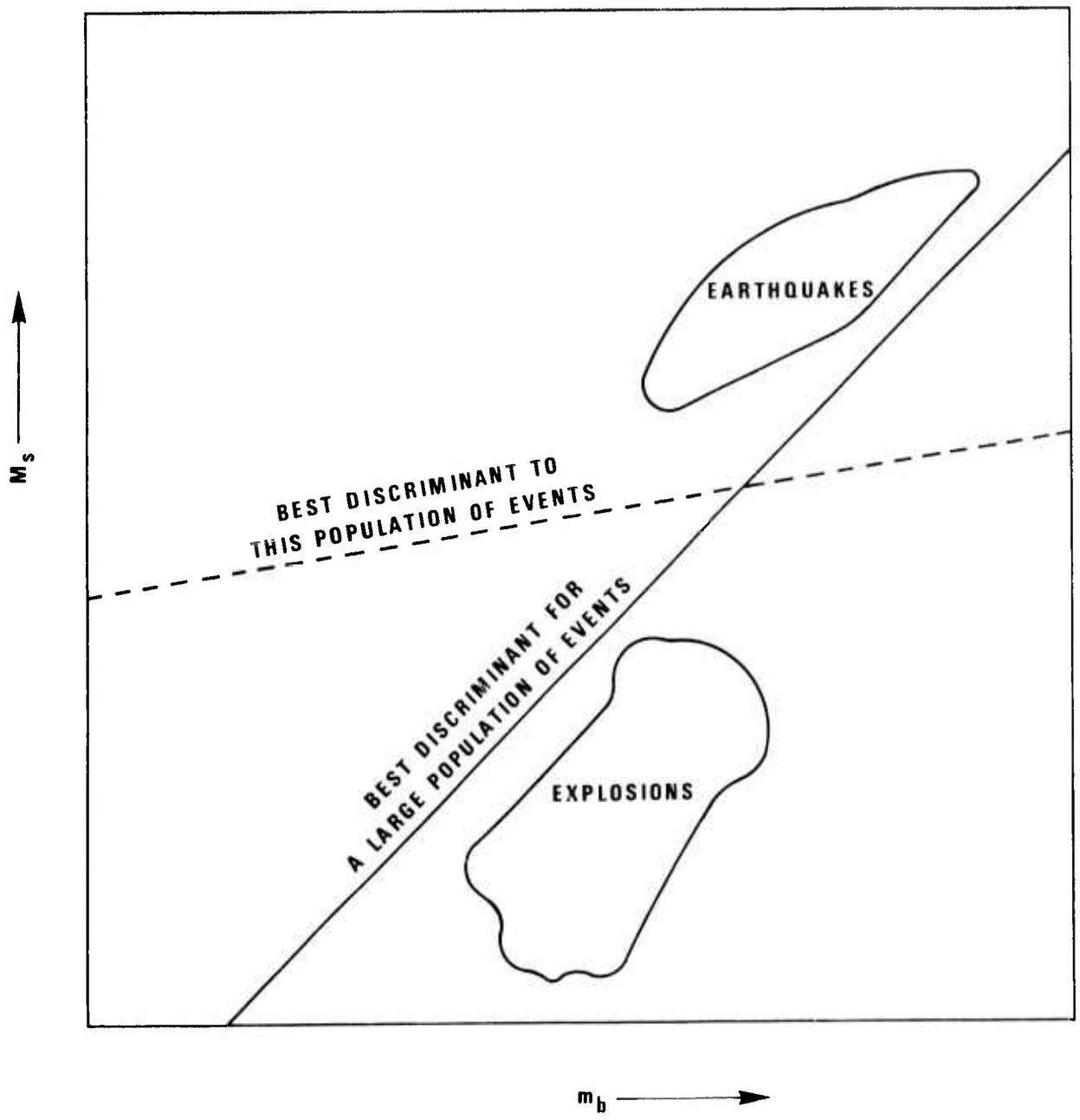

Figure 14. Hypothetical discrimination exhibiting magnitude bias.

Even with a large body of data encompassing a wide range of magnitudes for both earthquakes and explosions, an unrestricted analysis of raw data might be expected to exhibit a magnitude bias. Such a bias would tend to occur at least for the pair of variables M_s and m_b since M_s for large earthquakes tends to lie above the discriminant line by a larger amount than M_s for large explosions tends to lie below it. An analysis of the raw data might thus attempt to classify events (particularly if M_s was frequently not detected for small events) on the basis of a discriminant line of slope greater than unity. We therefore believe that the constraint of unit slope should be imposed upon the M_s versus m_b discriminant by analyzing data in terms of the single variable $(M_s - m_b)$.

We have extended the analogy of visual $(M_s - m_b)$ to our data base by "normalizing" all spectral magnitudes to those of the high-frequency P-wave magnitudes P_3 by subtracting from all magnitudes the quantity $\alpha \cdot P_3$, where α is a coefficient which is to be determined. The short-and long-period P-wave magnitudes P_2, P_3, LP_1, LP_2 and LP_3 are thereby converted from magnitudes to spectral ratios. The worth of these spectral ratios to the problem of discrimination lies in the relative enhancement of high frequencies for explosions. For the high-frequency band P_3 this enhancement is due to the higher corner frequencies of explosions than of earthquakes and to the (admittedly arguable) slower high-frequency decay rate of explosions than that of earthquakes, f^{-2} versus f^{-3}. With signals originating in so many diverse tectonic regions, however, these differences may be overwhelmed by differences in t*. The lower frequency bands are expected to contain less energy, relative to that in P_3, for explosions than for (deeper) earthquakes on account of cancellation of the signal by pP. Subtracting $\alpha \cdot P_3$ from the S, LR, and LQ magnitudes converts them to measures of the relative shear wave-to-compressional wave excitation ratio for the event. This quantity is expected to be higher for earthquakes than for explosions, but we note that this will be affected strongly by the focal mechanism and depth of the earthquakes.

In order to maintain a strict analogy with classical $M_s - m_b$ differences, all magnitudes should have been normalized to the middle-frequency P-wave magnitude P_2 rather than to P_3, since visual m_b measurements are usually made of signals of about 1 sec period. The higher frequency band was chosen instead

in order to utilize the largest possible frequency contrast between the short-period and the long-period data. As a result of this choice, the spectral analog of the M_s versus m_b discriminant will have a slope which is steeper than the unit slope which has thus far been assumed. Normalization of all magnitudes to P_3 generates two short-period discrimination variables, namely the P-wave spectral ratios of P_1 to P_3 and of P_2 to P_3. In order to more fully characterize the shape of the P-wave spectrum, which is assumed to be a valuable discriminant, an additional spectral ratio was used, namely that of P_1 to P_2. That the three short-period discrimination variables are not redundant can be seen by considering the expressions for the spectral ratios:

$$\begin{aligned} V_1 &= P_1 - \alpha_{13} P_3 \\ V_2 &= P_2 - \alpha_{23} P_3 \\ V_3 &= P_1 - \alpha_{12} P_2 \end{aligned} \tag{30}$$

It can easily be shown that the three discrimination variables V_1, V_2 and V_3 are linearly independent if $\alpha_{13} \neq \alpha_{12} \cdot \alpha_{23}$.

In order to determine suitable values of the coefficients α, we have plotted in Figure 15 P_1 as a function of P_2 for both the earthquake and explosion populations. Those events which were classified a priori on the basis of their epicenters and/or origin times as being explosions were:

Semipalatinsk Area - 14, 17, 20, 79, 81, 189, 266, 267, 268, 276, 277, 278

Novaya Zemlya - 19, 33

West Kazakh (Volga River/Caspian Sea) - 22,274

Siberia and Lake Baikal - 1, 16, 18, 21, 269, 270, 273

In addition, three other events were identified by epicenter and origin time data as being explosions, but inspection of their P-wave signals revealed them to be multiple events. These presumed shot arrays are events 53, 265, and 271, and they are denoted by a special symbol in Figure 15. All other events were classified a priori as earthquakes. It has already been noted that events occurring in different regions can appear dissimilar on account of propagation path effects even if their source mechanisms are identical. There thus exists the possibility that the P_1 versus P_2 "discriminant" illustrated in Figure 15 does not so much separate earthquakes from explosions as it

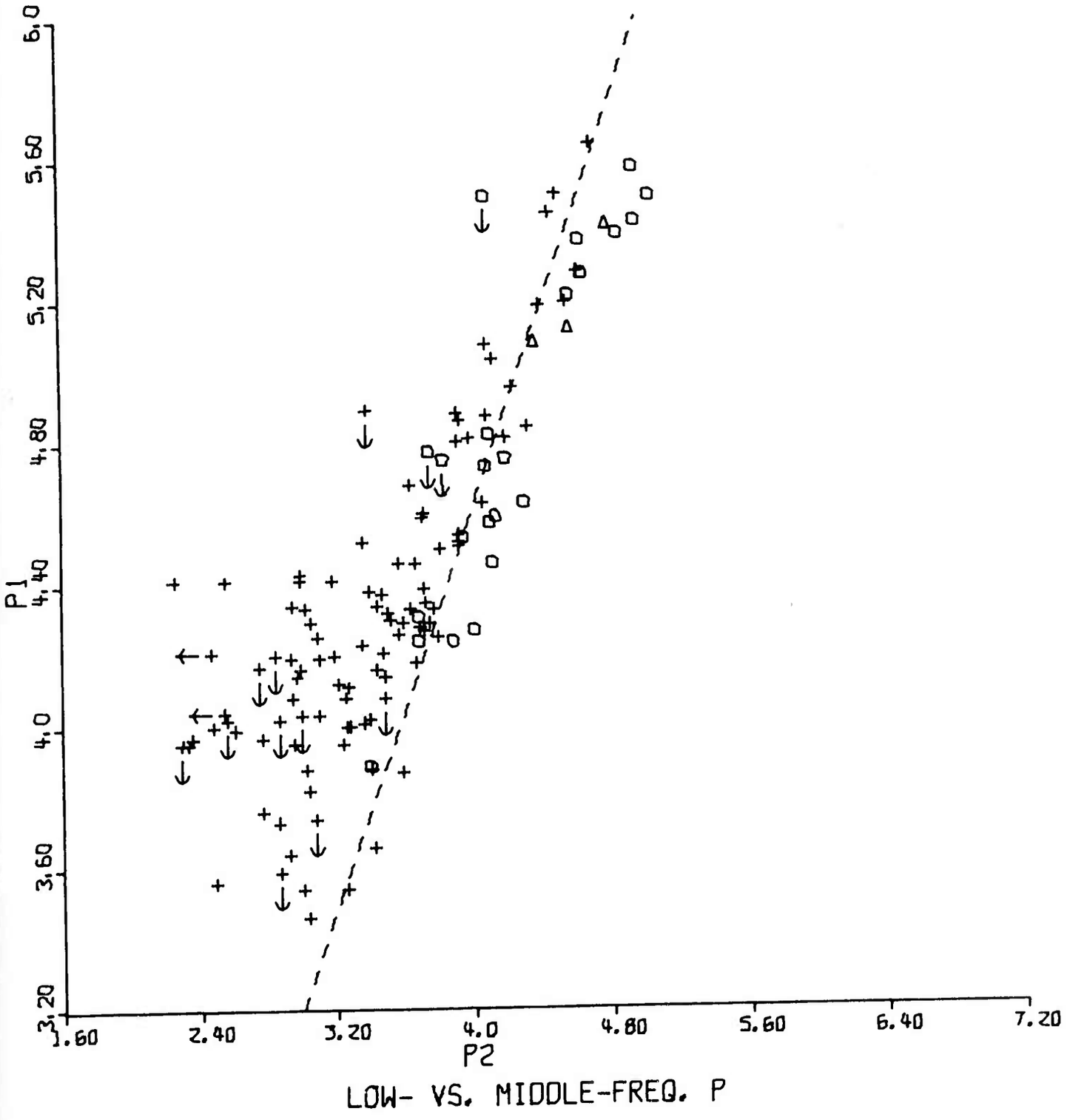

Figure 15. Low-frequency P-wave magnitude P_1 of presumed earthquakes and explosions as a function of the middle-frequency P-wave magnitude P_2. Earthquakes are denoted by crosses, single explosions by circles, and multiple explosions by triangles.

separates events in "explosion regions" (defined above) from events in all other regions listed in Table II. This possibility will be investigated further in a later section of this report. The same separation of events into earthquake and explosion populations was used in Figure 16 to determine the coefficients α which were to be used to calculate discrimination variables based on the normalization to P_3 of the other fourteen spectral magnitudes.

Many data points in Figures 15 and 16 have arrows attached to them pointing either down or to the left; such points are the previously mentioned 90% confidence limit upper bounds to the true magnitudes, calculated from measurements of only noise and not signal. The true magnitude of each point is assumed to lie in the direction of the arrow. Not appearing in the figures are those points for which the values of both the abscissa and ordinate magnitude variables were approximated by upper bounds, since these points cannot contribute any useful information to the discrimination between the two populations of events. The dashed lines in Figures 15 and 16 were visually fit to be either coincident with or parallel to other lines (not shown) which as nearly as possible separate the explosions from the earthquakes. The two populations overlap for every pair of magnitude variables shown in the figures, so in no case was perfect separation possible. The reason that the lines plotted on the figures are in some cases parallel to, rather than coincident with, the "best" discriminant lines is that it is only the slopes of these lines, and not their intercepts, which affect their discrimination capability. That this is so may be seen from equation (30), which may be interpreted geometrically in terms of Figures 15 and 16 as meaning that the value of the discrimination variable for a given point on one of those plots is given by the vertical distance from the given point to the dashed line. If the intercept of the line is changed but not its slope, a constant will be added to the value of the discrimination variable for every point on the plot. This additive constant does not affect the separation between the earthquake and explosion populations, and hence it may be chosen arbitrarily. In Figure 15 and 16 this constant has been chosen in such a manner as to utilize as fully as possible those magnitudes which were approximated by upper bounds. Specifically, the intercepts of the lines were visually adjusted to maximize the number of explosion upper bounds and minimize the number of earthquake upper bounds lying on the "explosion" side of the discriminant line. The reason that such adjustment is advantageous is that all upper bounds

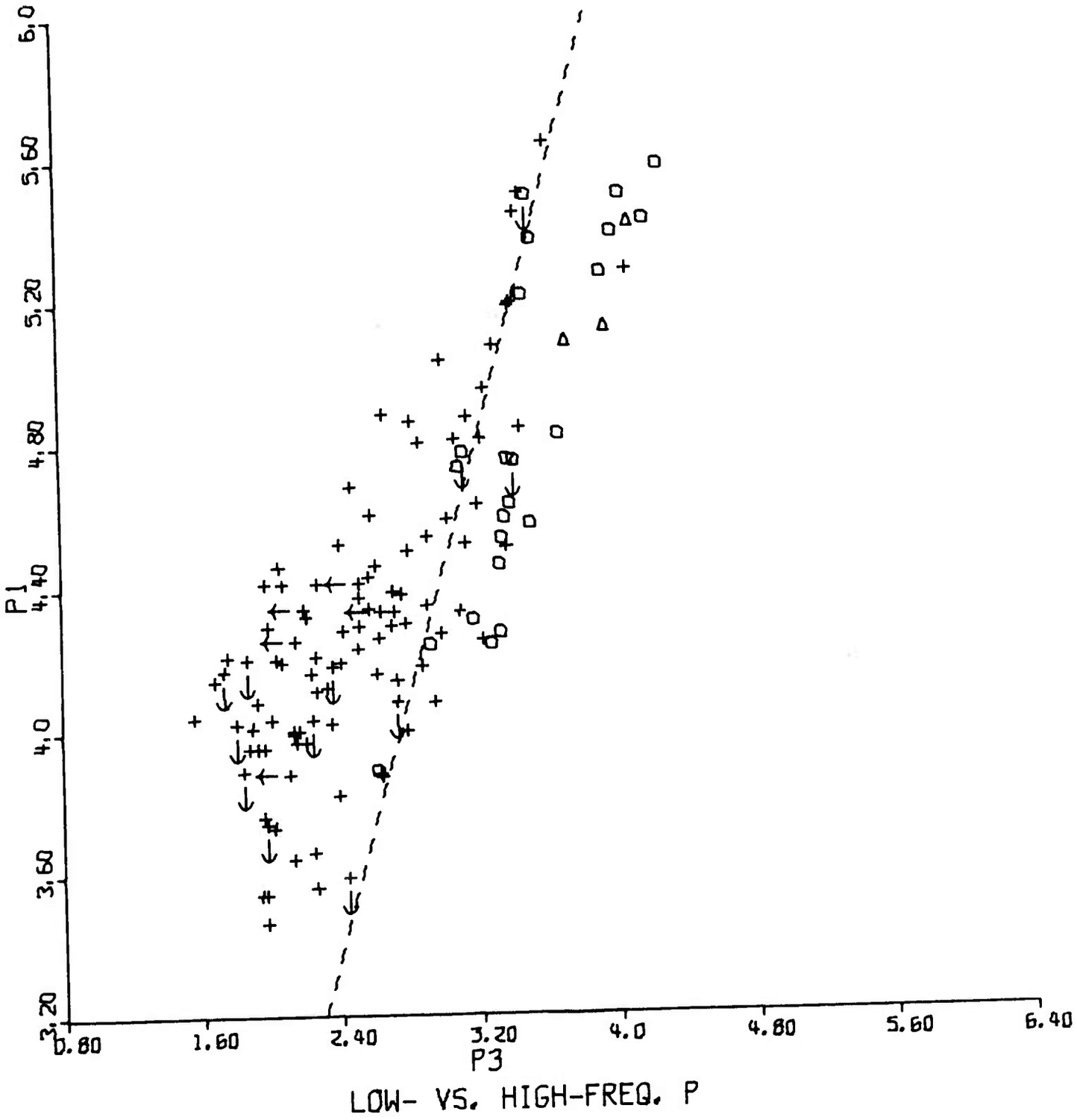

Figure 16a. Low-frequency P-wave magnitude P_1. Spectral magnitudes of presumed earthquakes and explosions as a function of the high-frequency P-wave magnitude P_3. Earthquakes are denoted by crosses, single explosions by circles, and multiple explosions by triangles.

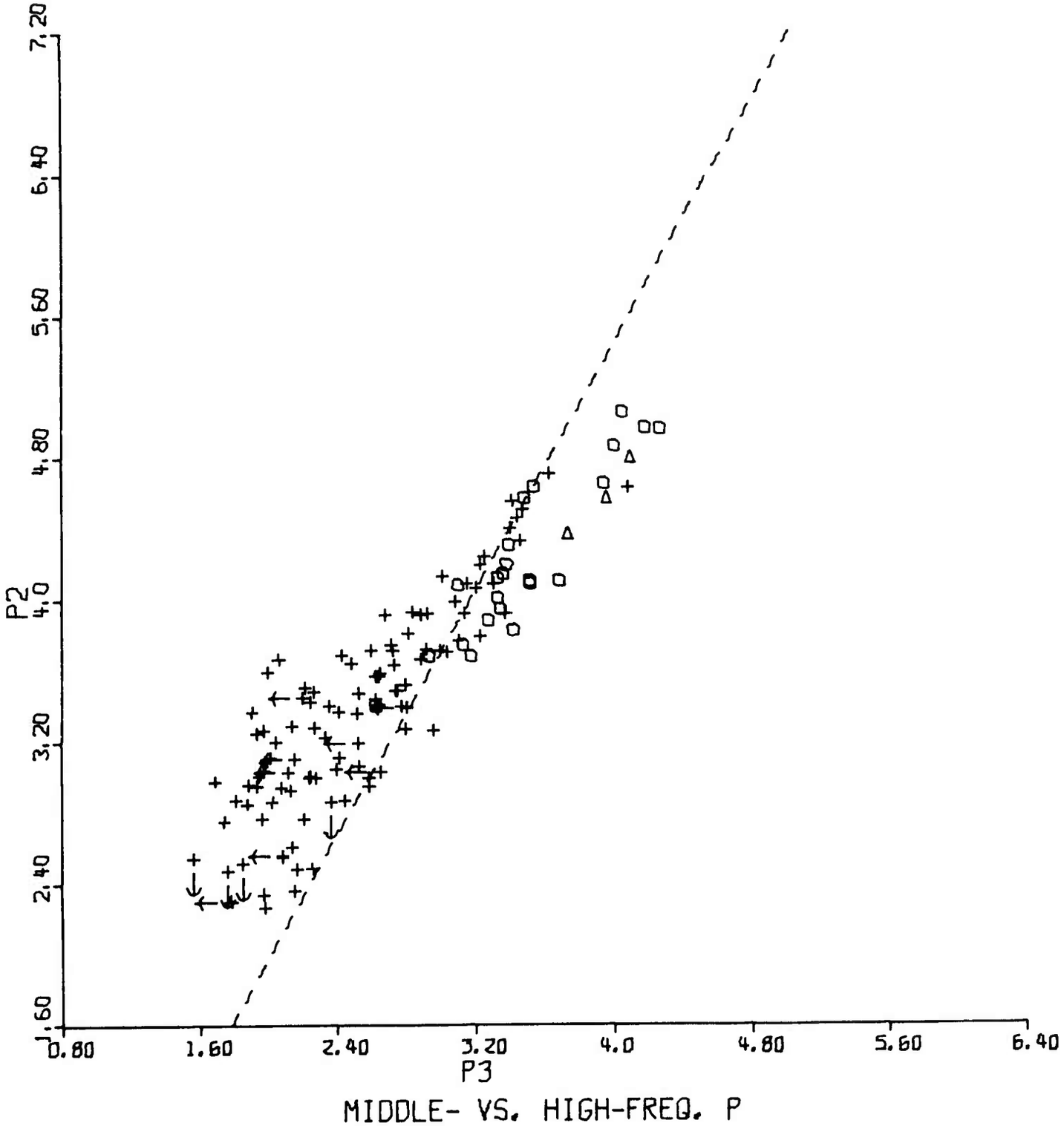

Figure 16b. Middle-frequency P-wave magnitude P_2. Spectral magnitudes of presumed earthquakes and explosions as a function of the high-frequency P-wave magnitude P_3. Earthquakes are denoted by crosses, single explosions by circles, and multiple explosions by triangles.

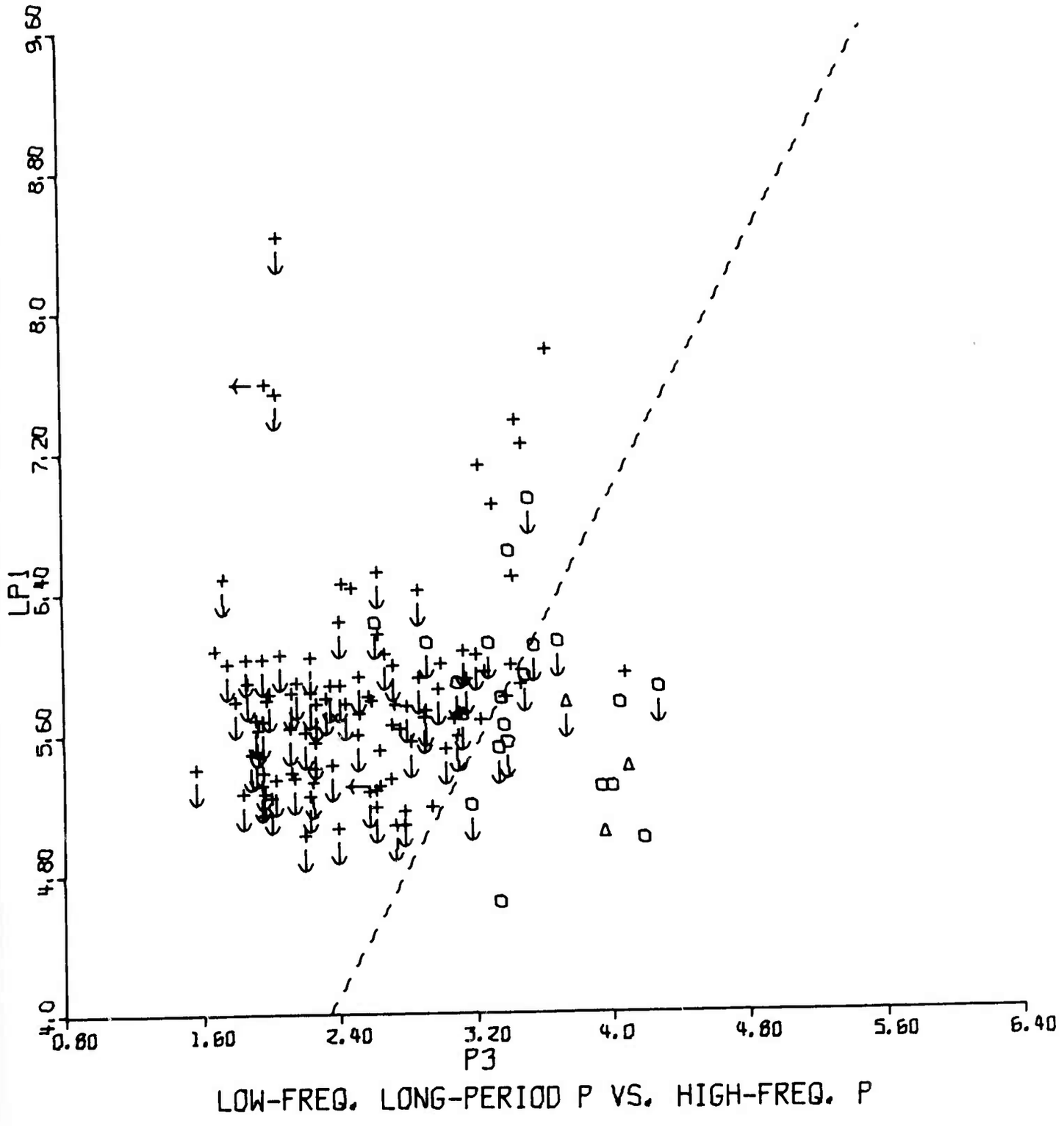

Figure 16c. Low-frequency long-period P-wave magnitude LP_1. Spectral magnitudes of presumed earthquakes and explosions as a function of the high-frequency P-wave magnitude P_3. Earthquakes are denoted by crosses, single explosions by circles, and multiple explosions by triangles.

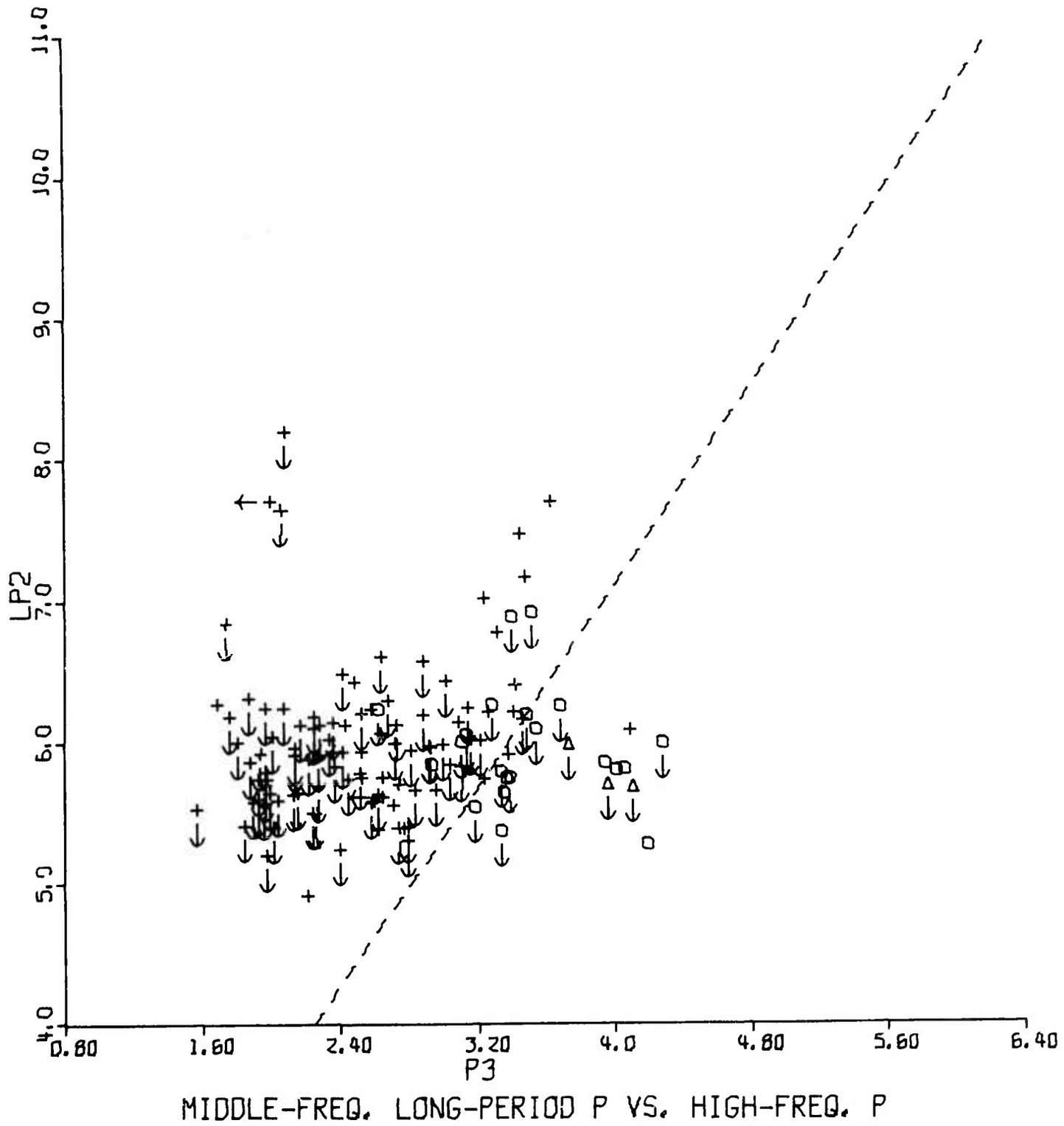

Figure 16d. Middle-frequency long-period P-wave magnitude LP_2. Spectral magnitudes of presumed earthquakes and explosions as a function of the high-frequency P-wave magnitude P_3. Earthquakes are denoted by crosses, single explosions by circles, and multiple explosions by triangles.

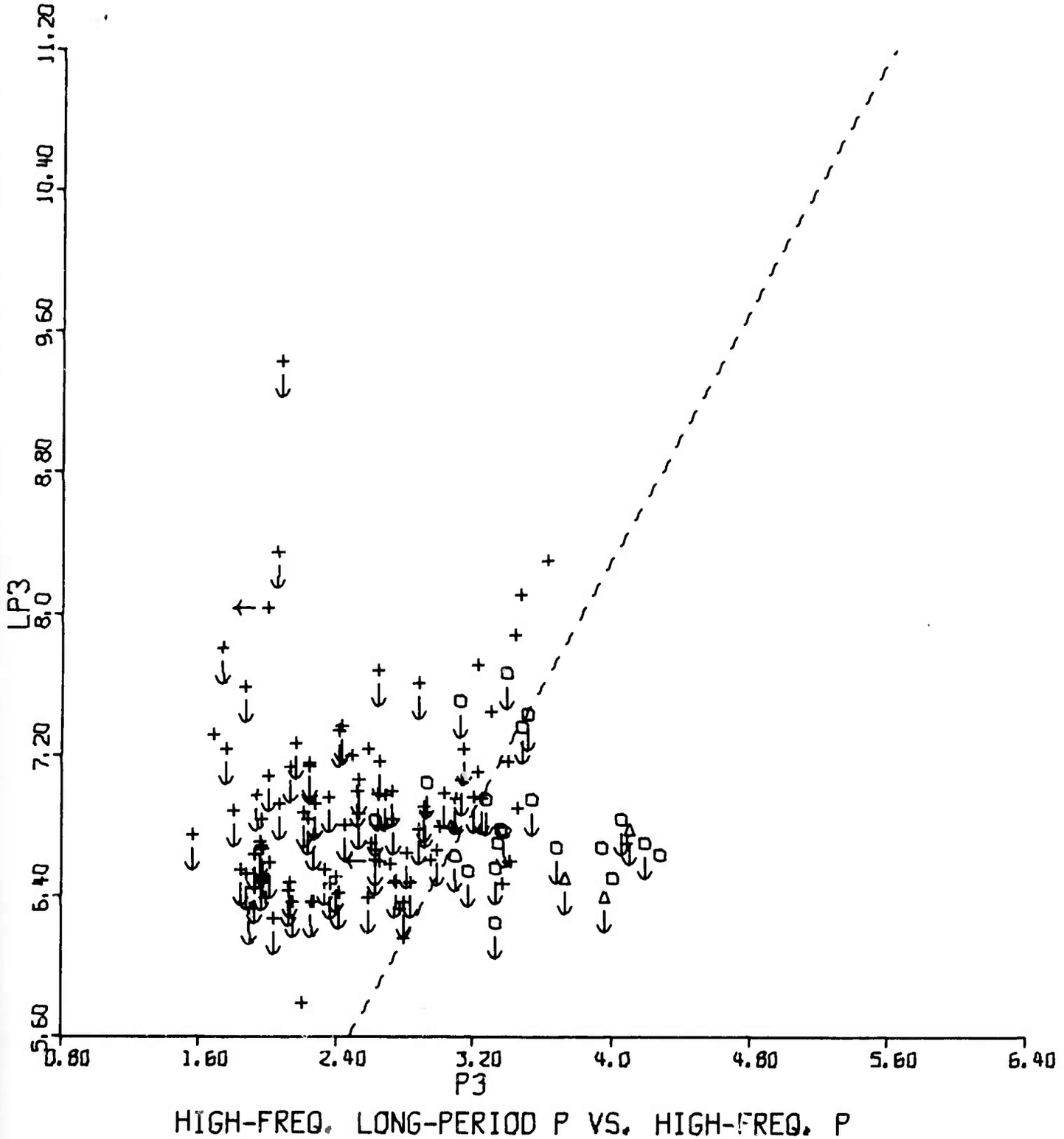

Figure 16e. High-frequency long-period P-wave magnitude LP_3. Spectral magnitudes of presumed earthquakes and explosions as a function of the high-frequency P-wave magnitude P_3. Earthquakes are denoted by crosses, single explosions by circles, and multiple explosions by triangles.

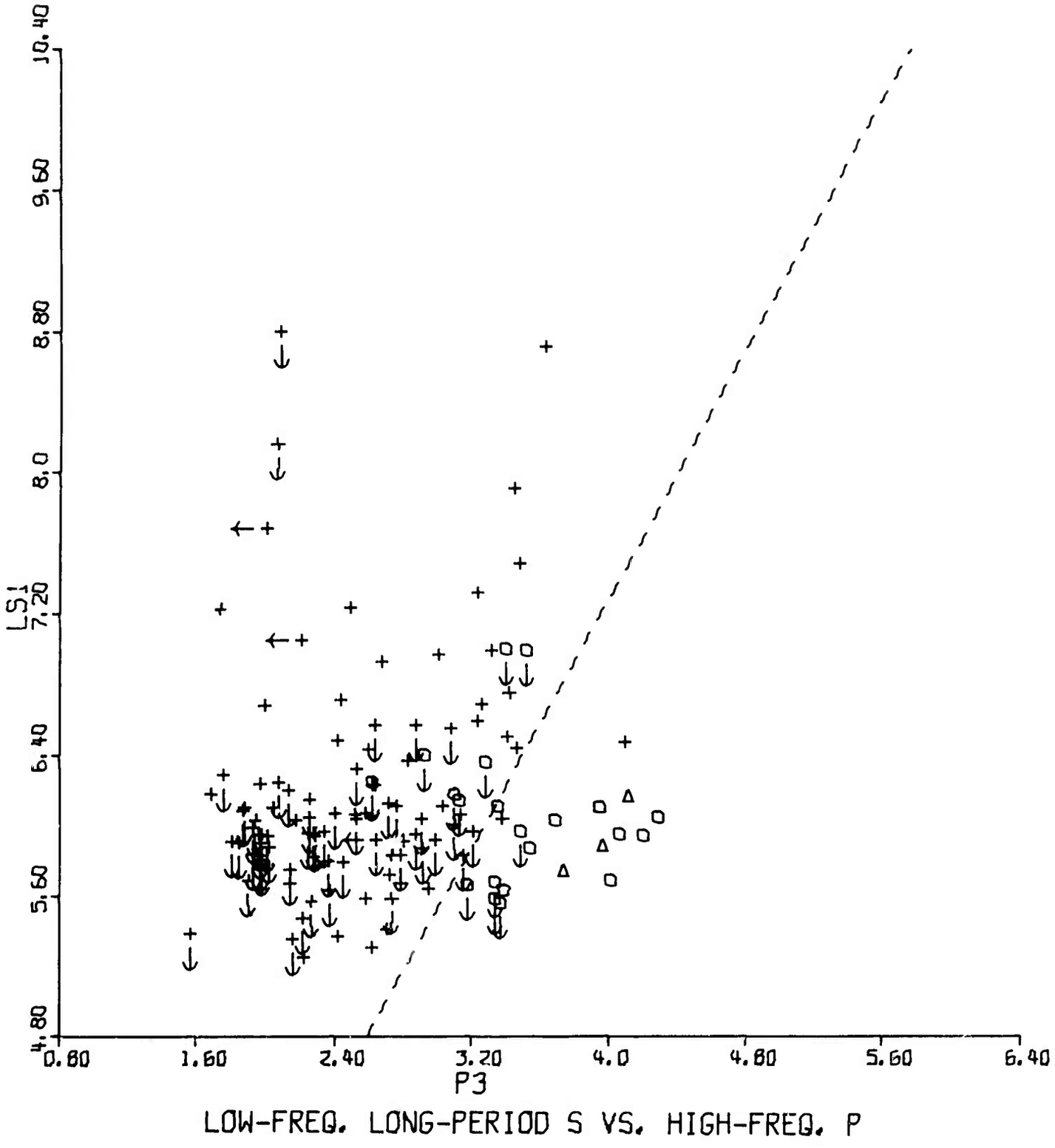

Figure 16f. Low-frequency long-period S-wave magnitude LS_1. Spectral magnitudes of presumed earthquakes and explosions as a function of the high-frequency P-wave magnitude P_3. Earthquakes are denoted by crosses, single explosions by circles, and multiple explosions by triangles.

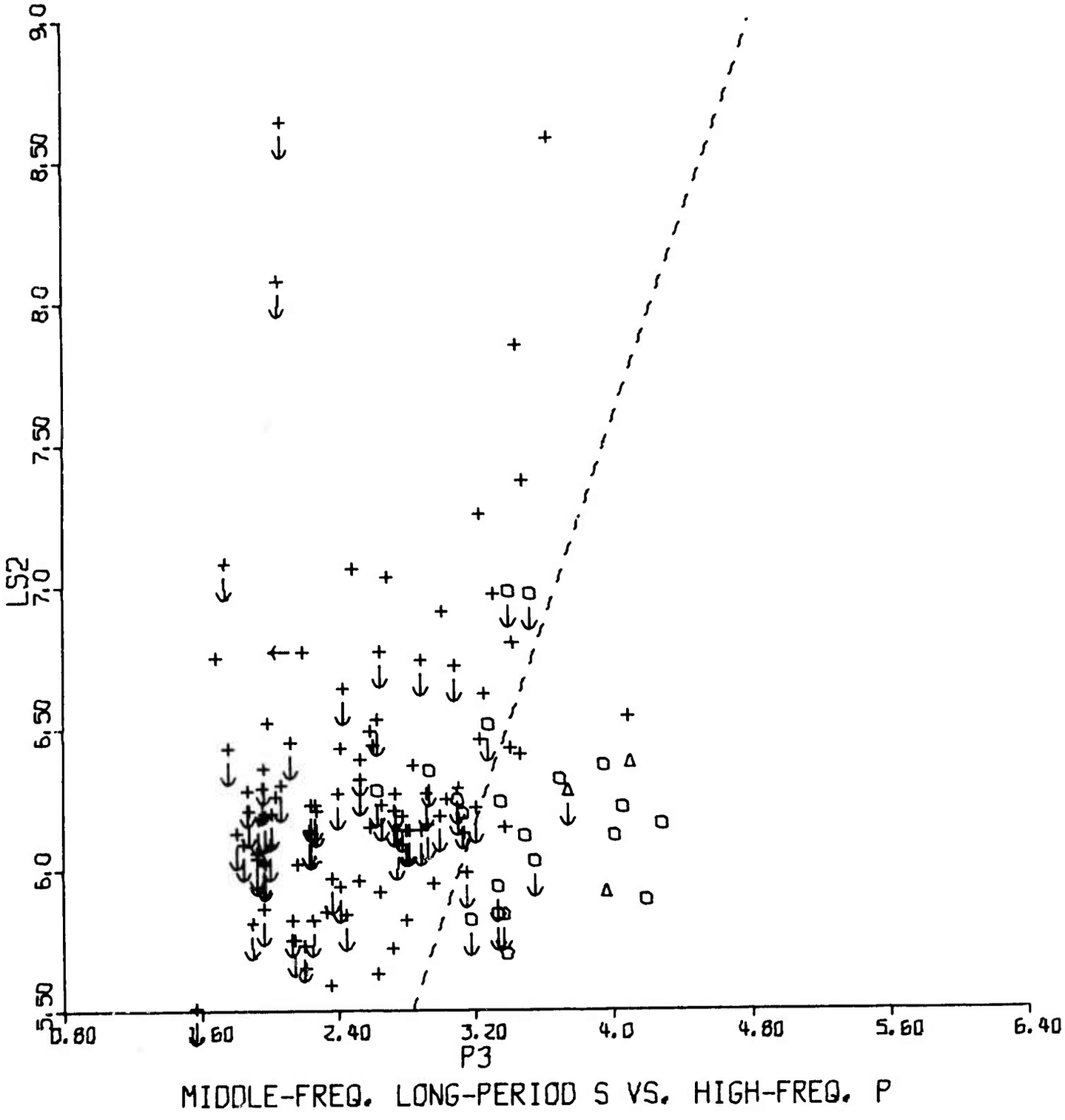

Figure 16g. Middle-frequency long-period S-wave magnitude LS_2. Spectral magnitudes of presumed earthquakes and explosions as a function of the high-frequency P-wave magnitude P_3. Earthquakes are denoted by crosses, single explosions by circles, and multiple explosions by triangles.

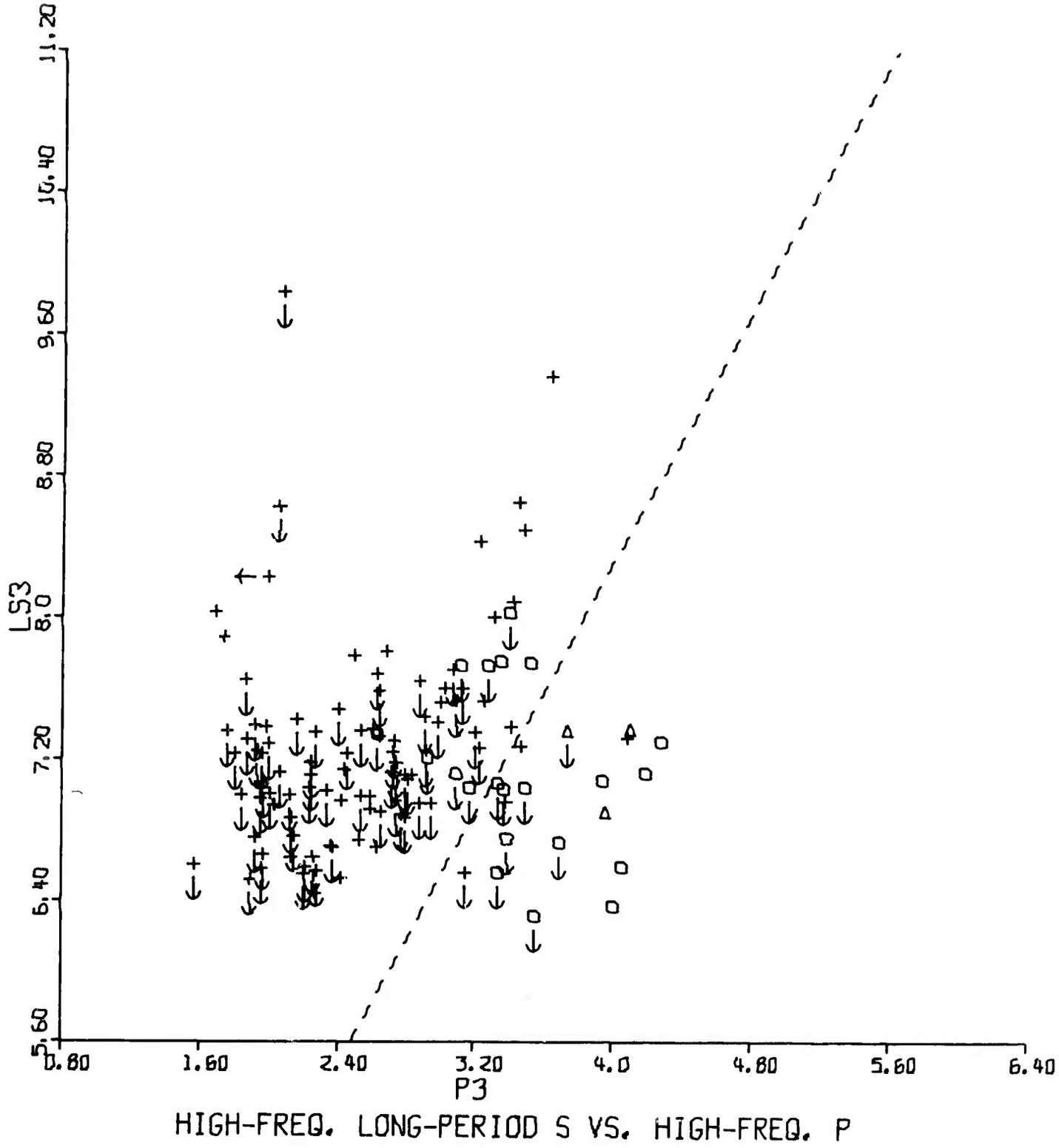

Figure 16h. High-frequency long-period S-wave magnitude LS_3. Spectral magnitudes of presumed earthquakes and explosions as a function of the high-frequency P-wave magnitude P_3. Earthquakes are denoted by crosses, single explosions by circles, and multiple explosions by triangles.

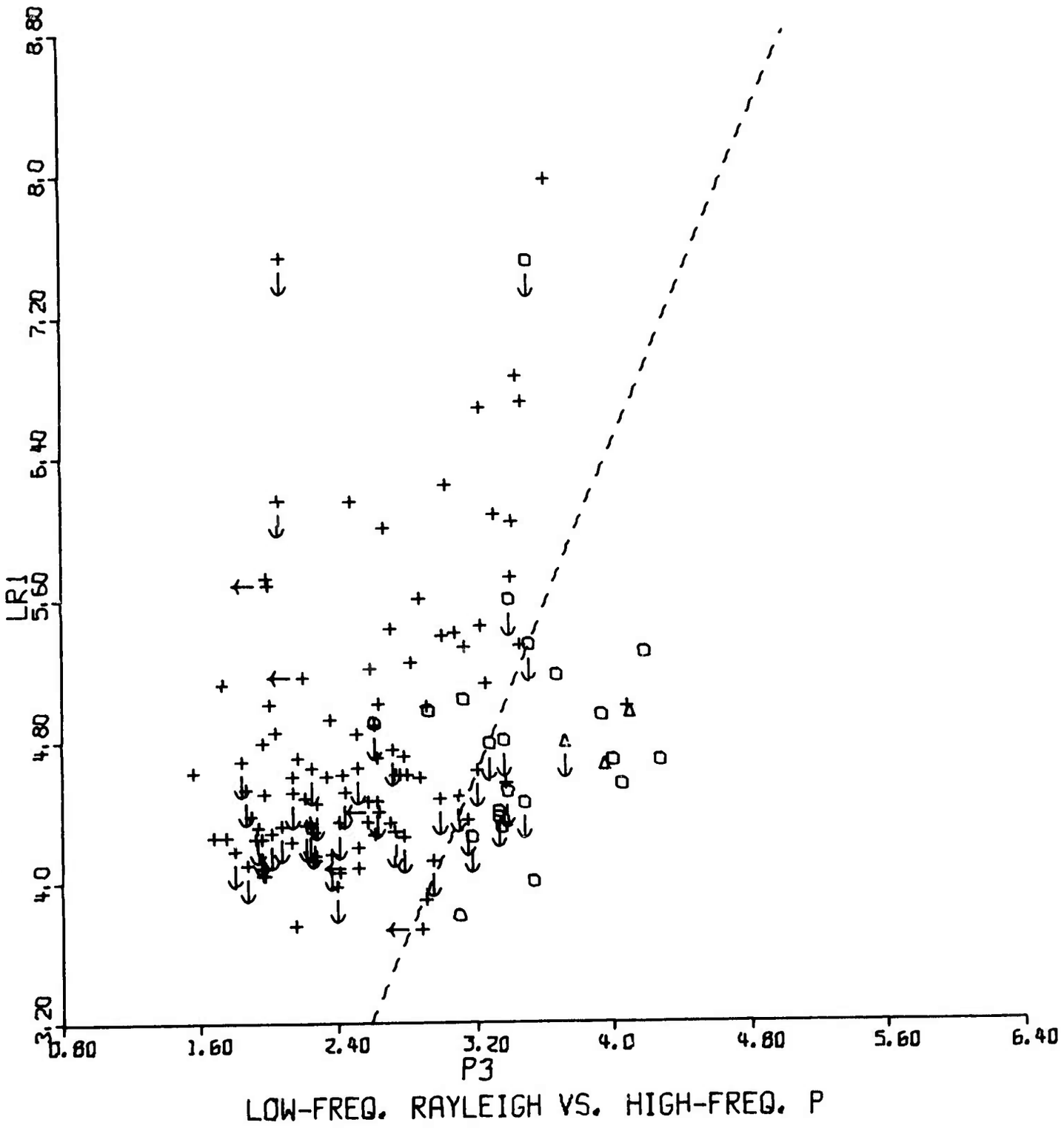

Figure 16i. Low-frequency Rayleigh-wave magnitude LR_1. Spectral magnitudes of presumed earthquakes and explosions as a function of the high-frequency P-wave magnitude P_3. Earthquakes are denoted by crosses, single explosions by circles, and multiple explosions by triangles.

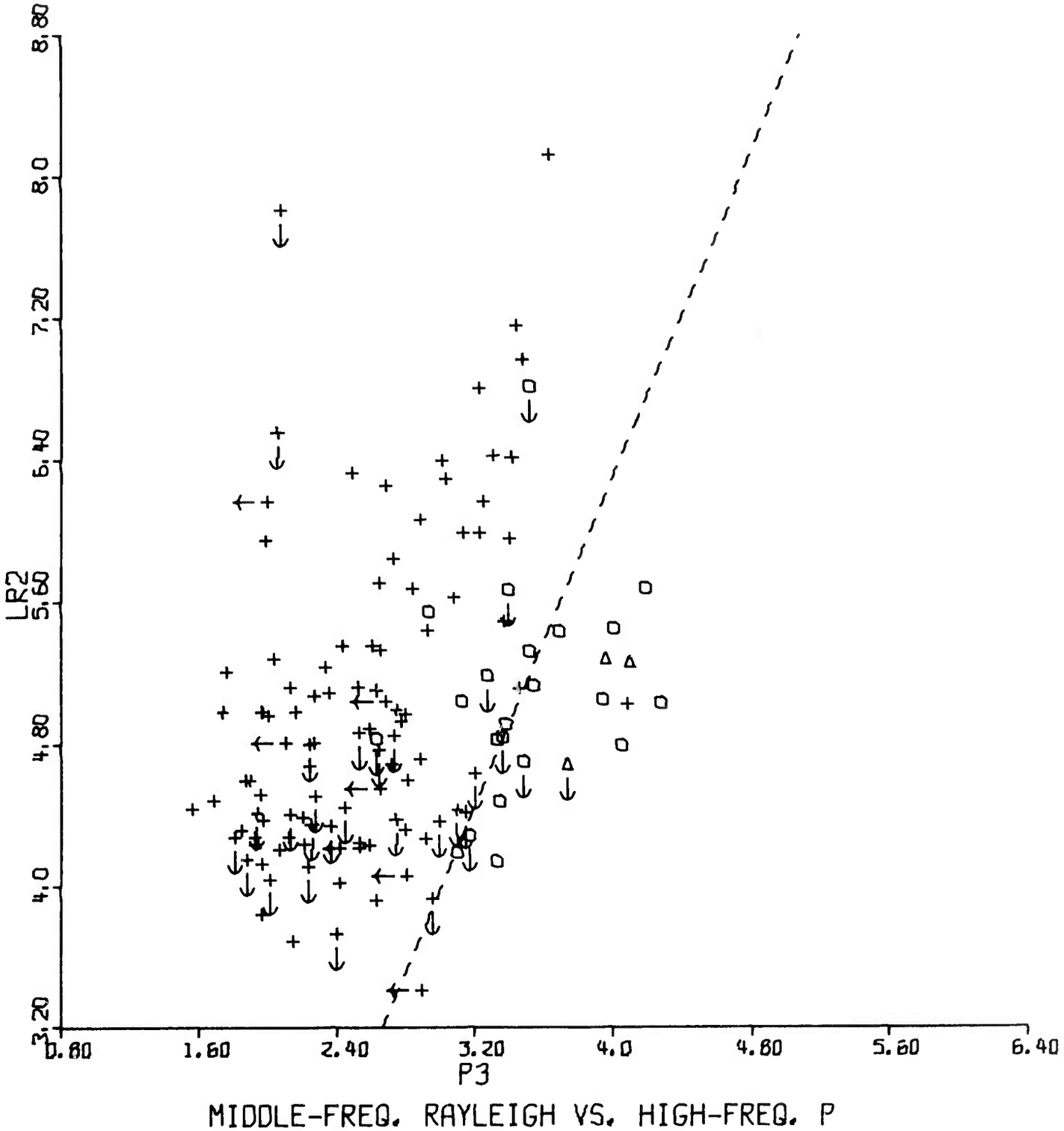

Figure 16j. Middle-frequency Rayleigh-wave magnitude LR_2. Spectral magnitudes of presumed earthquakes and explosions as a function of the high-frequency P-wave magnitude P_3. Earthquakes are denoted by crosses, single explosions by circles, and multiple explosions by triangles.

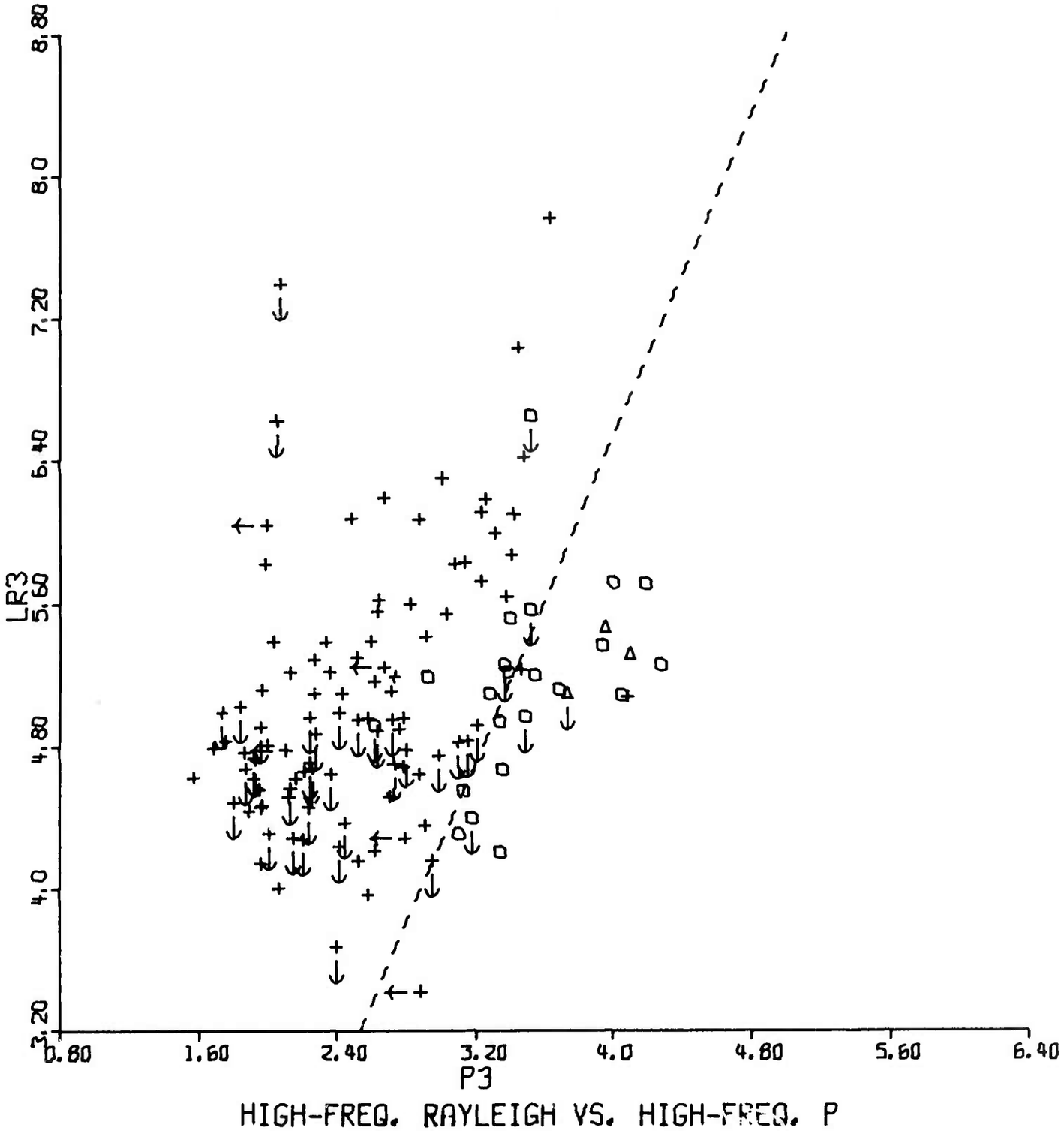

Figure 16k. High-frequency Rayleigh-wave magnitude LR_3. Spectral magnitudes of presumed earthquakes and explosions as a function of the high-frequency P-wave magnitude P_3. Earthquakes are denoted by crosses, single explosions by circles, and multiple explosions by triangles.

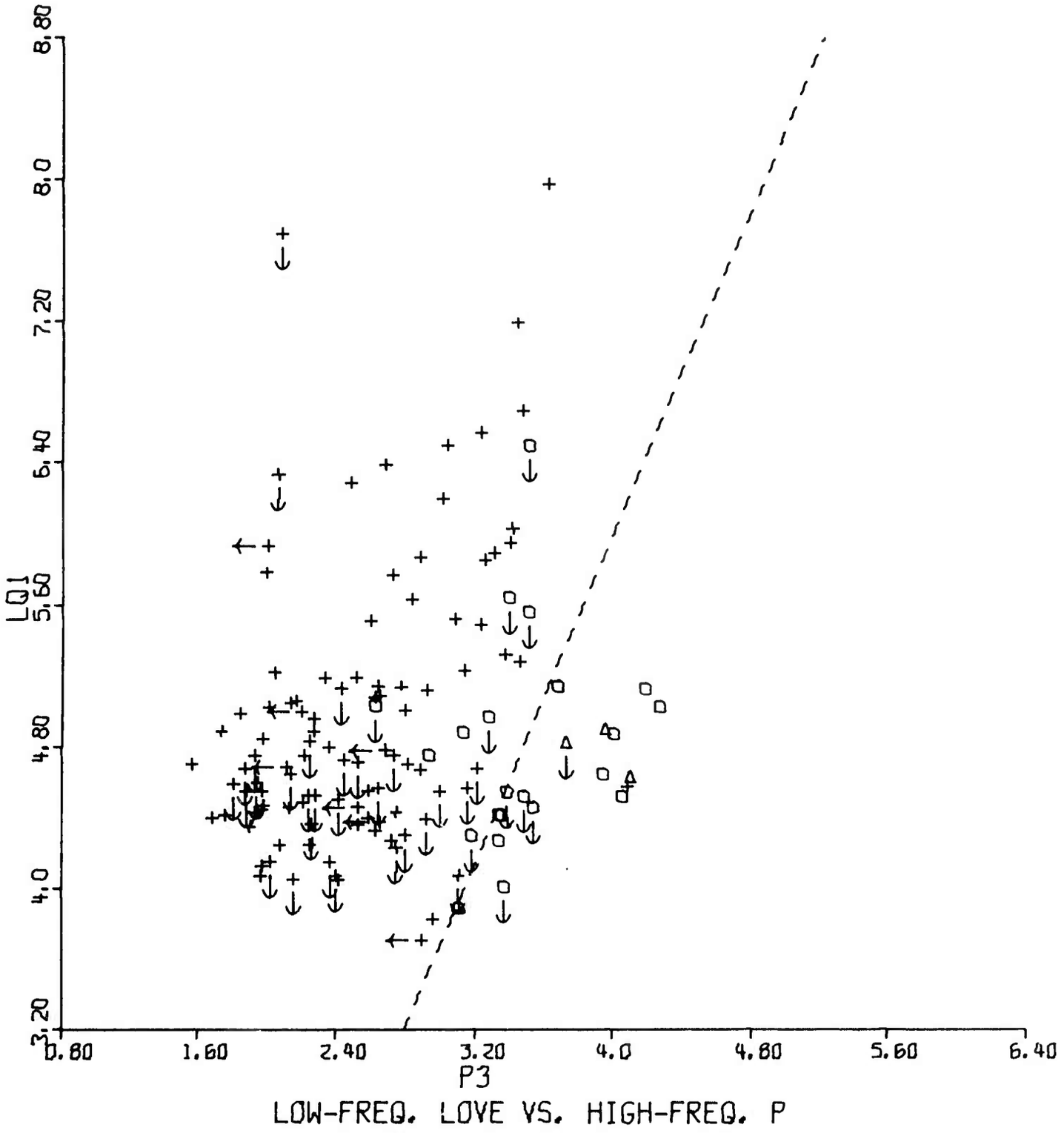

Figure 161. Low-frequency Love-wave magnitude LQ_1. Spectral magnitudes of presumed earthquakes and explosions as a function of the high-frequency P-wave magnitude P_3. Earthquakes are denoted by crosses, single explosions by circles, and multiple explosions by triangles.

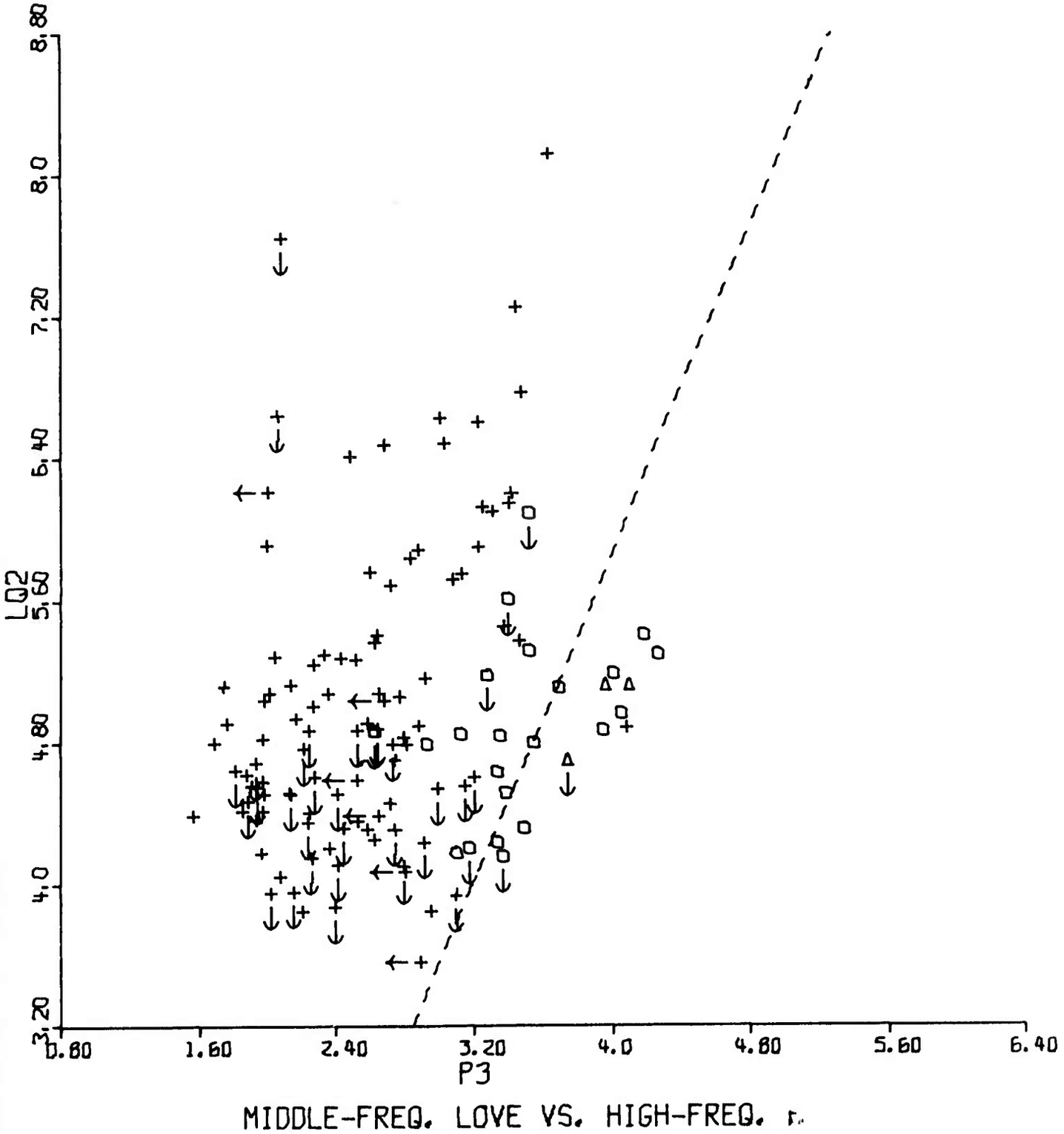

Figure 16m. Middle-frequency Love-wave magnitude LQ_2. Spectral magnitudes of presumed earthquakes and explosions as a function of the high-frequency P-wave magnitude P_3. Earthquakes are denoted by crosses, single explosions by circles, and multiple explosions by triangles.

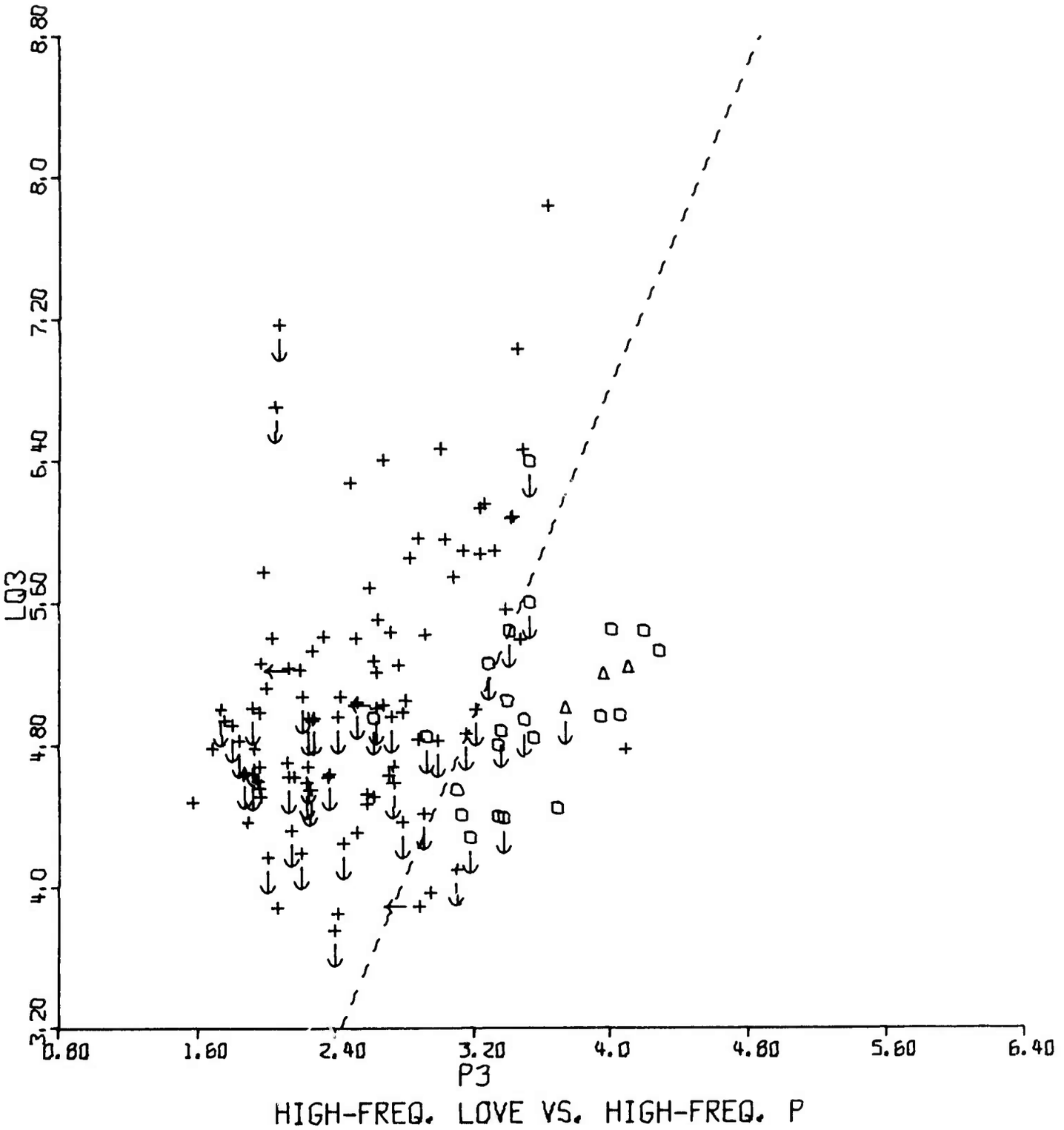

Figure 16n. High-frequency Love-wave magnitude LQ_3. Spectral magnitudes of presumed earthquakes and explosions as a function of the high-frequency P-wave magnitude P_3. Earthquakes are denoted by crosses, single explosions by circles, and multiple explosions by triangles.

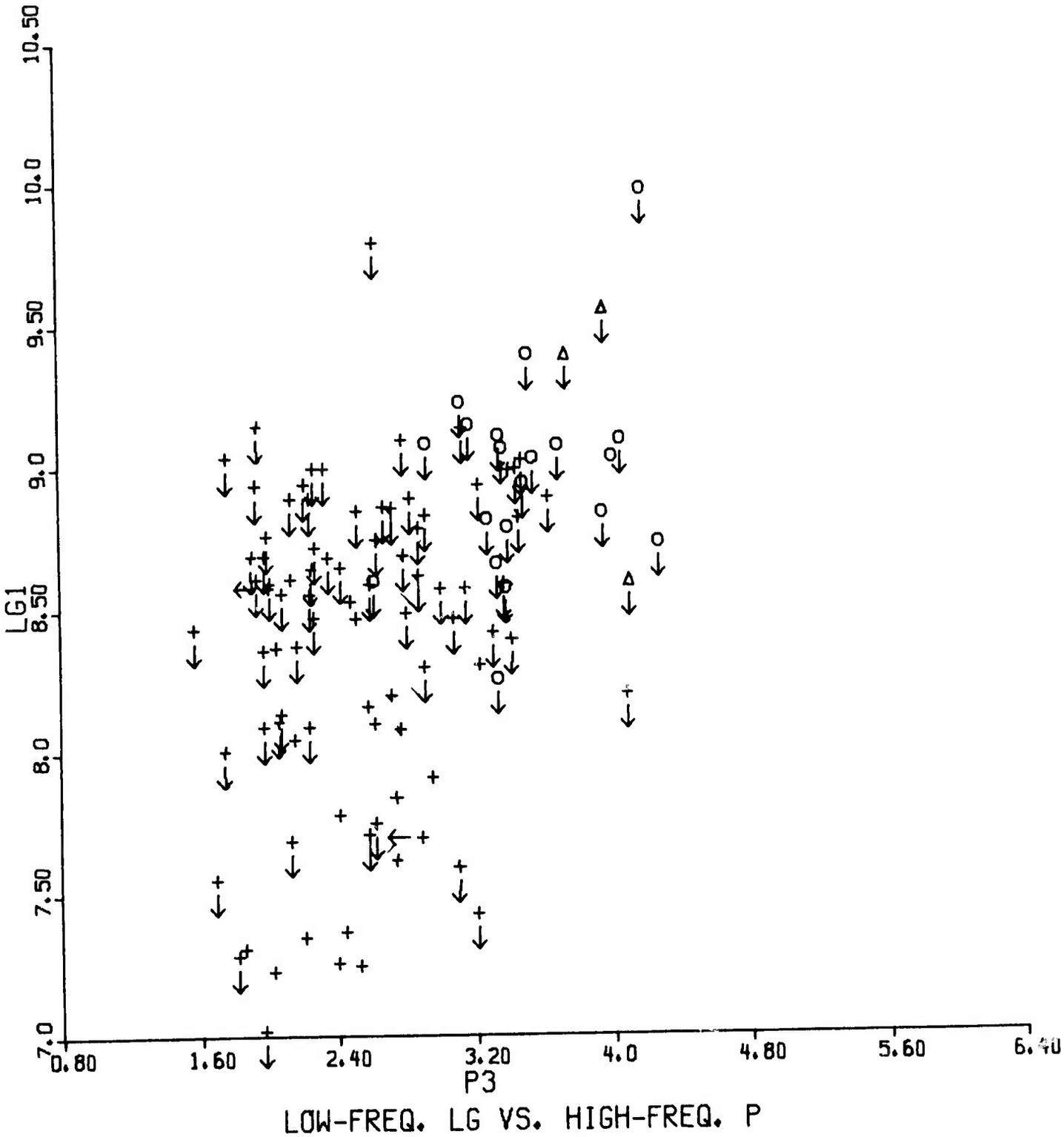

Figure 16o. Low-frequency Lg-wave magnitude Lg_1.
Spectral magnitudes of presumed earthquakes and explosions as a function of the high-frequency P-wave magnitude P_3.
Earthquakes are denoted by crosses, single explosions by circles, and multiple explosions by triangles.

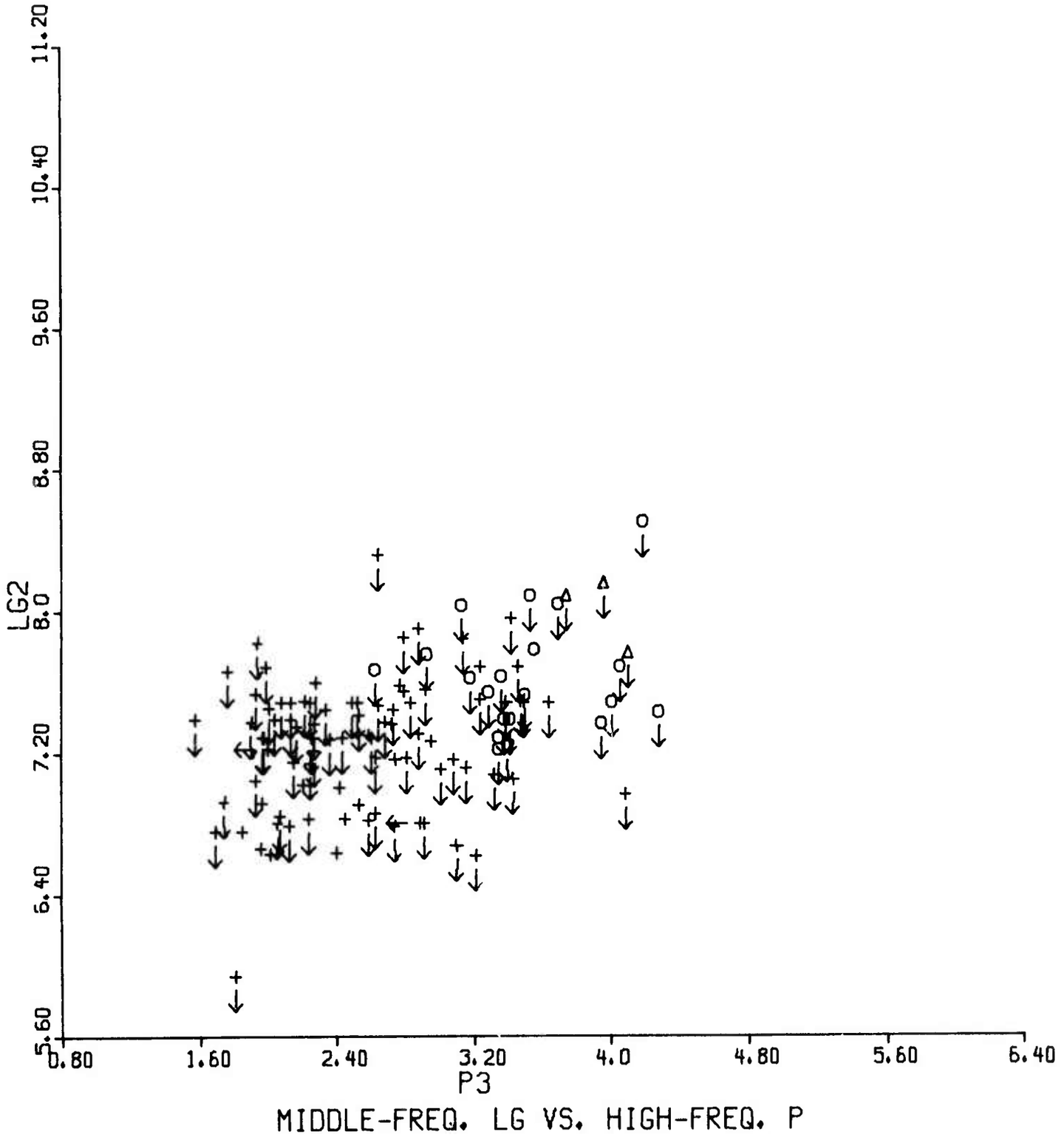

Figure 16p. Middle-frequency Lg-wave magnitude Lg_2. Spectral magnitudes of presumed earthquakes and explosions as a function of the high-frequency P-wave magnitude P_3. Earthquakes are denoted by crosses, single explosions by circles, and multiple explosions by triangles.

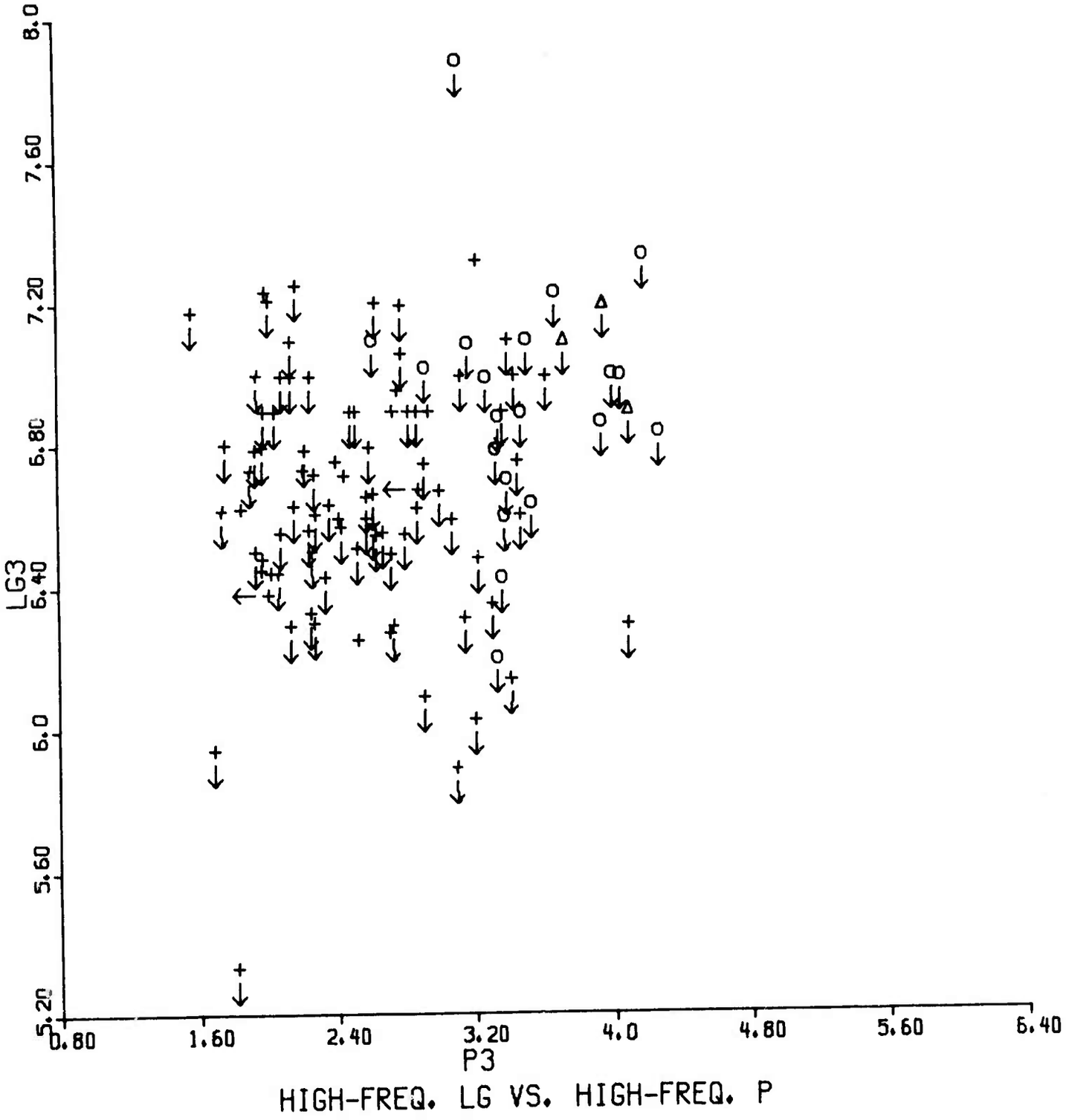

Figure 16q. High-frequency Lg-wave magnitude Lg_3. Spectral magnitudes of presumed earthquakes and explosions as a function of the high-frequency P-wave magnitude P_3. Earthquakes are denoted by crosses, single explosions by circles, and multiple explosions by triangles.

lying below the discriminant line may be presumed to lie within the explosion population, even though the true positions of these points are unknown. Physically, this geometrical argument is equivalent to identifying as explosions all those events for which the spectral ratio defined by

$$\text{spectral ratio} = \text{amplitude variable}_1/(\text{amplitude variable}_2)^{\alpha} \qquad (31)$$

is less than some specified threshold which explosions are presumed to exceed. Adjusting the intercept of the discriminant line to reflect this threshold and then retaining as useful data those upper bounds which fall below the line and rejecting those which lie above it is an application of the principle of negative discrimination. Moving the discriminant lines parallel to themselves in Figures 15 and 16 would have the effect merely of changing the number of upper bounds which are retained as useful data points. If for some reason it was believed that negative discrimination should not be applied, the intercepts of the discriminant lines could be chosen to be so low that only actual measurements, and no upper bounds, are retained in the data base.

Table XIII lists the discriminant lines which are shown in Figures 15 and 16. The lines were fit visually, and their exact values were chosen to be consistent with those of a companion study employing a somewhat larger data base (Rivers et al, 1979). It can be seen that the slope of the short-period P-wave spectral ratio increases with increasing separation of the ratioed frequency bands and then stays constant as the separation is increased from P_1/P_3 to LP_1/P_3. This same constant slope also applies to long-period S. This consistency perhaps indicates that the determination of the coefficients α, although empirical, does in fact measure some real physical effect. The slopes of the discriminant lines for surface waves differ from the unit slope of the classical M_s:m_b discriminant, but this difference was anticipated since the P-wave magnitude P_3 is measured at a higher frequency than is m_b. A steeper slope should result for the M_s:m_b discriminant if m_b is measured on the decaying asymptote of the P-wave spectrum rather than near the corner frequency.

Rivers, D. W., D. H. von Seggern, B. L. Elkins, P. J. Klouda, J. A. Burnetti, and I. Megyesi (1979). (S) A statistical discrimination experiment for Eurasian events using the Priorities I and II networks (U), SDAC Report No. TR-79-2, Teledyne Geotech, Alexandria, Virginia.

TABLE XIII

Discriminant Lines Fit to Figures 15-17

$$P_1 = 1.41\ P_2 - 1.03$$
$$P_2 = 1.72\ P_3 - 1.45$$
$$P_1 = 1.77\ P_3 - 0.87$$

$$LP_1 = 1.77\ P_3 - 0.14$$
$$LP_2 = 1.77\ P_3 + 0.02$$
$$LP_3 = 1.77\ P_3 + 1.22$$

$$LS_1 = 1.77\ P_3 + 0.21$$
$$LS_2 = 1.77\ P_3 + 0.50$$
$$LS_3 = 1.77\ P_3 + 1.22$$

$$LR_1 = 2.31\ P_3 = 2.79$$
$$LR_2 = 2.31\ P_3 - 2.94$$
$$LR_3 = 2.27\ P_3 - 2.55$$

$$LQ_1 = 2.30\ P_3 - 3.21$$
$$LQ_2 = 2.30\ P_3 - 3.34$$
$$LQ_3 = 2.30\ P_3 - 2.39$$

$$\Omega_o(-2) = -3fc(-2) + 5.93$$
$$\Omega_o(-3) = -3fc(-3) + 5.97$$

It can be seen from Table XIII that the slopes for all six discriminants of the form $M_s:m_b$ were not quite equal. The differences are probably only a statistical fluctuation, and a slope of 2.30 could probably have been imposed upon each of the six discriminants without significantly changing the separation between the two populations.

No discriminants involving L_g were computed since, as is shown in Figures 16 o-q, insufficient explosion data existed to permit such discriminants to be found. This deficiency is due partly to nondetection but mainly to the omission of the L_g window from the archived data set, especially at stations such as KAAO and MAIO which are at regional distances to many events. The failure to construct a discriminant utilizing L_g, at certain stations if not averaged over an entire network, and to compare its effectiveness with that of the teleseismic discriminants must be regarded as one of the major disappointments of this experiment.

The discrimination value of the spectral-fitting algorithm which was illustrated in Figure 2 lies in the determination of low-frequency spectral level as a function of corner frequency. For a given level, explosions should have a higher corner frequency than do earthquakes because their source time dimensions are smaller (Hanks and Thatcher, 1972). Figure 17 at least suggests that this effect can be measured from the spectral fitting algorithm, using either the f^{-2} or the f^{-3} decay models, but it hardly demonstrates that it contains much discrimination power. The lines drawn between the two populations in Figures 17a and 17b have slope -3, which is the theoretical value for events having a given stress drop. The intercepts of these lines are irrelevant, since no upper bounds are applicable to noise measurements of this pair of parameters.

Hanks, T., and W. Thatcher (1972). A graphical representation of seismic source parameters, J. Geophys. Res., 77, 4393.

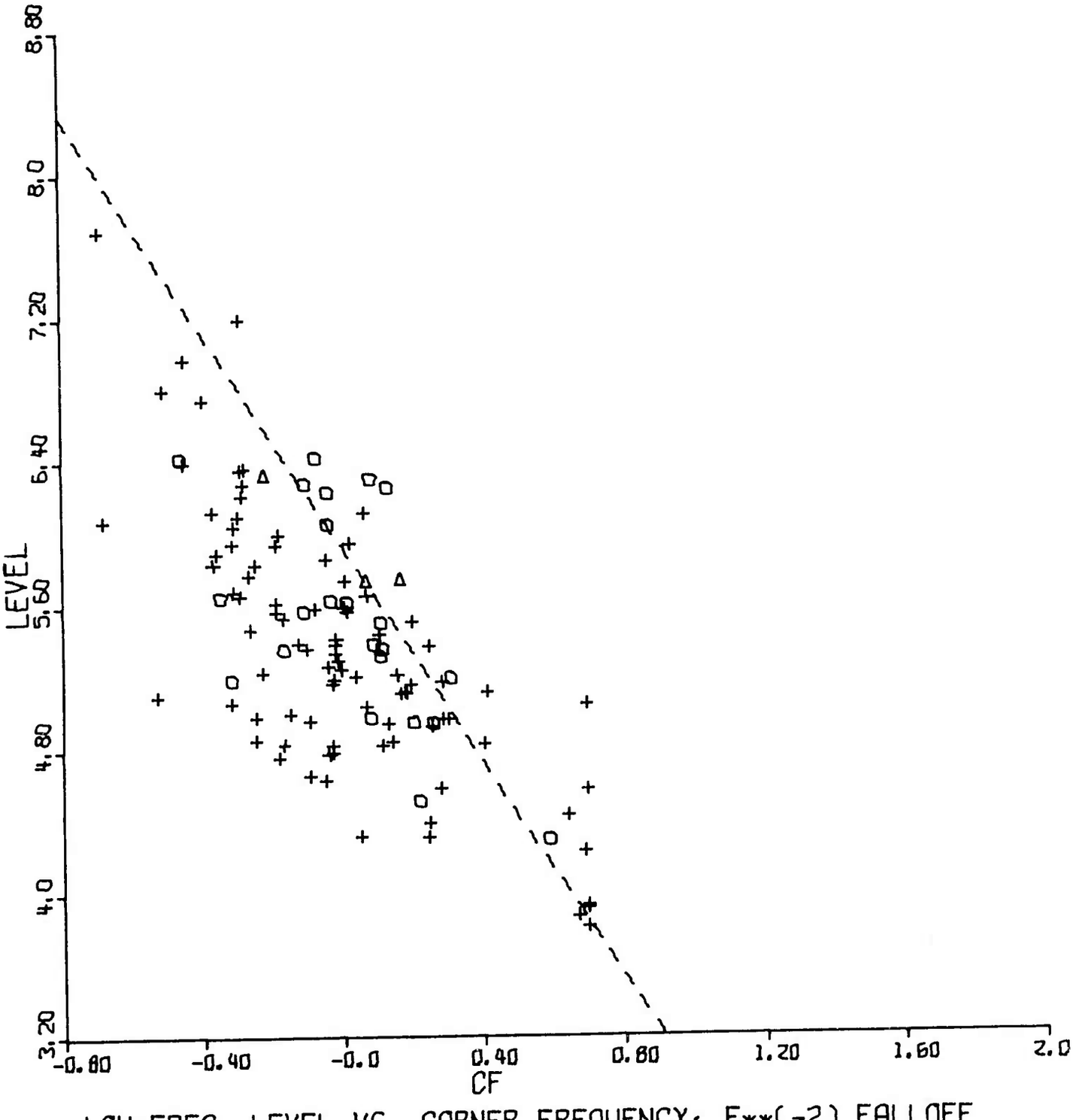

Figure 17a. f^{-2} spectral fit.
Low-frequency spectral level of presumed earthquakes and explosions as a function of corner frequency. Earthquakes are denoted by crosses, single explosions by circles, and multiple explosions by triangles.

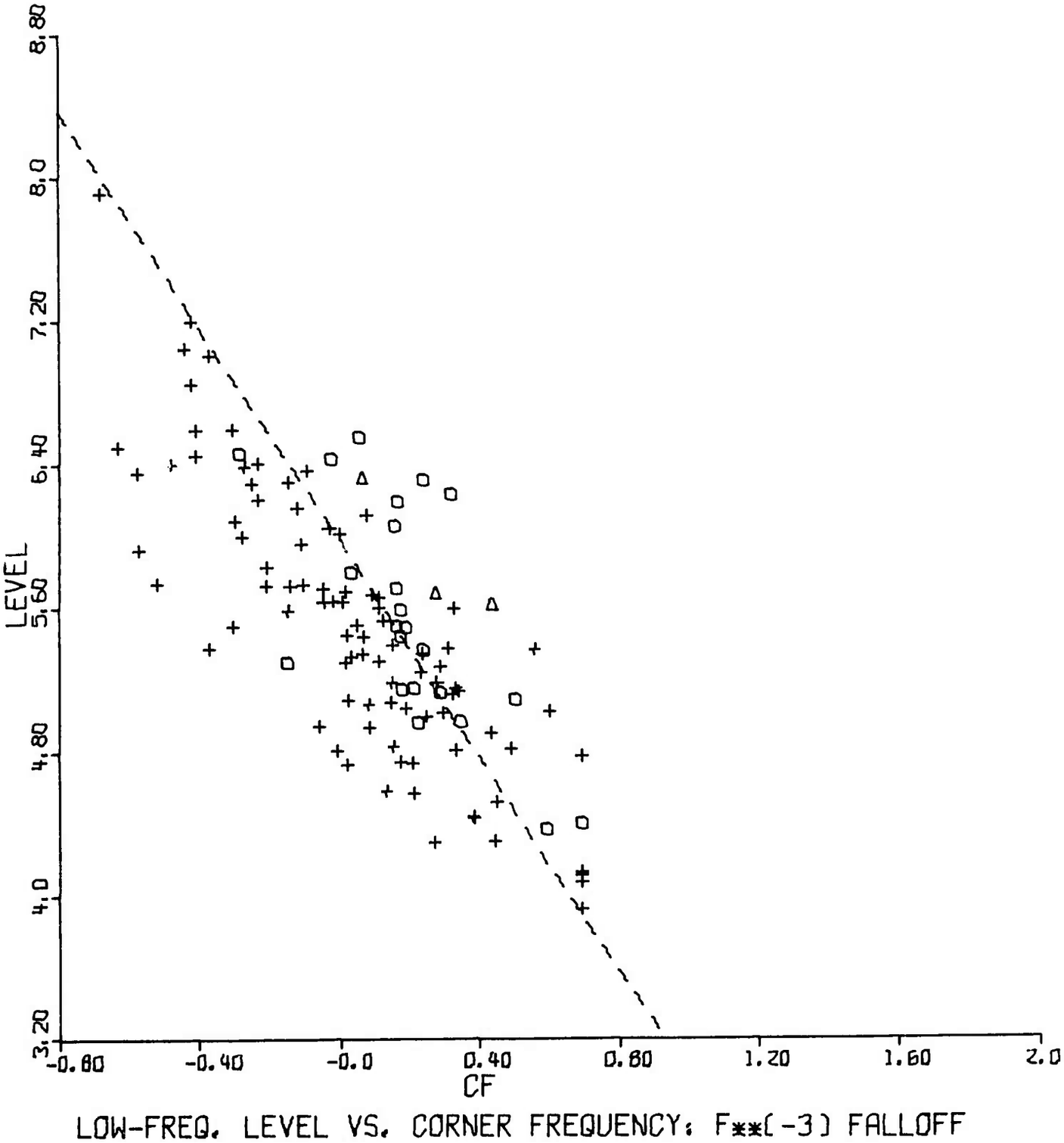

Figure 17b. f^{-3} spectral fit.
Low-frequency spectral level of presumed earthquakes and explosions as a function of corner frequency. Earthquakes are denoted by crosses, single explosions by circles, and multiple explosions by triangles.

The failure of the two populations to separate clearly in Figure 17 is probably due to the distortion of the source spectra by signal propagation effects. As was mentioned in the description of the spectral-fitting algorithm, the values chosen for Ω_o and f_c are critically dependent on the value chosen for t*, so at least part of the weakness of this discriminant may be attributable to an erroneous attenuation correction. It may be that this discriminant is too strongly influenced by errors in the values which were calculated for t* for each epicenter-to-receiver path to permit meaningful network averages to be formed. The power of the discriminant might thus be enhanced if the propagation paths were made constant by applying the Ω_o versus f_c discriminant only to data from events occurring at the same depth within a single tectonic region as recorded at a single station. Another way of improving the discriminant's power would be to use network-averaged values of Ω_o and f_c, as was done in Figure 17, but to use better values of t* in the calculation of the spectral fits. It will be recalled that a value of t* was calculated for each individual spectral fit, and so these values were subject to a significant statistical fluctuation. This fluctuation was particularly large for those cases in which the data from only a narrow spectral band was of a sufficient signal-to-noise ratio to be used. A more reliable attenuation correction might thus be made by using not the value of t* for a given individual case but rather one which is determined by averaging the individual values found for all events occurring within that same tectonic region as measured at that same station (and using the same theoretical model, either f^{-2} or f^{-3}). The scatter of the individual values about these averages is shown in Appendix III. The scatter in the values which were used for t* for the same path for different events is clearly too large, so more reliable (or at least more self-consistent) values would have been found for Ω_o and f_c had the same value been used for t* every time. Another suggestion for improvement of this discriminant was made earlier in this report, namely that spectra be used only from those stations for which $30° < \Delta < 90°$, in order to avoid uncertainties introduced into the calculation of the magnitude of the low-frequency level by the correction for geometrical spreading of the wavefront. It should also be noted that this discriminant is probably strongly affected by the assumption of zero depth for all events. In light of these errors introduced into this discriminant by propagation effects, it is hardly surprising

that Figure 17 shows such large scatter. For the purposes of this experiment, we merely note that this scatter exists, and then we calculate the Ω_o versus f_c discrimination variable using a slope of -3.

The final discrimination variables are the (logarithmic) P-wave complexities. The distributions of the complexities for the earthquake and the explosion populations are shown in Figure 18. The separation between the two populations is seen to increase with increasing length of the time window during which the complexity was measured. The two populations have a large overlap, and certain events are conspicuous outliers. Some of these outliers are due to insufficient data, being based upon only one or two observations (cf. Appendix II), but others reflect real source or path effects. In particular, deep earthquakes are characterized by small complexities since their waveforms pass through the crust once rather than twice. Two of the multiple explosions, events 265 and 271, show large complexities on account of the large amount of energy arriving from the second explosion during the coda window of the first. Although the other multiple explosion, event 53, should also be expected to have an anomalously large complexity for the same reason, it does not do so. A possible explanation for the explosion-like complexity of event 53 is that some of the energy from the second explosion arrives within the signal window of the first, making the "signal" of the hypothetical single event look large relative to its "coda". The outlying events in Figure 18 may be particularly prone to misclassification, and special note will be made of them in the analysis of the discrimination results.

The twenty variables which were used as the basis for the multivariate discrimination are listed in Table XIV, and their values for each event are given in Appendix IV. Also in Table XIV are listed the number of events to which each discriminant was inapplicable, either because there was no measurement at any station of one of the magnitude variables used in the discriminant or because the magnitudes of both variables in the discriminant were upper bounds estimated from noise measurements only. Next are listed the number of events for which one of the magnitude variables was an upper bound and for which the discriminant variable was deleted from the data set because the true value could lie within either of the two populations. These rejected events are those which are shown in Figures 15 and 16 as points with arrows attached

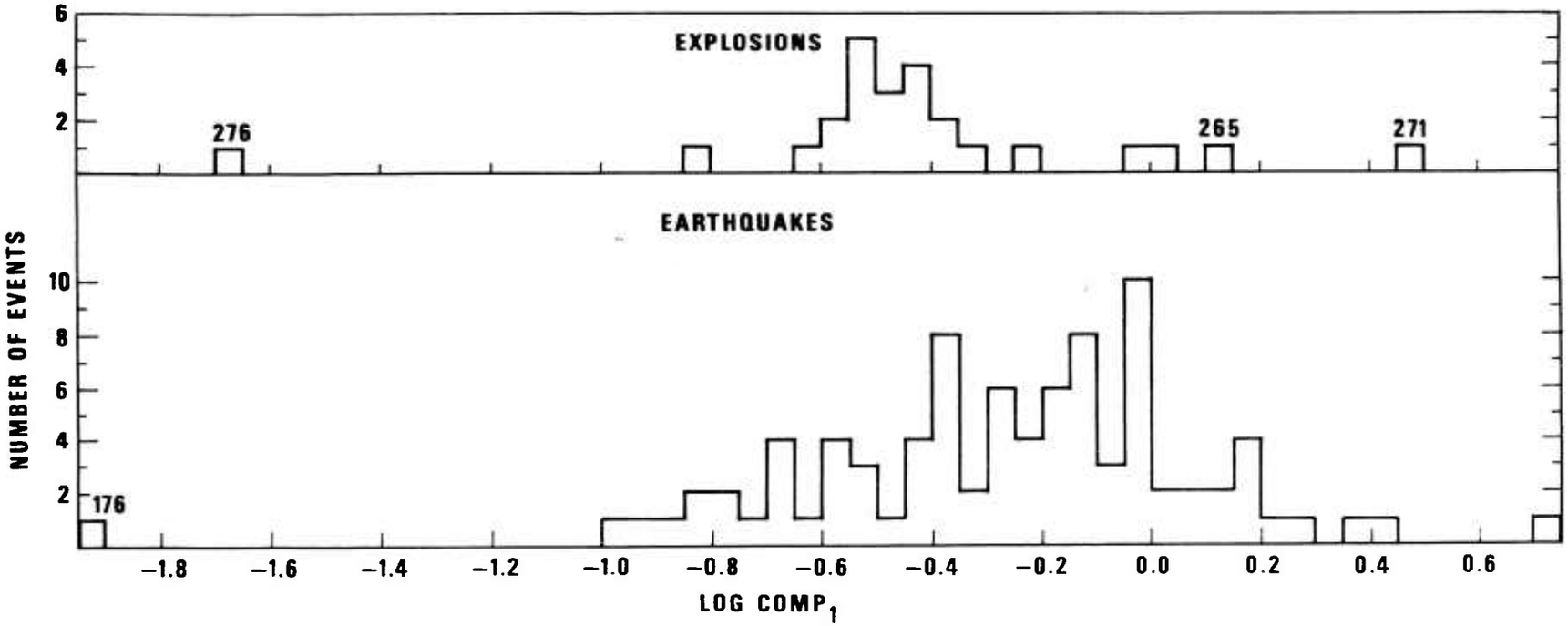

Figure 18a. Short time window.
Complexity for presumed earthquakes and explosions. Certain outliers are identified.

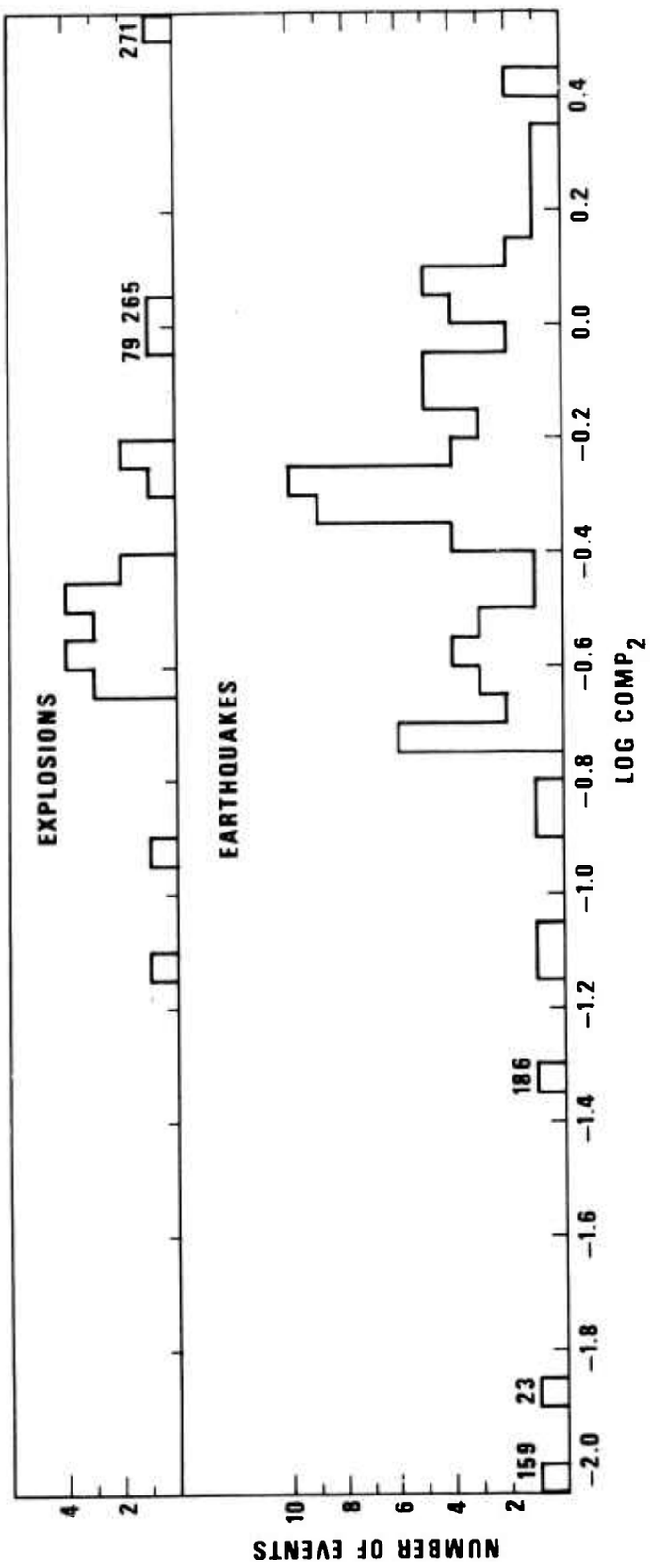

Figure 18b. Middle time window.
Complexity for presumed earthquakes and explosions. Certain outliers are identified.

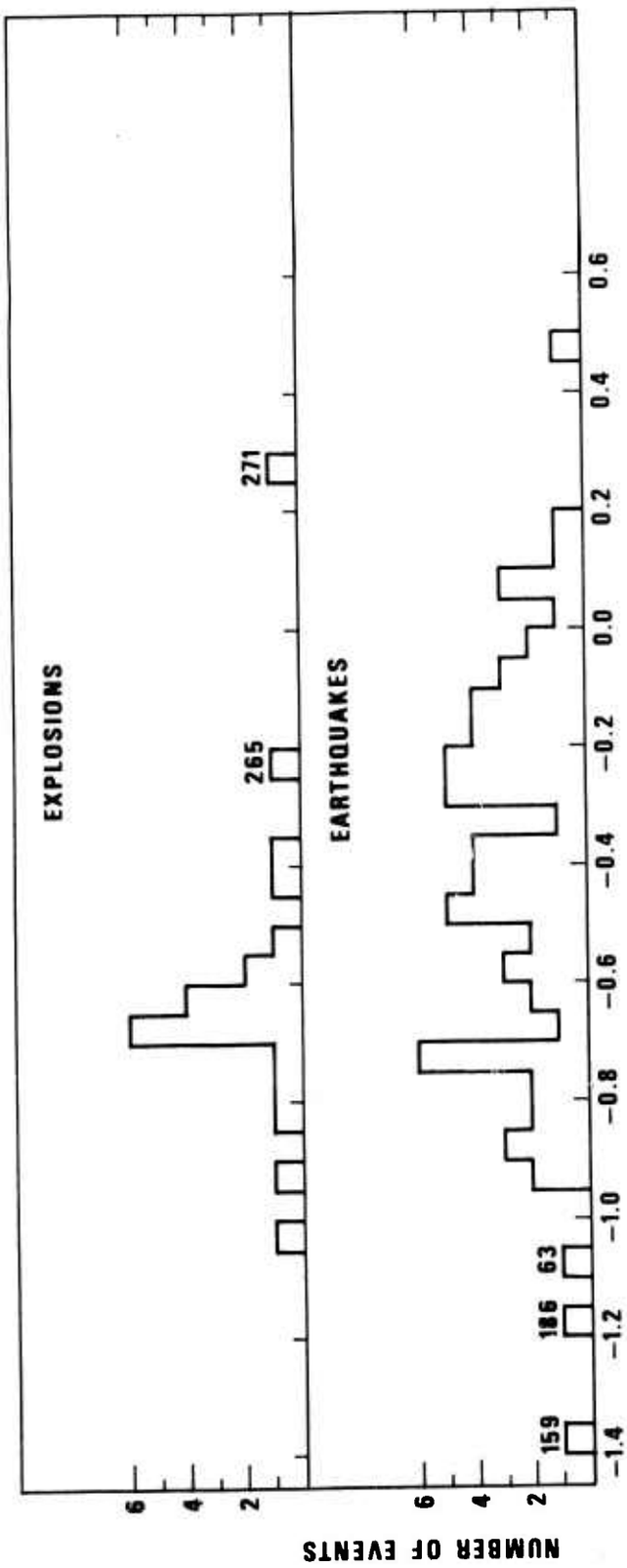

Figure 18c. Long time window.
Complexity for presumed earthquakes and explosions. Certain outliers are identified.

TABLE XIV

Variables Employed in Discrimination

A) Number of events to which the discriminant is inapplicable due to insufficient data.

B) Number of events for which an upper bound to the variable was computed but then rejected because the true value could lie on either side of the discriminant line.

C) Number of events for which the discrimination variable was approximated by an upper bound.

D) Number of events for which the true value of the discrimination variable was calculated.

E) Number of events for which the discrimination variable is non-zero. (Sum of (C) and (D).)

Variable Number	Discription	A	B	C	D	E
1	P_1-1.41 P_2	5	13	2	112	114
2	P_2-1.72 P_3	3	5	7	117	124
3	P_1-1.77 P_3	6	11	6	109	115
4	$\Omega_o(-2)$+3 fc(-2)	16	--	--	116	116
5	$\Omega_o(-3)$+3 fc(-3)	16	--	--	116	116
6	$comp_1$	19	--	--	113	113
7	$comp_2$	22	--	--	110	110
8	$comp_3$	40	--	--	92	92
9	LP_1-1.77 P_3	12	67	9	44	53
10	LP_2-1.77 P_3	11	75	13	33	46
11	LP_3-1.77 P_3	12	71	17	32	49
12	LS_1-1.77 P_3	10	60	8	54	62
13	LS_2-1.77 P_3	12	63	8	49	57
14	LS_3-1.77 P_3	12	68	10	42	52
15	LR_1-2.31 P_3	7	33	13	79	92
16	LR_2-2.31 P_3	5	29	9	89	98
17	LR_3-2.27 P_3	7	38	7	80	87
18	LQ_1-2.30 P_3	5	35	12	80	92
19	LQ_2-2.30 P_3	6	33	8	85	93
20	LQ_3-2.30 P_3	9	38	9	76	85

to them which point towards the (dashed) discriminant line. The next column of Table XIV shows the number of events for which the upper bound estimate was retained in the data base as an approximation to the true value of the discrimination variable. These events, to which the principle of negative discrimination is applicable, are those which are shown in Figures 15 and 16 as points with arrows attached which point away from the discriminant line. Next are shown the number of events for which the discrimination variable was actually measured, and finally there are listed the total number of events to which the discriminant is applicable. Table XIV shows that for every discriminant except those involving long-period body waves more than 85% of the magnitudes retained in the data base were "true" values, rather than upper bounds.

MULTIVARIATE DISCRIMINATION

Discrimination can be performed using as many of the nineteen variables as desired; instead of a line separating the earthquake and explosion populations as with the classical M_s versus m_b discriminant, the two populations are separated by an N-1 dimensional hyperplane in the space spanned by the N chosen variables. A practical limit is imposed upon the number of variables, however, by the fact that as more variables are used in a single discriminant, there are fewer events in the data base for which all the chosen variables are non-zero. The N coefficients determining the hyperplane are referred to as the "discriminant function".

The discrimination was performed using the stepwise discriminant analysis program BMD07M developed by Jennrich (1977). The first step of the discrimination consists of the a priori classification of a suite of events as earthquakes or explosions, as was done in the previous section of this report. These events are used as a "training set" to calculate the discriminant function which best separates the two populations, and this function is then applied to the remaining events. As a check against misclassified events' being used in the training set, the discriminant function is used to calculate a posteriori probabilities of correct classification for all events of the training set before the discriminant is applied to unknowns. Unknown events are classified as explosions or earthquakes depending upon on which side of the hyperplane they lie, and probabilities of misclassification are given by their proximity to the other population.

Output of the multivariate discrimination program consists not only of the discriminant function and the a posteriori probabilities but also of a table which ranks the N chosen variables in the order of their importance in determining the equation of the discriminant hyperplane. This ranking is calculated by a stepwise process that computes which of the N-m remaining variables will yield the most improvement in discrimination of the training set when added to the m variables already used in the previous steps. The stepwise process re-evaluates the weight assigned to each variable whenever a new one is added,

---

Jennrich, R. I. (1977). Stepwise discriminant analysis, in Statistical Methods for Digital Computers, edited by K. Enslein, A. Ralston, and H. S. Wiff, John Wiley and Sons, New York.

and it may then delete one of the previously used variables if it is deemed to yield superfluous or contradictory information to the discrimination. This ranking of variables is described in detail by von Seggern and Rivers (1979).

All 132 events, with the exception of the three multiple explosions, are to be used in the training set, so the discrimination experiment will essentially be a test of whether each event's a posteriori classification agrees with the classification which was assigned to it a priori. Although the a posteriori classification in effect regards the training set events as unknowns, the only true unknowns (in the sense of not having been used to calculate the discriminant functions) are the three shot arrays. The question then arises: how effective will the discriminant functions be when they are applied not to the 129 events of the training set but rather to the next group of, say, fifty events which are true unknowns? The a posteriori discrimination provides an approximate answer to that question, in that the classification probability of each event computed on the basis of the 129-event training set is a good approximation to that probability which would result from the use of only the other 128 events in the training set. Classification of the next fifty unknowns should thus work approximately as well as that of the training set. In practice, seismic discrimination ought to be a learning process, and the fifty newly-classified events should be added to the training set so that the next group of events can be classified using a 179-event training set. The influence exerted on the discrimination by the size of the training set will be measured in a subsequent section of this report.

DISCRIMINATION RESULTS

Using the number of events to which each discrimination variable is applicable, as listed in the final column of Table XIV, a systematic approach may be devised to the problem of collecting various subsets of the twenty variables to form multivariate discriminants. Neglecting for the moment the three multiple explosions, to which all of the twenty variables are applicable, Table XIV shows that the least frequently observed variable, the spectral ratio of the middle-frequency long-period P-wave magnitude LP_2 to the high-frequency short-period P-wave magnitude P_3, is applicable to 43 of the 129 events to which an a priori classification has been assigned. A twenty-variable discriminant can thus be applied to at most 43 events in the training set. It turns out, however, that at least one of the nineteen other variables is inapplicable to 19 of these 43 events, so the twenty-variable discriminant can actually be applied to only 24 events. The next least frequently observed variable is applicable to 46 events, but at least one of the remaining eighteen variables is inapplicable to eighteen of them, so the discriminant formed from the nineteen most frequently observed variables can be applied to only 28 events. Proceeding in this manner, at each step deleting from the subset of variables used in the multivariate discriminant the next least frequently observed variable, it is possible to construct the systematic incrementation of variables which is shown in Table XV. No two-variable discriminant is listed in the table, since it was not desired to create a multivariate discriminant which included the $\Omega_o(-2)$ versus $f_c(-2)$ variable but not the $\Omega_o(-3)$ versus $f_c(-2)$ variable, or vice versa. The first attempt at an a posteriori classification of the 132 events consisted of applying each of the nineteen discriminants listed in Table XV to the training set and seeing how many events each discriminant classified "correctly" (i.e., in agreement with the a priori classification).

Results of the a posteriori classification of the training set (and also of the three multiple explosions, events 53, 265, and 271) are shown in Table XVI. Listed alongside each event in that table is its a priori classification: "S" for "shot", "Q" for "quake", or "M" for "multiple". Next are listed the a posteriori classifications generated by each of the nineteen multivariate discriminants shown in Table XV. Events are classified as being

TABLE XV

Classification of the 129-Event Training Set by the Systematic Incrementation of Variables,
Refer to Table XIV for Explanation of the 20 Variables.

number of variables	which variables	no. of events to which the discriminant is applicable	no. of shots right	no. of shots wrong	no. of quakes right	no. of quakes wrong
20	1-20	24	12	0	12	0
19	1-9, 11-20	28	12	0	15	1
18	1-9, 12-20	31	12	0	18	1
17	1-9, 12, 13, 15-20	34	12	0	21	1
16	1-8, 12, 13, 15-20	38	12	0	25	1
15	1-8, 12, 15-20	38	12	0	25	1
14	1-8, 15-20	51	13	0	37	1
13	1-8, 15-19	54	13	1	39	1
12	1-8, 15, 16, 18, 19	56	13	1	41	1
11	1-7, 15, 16, 18, 19	61	12	2	46	1
10	1-7, 16, 18, 19	62	12	2	47	1
9	1-7, 16, 19	64	14	1	48	1
8	1-7, 16	71	15	1	53	2
7	1-7	93	15	5	70	3
6	1-6	94	15	5	70	4
5	1-5	102	14	6	78	4
4	2-5	103	16	5	78	4
3	2, 4, 5	111	12	11	84	4
1	2	121	11	12	94	4

TABLE XVI

RESULTS OF THE DISCRIMINATION USING THE SYSTEMATIC INCREMENTATION OF VARIABLES
REFER TO TABLE XIII FOR A DESCRIPTION OF THE MULTIVARIATE DISCRIMINANTS

EVENT	CLASS	NUMBER OF VARIABLES IN THE DISCRIMINANT : 20	19	18	17	16	15	14	13	12	11	10	9	8	7	6	5	4	3	1
1	(S)							S	S	S	S	S	S	S	Q*	Q*	Q*	Q*	Q*	
3	(Q		S*	Q	Q	Q	Q	Q	Q	Q	Q	Q	Q	Q	Q	Q	Q	Q	Q	Q
4	Q																		Q	
6	Q																			
7	Q				Q	Q	Q	Q	Q	Q	Q	Q	Q	Q	Q	Q	Q	Q	Q	Q*
8	Q																			Q
9	Q																			Q
10	Q									Q	Q	Q	Q	Q	Q	Q	Q	Q	Q	Q
14	S	S	S	S	S	S	S	S	S	S	S	S	S	S	S	S	S	S	S	S*
16	S	S	S	S	S	S	S	S	S	S	S	S	S	S	S	S	S	S	S	S*
17	S	S	S	S	S*	S*	S*	S*	Q*	Q*	Q*	Q*	S*	S	S	S*	S*	S*	S*	S*
18	S														S*		S*	S*	S*	S*
19	S	S	S	S	S	S	S	S	S	S	S	S	S	S	S	S	S	S	S	S*
20	S	S	S	S	S	S	S	S	S	S	S	S	S	S	S	S	S	S	S	S*
21	S														S*	S*	S*	S*	S*	S*
22	S	S	S	S	S	S	S	S	S	S	S	S	S	S	S	S	S*	S*	S*	S*
23	S																			S
24	Q																			Q
25	Q							Q	Q	Q	Q	Q	Q	Q	Q	Q	Q	Q	Q	Q
26	Q																			Q
27	Q							Q	Q	Q	Q	Q	Q	Q	Q	Q	Q	Q	Q	Q
28	Q																Q*	Q*	Q*	Q*
29	Q				Q	Q	Q	Q	Q	Q	Q	Q	Q	Q	Q	Q	Q	Q	Q	Q*
30	Q	Q	Q	Q	Q	Q	Q	Q	Q	Q	Q	Q	Q	Q	Q	Q	Q	Q	Q	Q*
31	Q																			Q
32	Q																			Q
33	S								S	S*	Q*	Q*	Q*	Q	Q	Q	Q	Q	Q	Q
34	Q																			Q
35	Q	Q	Q	Q	Q	Q	Q	Q	Q	Q	Q	Q	Q	Q	Q	Q	Q	Q	Q	Q
36	Q																			Q
37	Q							Q	Q	Q	Q	Q	Q	Q	Q	Q	Q	Q	Q	Q
38	Q																			Q
39	Q		Q	Q	Q	Q	Q	Q	Q	Q	Q	Q	Q	Q	Q	Q	Q*	Q*	Q	Q
41	Q																			Q
45	Q										Q	Q	Q	Q	Q	Q	Q	Q	Q	Q
46	Q								Q	Q	Q	Q	Q	Q	Q	Q	Q	Q	Q	Q
47	Q					Q	Q	Q	Q	Q	Q	Q	Q	Q	Q	Q	Q	Q	Q	Q
48	Q													Q*	Q*	Q*	Q	Q	Q	Q
49	Q	Q	Q	Q	Q	Q	Q	Q	Q	Q	Q	Q	Q	Q	Q	Q	Q	Q	Q	Q
50	Q	Q	Q	Q	Q	Q	Q	Q	Q	Q	Q	Q	Q	Q	Q	Q	Q	Q	Q	Q
53	Q	Q	Q	Q	S*	Q*	Q*	S	S	S	S	S	S	S	Q	Q	Q	Q	Q	Q
55	Q																			Q
56	Q																			Q
57	Q														Q	Q	Q	Q	Q	Q
58	Q																Q	Q	Q*	Q
59	Q																			Q

TABLE XVI (CONTINUED)

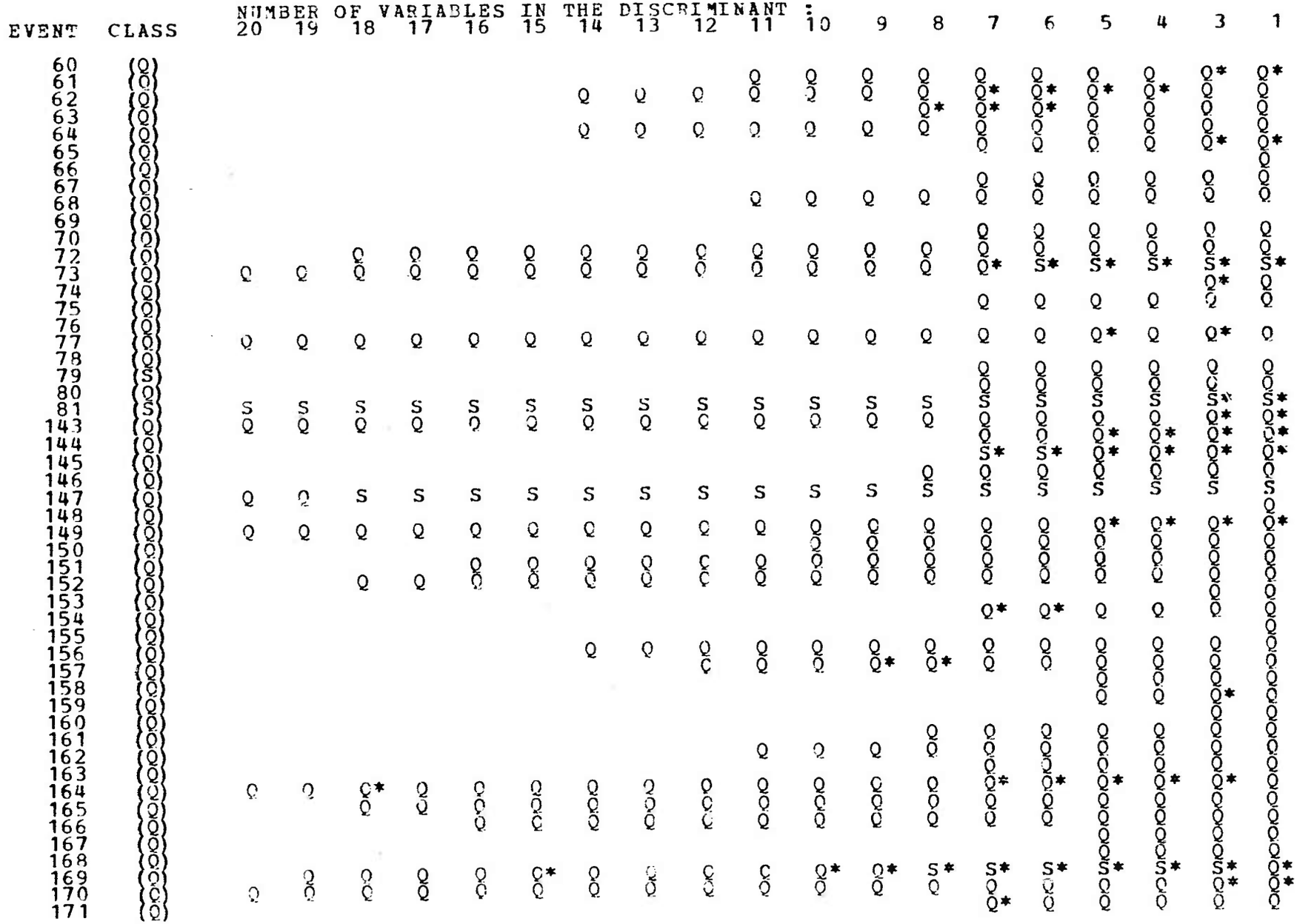

TABLE XVI (CONTINUED)

explosions or earthquakes depending upon whether the computed probability of being an explosion is greater than or less than one-half. Asterisks appear beside those classifications for which this probability lies between twenty and eighty percent. Denoting the probability of being an explosion by P(EX), the classification system used in Table XVI may be written as:

$$\text{Classification} \quad \begin{cases} S & \text{if } 0.8 < P(EX) < 1.0 \\ S^* & \text{if } 0.5 < P(EX) < 0.8 \\ Q^* & \text{if } 0.2 < P(EX) < 0.5 \\ Q & \text{if } 0.0 < P(EX) < 0.2 \end{cases} \tag{32}$$

For each multivariate discriminant Table XV shows the number of instances in which the a priori and a posteriori classifications were in agreement or in disagreement. It is shown that, as one would expect, the applicability of the discriminants increases but their reliability decreases as the number of variables decreases from twenty to one. In fact, the one-variable discriminant $P_2 - 1.72\ P_3$ misclassifies more explosions than it classifies correctly, although it does correctly classify some 95% of the earthquakes to which it is applicable. This asymmetry is brought about by the difference in the sizes of the two populations in the training set and by the discrimination algorithm's treatment of both types of misclassification as being equally undesirable. It will be shown later that a better classification percentage may be obtained for the explosions (at the expense of that of the earthquakes) by weighting the two populations unequally.

Thus far 121 of the 132 events have been examined using as many as nineteen, or as few as one, different multivariate discriminants. Considering now the 121 events to be unknowns, it must be determined which one of these discriminants should be used to assign the best possible classification to each event. In general the "best" such discriminant would be expected to be the one which utilizes the most information about each unknown event, i.e., the one containing the most variables. Table XV shows, however, that the discriminants which employ the most variables are poorly calculated since the number of events in the training set which was used to calculate them does not greatly exceed the number of variables. Such discriminants should be regarded as too unreliable to use for classifying unknowns since their exact form is too strongly dependent upon the selection of events comprising the training set. A subjective evaluation must be made of the trade-off between

the amount of information used by each discriminant, as measured by the number of variables, and the discriminant's reliability, as measured by the number of events of both populations in the training set. For the purposes of this report, it was decided to reject as being unreliable those discriminants listed in Table XV which contain fifteen or more variables, since they were calculated using 38 or fewer data points. The discriminants containing fourteen or fewer variables were calculated using 51 or more data points, however, and it was somewhat arbitrarily decided that they should be regarded as reliable. The rule which was used for classification, then, was to classify each of the 121 events using the discriminant with the greatest possible number of variables, up to a maximum of fourteen. The results of applying the criterion for classification are shown in Table XVII. Refering to the description of the discriminants as given in the second column of Table XV, it can be seen that no discriminant containing fourteen or fewer variables uses any of the long-period body-wave variables, numbers 9-14 in Table XIV. The discrimination results which are presented herein are therefore unaffected by all the measurements which were made of long-period P-and S-waves. Figures 16 c-h nevertheless show that these deleted variables are effective discriminants, and their worth should not be ignored in future studies.

The systematic incrementation of variables which was described in Table XV and applied in Table XVI is only one of a multitude of methods for creating the multivariate discriminants. For example, there are $\binom{20}{10}$ = 184,756 different ten-variable discriminants alone. It is entirely possible, if not indeed probable, that one of the 184,755 other combinations would work better than the particular one which resulted from the incrementation shown in Table XV. In particular, many of the other ten-variable discriminants might be applicable to certain events to which the chosen ten-variable discriminant could not be applied. Thus in Table XVII many events were classified using fewer variables than had been determined for them. For example, because discrimination variable number 6 was inapplicable to event 26, that event was classified using five variables, although it is shown in Appendix IV that ten of the fourteen variables used for discrimination could have been applied to it. Worse, nine events (designated "unk." in Table XVII) were not classified at all by the systematic incrementation of variables because discrimination

TABLE XVII

Summary of the Discrimination Results Using the Multivariate Incrementation Scheme of Table XV

Event	Number of Variables	Classification	Event	Number of Variables	Classification	Event	Number of Variables	Classification	Event	Number of Variables	Classification
1	14	S	45	11	Q	144	7	Q	179	14	Q
3	14	Q	46	13	Q	145	7	S*	180	7	Q
4	3	Q	47	14	Q	146	8	Q	182	9	Q
6		unk.	48	8	Q*	147	14	S	183	14	Q
7	14	Q	49	14	Q	148	1	Q	184	6	Q
8	1	Q*	50	14	Q	149	14	Q	185	3	Q
9	1	Q	53	14	S	150	10	Q	186		unk.
10	12	Q	55	7	Q	151	14	Q	187	3	Q
14	14	S	56		unk.	152	14	Q	188	14	Q
16	14	S	57	7	Q	153	3	Q	189	8	S*
17	14	S*	58	1	Q	154	7	Q*	190	14	Q
18	7	S*	59	5	Q	155	1	Q	191	7	Q
19	14	S	60		unk.	156	14	Q	192	1	Q
20	14	S	61	11	Q	157	12	Q	193	8	Q
21	7	S*	62	14	Q	158	5	Q	194	1	Q
22	14	S	63	8	Q*	159	5	Q	195	14	Q
23	1	Q	64	14	Q	160	3	Q	264	14	Q
24	1	Q	65	7	Q	161	8	Q	265	14	S
25	14	Q	66	1	Q	162	11	Q	266	9	S*
26	5	Q	67	7	Q	163	7	Q	267	14	S
27	14	Q	68	11	Q	164	14	Q	268	14	S
28	5	Q*	69		unk.	165	14	Q	269	14	S
29	14	Q	70	7	Q	166	14	Q	270	14	S
30	14	Q	72	14	Q	167	5	Q	271	14	Q*
31	7	Q	73	14	Q	168	5	Q	272	13	Q
32	7	Q	74	3	Q*	169	14	Q	273	14	S
33	13	S	75	7	Q	170	14	Q	274	4	S*
34	5	Q	76		unk.	171	7	Q*	275		unk.
35	14	Q	77	14	Q	172	14	Q	276	3	S*
36	8	Q	78		unk.	173	11	Q	277	3	S*
37	14	Q	79	7	Q	175	14	Q	278	7	S*
38		unk.	80	7	Q	176	7	Q			
39	14	Q	81	14	S	177	14	Q			
41	7	Q	143	14	Q	178	14	Q			

variable number 2, which was used in all the multivariate discriminants, was not applicable to them. Special multivariate discriminants were therefore created and applied to events such as number 26 in order to classify them using as much information as possible. Table XVIII lists these special discriminants, their effectiveness is classifying the 129 events of the training set, and the classifications which result from applying them to the specific events for which they were created. These classifications are to be considered more reliable for these particular events than the classifications given for them in Table XVII.

The most reliable classification for each event is thus given either in Table XVIII for all the events listed there or in Table XVII for all other events. A summary of these most reliable classifications is presented in Table XIX. Alongside the a priori classification which was assigned to each event ("EX" for explosion, "Q" for earthquake, "M" for multiple explosion) there are listed the number of variables which were used for the most reliable a posteriori classification. Next are listed the a posteriori classifications if they are uncertain or if they are in disagreement with the a priori assignations. It can be seen from the table that the multivariate discrimination employed in this report resulted in some six misclassifications (assuming, of course, that the a priori classifications are in fact correct). The percentage of misclassifications should not be regarded as a definitive measure of the reliability of the discrimination process, however, since it is obviously dependent upon the particular suite of events chosen for use in the analysis and since no mention has been made of the uncertainty associated with the classification of each event. It is difficult to make any quantitative assessment of the confidence with which any given event may be classified since uncertainty enters into the discrimination at several different stages. Sources of the uncertainty are:

1) Measurement of the 27 parameters listed in Table VI. These measurements are affected by the starting point and length of the data windows in the time domain, amplitude leakage between discrete frequencies in the computation of the spectra, etc.

2) Calculation of the magnitudes from the 27 measured parameters. Errors arise in these calculations due to errors in the assumed values of

TABLE XVIII

Summary of the Discrimination Results Using Special Multivariate Discriminants for Specific Events.

Event	number of variables	variables used in the discriminant (refer to Table XIV for description)	number of shots right	number of shots wrong	number of quakes right	number of quakes wrong	classification
4	9	2, 4, 5, 15-20	13	1	47	1	Q
6	5	15-19	13	2	55	1	Q
8	6	2, 6, 8, 16, 17, 19	13	1	42	2	S*
9	12	1-3, 6-8, 15-20	12	1	39	1	Q
23	3	2, 6, 7	12	9	79	2	Q
24	12	1-3, 6-8, 15-20	12	1	39	1	Q
26	10	1-5, 16-20	12	1	46	2	Q
28	8	1-5, 18-20	12	2	48	2	Q
34	10	1-5, 16-20	12	1	46	2	Q
38	10	1, 3, 6, 7, 15-20	12	1	45	1	Q
56	5	16-20	13	1	55	1	Q
58	11	1-3, 6-8, 15, 16, 18-20	12	1	41	1	Q
59	10	1-5, 16-20	12	1	46	2	Q
60	2	7, 19	15	1	56	1	Q
66	8	1-3, 6-8, 15, 16	15	1	46	2	Q
69	2	18, 19	14	2	66	3	S*
76	3	16, 18, 19	13	2	66	1	Q
78	9	1, 3, 6, 15-20	12	1	46	1	Q
148	9	1-3, 15-20	12	1	48	1	Q
153	7	2, 4, 5, 15, 16, 18, 19	14	1	54	1	Q
155	3	1-3	14	6	84	4	Q
160	5	2, 4-7	12	9	73	3	Q
185	11	2, 4-7, 15-20	13	0	43	1	Q
186	11	1, 3-8, 15, 16, 18, 19	13	1	42	1	Q
187	10	2, 4-8, 15, 16, 18, 19	14	0	42	1	Q
192	5	2, 16, 17, 19, 20	13	1	54	1	Q
276	5	2, 4-7	12	9	73	3	S
277	10	2, 4-6, 15-20	13	1	43	1	S

TABLE XIX

Summary of the Multivariate Discrimination

Event	a priori classification	number of variables used	classification	Event	a priori classification	number of variables used	classification
1	EX	14		45	Q	11	
3	Q	14		46	Q	13	
4	Q	9		47	Q	14	
6	Q	5		48	Q	8	Q*
7	Q	14		49	Q	14	
8	Q	6	EX*	50	Q	14	
9	Q	12		53	M	14	
10	Q	12		55	Q	7	
14	EX	14		56	Q	5	
16	EX	14		57	Q	7	
17	EX	14	EX*	58	Q	11	
18	EX	7	EX*	59	Q	10	
19	EX	14		60	Q	2	
20	EX	14		61	Q	11	
21	EX	7	EX*	62	Q	14	
22	EX	14		63	Q	8	Q*
23	Q	3		64	Q	14	
24	Q	12		65	Q	7	
25	Q	14		66	Q	8	
26	Q	10		67	Q	7	
27	Q	14		68	Q	11	
28	Q	8		69	Q	2	EX*
29	Q	14		70	Q	7	
30	Q	14		72	Q	14	
31	Q	7		73	Q	14	
32	Q	7		74	Q	3	Q*
33	EX	13		75	Q	7	
34	Q	10		76	Q	3	
35	Q	14		77	Q	14	
36	Q	8		78	Q	9	
37	Q	14		79	EX	7	Q
38	Q	10		80	Q	7	
39	Q	14		81	EX	14	
41	Q	7		143	Q	14	
				144	Q	7	

TABLE XIX (Continued)

Summary of the Multivariate Discrimination

Event	a priori classification	number of variables used	classification
145	Q	7	EX*
146	Q	8	
147	Q	14	EX
148	Q	9	
149	Q	14	
150	Q	10	
151	Q	14	
152	Q	14	
153	Q	7	
154	Q	7	Q*
155	Q	3	
156	Q	14	
157	Q	12	
158	Q	5	
159	Q	5	
160	Q	5	
161	Q	8	
162	Q	11	
163	Q	7	
164	Q	14	
165	Q	14	
166	Q	14	
167	Q	5	
168	Q	5	
169	Q	14	
170	Q	14	
171	Q	7	Q*
172	Q	14	
173	Q	11	
175	Q	14	
176	Q	7	
177	Q	14	
178	Q	14	
179	Q	14	
180	Q	7	
182	Q	9	
183	Q	14	
184	Q	6	
185	Q	11	
186	Q	11	
187	Q	10	
188	Q	14	
189	EX	8	EX*
190	Q	14	
191	Q	7	
192	Q	5	
193	Q	8	
194	Q	1	
195	Q	14	
264	Q	14	
265	M	14	
266	EX	9	EX*
267	EX	14	
268	EX	14	
269	EX	14	
270	EX	14	
271	M	14	Q*
272	Q	13	
273	EX	14	
274	EX	4	EX*
275	EX		unk.
276	EX	5	
277	EX	10	
278	EX	7	EX*

the B-factors, attenuation coefficients, distances, etc.

3) Calculation of the maximum-likelihood estimates of the 27 magnitudes. As a rule of thumb, the most reliable estimates are those which are (a) based on magnitudes from the greatest number of stations, and (b) based on the most signal detections and the fewest noise levels. A rough idea of the relative uncertainty of the network estimates of each magnitude for each event may thus be gained from inspection of Appendix II. That this rule of thumb is only an approximate guideline may be seen, however, by considering two events for which all the measurements of one of the parameters were based on signal detections rather than noise levels. Although the standard deviation of the mean for the magnitude of that parameter is likely to be smaller for the event which was observed at more stations than was the other, there is certainly no guarantee that this is the case. The less frequently observed event may in fact be better determined, and the only sure comparison of the relative uncertainty in the two event magnitudes is given by the standard deviation of the means for both. It should be noted that if noise levels as well as signal detections were used to compute a given maximum-likelihood estimate, then the standard deviation of the mean cannot be used but an analogous confidence limit can be given by the Cramer-Rao bound (Ringdal, 1976).

4) Determination of the discrimination variables. Certain of the coefficients α in equation (31) are more poorly determined than others, and so some of the twenty (later decreased to fourteen) discrimination variables result in more misclassifications than do others. Although an estimate can be made of the relative reliability of each discrimination variable, it is not necessary to do so, since the reliability of the multivariate discriminant functions (considered next) can be determined independently of that of the individual variables of which they are composed.

5) Formation of the multivariate discrimination functions. It has already been explained that the reliability of the discriminants is a tradeoff between the number of events in the training set used to determine them and the fraction of those events which are misclassified

by them. This information is presented in Tables XV and XVIII. It can thus be seen that the classification of events such as number 194, which Table XVII shows to have been classified on the basis of a one-variable discriminant, should be regarded as highly uncertain, since Table XV indicates that this discriminant has a high misclassification rate.

6) Computation of the classification probabilities. Even if the locations in the multivariate space of the discriminant hyperplanes (considered above) were taken to be perfectly determined, uncertainty would arise in the classification of a given event due to the proximity of that event's data point to the particular hyperplane used for discrimination. Data points which lie distant from the hyperplane lie well within the boundaries of either the earthquake or explosion populations and hence have a low probability of having been misclassified, but data points near the hyperplane are within a region of some overlap of the two populations, and hence their classification is uncertain. A measure of this uncertainty is given by the designations which are explained in equation (32) and applied to Tables XVII and XVIII. Table XIX shows that there were twelve events which were correctly classified using computed probabilites of being an explosion P(EX) which lie between 0.2 and 0.8.

Uncertainty in the discrimination process is obviously cumulative, so the factors listed above (or at least numbers 3, 5, and 6, which are highly variable from event to event) should be considered in evaluating the uncertainty associated with the classification of any given event.

Even though the number of misclassified events cannot be used by itself to evaluate the effectiveness of the discrimination process, it is instructive to examine on a case-by-case basis the six misclassified events in order to determine the weaknesses of the method and to determine whether any particular type of event exists which is more prone to misclassification than others. These six events are:

1) Event 8. This event was classified on the basis of six discrimination variables, two of which were P-wave signal complexity windows. The

complexity was based on a measurement at only one station, KSRS, and hence may be unreliable. It should be noted that at KSRS the P-wave spectral amplitudes P_1 and P_3 were flagged as falling below the threshold SNR of 1.5; since the signal at that station was so noisy, it is very likely that the complexity of the coda was also dominated by noise. When a four-variable discriminant not using complexity was applied to this event, it was classified as an earthquake. This event was very poorly observed, since, as is shown in Appendix II, the single P_2 measurement at KSRS was the only P-wave observation in the entire data base. (However, there did exist data windows for short-period P at certain other stations which could not be measured due to signal processing problems.) Appendix IV shows that, as a result, the P_1:P_2 and P_1:P_3 spectral ratios could not be used for discrimination and that the P_2:P_3 spectral ratio which was used was actually an upper bound. In Figure 16b event 8 is indicated by one of the crosses which lie on the left of the discriminant line and which have arrows attached to them pointing toward the left. If the magnitude of P_3 had been represented by an actual measurement rather than by an upper bound, this data point would have moved farther into the earthquake population. The misclassification of event 8 is thus due mainly to an insufficiently (and possibly incorrectly) determined value for the complexity, and the discrimination was influenced heavily by the unreliable complexity value since there were too few observations of short-period P-waves to compute accurately the spectral ratios P_1:P_2, P_1:P_3, and P_2:P_3.

2) Event 69. The NEIS depth for this event is 255 km. It was classified on the basis of the two-variable discriminant consisting of the spectral ratios LQ_1:P_3 and LQ_2:P_3. Appendix II shows that the P_3 magnitude was actually an upper bound based on no signal measurements and on only one noise measurement (at ILPA). The LQ magnitudes were based on eight noise measurements and one signal measurement. That one measurement was made at KAAO, at a distance of $\Delta = 2.8°$. The uncertainties which are introduced into the network-averaged magnitude calculations by close-in surface-wave data such as this have already been discussed, and it would probably have been better to delete this

single observation from the data base. This deletion would have left no discrimination variables applicable to this event, and it would have been classified as an unknown. Even if the LQ magnitudes had been retained, the two spectral ratios should be regarded as unreliable since the P_3 magnitude was computed using a single measurement, and one which furthermore was noise rather than signal.

3) Event 79. This explosion was misclassified using a seven-variable discriminant including the two complexity measurements $comp_1$ and $comp_2$. It was noted on Figure 18b that $comp_2$ is anomalously large for this event, and Appendix II shows that the value used for $comp_2$ was based upon a single observation. When the complexity variables are deleted from the discriminant, this event is still misclassified as an earthquake, but less strongly so. Indeed, comparing the magnitudes listed in Appendix I for this event with the short-period discriminants plotted in Figures 16a-c and Figures 17a-b shows that event 79 is at least weakly earthquake-like with regard to each discriminant, and Table XVI confirms this. This event was misclassified because no long-period discrimination parameters could be used, and, as Table XV demonstrates, explosions tend to be misclassified in the absence of M_s:m_b data. In the next section of this report we shall show how the short-period-only discriminants can be made more effective for identifying explosions.

4) Event 145. The NEIS depth for this event is 540 km. When complexity is deleted from the eight-variable discriminant used for this event, it is classified as an earthquake.

5) Event 147. The NEIS depth for this event is 479 km. It was classified on the basis of the fourteen-variable discriminant, and it was explosion-like with regard to each of the variables. In practice, however, this event would have been classified as an earthquake, since visual inspection of the short-period P-wave seismogram recorded at CHTO (Figure 19) reveals a strong dilatant first motion.

6) Event 271. It was noted in Figure 18 that this shot array has a large complexity. When the three complexity variables are deleted from the fourteen-variable discriminant which was applied to it, it

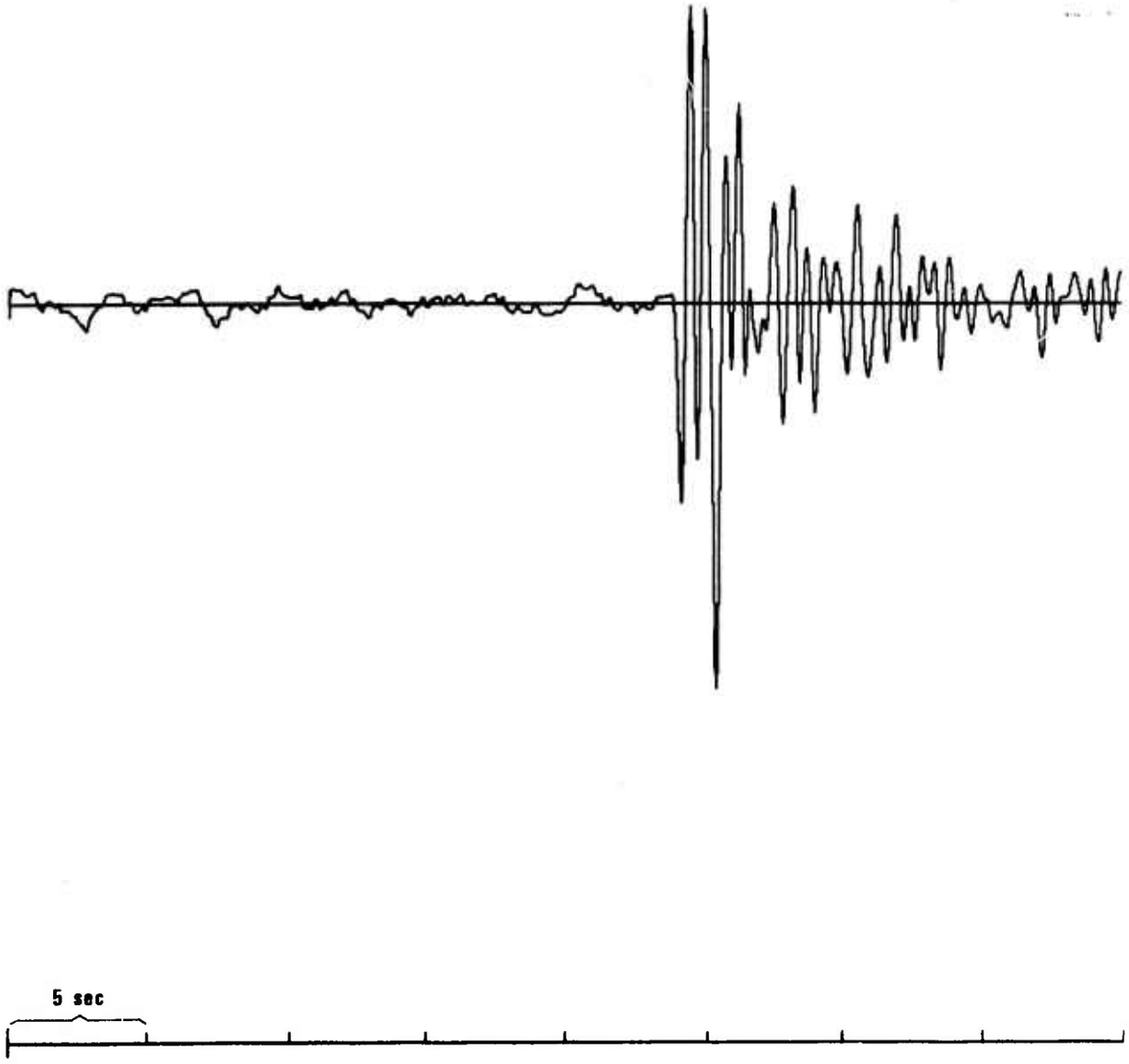

Figure 19. Short-period P seismogram of event 147 recorded at CHTO.

is classified as an explosion.

7) As previously noted, event 275 was deleted from the classification because no seismograms for that event were retained in the data base. It thus remains unknown.

It is thus seen that the two principal causes of misclassification were insufficient detections for both earthquakes and explosions and depth of the hypocenter for earthquakes. Earthquakes at greater than crustal depths are seen to resemble explosions in many respects, and this resemblance is especially strong with regard to complexity. The systematic misclassification of deep events, particularly by means of the P-wave signal complexity, has been demonstrated in several previous investigations (Dahlman and Israelson, 1977).

Special attention should be paid to the classification of the three multiple explosions, events 53, 265, and 271. Figures 16 and 17 show that the spectral ratios for these events lie in every case within the explosion populations, but as we have seen, event 271 was misclassified. Figure 15 shows that the earthquake-like aspect of each of these events is the complexity. It is thus seen that complexity may lead to the misclassification of not only deep earthquakes but also multiple explosions. This suggests that in practice perhaps each discriminant function should be applied to unknown events twice, once with and one without the complexity variables. A classification criterion might then be established as follows:

with complexity	without complexity	classification
earthquake	earthquake	earthquake
earthquake	explosion	possible multiple explosion
explosion	earthquake	possible deep earthquake (33)
explosion	explosion	explosion

Application of such a criterion would of course fail to eliminate all deep earthquakes from the list of events classified as explosions, since earthquakes such as event 147 appear explosion-like with respect to $M_s:m_b$ and/or P-wave

---

Dahlman, R., and H. Israelson (1977). Monitoring Underground Nuclear Explosions, Elsevier North Holland Inc..

spectral ratios as well as complexity. Similarly, for certain configurations of multiple explosions, the spectral ratios of long-to-short period variables as well as complexity could be made to resemble earthquakes. In such cases, however, the short-period P-wave spectral ratios would still appear explosion-like.

DISCUSSION

It was explained in a previous section of this report that the multivariate discrimination algorithm is a stepwise process and that at each step in the computation of an n-variable discriminant a search is made over the n-m unused variables in order to find the one which will most strongly improve the discrimination capability when added to the m variables already entered into the discriminant. After the new m + 1 variable discriminant is computed, the m + 1 variables are ranked in order of their contribution to the separation of the earthquake and explosion populations, and then a new search is made over the remaining n-m-1 variables. The results of this procedure for the fourteen-variable case are shown in Table XX. It should be noted that the results would be somewhat different in, for example, the ten-variable case because the training set would be different and because the relative importance of each of the ten common variables would be affected by the absence of the other four. Because the fourteen-variable discriminant was judged to be the "best" one examined, however, the ranking of the fourteen variables shown in Table XX will be assumed to impart the best information available about the relative value of each of the individual discrimination variables. The table shows that the order in which the variables are entered into the discriminant function differs from the order in which they are ranked following the final step. This difference is to be expected, since after the final step the importance of each variable is compared with that of all the variables which were eventually entered into the discriminant, rather than with that of just those which had been entered before it. The final ranking thus presents the best measure of the relative value of each of the individual variables, but the order in which the first m variables are entered into the discriminant function serves to define the best possible m-variable discriminant. (It should be emphasized that in this context the "best possible" discriminant is the one which yields the best separation between the earthquakes and explosions of the 51 event training set used for the fourteen-variable discriminant. This "best possible" m-variable discriminant may be of limited applicability and/or effectiveness as a discriminant for the other 81 events in the data base.) By this criterion it may be seen that the best single-variable discriminant is the spectral ratio of middle-frequency Love waves to high-frequency P waves. When all fourteen

TABLE XX

Ranking of the Variables in the Fourteen-Variable Discriminant

Order in which the variables are entered:

step number	variable entered	F-statistic	degrees of freedom
1	LQ_2 -2.31 P_3	79.9171	1,49
2	P_2 -1.72 P_3	7.6636	1,48
3	$\Omega_o(-2)$ + 3 fc (-2)	2.6590	1,47
4	$comp_2$	1.6107	1,46
5	LQ_1 -2.30 P_3	0.4096	1,45
6	LR_1 -2.31 P_3	1.1904	1,44
7	P_1 -1.41 P_2	0.6782	1,43
8	P_1 -1.77 P_3	0.3763	1,42
9	$comp_1$	0.3536	1,41
10	LR_3 -2.27 P_3	0.1770	1,40
11	LQ_3 -2.30 P_3	0.1155	1,39
12	$comp_3$	0.1086	1,38
13	$\Omega_o(-3)$ + 3 fc (-3)	0.0136	1,37
14	LR_2 -2.31 P_3	0.0009	1,36

After all 14 variables are entered:

Order	variable	F-statistic (degrees of freedom = 1,36)
1	LQ_2 -2.31 P_3	2.3203
2	LQ_1 -2.30 P_3	1.4501
3	LR_1 -2.31 P_3	1.2004
4	P_1 -1.41 P_2	0.7366
5	$\Omega_o(-2)$ + 3 fc (-2)	0.4739
6	P_1 -1.77 P_3	0.3159
7	$comp_1$	0.1798
8	LR_3 -2.27 P_3	0.1535
9	LQ_3 -2.30 P_3	0.0930
10	$comp_3$	0.0915
11	$comp_2$	0.0783
12	P_2 -1.72 P_3	0.0544
13	$\Omega_o(-3)$ + 3 fc (-3)	0.0114
14	LR_2 -2.31 P_3	0.0009

variables are used, the discrimination algorithm assigns the top two rankings to the spectral ratios LQ_2:P_3 and LQ_1:P_3 and the third highest ranking to the spectral ratio LR_1:P_3. It is thus seen that, as is well known, M_s:m_b is a valuable discriminant, but it happens that in this experiment its most important form is LQ:P rather than the traditional LR:P. It is perhaps not surprising that Love waves are a more effective discriminant than are Rayleigh waves, since in an idealized case Love waves should be an infallible discriminant, their very existence being diagnostic of an earthquake. The Rayleigh-wave radiation of an idealized explosion, by contrast, is not more than an order of magnitude smaller than that of a shallow earthquake with the same seismic moment (von Seggern and Rivers, 1979). In practice, however, Love waves are emitted by explosions due to mode conversion and to deviation of the source mechanism from a purely radial presure pulse, but they are still emitted in small enough amplitudes that they remain a better discriminant than Rayleigh waves. In fact, even though the spectral ratio of middle-frequency Love waves to high-frequency P-waves was the best single-variable discriminant, Table XX shows that the corresponding ratio for Rayleigh waves is the last variable entered into the fourteen-variable discriminant function. It should not be concluded from this ranking that M_s:m_b measured by means of Rayleigh waves is a poor discriminant; Figure 16j shows that this is clearly not the case. Rather, what this ranking indicates is that after (LQ_2 -2.31 P_3) has been entered into the discriminant and assigned heavy weight, most of the information contained in the (LR_2 -2.31 P_3) variable becomes redundant, and the discrimination algorithm regards this variable as superfluous. It should be remembered that the surface-wave magnitudes used in the discrimination are averages taken over a network of many stations; for data from a single station, Love waves and Rayleigh waves are likely to be complementary rather than redundant, since for many source geometries the nodes of one type of surface-wave radiation pattern are coincident with the lobes of the other type of pattern. Attention should be paid to the ranking in Table XX of the three complexity variables. It has already been mentioned that discrimination based on complexity can be misleading, particularly for deep earthquakes and for multiple explosions.

No assessment was made of the importance of the six variables which were not employed in the fourteen-variable discriminant function, namely the spectral ratios to P_3 of the six magnitudes of the long-period body waves. Although Tables XIV and XV show that these variables were observed too seldom to permit the accurate determination of any multivariate discriminant function containing them, Figures 16c-h show that each of these six variables considered individually shows considerable discrimination capability. Some of this capability, of course, is due to the fact that long-period body waves are usually detected only for large events, and in such cases many different discriminants are usually effective. Nevertheless, these six variables apparently would supply valuable information to any multivariate discriminant function containing them, and in any future investigations of statistical seismic discrimination techniques they should be routinely measured for all events in order to build up a suitable training set of events to which they are applicable.

It was noted in the previous section of this report that of the earthquakes misclassified as explosions, several are deep events. These misclassifications were undoubtedly influenced by noise and missing data, as in the cases of the other misclassifications, but the possibility remains that systematic errors were made which affected deep events more severely than shallow ones. One such systematic error could be the use of zero-depth B-factors in the computation of the body-wave magnitudes P_1, P_2, P_3, LP_1, LP_2, LP_3, LS_1, LS_2 and LS_3. Another would be the use of a zero-depth geometrical spreading correction in the computation of the low-frequency spectral levels $\Omega_o(-2)$ and $\Omega_o(-3)$. Although these errors are systematic, their effect is unpredictable, being dependent upon the epicenter-to-station distances for the particular network of stations used for a given event. The hypothesis of systematic error is thus not necessarily incompatible with the fact that several deep events were correctly identified as earthquakes. As has been pointed out, there could also be certain real differences between deep earthquakes and shallower ones such as comprised most of the training set. Certainly the surface-wave excitation is less for deep events. The P-wave spectra (and hence the spectral ratios P_1:P_2, P_1:P_3, and P_2:P_3) may also be different for deep earthquakes on account of certain features of their source mechanisms. For example, at least some deep earthquakes may involve smaller source dimensions and larger stress drops than do those at shallower depths, causing

them to have higher corner frequencies and more high-frequency spectral content. Their mechanisms might also be explosion-like in that they could involve a volume change due to a mineralogic phase transition. The spectra of deep earthquakes might also differ from those of the other earthquakes in the training set on account of differences in the propagation paths of the signals; P waves from deep events travel through the earth's crust and upper mantle only once, not twice. The P-wave signal complexity is also affected by the differences in propagation paths, and it has already been shown that the anomalously low values of the complexity for deep events can be sufficent to cause misclassification.

In an actual operational procedure of detecting, locating, and discriminating unknown events, however, events which had been determined to be deep would be deleted from the list of unknowns prior to the application of the multivariate discriminant functions. In order to evaluate the effect of using hypocentral depth as a discriminant, a three-stage discrimination process was performed which resembled ones described by Dahlman and Israelson (1977). The results of this three-stage process are shown in Table XXI. Listed in this table are, in each instance in which they are available, the hypocentral depths in km for every event as they are given in the bulletins produced by the NEIS and by the Network Event Processor (NEP) at the Seismic Data Analysis Center. No values are given for those events whose depths were restricted by the NEP to be zero. The first stage of the discrimination consists of classifying as earthquakes all events whose depths are believed to be greather than 100 km. Table XXI shows that there are 24 such events. (One of them, event 50, was restricted by the NEP to a depth of 40 km, but was classified as an earthquake on the basis of its NEIS depth of 400 km.) The second stage of the discrimination was the application to the other 109 events of those multivariate discriminant functions which contained at least one of the six M_s:m_b variables, numbers 15 through 20 in Table XIV. This stage was somewhat different from that of Dahlman and Israelson (1977) in that these multivariate discriminants contain not only M_s:m_b but also the short-period spectral ratios, complexity, and low-frequency level versus corner frequency. Table XXI shows that the application of these discriminants, taken from Tables XVII and XVIII, results in the classification of 82 more events, two of them (events 8 and 271) incorrectly. The third stage consists of the classification of the remaining

TABLE XXI

Three-stage Classification of Events

Event	NEIS depth	NEP depth	depth classification	long-and short-period data	short-period data only	correct classification
1	0			EX		
3	33			Q		
4	104		Q			
6				Q		
7	15			Q		
8				EX		Q
9	68			Q		
10	163		Q			
14	0			EX		
16	2			EX		
17	0			EX		
18	0				EX	
19	0			EX		
20	0			EX		
21	33				EX	
22	0			EX		
23					Q	
24				Q		
25				Q		
26	167		Q			
27	33			Q		
28	157	119	Q			
29				Q		
30	33			Q		
31	33				Q	
32	33				Q	
33	0			EX		
34	33			Q		
35	33			Q		
36				Q		
37	33			Q		
38	257		Q			
39	33			Q		
41	140		Q			
45	97			Q		
46				Q		
47	41			Q		
48	233		Q			
49	62	52		Q		
50	400	40	Q			
53	0			EX		
55					Q	
56				Q		
57					Q	
58				Q		
59	33	78		Q		
60				Q		
61	33			Q		

TABLE XXI (Continued)

Three-stage Classification of Events

Event	NEIS depth	NEP depth	depth classification	long-and short-period data	short-period data only	correct classification
62	59	58		Q		
63	165		Q			
64	66	26		Q		
65					Q	
66				Q		
67	114		Q			
68	33			Q		
69	255		Q			
70	230		Q			
72	120	76	Q			
73	33	105	Q			
74					Q	
75					Q	
76				Q		
77	33	106	Q			
78				Q		
79					Q	EX
80		22			Q	
81	0			EX		
143	15	34		Q		
144	163		Q			
145	540	575	Q			
146				Q		
147	479	500	Q			
148	33			Q		
149	33	33		Q		
150				Q		
151	33			Q		
152				Q		
153				Q		
154	502	585	Q			
155	239		Q			
156				Q		
157	132	130	Q			
158					Q	
159					Q	
160		475	Q			
161	77	85		Q		
162	33	16		Q		
163	33	26			Q	
164	38	40		Q		
165	33			Q		
166	33			Q		
167	33	9			Q	
168	33				Q	
169	118	125	Q			
170	33			Q		
171	33	65			Q	

TABLE XXI (Continued)

Three-stage Classification of Events

Event	NEIS depth	NEP depth	depth classification	long-and short-period data	short-period data only	correct classification
172	33			Q		
173	33			Q		
175	20			Q		
176					Q	
177	33			Q		
178	33	136	Q			
179	53	27		Q		
180					Q	
182	33			Q		
183		35		Q		
184	10				Q	
185	34			Q		
186				Q		
187				Q		
188				Q		
189	0			EX		
190	38	35		Q		
191					Q	
192				Q		
193				Q		
194					Q	
195	3			Q		
264	0120			Q		
265	0			EX		
266				EX		
267				EX		
268		1		EX		
269				EX		
270				EX		
271				Q		EX
272				Q		
273				EX		
274					EX	
275					unk.	EX
276	0				EX	
277	0			EX		
278	0				EX	
earthquakes correct		24		61	20	
earthquakes incorrect		0		1	0	
explosions correct		0		19	5	
explosions incorrect		0		1	1	
unidentified					1	

26 events using only short-period discriminants. One of these events was misclassified. It should be noted that the training sets used in calculating the discriminants applied in the second and third stages included the 24 events identified in stage one as being deep. It is doubtful that using only shallow events in the training sets would improve the discrimination, because some of the unknown events remaining after stage one are actually deep, and shallow-event discriminants might systematically misclassify them. In comparing Table XXI of this report with Table 10.4 of Dahlman and Israelson (1977), it should be remembered that short-period discriminants were applied in both the second and third stages in this report but in only the final stage by Dahlman and Israelson. It ought to be noted that several of the 24 events which could be identified as earthquakes on the basis of their depth were assigned uncertain classifications, denoted by asterisks, in Tables XVII and XVIII.

So far in the calculation of all the discriminant functions examined in this report it has been assumed that the misclassification of earthquakes is as undesirable as that of explosions. In practice, unidentifed explosions are a more serious error than are false alarms, so one might wish to adjust the discriminant functions to decrease the number of misclassified explosions, even if such adjustment increases, by a greater amount, the number of misclassified earthquakes. Such an adjustment can be made by assigning more weight in the discrimination algorithm to explosions. This assignation of weights may be interpreted geometrically as moving the discriminant hyperplane parallel to itself in the direction of the earthquake population so that all explosions, including the outliers, lie on the same side of the hyperplane's new position. For example, the three-variable discriminant function which uses only the short-period P-wave spectral ratios is given by

$$D(V_1, V_2, V_3) = -1.863\ V_1 - 1.727\ V_2 - 1.366\ V_3 + \text{const.} \qquad (34)$$

where (cf. Table XIV)

$$\begin{aligned} V_1 &= P_1 - 1.42\ P_2 \\ V_2 &= P_2 - 1.72\ P_3 \\ V_3 &= P_1 - 1.77\ P_3 \end{aligned} \qquad (35)$$

The value of the constant in equation (34) was -6.602 in the three-variable discriminant function which was used for classifying event 155 in Table XVIII.

As is shown there, this discriminant is highly unreliable, misclassifying six explosions and four earthquakes. The effect upon this discriminant of assigning more weight to explosions is shown in Table XXII. It is demonstrated that by changing the constant from -6.602 to -5.321, the total number of misclassifications is raised from ten to sixteen, but the number of misclassified explosions is reduced to two. By allowing the constant to take on some intermediate value (i. e., by assigning an intermediate weight to explosions) it is possible to satisfy some arbitrary criterion chosen as the most acceptable trade-off between the number of undetected explosions and the number of false alarms. In an actual discrimination routine it would probably be advantageous to choose some such optimum trade-off and then weight the two populations in the discriminant functions accordingly.

The multivariate discriminants which have thus far been described used a training set of between 51 and 121 events. The question will now be addressed: since all the "unknown" events (except the multiple explosions) had in fact been assigned a priori classifications, would the discrimination have worked as well on a suite of true unknowns? In order to investigate this question, certain of the multivariate discriminant functions were re-computed using only a fraction of events previously used in the training set. These new discriminants were then applied to all the events, including those which were not used in the training set and which may therefore be regarded as true unknowns. If the discrimination works almost as well using a small training set, then the discriminant functions are fairly stable, and the results described in this report may be applied to an actual discrimination routine with more confidence than they could be otherwise. It is shown in Table XXIII that the four variable discriminant was in fact rather stable against perturbations introduced by changing the training set. The performance of this discriminant was not greatly deteriorated by the use of 69 or even 34 events in the training set rather than the full suite of 103 events. Table XXIV shows that the classifications based on the eight-variable discriminant were scarcely changed when the training set was reduced from 71 events to 23, but this is misleading, since the misclassification rate tripled when 48 events were used. It is not surprising that an eight-variable discriminant function is poorly determined by 48 events, and it was on account of the likelihood of a similarly poor determination that no

TABLE XXII

Effect on a Three-variable Discriminant Function of Assigning More Weight to Explosions

discrimination variables (cf. Table XIV) : 1, 2, 3

constant term in the discriminant function		classification	
		shot	quake
-6.602	shot	14	6
	quake	4	84
		shot	quake
-6.219	shot	15	5
	quake	4	84
		shot	quake
-5.968	shot	16	4
	quake	6	82
		shot	quake
-5.740	shot	17	3
	quake	8	80
		shot	quake
-5.321	shot	18	2
	quake	14	74

TABLE XXIII

Effect on the Four-variable Discriminant
Function of Changing the Size of the Training Set

number of events in the training set		classification: shot	quake
7 shots	shot	14	7
27 quakes	quake	6	76
		shot	quake
14 shots	shot	14	7
55 quakes	quake	4	78
		shot	quake
21 shots	shot	16	5
82 quakes	quake	4	78

	probability of being an explosion: event 189	event 195
complete training set	0.500	0.012
delete event 189 only	0.468	0.011
delete event 195 only	0.498	0.013

TABLE XXIV

Effect on the Eight-variable Discriminant
Function of Changing the Size of the Training Set

number of events in the training set		classification: shot	quake
5 shots	shot	15	1
18 quakes	quake	3	52
		shot	quake
11 shots	shot	11	5
37 quakes	quake	4	51
		shot	quake
16 shots	shot	15	1
55 quakes	quake	2	53

	probability of being an explosion: event 189	event 195
complete training set	0.696	0.001
delete event 189 only	0.595	0.001
delete event 195 only	0.692	0.001

use was made of the discriminants involving fifteen or more variables but determined by 38 or fewer events (cf. Table XV). Tables XXIII and XXIV thus show that at least the four-and eight-variable discriminants are fairly well determined and may be used to classify events not contained in the training set with about the same degree of success as for the training set events.

The tables also show the results of another test of discriminant stability, namely the deletion of specific single events from the training set. The events which were selected for deletion were number 189, marginally classified by both the four-and eight-variable discriminants as an explosion, and number 195, strongly classified by both as an earthquake. Table XXIV shows that had either event not been assigned an a priori classification, it would still have been correctly classified by the eight-variable discriminant computed on the basis of the other 80 events in the training set. Table XXIII shows, however, that the deletion of event 189 from the training set of the four-variable discriminant function results in the misclassification of that event as an earthquake. This test shows that, as one would expect, the classification of data points lying close to the discriminant hyperplanes can change when the positions of the hyperplanes shift slightly, and such shifts do in fact occur when data points close to the hyperplanes are added to or are deleted from the training set. It was for this reason that the classification of events in Table XVII and XVIII was noted as uncertain if the probability of being an explosion was between 0.2 and 0.8. In an actual discrimination process, then, in which event 189 was a true unknown and hence was assigned no a priori classification, the four-variable discriminant would classify that event marginally as an earthquake. Had more events been used in the training set, however, the discriminant function might have been slightly different (such slight differences are not incompatible with the previous assertion of discriminant stability), and event 189 might have been classified marginally as an explosion. An operative discrimination routine would be a learning process in which newly-classified events would be added periodically to the training set and the discriminant functions would then be re-calculated. The a posteriori classification resulting from this re-calculation might reveal that some of the previous classifications of training set events are wrong or at least uncertain. Events with marginal classifications like event 189 should not be added to the training

set unless their classifications could be verified by independent information such as dilatational first motions, photographic evidence of cratering, etc. After the discriminant functions are re-calculated they should then be re-applied to the events with marginal classifications, and the resulting new classifications should be regarded as more reliable.

Although the tests which are shown in Tables XXIII and XXIV demonstrate that the discriminant functions are fairly insensitive to the total number of events used in the training set, there remains the possibility that the discriminants are sensitive to the geographical distribution of these events. No assessment can be made of the value of the discrimination techniques until it is determined to what extent, if any, the discrimination between the earthquake and explosion populations was actually discrimination between certain characteristics of the source regions of the two populations. If the discrimination is due to epicenter-to-receiver path effects rather then to source mechanisms, it will lose its value when applied to explosions in seismically active regions or to earthquakes at test sites. Some assurance that the discrimination was not solely a path effect may be gained by noticing that the data base did in fact include at least two examples of earthquakes and explosions occurring close to each other. Table I shows that event 21, an explosion, occurred at a distance of about 150 km from event 65, an earthquake. The multivariate discriminants correctly classified both of these Lake Baikal events. Table I also shows that event 264, an earthquake, occurred close to the Semipalatinsk explosions. This event was also classified correctly, so it seems that path effects did not dominate the multivariate discrimination. Certain individual discriminants may have been affected by differences between the earthquake and explosion source regions, however; in particular, it has already been noted that attenuation differences may have enhanced the discrimination power of the short-period P-wave spectral ratios. The differences in the attenuation coefficient t* for various source region-to-station paths are shown in Appendix IV.

It has been emphasized that the training set of events used for this report was not geographically homogeneous. The question is now addressed of whether there does indeed exist a single earthquake population and a single explosion population for all Eurasian events, as has been assumed in this

report, or whether there are in fact several distinct populations characteristic of different regions. If region-dependent populations exist, then the same discriminant functions may not work equally well for all of them. There may in fact exist anomalous regions for which the earthquake population has a large intersection with the total "Eurasian" explosion population or for which the explosions are contained within the "Eurasian" earthquake population. It must be known whether the discrimination is region-dependent before the results of this report may be applied to the classification of events occurring in regions not adequately sampled by the 129 events which were used in the training set. In order to test for the existence of regional sub-populations of the "Eurasian" earthquake population, a test was made of whether earthquakes in different tectonic regions may be discriminated from each other. This procedure will first be described, and then the results will be discussed.

Throughout this report it has been assumed that the process of discrimination consists of classifying unknown events as being members of one or the other of exactly two groups. Inspection of the formulas for the calculation of the discriminant functions (von Seggern and Rivers, 1979), however, shows that it is a straightforward process to generalize the discrimination to include an arbitrarily large number of groups, and the computer program (Jennrich, 1977) which was used for the multivariate analysis has the capability of performing multi-population discrimination. Discrimination between several groups involves the calculation of a different multivariate classification function for each pair of groups, a process which is geometrically equivalent to the determination of a set of hyperplanes whose intersection partitions space into cells, one cell per group. The classification function may then be applied to unknown events in order to determine in which cell they lie, i.e., to which population they belong. This process ought not to be confused with cluster analysis. Cluster analysis attempts to find how many statistically significantly different populations exist within a given training set, and then unknown events are assigned to one or another of those thus determined populations ("clusters"). Discriminant analysis, on the other hand, begins with an *a priori* specification of the number of populations and of which events in the training set belong to each one, and then unknown events are assigned to one

or another of those given populations. Cluster analysis thus determines the most statistically significant partitioning of the training set into groups, and the investigator must attempt to infer the physical basis for the similarity between the events in each group (explosions, shallow dip-slip earthquakes, earthquakes in Tibet, etc). In discriminant analysis the investigator specifies the criteria whereupon the events are to be grouped (explosions, strike-slip earthquakes in the Ural Mountains, earthquakes occuring on a Tuesday, etc.) and then the analysis reveals whether the groups are statistically significant, i. e., non-overlapping.

In order to evaluate the influence of the geographical distribution of events upon their classification, a multi-population discrimination was performed which attempted to determine whether earthquakes occurring in different tectonic regions were significantly different from one another. The results of this discrimination are shown in Table XXV. In the first test shown, the classification functions based on the three short-period P-wave spectral ratios were applied to three populations of events, namely earthquakes in Kamchatka, in Tibet, and in the Pamirs-Hindu Kush region. The table shows how many events were classified a posteriori into each group and also which events they were. It can be seen that with respect to the three chosen variables the Kamchatka and Tibet populations are rather different from each other, and the Pamirs population is quite different from both of them. The second test shows the addition of the three LR:P spectral ratios further separates the Kamchatka earthquakes from those in Tibet. Although these tests were, of necessity, based on a sparse data set, it appears that there may indeed exist regional sub-populations of the large population of earthquakes which was used for calculating the multivariate discriminant functions. Unfortunately, the data is too scanty to determine whether there also exist regional sub-populations of the explosion population. If such sub-populations do exist, then the discriminant functions may differ significantly from region to region, in which case the results of this report cannot be applied confidently to the discrimination of other suites of events. It is only when the discriminant functions are understood quantitatively on the basis of the physics of event source mechanisms and propagation path effects, rather than just on an empirical basis as in this report, that they may be applied to the classification of events occurring in regions not sampled by the training set.

TABLE XXV

Discrimination Between Earthquakes in Different Tectonic Regions

discrimination variables (cf. Table XIV)	classification			
1, 2, 3		Kamchatka	Tibet	Pamirs
	Kamchatka	11: 50, 64, 143, 148, 157 165, 169, 171, 178, 180 182	5: 146, 156, 158, 176, 193	2: 58, 183
	Tibet	6: 7, 27, 30, 34, 190 191	9: 31, 32, 35, 39, 46 68, 75, 151, 166	3: 24, 27, 29
	Pamirs	1: 72	2: 9, 26	10: 10, 28, 41, 45, 48, 67, 70, 155, 161, 179
1, 2, 3, 15, 16, 17		Kamchatka	Tibet	
	Kamchatka	8: 50, 143, 148, 156, 165 169, 182, 183	2: 64, 178	
	Tibet	2: 7, 151	10: 27, 29, 30, 34, 35 39, 46, 68, 166, 190	

It has already been pointed out that systematic errors may have occurred in the computation of the magnitudes of deep events. Certain other systematic errors may have been made which affected all the events equally. Specifically, no station corrections were applied for any station, and magnitude biases may have been thereby introduced into the network averages. The station corrections which should be applied for a given station are a function both of the phase (e.g., LP or LS) and of the frequency (e.g., P_2 or P_3). These corrections should be determined by comparing the magnitudes of each measured parameter at a single station with the values obtained by averaging over the network. Unfortunately, so many measurements used in computing the network magnitudes were noise levels and so many different sub-networks of stations were used for different events that such a calculation employing this data base could yield only questionable results. Station corrections would best be determined by using a data base of large events, which would be detected with a high signal-to-noise ratio at all stations of a network which remains constant from event to event. In any case, we note that the addition of station corrections to the magnitudes would have changed the values calculated by the Ringdal (1976) algorithm, perhaps (at least in some cases) by a significant amount.

A subtle bias may have been introduced into the calculation of the magnitudes for many of the events by the geographical distribution of stations in the network. Specifically, the use of all five stations BFAK, UCAK, NJAK, CNAK, and TNAK may have placed undue emphsis on signals recorded in one small sector of the radiation pattern for events teleseismic to Alaska. This problem could be particularly acute if these stations were close to a node in the radiation pattern for one or more of P, SH, SV, LR, or LQ. This potential bias might be investigated by computing network magnitude estimates using only one of these five stations and then repeating the discrimination analysis in order to see whether the discrimination capability of the network was thereby significantly diminished or, at least for certain events, somewhat enhanced. Another way of testing whether too much weight was given to the Alaskan sites would be to assign each of the stations a weight of one-fifth when computing the network magnitude estimates. The procedure of deleting certain stations from the network and repeating the discrimination could also be applied to each of the twenty-seven stations one at a time in order to gain some assessment of the contribution of each station (perhaps in a negative sense) to the

network discrimination capability . This assessment could then be used in assigning weights to the stations, and these in turn could be used to calculate new values of the network magnitude estimates. As was pointed out in the discussion of station corrections, however, the over-abundance of noise measurements relative to signals and the inconstancy from event to event of the sub-network of stations which were actually used would tend to introduce a large element of uncertainty into such an assignment of weights.

CONCLUSIONS

The following conclusions may be drawn from the statistical discrimination experiment described in this report:

1) Inclusion of SRO/ASRO stations in the data base increases the volume of useful long-period data, thereby enhancing the discrimination capability. Stations KAAO and MAIO, being close to the Area of Interest, are particularly useful for detecting long-period signals. The beam-forming capabilities of the four large arrays make them valuable for this purpose also.

2) Inclusion of SRO/ASRO stations helps better determine the parameters which are used for short-period discrimination. The SNR at these stations is good, but as is shown in Figure 1, weak signals are systematically unreported.

3) Whenever an event is large enough for surface waves to be detected, M_s:m_b is a valuable discriminant. Its value is even greater when Love waves rather than Rayleigh waves are used to measure M_s.

4) If a seismogram contains no visible signal in the data window surrounding a predicted arrival time, the level of the background noise in that window should be measured for use in a maximum-likelihood estimate of the magnitude of the unseen signals.

5) Even if a certain signal is undetected at every station in the network, an upper bound to the magnitude of that signal can be computed from noise measurements. This upper bound may (or may not) be useful for negative discrimination.

6) Deep earthquakes are more prone to misclassification than are shallow ones. Hypocentral locations and the detection of depth phases should therefore be used in order to eliminate as many deep events as possible from the data base of unknowns before the statistical discrimination is performed.

7) Deep earthquakes and multiple explosions are especially prone to misclassification on the basis of P-wave signal complexity. Application of the criterion shown in equation (33) may reduce the number of misclassifications due to complexity.

8) As is shown in Figure 19, the observation of dilatant first motions may be used to identify as earthquakes some events which the purely statistical discrimination process would misclassify as explosions.

9) In order to avoid problems introduced by a magnitude bias between the explosion and earthquake populations, spectral ratios of the form ($\text{magnitude}_1 - \text{coefficient} \cdot \text{magnitude}_2$) should be used as discrimination variables, rather than the magnitudes themselves.

10) Multivariate discrimination is preferable to any particular univariate discriminant. The multivariate discrimination should employ as many variables as possible for any given unknown event, as long as the discriminant function was calculated using a suitably large training set of events whose classification is known a priori.

11) Statistical discrimination should be a learning process. When a group of unknown events has been classified by the multivariate analysis, it should then be added to the training set used to calculate the discrimination variables and the multivariate discriminant functions. As the data base enlarges, the discrimination becomes more reliable, and it may then be concluded from a posteriori classifications that some of the classifications of events in the training set are wrong. Events which could be classified only marginally should not be added to the training set unless their classifications can be verified by independent evidence. As the training set expands, classifications previously noted as uncertain should be repeated.

RECOMMENDATIONS

The authors make the following recommendations for future research pertaining to seismic discrimination:

1) A determination of station corrections should be made for P-, S-, and surface waves in every frequency band in order to eliminate station bias from the network estimates of event magnitudes.

2) Weights should be assigned to each station in the network for use in the calculation of event magnitudes. These weights should be determined on the basis of the scatter in the magnitude calculation, i. e., the repeatibility of measurement, at each station. Considering a large group of events having the same network-averaged magnitude, the station bias at some given station is the difference between that common magnitude and the average of the individual magnitudes measured at that station for the events in the group, and the weight which should be assigned to the station is inversely proportional to the size of the "error bars" around that average magnitude.

3) Because the individual discriminants employed in this study have been empirically determined, an investigation should be made of their physical basis. Such an investigation would attempt to determine circumstances under which particular discriminants might be useless or misleading, as was the case, for example, with complexity for deep earthquakes. This study would address the question of whether the discriminant lines shown in Figures 15 and 16 are in fact straight lines or whether they bend at low (or high) magnitudes, whether their slopes can be theoretically predicted, as was the case in Figure 17, whether these discriminants are sensitive to the ambient stress level or to the geological medium at the source, etc.

4) A study should be made of the influence exerted upon the discrimination by the geographical distribution of events used in the training set. It has already been noted that serious questions may be raised about the reliability of a discriminant function which was calculated using earthquakes in one geographical region and explosions in another. Still more questions may be raised about the applicability

of this discriminant function to unknown events which occur in some third region. Only when a quantitative assessment can be made of the various source region and propagation path effects can the statistical discrimination techniques be applied with confidence to those circumstances in which they would most be needed in actual practice, namely explosions detonated at previously unknown test sites.

5) An effort should be made to identify and analyze anomalous events which are especially prone to misclassification.

6) A discrimination experiment should be performed which uses Pearce's (1977) algorithm based on the detection or non-detection of pP and sP. This experiment would determine both the reliability and the magnitude threshold of the applicability of this technique relative to that of the statistical techniques investigated in this report.

7) A comparison should be made between the teleseismic discriminants used in this report and regional discriminants based upon such phases as Pg and Lg. Such a study would reveal whether the use of stations located within the Area of Interest would enhance discrimination as well as detection. This study should use events in the Southwestern United States in order to insure uniformity of the regional paths for signals from both explosions and earthquakes.

Pearce, R. G. (1977). Fault plane solutions using relative amplitudes of P and pP, Geophys J. R. Astr. Soc., 50, 381.

ACKNOWLEDGEMENTS

We appreciate the assistance in this project of J. R. Woolson and his group, especially J. McNear, B. D. Dillard, and K. C. Smith, who have, on an almost daily basis, rectified various problems which were encountered in processing the digital data. The authors have benefited greatly from many discussions with R. R. Blandford at all stages throughout this experiment. We are also indebted to A. C. Chang for a discussion of the multiple P arrivals such as are shown in Figure 8.

The authors would especially like to express their gratitude to J. A. Burnetti, P. J. Klouda, I. Megyesi, and G. R. Naylor, whose diligence in the visual analysis of the huge data base reflected in Table V was the sine qua non of this experiment.

REFERENCES

Ben-Menahem, A., S. W. Smith, and T. L. Teng (1965). A procedure for source studies from spectrums of long-period seismic body waves, Bull. Seism. Soc. Am., 55, 203.

Booth, D. C., P. D. Marshall, and J. B. Young (1974). Long and short period P-wave amplitudes from earthquakes in the range 0°-114°, Geophys. J. R. Astr. Soc., 39, 523.

Dahlman, O., and H. Israelson (1977). Monitoring Underground Nuclear Explosions, Elsevier North Holland Inc., New York.

Gutenberg, B. (1945). Amplitudes of P, PP and S and magnitudes of shallow earthquakes, Bull. Seism. Soc. Am., 35, 57.

Gutenberg, B., and C. F. Richter (1956). Magnitude and energy of earthquakes, Annali Geofisica, 9, 1.

Hanks, T., and W. Thatcher (1972). A graphical representation of seismic source parameters, J. Geophys. Res., 77, 4393.

Jennrich, R. I. (1977). Stepwise discriminant analysis, in Statistical Methods for Digital Computers, edited by K. Enslein, A. Ralston, and H. S. Wiff, John Wiley and Sons, New York.

Mitchell, B. J., L. W. B. Leite, Y. K. Yu, and R. B. Herrmann (1976). Attenuation of Love and Rayleigh waves across the Pacific at periods between 15 and 110 seconds, Bull. Seism. Soc. Am., 66, 1189.

Pearce, R. G. (1977). Fault plane solutions using relative amplitudes of P and pP, Geophys J. R. Astr. Soc., 50, 381.

Ringdal, F. (1976). Maximum-likelihood estimate of event magnitude, Bull. Seism. Soc. Am., 66, 789.

Rivers, D. W., D. H. von Seggern, B. L. Elkins, P. J. Klouda, J. A. Burnetti, and I. Megyesi (1979). (S) A statistical discrimination experiment for Eurasian events using the Priorities I and II networks (U), SDAC Report No. TR-79-2, Teledyne Geotech, Alexandria, Virginia.

Romney, C. (1959). Amplitudes of seismic body waves from underground nuclear explosions, J. Geophys. Res., 64, 1489.

Sato, R., (1967). Attenuation of seismic waves, J. Phys. Earth, 15, 32.

Sobel, P. A., and D. H. von Seggern (1976). Study of selected events in the Tien Shan region in a seismic discrimination context, SDAC Report No. TR-76-9, Teledyne Geotech, Alexandria, Virginia.

Sobel, P. A., D. H. von Seggern, E. I. Sweetser, and D. W. Rivers (1977a). Study of selected events in the Pamirs in a seismic discrimination context, SDAC Report No. TR-77-3, Teledyne Geotech, Alexandria, Virginia.

Sobel, P. A., D. H. von Seggern, E. I. Sweetser, and D. W. Rivers (1977b). Study of selected events in the Baikal Rift Zone in a seismic discrimination context, SDAC Report No. TR-77-5, Teledyne Geotech, Alexandria, Virginia.

Sobel, P. A., D. H. von Seggern, E. I. Sweetser, and D. W. Rivers (1977c). Study of selected events in the Caucasus in a seismic discrimination context, SDAC Report No. TR-77-6, Teledyne Geotech, Alexandria, Virginia.

Sobel, P. A., and D. H. von Seggern (1978). Analysis of selected seismic events from Asia in a seismic discrimination context, SDAC Report No. TR-78-5, Teledyne Geotech, Alexandria, Virginia.

Veith, K., and G. Clawson (1972). Magnitudes from short-period P-wave data, Bull. Seism. Soc. Am., 62, 435.

von Seggern, D. H., and D. W. Rivers (1978). Comments on the use of truncated distribution theory for improved magnitude estimation, Bull. Seism. Soc. Am., 68, 1543.

von Seggern, D. H., and D. W. Rivers (1979). Seismic discrimination of earthquakes and explosions with application to the Southwest United States, SDAC Report No. TR-77-10, Teledyne Geotech, Alexandria, Virginia.

von Seggern, D. H., and P. A. Sobel (1977). Study of selected Kamchatka earthquakes in a seismic discrimination context, SDAC Report No. TR-76-10, Teledyne Geotech, Alexandria, Virginia.

APPENDIX I

Network estimates of parameters measured for each event

NETWORK ESTIMATES (RINGDAL MAXIMUM-LIKELIHOOD ALGORITHM) OF THE MAGNITUDES OF THE 27 PARAMETERS IN TABLE VI

ASTERISK INDICATES UPPER BOUND (AT THE NINETY PER CENT CONFIDENCE LEVEL) BASED ON NOISE ONLY

	EVENT :	1	3	4	6	7	8	9	10	14	16	17	18
1	P1	4.730	4.210	* 4.080	* 4.060	4.290	* 4.890	4.410	3.970	4.270	4.460	4.530	4.630
2	P2	4.080	3.480	3.490	* 2.820	3.740	* 3.390	2.260	2.770	4.010	4.122	3.940	4.307
3	P3	3.100	2.270	2.740	* 2.000	2.710	* 2.800	1.980	2.210	3.340	3.340	3.350	3.400
4	OMEGA-2	5.627	5.385	3.868	0.0	5.835	0.0	0.0	3.930	4.948	5.613	5.196	5.506
5	CR.FR-2	-0.028	-0.016	0.670	0.0	-0.366	0.0	0.0	0.697	0.201	0.015	0.307	0.109
6	T*-2	0.0	0.0	0.0	0.0	0.0	0.0	0.0	0.0	0.0	0.0	0.0	0.0
7	OMEGA-3	5.584	5.700	4.073	0.0	5.991	0.0	0.0	4.130	4.971	5.706	5.088	5.792
8	CR.FR-3	0.177	-0.048	0.697	0.0	-0.271	0.0	0.0	0.697	0.350	0.162	0.505	0.033
9	T*-3	0.0	0.0	0.0	0.0	0.0	0.0	0.0	0.0	0.0	0.0	0.0	0.0
10	COMP1	-0.557	-0.042	0.0	0.0	-0.263	-0.175	0.005	-0.020	-0.437	-0.639	-0.514	-0.553
11	COMP2	-0.647	-0.182	0.0	0.0	0.018	0.0	-0.259	-0.515	-0.493	-0.273	-0.623	-0.615
12	COMP3	-0.761	-0.335	0.0	0.0	-0.486	-0.916	-0.237	-0.599	-0.722	-0.406	-0.928	-0.624
13	LG1	0.0	* 8.473	7.620	8.580	0.0	0.0	0.0	7.023	7.225	7.287	* 9.105	* 8.785
14	LG2	0.0	* 7.213	* 6.790	7.220	0.0	0.0	0.0	6.727	* 6.783	* 6.199	* 7.877	* 6.699
15	LG3	0.0	* 6.300	* 6.290	6.380	0.0	0.0	0.0	4.630	5.020	5.510	5.790	6.620
16	LP1	* 5.880	5.410	5.760	* 7.580	5.340	* 5.840	5.140	* 5.020	4.910	* 5.370	* 5.790	5.640	* 6.880
17	LP2	* 6.000	* 5.690	5.700	* 7.700	5.550	* 5.920	* 5.200	4.910	* 5.370	* 6.250	* 6.560	6.700	* 7.660
18	LP3	* 6.630	6.370	6.490	* 8.030	6.580	* 6.710	6.480	5.790	* 6.250	* 6.560	* 6.680	6.110	* 7.000
19	LS1	* 6.180	5.820	5.830	7.680	5.410	* 5.890	* 5.810	5.470	* 5.580	* 5.680	* 5.840	6.240	* 6.980
20	LS2	* 6.250	6.030	6.140	* 7.640	5.720	* 5.870	* 6.020	* 5.730	* 5.940	* 5.840	* 6.560	7.750	* 8.020
21	LS3	* 7.120	6.440	* 6.970	8.220	* 7.130	* 6.910	* 6.660	* 6.550	* 7.060	* 6.560	4.370	4.310	* 5.590
22	LR1	3.810	4.130	4.610	5.680	4.340	* 4.300	4.040	4.480	4.400	4.370	4.820	4.480	* 5.660
23	LR2	4.190	5.070	4.990	6.160	4.690	4.060	4.380	4.390	4.140	4.820	4.940	4.670	5.520
24	LR3	4.310	5.290	5.190	6.040	4.520	4.290	4.470	* 4.280	4.210	4.940	4.420	4.420	* 5.640
25	LQ1	3.890	4.960	4.430	5.930	4.270	* 4.390	4.470	4.490	4.270	4.420	4.640	4.840	* 5.610
26	LQ2	4.180	5.240	4.700	6.210	4.460	* 4.070	4.510	3.850	4.240	4.640	* 4.880	* 5.440
27	LQ3	4.550	5.330	4.680	* 6.180	4.630	* 4.450	4.510	* 4.190	4.400	4.800		

	EVENT :	19	20	21	22	23	24	25	26	27	28	29	30
1	P1	5.382	5.570	4.590	4.820	* 4.020	4.000	4.030	3.760	4.390	4.080	4.000	5.640
2	P2	4.857	4.953	4.140	4.100	* 2.560	2.480	3.110	2.770	3.710	3.260	3.270	4.700
3	P3	4.010	4.280	3.366	3.685	* 2.080	2.170	2.010	1.960	2.720	2.950	2.790	3.630
4	OMEGA-2	6.224	6.245	5.382	5.357	0.0	7.191	5.995	3.805	5.164	4.578	5.105	6.966
5	CR.FR-2	-0.035	0.129	0.089	0.112	0.0	-0.289	-0.177	0.697	0.192	0.697	-0.526	-0.446
6	T*-2	0.0	0.0	0.0	0.0	0.0	0.0	0.0	0.0	0.0	0.0	0.0	0.0
7	OMEGA-3	6.133	6.303	5.495	5.436	0.0	7.349	6.386	3.920	5.394	4.772	4.731	7.197
8	CR.FR-3	0.167	0.242	0.165	0.175	0.0	0.0	-0.266	0.697	0.153	0.697	0.020	-0.419
9	T*-3	0.0	0.0	0.0	0.0	0.0	0.0	0.0	0.0	0.0	0.0	0.0	0.0
10	COMP1	-0.352	-0.470	-0.514	-0.840	-0.443	0.366	-0.274	0.0	-0.100	0.0	-0.160	0.195
11	COMP2	-0.402	-0.454	-0.552	-0.923	-1.885	0.348	-0.125	0.0	-0.227	0.0	-0.311	0.094
12	COMP3	-0.546	-0.559	-0.699	-1.021	0.0	0.131	-0.125	0.0	-0.733	0.0	-0.192	-0.160
13	LG1	9.029	* 8.732	* 9.060	* 9.071	* 7.968	* 8.375	* 8.593	* 7.021	8.200	7.910	* 8.690	* 8.890
14	LG2	* 7.487	* 7.428	* 7.391	* 8.041	* 6.804	* 7.352	* 7.456	6.660	7.370	7.270	7.550	* 7.490
15	LG3	* 6.995	* 6.831	* 6.425	* 7.225	* 6.789	* 7.250	* 7.208	6.449	6.270	6.890	* 7.190	* 6.990
16	LP1	5.290	* 5.850	5.640	* 6.110	* 6.010	* 5.890	* 5.820	* 5.310	5.650	5.180	5.080	7.770
17	LP2	5.300	* 5.990	5.740	* 6.250	* 6.260	* 6.120	* 6.040	* 5.570	* 5.990	* 5.660	* 5.300	7.690
18	LP3	6.500	6.640	6.780	* 6.680	* 7.260	* 7.270	* 7.090	* 6.710	* 7.000	6.610	6.160	8.300
19	LS1	5.990	6.050	* 5.560	6.030	* 6.100	6.030	* 5.940	* 5.950	* 6.130	5.640	5.670	8.700
20	LS2	6.120	6.160	* 5.840	6.320	* 6.210	6.020	* 6.090	* 6.290	* 6.210	5.950	5.820	8.580
21	LS3	6.370	7.300	* 7.030	* 6.730	* 6.940	* 7.420	* 7.290	* 6.980	* 7.240	* 6.950	* 6.870	9.350
22	LR1	4.690	* 4.690	* 4.800	5.170	* 4.460	4.700	5.010	* 4.250	5.430	* 4.120	4.710	7.970
23	LR2	5.450	5.030	* 4.840	5.430	* 4.370	4.980	4.960	4.520	5.840	* 3.930	4.970	8.118
24	LR3	5.720	5.260	* 5.260	5.120	* 4.570	4.620	4.810	4.560	5.110	* 4.160	4.960	7.760
25	LQ1	4.870	5.020	* 4.010	5.140	* 4.540	5.060	5.020	4.070	5.770	3.820	5.010	7.970
26	LQ2	5.140	5.300	* 4.160	5.110	* 4.310	4.940	5.080	4.180	5.690	3.850	4.830	8.120
27	LQ3	5.450	5.330	* 4.390	4.450	* 4.270	4.620	5.120	4.600	5.430	3.970	4.980	7.840

NETWORK ESTIMATES (RINGDAL MAXIMUM-LIKELIHOOD ALGORITHM) OF THE MAGNITUDES OF THE 27 PARAMETERS IN TABLE VI

ASTERISK INDICATES UPPER BOUND (AT THE NINETY PER CENT CONFIDENCE LEVEL) BASED ON NOISE ONLY

	EVENT :	31	32	33	34	35	36	37	38	39	41	45	46
1	P1	4.460	4.340	4.240	4.230	4.680	4.520	4.120	* 4.210	4.290	4.330	4.430	4.080
2	P2	3.660	3.450	3.680	3.360	3.640	3.370	3.220	* 2.470	3.590	3.770	3.000	2.950
3	P3	2.060	* 2.200	2.930	2.520	2.490	2.420	2.340	1.760	1.990	3.100	2.580	1.930
4	OMEGA-2	5.657	5.438	4.941	5.682	5.828	7.686	4.947	0.0	5.595	5.266	6.071	5.418
5	CR.FR-2	0.070	0.105	0.255	-0.310	-0.243	-0.687	0.129	0.0	0.007	-0.037	-0.681	-0.014
6	T*-2	0.0	0.0	0.0	0.0	0.0	0.0	0.0	0.0	0.0	0.0	0.0	0.0
7	OMEGA-3	6.043	5.598	5.141	6.348	6.400	7.910	5.073	0.0	5.669	5.298	5.722	5.826
8	CR.FR-3	-0.030	0.110	0.178	-0.578	-0.480	-0.680	0.148	0.0	0.092	0.017	-0.206	-0.205
9	T*-3	0.0	0.0	0.0	0.0	0.0	0.0	0.0	0.0	0.0	0.0	0.0	0.0
10	COMP1	-0.994	-0.716	-0.226	0.0	-0.031	-0.221	0.127	-0.337	-0.392	-0.021	-0.023	-0.617
11	COMP2	-0.875	-0.316	-0.240	0.0	-0.104	-0.314	0.097	-0.346	-0.354	-0.291	0.069	-0.263
12	COMP3	-0.052	-0.360	-0.637	0.0	-0.206	-0.034	-0.114	0.0	0.054	-0.492	0.0	-0.121
13	LG1	* 8.110	* 8.202	* 9.081	8.470	8.530	0.0	* 8.995	* 9.036	* 8.760	* 7.594	* 7.712	* 8.935
14	LG2	* 6.810	* 7.081	* 7.756	* 7.490	* 7.490	0.0	* 7.451	* 7.664	* 7.690	* 6.676	* 6.827	* 7.539
15	LG3	* 6.440	* 7.068	* 7.016	* 6.890	* 6.890	0.0	* 6.429	* 6.799	7.230	* 5.893	* 6.652	* 6.785
16	LP1	* 7.530	* 6.670	* 6.110	* 5.590	6.420	* 6.230	* 5.800	* 6.000	5.790	* 5.580	* 5.270	* 5.680
17	LP2	* 7.640	* 6.730	5.840	* 5.780	6.420	* 6.480	* 6.020	* 6.180	* 5.640	* 5.830	* 5.570	* 5.600
18	LP3	* 8.340	* 7.410	* 7.050	* 7.000	7.200	* 7.340	* 6.550	* 7.240	6.390	* 6.960	* 6.390	* 6.640
19	LS1	* 8.160	7.050	* 6.400	6.060	7.230	5.370	* 5.970	* 6.290	6.680	* 6.010	5.580	* 5.990
20	LS2	* 8.080	6.770	* 6.350	5.960	7.060	* 5.940	* 5.850	* 6.430	6.520	* 6.290	6.150	* 6.060
21	LS3	* 8.620	* 7.740	* 7.210	6.740	7.780	6.530	* 7.020	* 7.360	7.380	* 7.530	6.990	* 7.390
22	LR1	* 6.160	5.160	4.970	4.840	6.150	* 4.340	4.600	4.260	5.720	* 4.490	4.340	4.250
23	LR2	* 6.550	* 5.470	5.540	5.120	6.319	* 4.220	5.230	5.210	5.940	* 4.430	4.230	4.240
24	LR3	* 6.620	* 5.400	5.190	5.300	6.080	* 4.990	5.390	4.830	5.820	* 4.820	3.970	4.620
25	LQ1	* 6.330	5.090	4.750	5.190	6.280	* 4.500	5.190	4.420	5.780	* 4.070	4.550	4.430
26	LQ2	* 6.640	* 5.470	4.790	5.270	6.405	* 4.510	5.300	4.910	5.910	* 3.940	4.310	* 4.370
27	LQ3	* 6.700	5.220	* 4.850	5.400	6.270	* 4.960	5.410	4.940	5.770	* 4.100	4.470	* 4.640

	EVENT :	47	48	49	50	53	55	56	57	58	59	60	61
1	P1	4.500	4.300	5.070	5.030	5.410	4.250	* 4.550	3.660	3.950	4.380	* 4.180	4.380
2	P2	3.700	3.520	4.090	4.131	4.792	3.100	* 3.290	3.420	2.340	3.400	* 2.860	2.950
3	P3	3.030	2.790	3.310	3.010	4.101	* 2.150	* 2.680	2.250	1.970	2.770	2.370	2.580
4	OMEGA-2	5.886	4.964	6.036	6.272	6.327	4.779	0.0	5.043	0.0	4.827	0.0	4.844
5	CR.FR-2	-0.355	0.300	-0.309	-0.281	-0.216	-0.034	0.0	0.067	0.0	0.110	0.0	0.141
6	T*-2	0.0	0.0	0.0	0.0	0.0	0.0	0.0	0.0	0.0	0.0	0.0	0.0
7	OMEGA-3	6.081	4.901	6.198	6.397	6.323	4.738	0.0	5.042	0.0	4.805	0.0	4.996
8	CR.FR-3	-0.293	0.437	-0.228	-0.227	0.062	0.211	0.0	0.193	0.0	0.335	0.0	0.252
9	T*-3	0.0	0.0	0.0	0.0	0.0	0.0	0.0	0.0	0.0	0.0	0.0	0.0
10	COMP1	-0.484	-0.859	-0.380	-0.199	-0.385	-0.370	0.0	-0.115	-0.292	0.0	0.0	-0.018
11	COMP2	-0.535	-1.129	-0.312	-0.253	-0.453	-0.283	0.0	-0.081	-1.054	0.0	0.109	-0.609
12	COMP3	-0.546	0.0	-0.398	-0.556	-0.698	-0.504	0.0	-0.258	-0.731	0.0	0.0	0.0
13	LG1	0.0	* 9.096	* 8.418	* 8.573	* 8.594	* 8.427	0.0	* 8.555	0.0	8.080	0.0	8.159
14	LG2	0.0	* 7.856	* 7.080	* 7.112	* 7.767	* 7.156	0.0	* 7.145	0.0	7.580	0.0	7.307
15	LG3	0.0	* 7.057	* 6.351	6.668	* 6.994	* 6.445	0.0	* 6.326	0.0	6.950	0.0	* 6.590
16	LP1	* 5.510	* 5.160	6.390	5.990	5.400	* 5.820	* 6.090	* 6.030	* 6.020	5.620	* 5.420	5.810
17	LP2	* 5.940	* 5.400	6.770	* 6.430	* 5.680	* 5.990	* 6.150	* 6.180	* 6.240	5.390	* 5.830	6.230
18	LP3	* 6.990	* 6.370	7.450	6.800	* 6.780	* 7.280	* 7.310	* 7.160	6.840	6.330	* 6.470	7.240
19	LS1	6.110	* 5.830	6.990	6.970	6.170	* 5.940	* 6.040	* 6.150	6.240	* 6.110	* 5.630	6.070
20	LS2	6.250	* 6.140	6.970	6.910	6.380	* 6.170	* 6.260	* 6.230	* 6.360	* 6.190	* 5.970	6.490
21	LS3	7.600	* 7.110	8.000	7.520	7.370	* 7.090	* 7.030	* 7.110	7.040	* 6.890	* 6.700	6.920
22	LR1	6.240	* 4.260	6.070	5.390	4.960	* 4.590	* 4.510	* 4.650	4.790	4.610	* 4.160	4.460
23	LR2	6.290	4.320	6.420	6.390	5.260	* 4.690	5.040	* 4.800	4.980	4.930	* 4.340	4.890
24	LR3	5.540	4.690	5.990	6.300	5.320	* 4.700	5.250	* 4.970	* 4.910	4.900	* 4.650	4.960
25	LQ1	6.490	* 4.300	5.890	6.190	4.630	* 4.710	4.780	* 4.830	4.550	5.140	* 4.150	4.400
26	LQ2	6.480	* 4.100	6.100	6.620	5.130	* 4.580	5.040	* 4.870	4.820	5.060	* 4.210	4.910
27	LQ3	5.950	* 4.370	5.890	6.460	5.240	* 4.740	5.020	* 4.950	4.930	5.250	* 4.640	4.530

NETWORK ESTIMATES (RINGDAL MAXIMUM-LIKELIHOOD ALGORITHM) OF THE MAGNITUDES OF THE 27 PARAMETERS IN TABLE VI

ASTERISK INDICATES UPPER BOUND (AT THE NINETY PER CENT CONFIDENCE LEVEL) BASED ON NOISE ONLY

	EVENT :	62	63	64	65	66	67	68	69	70	72	73	74
1	P1	3.870	4.350	4.020	3.560	3.970	4.140	4.200	* 3.969	3.820	4.160	4.510	* 3.590
2	P2	3.580	3.720	3.400	2.490	2.360	3.490	3.200	* 3.115	3.050	3.440	3.920	2.870
3	P3	2.650	2.910	2.360	2.260	2.150	2.740	2.040	* 2.888	2.400	2.620	3.380	2.450
4	OMEGA-2	5.110	5.170	5.192	5.468	0.0	4.964	5.003	0.0	4.233	5.566	5.584	3.909
5	CR.FR-2	0.165	-0.024	-0.021	-0.260	0.0	0.286	-0.144	0.0	0.687	-0.183	-0.072	0.697
6	T*-2	0.0	0.0	0.0	0.0	0.0	0.0	0.0	0.0	0.0	0.0	0.0	0.0
7	OMEGA-3	5.186	5.187	5.331	5.347	0.0	5.121	5.493	0.0	4.441	5.629	5.654	4.109
8	CR.FR-3	0.282	0.150	0.033	0.065	0.0	0.329	-0.302	0.0	0.386	-0.046	0.113	0.697
9	T*-3	0.0	0.0	0.0	0.0	0.0	0.0	0.0	0.0	0.0	0.0	0.0	0.0
10	COMP1	-0.580	-0.671	-0.361	-0.104	0.171	-0.161	-0.507	0.0	-0.247	-0.240	-0.086	0.0
11	COMP2	-0.454	-0.737	-0.281	-0.734	-0.539	0.296	-0.141	0.0	0.024	-0.683	-0.071	0.0
12	COMP3	-0.464	-1.063	-0.446	-0.399	-0.595	0.046	0.0	0.0	0.0	-0.849	-0.100	0.0
13	LG1	0.0	* 8.300	* 8.684	* 8.643	8.047	7.840	8.370	7.700	7.260	* 7.750	* 8.590	7.370
14	LG2	0.0	* 6.808	* 7.279	* 7.291	* 7.154	7.170	* 7.390	6.810	6.640	* 6.860	* 7.490	6.830
15	LG3	0.0	* 6.091	* 6.630	* 6.500	* 6.628	6.890	* 6.890	6.670	6.753	* 6.576	* 6.890	6.710
16	LP1	5.500	* 5.690	* 5.870	* 5.330	* 5.350	* 5.080	* 5.340	* 5.020	* 5.060	5.280	5.800	* 5.770
17	LP2	* 5.750	* 5.970	* 6.140	* 5.500	* 5.640	* 5.390	* 5.590	* 5.170	* 5.240	5.380	5.910	* 5.740
18	LP3	* 7.170	* 6.910	* 6.970	* 6.370	* 6.370	* 6.480	* 6.270	* 6.690	* 6.510	* 6.660	6.470	* 6.810
19	LS1	* 5.920	* 6.040	* 5.800	* 5.570	* 5.350	* 5.580	6.100	* 5.970	* 6.070	5.300	6.040	* 5.790
20	LS2	* 6.230	* 6.270	5.590	* 5.820	* 5.750	* 6.090	6.260	* 6.330	* 6.270	5.630	6.150	* 5.840
21	LS3	* 6.900	* 7.440	6.710	* 6.650	* 6.770	* 7.180	6.940	* 7.180	* 7.480	6.700	6.960	* 7.230
22	LP1	5.010	3.900	4.920	* 4.290	3.750	* 4.290	4.850	3.730	* 3.980	4.270	4.560	* 4.510
23	LP2	5.330	4.270	5.090	* 4.350	3.690	* 4.380	5.280	3.410	* 3.730	3.920	5.490	* 4.450
24	LP3	5.620	4.360	5.220	* 4.680	* 4.290	* 4.700	5.390	3.420	* 3.670	4.220	5.640	* 4.380
25	LQ1	5.090	* 4.390	4.830	* 4.370	* 4.060	* 4.230	5.220	3.700	* 4.070	4.330	5.320	* 4.730
26	LQ2	5.080	* 4.240	5.080	* 4.150	* 3.960	* 4.310	5.290	3.560	* 3.870	4.260	5.460	* 4.320
27	LQ3	5.500	* 4.420	4.620	* 4.550	* 4.320	* 4.590	5.400	3.890	* 3.750	4.510	5.560	* 4.250

	EVENT :	75	76	77	78	79	80	81	143	144	145	146	147
1	P1	4.410	* 3.890	4.950	4.040	3.890	3.950	5.490	5.498	4.270	4.630	4.320	5.280
2	P2	2.550	* 2.510	4.243	* 2.540	3.400	2.960	5.046	4.506	3.710	4.060	3.500	4.621
3	P3	2.080	1.850	3.255	1.570	2.620	1.880	4.055	3.481	2.990	3.210	2.220	4.090
4	OMEGA-2	5.065	0.0	5.858	0.0	5.189	4.630	6.414	6.745	5.118	5.532	5.250	5.945
5	CR.FR-2	-0.318	0.0	-0.039	0.0	-0.317	-0.043	-0.068	-0.391	0.416	-0.162	-0.001	0.023
6	T*-2	0.0	0.0	0.0	0.0	0.0	0.0	0.0	0.0	0.0	0.0	0.0	0.0
7	OMEGA-3	4.744	0.0	6.007	0.0	5.292	4.806	6.542	7.006	5.269	5.630	5.442	6.108
8	CR.FR-3	0.177	0.0	-0.002	0.0	-0.149	-0.008	0.055	-0.369	0.292	0.009	0.066	0.076
9	T*-3	0.0	0.0	0.0	0.0	0.0	0.0	0.0	0.0	0.0	0.0	0.0	0.0
10	COMP1	-0.784	0.0	-0.122	-0.423	0.032	-0.101	-0.424	-0.368	0.161	-0.699	-0.572	-0.677
11	COMP2	-0.609	0.0	-0.277	0.0	-0.049	0.442	-0.494	-0.293	0.057	-0.729	-0.652	-0.712
12	COMP3	0.0	0.0	-0.375	0.0	0.0	0.0	-0.653	-0.275	-0.846	-0.881	-0.602	-0.876
13	LG1	* 8.560	7.310	0.0	* 8.437	* 8.600	0.0	* 9.090	* 9.021	0.0	* 7.430	* 8.942	* 8.199
14	LG2	* 7.490	6.760	0.0	* 7.390	* 7.670	0.0	* 7.690	* 7.485	0.0	* 6.625	* 7.494	* 6.968
15	LG3	* 6.990	6.620	0.0	* 7.174	* 7.090	0.0	* 6.990	* 6.601	0.0	* 6.027	* 6.785	* 6.291
16	LP1	* 8.420	* 5.260	5.940	* 5.410	* 6.220	* 5.890	5.760	7.230	* 5.850	* 6.040	* 5.610	5.930
17	LP2	* 8.190	* 5.410	6.210	* 5.530	* 6.230	* 5.960	5.810	7.160	* 5.980	* 6.010	* 5.880	6.080
18	LP3	* 9.420	* 6.550	* 6.960	* 6.750	* 6.830	* 6.530	* 6.840	8.100	* 6.660	* 6.970	* 6.880	6.700
19	LS1	* 8.790	* 5.900	6.690	* 5.390	* 6.250	* 6.100	5.950	7.490	* 5.920	* 5.970	5.250	6.470
20	LS2	* 8.640	* 6.090	6.620	* 5.510	* 6.280	* 6.210	6.220	7.370	* 6.190	* 6.220	5.650	6.540
21	LS3	* 9.830	* 7.000	7.530	* 6.610	* 7.340	* 7.310	6.590	8.490	* 7.410	* 7.350	* 6.590	7.320
22	LP1	* 7.530	* 4.690	5.120	4.620	* 4.990	* 4.100	4.550	6.700	* 4.470	* 4.630	* 4.330	4.990
23	LP2	* 7.810	4.320	6.160	4.440	* 4.830	* 4.150	4.790	6.960	* 4.370	* 4.640	4.240	5.020
24	LP3	* 7.390	* 5.020	6.180	4.630	* 4.920	* 4.680	5.090	6.420	* 4.750	* 4.920	4.660	5.080
25	LQ1	* 7.690	4.990	5.850	4.700	* 5.030	* 4.550	4.520	6.690	* 4.550	* 4.680	4.750	4.580
26	LQ2	* 7.640	4.420	6.120	4.390	* 4.860	* 4.470	4.970	6.770	* 4.540	* 4.610	* 4.770	4.890
27	LQ3	* 7.170	* 4.820	6.150	4.480	* 4.950	* 4.650	4.970	6.460	* 4.820	* 5.000	* 5.070	4.780

NETWORK ESTIMATES (RINGDAL MAXIMUM-LIKELIHOOD ALGORITHM) OF THE MAGNITUDES OF THE 27 PARAMETERS IN TABLE VI

ASTERISK INDICATES UPPER BOUND (AT THE NINETY PER CENT CONFIDENCE LEVEL) BASED ON NOISE ONLY

	EVENT :	148	149	150	151	152	153	154	155	156	157	158	159
1	P1	4.540	5.183	4.190	4.860	4.000	* 4.170	4.870	3.730	4.110	4.500	3.950	3.990
2	P2	3.920	4.396	2.940	3.930	3.290	2.750	4.090	2.860	3.280	3.810	3.250	2.610
3	P3	2.920	3.410	2.070	2.830	2.140	1.740	3.150	2.020	2.270	2.810	1.930	2.140
4	OMEGA-2	5.531	6.205	5.767	6.393	4.987	6.115	5.938	0.0	4.658	5.121	4.829	5.510
5	CR.PR-2	-0.0	-0.286	-0.263	-0.450	-0.244	0.065	-0.184	0.0	-0.090	0.176	0.409	0.196
6	T*-2	0.0	0.0	0.0	0.0	0.0	0.0	0.0	0.0	0.0	0.0	0.0	0.0
7	OMEGA-3	5.690	6.299	6.495	6.591	4.942	6.851	6.151	0.0	4.568	5.307	4.819	5.371
8	CR.PR-3	0.016	-0.143	-0.633	-0.407	-0.059	-0.419	-0.119	0.0	0.217	0.110	0.493	0.562
9	T*-3	0.0	0.0	0.0	0.0	0.0	0.0	0.0	0.0	0.0	0.0	0.0	0.0
10	COMP1	0.0	-0.297	-0.130	-0.190	-0.399	0.0	-0.655	-0.235	-0.036	-0.599	0.0	0.0
11	COMP2	0.0	-0.345	-0.340	-0.354	-0.200	0.0	-0.734	0.0	0.049	-0.711	-0.195	-2.044
12	COMP3	0.0	-0.450	0.0	-0.473	-0.289	-0.794	-0.904	0.0	-0.703	-0.729	0.464	-1.396
13	LG1	* 8.830	8.986	* 8.137	* 8.890	* 8.890	* 8.006	* 8.577	7.230	* 8.994	* 8.489	* 8.608	8.610
14	LG2	* 7.559	* 7.960	* 6.850	* 7.490	* 7.490	* 6.925	* 7.121	6.630	* 7.367	* 7.175	* 7.045	* 7.390
15	LG3	* 6.745	* 7.090	* 6.552	* 6.890	* 7.090	* 6.616	* 6.311	6.440	* 6.717	* 6.548	* 6.501	* 6.990
16	LP1	* 5.730	5.980	* 6.050	* 5.550	5.380	* 6.480	* 5.900	* 5.240	* 5.550	* 5.750	* 5.500	* 5.830
17	LP2	* 5.960	6.210	* 6.240	* 5.660	* 5.910	* 6.840	* 6.020	* 5.400	* 5.910	* 5.940	* 5.740	* 5.960
18	LP3	* 6.830	7.170	* 6.930	* 6.480	* 6.480	* 7.810	* 7.240	* 6.590	* 6.750	* 6.650	* 6.450	* 7.140
19	LS1	* 5.870	6.500	* 6.250	6.370	5.670	7.220	* 5.830	* 5.880	* 5.960	5.910	* 5.840	* 5.750
20	LS2	* 6.160	6.430	* 6.300	6.370	5.750	* 7.080	* 5.990	* 6.200	* 6.230	* 6.140	* 6.040	* 5.820
21	LS3	* 7.250	7.380	* 7.130	7.110	6.650	7.890	* 6.560	* 7.010	* 7.350	* 7.090	* 6.760	* 6.870
22	LR1	4.990	5.720	* 4.320	5.240	4.600	5.120	* 4.350	* 4.280	4.150	4.610	4.250	* 4.510
23	LR2	5.440	5.950	4.210	5.670	5.120	4.980	* 4.420	* 4.040	4.810	4.600	4.280	* 4.410
24	LR3	5.420	5.870	4.010	5.600	5.220	* 4.990	* 4.830	* 4.310	5.100	* 4.780	* 4.740	* 4.570
25	LQ1	5.120	5.940	4.250	5.630	5.050	4.890	* 4.570	* 4.150	4.890	4.700	* 4.750	* 4.650
26	LQ2	5.170	6.140	4.050	5.840	5.130	* 5.120	* 4.560	* 3.950	5.010	4.790	* 4.690	* 4.510
27	LQ3	5.420	6.070	3.880	5.850	5.230	* 5.000	* 4.860	* 4.170	4.940	5.050	* 5.010	* 4.620

	EVENT :	160	161	162	163	164	165	166	167	168	169	170	171
1	P1	* 4.020	4.190	4.800	3.880	5.190	4.260	4.880	4.140	4.410	4.840	5.444	4.330
2	P2	2.870	3.110	3.910	3.410	4.554	3.570	3.910	2.980	3.190	4.330	4.460	3.630
3	P3	1.810	2.420	2.880	2.640	3.420	2.640	2.680	1.690	* 2.530	3.465	3.450	2.730
4	OMEGA-2	4.431	4.392	6.093	4.958	6.349	5.296	6.360	4.756	5.333	5.739	6.802	5.212
5	CR.PR-2	0.638	0.245	-0.296	-0.090	-0.287	-0.008	-0.275	-0.177	-0.016	0.013	-0.505	0.154
6	T*-2	0.0	0.0	0.0	0.0	0.0	0.0	0.0	0.0	0.0	0.0	0.0	0.0
7	OMEGA-3	4.519	4.432	6.287	4.936	6.357	5.504	6.590	4.587	5.636	5.590	7.051	5.241
8	CR.PR-3	0.452	0.339	-0.245	0.085	-0.091	0.049	-0.301	0.134	-0.022	0.333	-0.440	0.237
9	T*-3	0.0	0.0	0.0	0.0	0.0	0.0	0.0	0.0	0.0	0.0	0.0	0.0
10	COMP1	-0.840	-0.362	-0.027	-0.009	-0.310	-0.057	-0.113	0.0	0.0	-0.128	0.079	-0.760
11	COMP2	-0.383	0.100	-0.185	-0.299	-0.147	0.044	-0.242	0.0	0.0	-0.081	-0.002	-0.817
12	COMP3	0.0	0.0	0.0	0.0	-0.175	0.097	-0.604	0.0	0.0	-0.286	-0.156	-0.721
13	LG1	* 7.287	7.780	* 8.620	* 9.788	* 8.394	* 8.747	* 8.859	* 7.557	0.0	* 8.820	* 8.990	* 8.854
14	LG2	* 5.941	7.010	* 7.900	* 8.322	* 7.056	* 7.469	* 7.375	* 6.759	0.0	* 7.497	* 7.690	* 7.450
15	LG3	* 5.330	6.590	* 6.890	* 7.201	* 6.141	* 6.545	* 6.552	* 5.943	0.0	* 6.751	* 6.990	* 6.492
16	LP1	* 5.780	* 5.870	* 6.410	* 6.510	6.480	6.160	* 6.050	6.070	* 5.830	5.970	7.370	* 5.980
17	LP2	* 6.000	* 5.930	* 6.570	* 6.600	6.400	6.060	* 6.290	6.270	5.930	* 6.160	7.460	* 6.120
18	LP3	* 6.990	* 6.420	* 7.610	* 7.680	6.600	* 6.980	* 6.980	7.320	* 6.990	6.900	7.880	* 6.840
19	LS1	* 5.910	6.480	* 6.570	* 6.570	6.750	6.230	6.930	6.180	* 5.920	6.440	7.900	5.720
20	LS2	* 6.130	6.430	* 6.740	* 6.770	6.800	5.920	7.030	6.750	* 5.940	6.410	7.850	* 6.270
21	LS3	* 7.230	6.970	* 7.640	* 7.580	8.090	7.330	7.810	8.030	* 6.840	7.270	8.640	* 7.300
22	LR1	* 4.180	4.060	5.600	* 4.460	6.030	4.700	6.000	4.260	4.080	5.340	6.850	* 4.750
23	LR2	* 4.280	4.020	6.060	* 4.770	6.410	5.700	6.250	4.490	4.220	5.110	7.150	* 4.850
24	LR3	* 4.490	* 4.240	6.070	* 4.890	6.100	5.560	6.190	4.790	* 4.420	5.230	7.030	* 4.950
25	LQ1	* 4.590	* 4.050	5.860	* 4.570	6.020	5.140	6.380	4.400	4.460	5.280	7.180	* 4.750
26	LQ2	* 4.650	* 4.110	5.890	* 4.380	6.200	5.410	6.470	4.800	4.590	5.380	7.250	* 4.790
27	LQ3	* 4.910	3.850	5.960	* 5.010	6.080	5.210	6.400	4.780	* 4.510	5.390	7.020	* 4.960

NETWORK ESTIMATES (RINGDAL MAXIMUM-LIKELIHOOD ALGORITHM) OF THE MAGNITUDES OF THE 27 PARAMETERS IN TABLE VI

ASTERISK INDICATES UPPER BOUND (AT THE NINETY PER CENT CONFIDENCE LEVEL) BASED ON NOISE ONLY

	EVENT :	172	173	175	176	177	178	179	180	182	183	184	185
1	P1	3.540	3.460	4.810	4.410	4.290	4.810	4.250	4.370	4.280	4.180	4.160	* 3.740
2	P2	3.260	3.040	3.980	3.000	3.060	4.196	3.790	3.470	3.690	3.660	3.000	3.090
3	P3	1.970	1.970	3.080	2.280	2.530	3.230	3.230	2.530	2.430	2.880	2.240	1.980
4	OMEGA-2	5.389	4.824	6.120	4.834	5.109	5.940	5.206	5.364	5.375	5.653	4.929	4.318
5	CR.FR-2	-0.121	-0.025	-0.368	-0.162	0.178	-0.313	0.040	-0.096	0.244	-0.290	0.253	0.053
6	T*-2	0.0	0.0	0.0	0.0	0.0	0.0	0.0	0.0	0.0	0.0	0.0	0.0
7	OMEGA-3	5.586	5.085	6.449	5.734	5.156	5.951	5.444	5.019	5.373	5.722	5.136	4.297
8	CR.FR-3	-0.146	0.023	-0.409	-0.521	0.336	-0.108	0.019	0.299	0.318	-0.140	0.343	0.275
9	T*-3	0.0	0.0	0.0	0.0	0.0	0.0	0.0	0.0	0.0	0.0	0.0	0.0
10	COMP1	0.065	-0.411	0.131	-1.919	-0.392	-0.257	0.271	0.034	-0.270	-0.546	-0.197	0.715
11	COMP2	-0.041	-0.427	-0.051	-0.569	-0.338	-0.251	0.213	0.156	-0.094	-0.243	0.0	0.414
12	COMP3	0.180	0.0	-0.234	-0.436	-0.208	-0.233	0.081	-0.300	-0.128	-0.414	0.0	0.0
13	LG1	* 8.360	* 8.090	* 8.471	* 8.721	7.250	* 8.933	8.306	* 8.847	* 8.651	* 8.786	* 8.092	* 8.690
14	LG2	* 7.290	6.920	* 7.167	* 7.600	6.910	* 7.506	7.688	* 7.419	* 7.289	* 7.315	* 6.835	* 7.290
15	LG3	* 6.790	6.480	* 6.587	* 6.604	6.250	* 6.478	7.316	* 6.508	* 6.569	* 6.618	* 6.559	* 6.890
16	LP1	* 5.380	* 5.670	5.680	* 5.770	5.710	7.110	5.670	* 5.920	6.450	* 5.910	* 5.250	5.260
17	LP2	* 5.700	* 5.790	6.140	* 6.120	5.750	7.010	5.740	* 6.200	6.120	* 6.190	* 5.500	5.740
18	LP3	* 6.690	* 6.520	6.790	* 6.930	* 6.870	7.710	7.110	* 7.060	* 7.370	* 6.780	* 6.840	* 6.670
19	LS1	* 5.830	* 5.900	* 6.550	* 5.940	* 6.040	7.320	6.590	* 6.320	6.710	* 5.950	* 5.960	* 5.950
20	LS2	* 5.960	* 6.030	* 6.720	* 6.210	* 6.320	7.250	6.460	* 6.390	* 6.640	* 6.140	* 6.140	* 6.190
21	LS3	* 6.580	* 7.230	* 7.700	* 6.570	* 7.360	8.420	* 7.260	* 6.990	7.140	* 6.950	* 7.040	* 7.070
22	LR1	4.080	4.040	5.410	* 4.450	4.200	6.670	5.450	* 4.650	4.610	4.590	* 4.340	4.500
23	LR2	4.130	3.840	5.620	* 4.510	4.250	6.801	5.980	* 4.860	5.350	4.720	* 4.110	4.980
24	LR3	4.460	4.140	5.820	* 4.870	4.160	6.110	5.730	* 4.950	5.100	4.650	* 4.460	5.120
25	LQ1	4.450	4.130	5.520	* 4.530	4.360	6.560	5.490	* 4.710	* 5.130	4.670	* 4.530	4.850
26	LQ2	4.580	4.420	5.720	* 4.610	4.360	6.600	5.900	* 4.870	5.280	4.900	* 4.350	5.040
27	LQ3	4.680	4.560	5.740	* 4.950	4.310	6.130	5.870	* 5.040	5.070	4.830	* 4.590	5.260

	EVENT :	186	187	188	189	190	191	192	193	194	195	264	265
1	P1	4.330	* 4.030	3.640	4.310	4.460	3.540	* 4.200	3.880	* 3.950	4.600	4.521	5.080
2	P2	3.030	3.010	2.930	3.680	3.570	3.010	2.850	3.030	* 2.300	3.710	3.921	4.364
3	P3	* 2.650	2.250	2.130	3.180	2.620	1.940	1.870	* 2.110	* 1.780	2.600	3.137	3.734
4	OMEGA-2	5.050	4.856	4.586	4.977	5.566	4.310	0.0	5.233	0.0	5.614	5.175	5.741
5	CR.FR-2	0.697	-0.244	0.275	0.078	0.016	0.240	0.0	-0.223	0.0	-0.185	0.282	0.163
6	T*-2	0.0	0.0	0.0	0.0	0.0	0.0	0.0	0.0	0.0	0.0	0.0	0.0
7	OMEGA-3	5.021	5.373	5.064	4.961	5.528	4.305	0.0	5.922	0.0	5.725	5.345	5.615
8	CR.FR-3	0.506	-0.368	0.082	0.229	0.123	0.449	0.0	-0.572	0.0	-0.104	0.239	0.438
9	T*-3	0.0	0.0	0.0	0.0	0.0	0.0	0.0	0.0	0.0	0.0	0.0	0.0
10	COMP1	-0.825	-0.559	-0.035	-0.455	-0.122	0.212	0.417	-0.527	0.0	0.192	-0.418	0.136
11	COMP2	-1.326	-0.519	-0.317	-0.585	-0.366	-0.149	0.0	-0.551	0.0	0.067	-0.618	0.015
12	COMP3	-1.199	-0.017	-0.781	-0.827	-0.704	0.0	0.0	-0.859	0.0	-0.094	-0.670	-0.237
13	LG1	* 8.828	* 8.890	* 7.690	* 9.143	8.100	* 9.145	0.0	* 8.490	* 8.490	* 8.590	* 9.135	* 9.390
14	LG2	* 7.433	* 7.490	* 6.790	* 7.621	* 7.180	* 7.826	0.0	* 6.670	* 6.710	* 7.290	* 7.846	* 8.090
15	LG3	* 6.563	* 6.990	* 6.290	* 7.085	* 6.660	* 6.996	0.0	* 5.820	* 6.080	* 6.790	* 6.991	* 7.090
16	LP1	5.300	* 5.830	* 5.630	* 5.190	* 5.180	* 5.620	* 6.020	* 5.900	* 5.670	5.780	* 6.060	* 5.770
17	LP2	5.610	* 6.100	* 5.630	* 5.540	* 5.630	* 5.920	* 6.310	* 6.080	* 6.000	5.580	* 6.240	* 5.980
18	LP3	6.600	* 7.140	* 6.430	* 6.540	* 6.610	* 6.980	* 7.590	* 7.030	* 6.860	6.700	* 7.060	* 6.500
19	LS1	5.920	* 6.050	* 6.200	* 5.660	* 6.230	* 6.030	* 6.090	* 5.960	* 6.080	6.430	6.060	5.740
20	LS2	* 6.370	* 6.130	* 6.450	* 5.820	* 6.530	* 6.180	* 6.280	* 6.210	* 6.270	6.440	6.130	* 6.280
21	LS3	* 7.540	* 7.180	* 7.000	* 7.040	* 7.680	* 7.250	* 7.650	* 6.950	* 7.410	7.370	* 7.600	* 7.360
22	LR1	4.400	4.320	4.230	* 4.260	4.890	* 4.310	* 4.530	* 4.690	* 4.520	5.210	5.330	* 4.790
23	LP2	4.550	4.680	4.280	* 4.290	5.100	* 4.420	4.600	4.810	* 4.570	5.350	5.980	* 4.690
24	LP3	* 4.830	* 4.710	4.520	* 4.400	5.170	* 4.730	4.770	4.780	* 4.940	5.390	5.830	* 5.100
25	LQ1	4.380	4.250	4.460	* 4.300	5.080	* 4.600	* 4.680	4.690	* 4.490	5.510	5.230	* 4.920
26	LQ2	4.390	4.410	4.520	* 4.210	5.370	* 4.550	4.620	* 4.940	* 4.670	5.760	5.750	* 4.700
27	LQ3	* 4.840	* 4.680	4.700	* 4.280	5.270	* 4.780	4.630	* 5.140	* 4.980	5.680	5.890	* 5.010

NETWORK ESTIMATES (RINGDAL MAXIMUM-LIKELIHOOD ALGORITHM) OF THE MAGNITUDES OF THE 27 PARAMETERS IN TABLE VI

ASTERISK INDICATES UPPER BOUND (AT THE NINETY PER CENT CONFIDENCE LEVEL) BASED ON NOISE ONLY

	EVENT :	266	267	268	269	270	271	272	273	274	276	277	278
1	P1	4.570	5.420	5.270	5.367	4.750	5.120	4.010	5.211	* 4.748	* 5.490	* 4.770	4.240
2	P2	4.107	4.956	4.651	4.635	4.196	4.570	3.370	4.556	3.828	4.090	3.740	3.880
3	P3	3.518	4.193	3.942	3.540	3.398	3.962	1.900	3.490	3.423	3.520	3.130	3.280
4	OMEGA-2	5.320	6.297	6.046	6.273	5.570	5.739	4.783	6.418	4.515	5.647	4.296	5.361
5	CR.FR-2	0.106	0.082	-0.035	-0.101	-0.103	0.066	-0.023	-0.455	0.217	-0.346	0.586	-0.162
6	T*-2	0.0	0.0	0.0	0.0	0.0	0.0	0.0	0.0	0.0	0.0	0.0	0.0
7	OMEGA-3	5.364	6.223	6.052	6.424	5.490	5.682	4.831	6.454	4.368	5.126	4.403	5.150
8	CR.FR-3	0.244	0.323	0.160	-0.024	0.190	0.281	0.154	-0.280	0.596	0.293	0.697	0.216
9	T*-3	0.0	0.0	0.0	0.0	0.0	0.0	0.0	0.0	0.0	0.0	0.0	0.0
10	COMP1	-0.518	-0.444	-0.526	-0.469	-0.523	0.482	-0.907	-0.448	0.0	-1.676	-0.300	-0.012
11	COMP2	-0.575	-0.444	-0.535	-0.528	-0.555	0.514	-0.570	-0.538	0.0	-1.129	0.0	-0.233
12	COMP3	-0.646	-0.577	-0.653	-0.619	-0.668	0.287	-0.410	-0.660	0.0	0.0	0.0	-0.394
13	LG1	* 9.390	* 9.970	* 8.837	* 9.024	* 8.576	* 9.550	* 8.688	* 8.939	0.0	0.0	* 9.225	* 8.816
14	LG2	* 8.090	* 8.506	* 7.371	7.784	* 7.244	* 8.160	* 7.373	* 7.531	0.0	0.0	* 8.034	* 7.540
15	LG3	* 7.090	* 7.327	* 6.858	* 6.632	* 6.596	* 7.190	* 6.728	* 6.888	0.0	0.0	* 7.877	* 6.988
16	LP1	* 6.920	4.990	5.290	* 6.090	* 5.540	5.030	* 5.490	* 5.920	0.0	0.0	* 5.700	* 6.100
17	LP2	* 6.910	5.270	5.850	* 6.090	* 5.750	* 5.700	* 5.580	* 6.190	0.0	0.0	* 6.050	* 6.260
18	LP3	* 7.430	* 6.700	6.680	* 6.950	* 6.770	* 6.400	* 6.330	* 7.360	0.0	0.0	* 7.500	* 6.950
19	LS1	* 6.990	5.940	6.100	5.870	5.630	5.890	* 5.690	* 5.970	0.0	0.0	* 6.140	* 6.360
20	LS2	* 6.970	5.890	6.370	* 6.030	5.700	5.920	* 5.810	6.120	0.0	0.0	* 6.200	* 6.510
21	LS3	7.740	7.120	7.080	* 6.310	* 6.750	6.900	* 6.520	* 7.040	0.0	0.0	* 7.730	* 7.730
22	LR1	* 5.340	5.300	4.940	4.000	* 4.510	4.660	4.380	* 4.450	0.0	* 7.500	5.030	* 4.780
23	LR2	5.320	5.670	5.050	5.130	4.910	5.280	4.600	* 4.700	0.0	* 6.811	5.040	* 5.180
24	LR3	* 5.570	5.710	5.370	5.200	5.220	5.470	4.440	* 4.970	0.0	* 6.644	4.550	5.100
25	LQ1	* 5.560	5.130	4.650	* 4.460	* 4.540	4.900	4.350	* 4.520	0.0	* 6.490	4.880	* 4.970
26	LQ2	5.320	5.410	4.870	4.800	4.520	5.130	4.560	4.320	0.0	* 6.090	4.850	* 5.180
27	LQ3	* 5.600	5.440	4.960	4.840	5.050	5.200	4.370	* 4.940	0.0	* 6.390	4.410	* 5.260

APPENDIX II

Number of signal and noise measurements of each parameter for each event

NUMBER OF (1) NOISE AND (2) SIGNAL MEASUREMENTS USED TO COMPUTE THE NETWORK ESTIMATES OF THE MAGNITUDES OF THE 27 PARAMETERS IN TABLE VI

EVENT :	1	3	4	6	7	8	9	10	14	16	17	18
1 P1	3, 11	9, 5	5, 0	8, 0	6, 3	3, 0	7, 5	6, 4	6, 7	3, 4	6, 6	1, 5
2 P2	2, 12	4, 10	3, 2	8, 0	1, 8	2, 1	11, 1	6, 4	1, 12	0, 7	2, 10	0, 6
3 P3	2, 12	9, 5	0, 2	8, 0	3, 6	3, 0	10, 2	6, 4	1, 12	1, 6	2, 10	0, 6
4 OMEGA-2	0, 12	0, 6	0, 1	0, 0	0, 7	0, 0	0, 0	0, 1	0, 12	0, 6	0, 9	0, 6
5 CR.FR-2	0, 12	0, 6	0, 1	0, 0	0, 7	0, 0	0, 0	0, 1	0, 12	0, 6	0, 9	0, 6
6 T*-2	0, 12	0, 6	0, 1	0, 0	0, 7	0, 0	0, 0	0, 1	0, 12	0, 6	0, 9	0, 6
7 OMEGA-3	0, 12	0, 6	0, 1	0, 0	0, 7	0, 0	0, 0	0, 1	0, 12	0, 6	0, 9	0, 6
8 CR.FR-3	0, 12	0, 6	0, 1	0, 0	0, 7	0, 0	0, 0	0, 1	0, 12	0, 6	0, 9	0, 6
9 T*-3	0, 12	0, 6	0, 1	0, 0	0, 7	0, 0	0, 0	0, 1	0, 12	0, 6	0, 9	0, 6
10 COMP1	0, 6	0, 10	0, 1	0, 0	0, 6	0, 0	0, 3	0, 1	0, 5	0, 6	0, 9	0, 6
11 COMP2	0, 5	0, 9	0, 0	0, 0	0, 3	0, 0	0, 2	0, 1	0, 5	0, 6	0, 9	0, 6
12 COMP3	0, 5	0, 7	0, 0	0, 0	0, 2	0, 0	0, 2	0, 1	0, 5	0, 6	0, 9	0, 6
13 LG1	0, 0	1, 0	1, 0	1, 0	0, 0	0, 0	0, 0	0, 0	1, 0	1, 0	1, 0	1, 0
14 LG2	0, 0	1, 0	2, 0	1, 0	0, 0	0, 0	0, 0	0, 0	1, 0	1, 0	1, 0	1, 0
15 LG3	0, 0	1, 0	2, 0	1, 0	0, 0	0, 0	0, 0	0, 0	1, 0	1, 0	1, 0	1, 0
16 LP1	8, 0	9, 2	7, 2	12, 0	6, 1	8, 0	11, 0	13, 0	10, 1	9, 1	10, 1	6, 7
17 LP2	8, 0	11, 0	8, 1	12, 0	6, 1	8, 0	13, 0	12, 1	11, 0	9, 1	10, 1	7, 7
18 LP3	8, 0	9, 2	8, 1	12, 0	5, 1	8, 0	11, 0	12, 1	11, 0	9, 1	9, 1	7, 7
19 LS1	8, 0	8, 3	7, 1	10, 1	7, 1	7, 0	10, 0	11, 1	9, 1	8, 1	7, 1	7, 7
20 LS2	8, 0	8, 3	7, 1	11, 0	8, 1	7, 0	10, 0	11, 1	9, 1	8, 1	5, 1	7, 7
21 LS3	8, 0	10, 1	8, 0	10, 1	7, 1	7, 0	10, 0	10, 1	9, 1	7, 1	11, 1	7, 7
22 LR1	10, 1	12, 1	6, 3	14, 1	10, 2	11, 0	13, 0	10, 2	13, 2	3, 1	11, 1	7, 6
23 LR2	10, 1	7, 1	5, 4	14, 1	8, 2	10, 0	10, 2	12, 0	11, 2	7, 1	11, 1	7, 7
24 LR3	10, 1	8, 1	6, 3	14, 1	10, 2	10, 0	11, 2	11, 0	12, 1	7, 1	11, 1	7, 7
25 LQ1	10, 1	11, 3	6, 4	15, 1	12, 1	12, 0	12, 3	12, 1	12, 1	6, 2	11, 1	7, 7
26 LQ2	10, 1	9, 5	6, 4	13, 3	11, 2	11, 0	10, 5	11, 0	11, 2	6, 2	10, 2	7, 7
27 LQ3	9, 2	10, 4	7, 3	16, 0	11, 2	12, 0	11, 4	11, 0	12, 1	6, 2	12, 0	7, 7

EVENT :	19	20	21	22	23	24	25	26	27	28	29	30
1 P1	0, 10	1, 8	4, 8	2, 4	9, 0	9, 2	10, 1	12, 1	6, 5	3, 2	2, 1	2, 11
2 P2	0, 10	0, 9	1, 12	1, 5	7, 0	10, 2	7, 1	11, 1	3, 5	3, 2	2, 1	1, 11
3 P3	1, 9	1, 9	0, 11	0, 5	9, 0	9, 2	9, 1	11, 1	6, 5	3, 2	2, 1	2, 11
4 OMEGA-2	0, 10	0, 10	0, 11	0, 5	0, 0	0, 2	0, 1	0, 1	0, 6	0, 2	0, 1	0, 11
5 CR.FR-2	0, 10	0, 10	0, 11	0, 5	0, 0	0, 2	0, 1	0, 1	0, 6	0, 2	0, 1	0, 11
6 T*-2	0, 10	0, 10	0, 11	0, 5	0, 0	0, 2	0, 1	0, 1	0, 6	0, 2	0, 1	0, 11
7 OMEGA-3	0, 10	0, 10	0, 11	0, 5	0, 0	0, 2	0, 1	0, 1	0, 6	0, 2	0, 1	0, 11
8 CR.FR-3	0, 10	0, 10	0, 11	0, 5	0, 0	0, 2	0, 1	0, 1	0, 6	0, 2	0, 1	0, 11
9 T*-3	0, 10	0, 9	0, 11	0, 5	0, 0	0, 2	0, 1	0, 1	0, 6	0, 2	0, 1	0, 11
10 COMP1	0, 9	0, 9	0, 9	0, 2	0, 0	0, 1	0, 1	0, 1	0, 4	0, 2	0, 1	0, 9
11 COMP2	0, 9	0, 8	0, 8	0, 1	0, 0	0, 1	0, 1	0, 1	0, 4	0, 2	0, 1	0, 8
12 COMP3	0, 9	1, 7	0, 8	0, 1	0, 0	0, 1	0, 1	0, 1	0, 4	0, 2	0, 1	0, 7
13 LG1	0, 1	0, 1	1, 0	1, 0	1, 0	1, 0	1, 0	1, 0	1, 0	1, 0	1, 0	1, 0
14 LG2	1, 0	1, 0	1, 0	1, 0	1, 0	1, 0	1, 0	1, 0	1, 0	1, 0	1, 0	1, 0
15 LG3	1, 0	1, 0	1, 0	1, 0	1, 0	1, 0	1, 0	1, 0	1, 0	1, 0	1, 0	1, 0
16 LP1	7, 1	9, 1	8, 1	4, 1	10, 1	11, 1	12, 1	13, 1	8, 1	10, 1	9, 1	6, 1
17 LP2	5, 3	8, 2	8, 1	4, 1	10, 1	11, 1	12, 1	13, 1	9, 1	9, 1	9, 1	6, 1
18 LP3	6, 2	8, 2	8, 1	4, 1	9, 1	8, 1	12, 1	12, 1	6, 1	7, 1	7, 1	5, 1
19 LS1	6, 2	8, 2	8, 1	2, 1	10, 1	9, 1	12, 1	12, 1	6, 1	8, 1	5, 1	4, 1
20 LS2	5, 3	8, 2	8, 1	3, 1	10, 1	8, 1	11, 1	12, 1	6, 1	8, 1	7, 1	3, 1
21 LS3	7, 1	8, 2	8, 1	4, 1	9, 1	9, 1	11, 1	14, 1	6, 1	8, 1	9, 1	4, 1
22 LR1	11, 1	7, 1	8, 1	2, 1	10, 1	8, 1	13, 1	13, 1	9, 1	12, 1	7, 1	3, 1
23 LR2	4, 1	7, 1	8, 1	3, 1	10, 1	9, 1	11, 1	11, 1	6, 1	12, 1	8, 1	3, 1
24 LR3	4, 1	8, 1	8, 1	4, 1	10, 1	8, 1	13, 1	13, 1	6, 1	11, 1	10, 1	4, 1
25 LQ1	8, 1	7, 1	11, 1	6, 1	10, 1	9, 1	11, 1	15, 1	11, 1	11, 1	10, 1	4, 1
26 LQ2	6, 2	8, 1	11, 1	6, 1	10, 1	10, 1	10, 1	15, 1	10, 1	11, 1	10, 1	4, 1
27 LQ3	6, 6	8, 1	11, 0	9, 1	10, 0	11, 1	11, 3	15, 1	13, 4	11, 1	10, 1	2, 11

NUMBER OF (1) NOISE AND (2) SIGNAL MEASUREMENTS USED TO COMPUTE THE NETWORK ESTIMATES OF THE MAGNITUDES OF THE 27 PARAMETERS IN TABLE VI

	EVENT :	31	32	33	34	35	36	37	38	39	41	45	46
1	P1	13, 2	7, 5	8, 4	3, 3	8, 6	2, 2	9, 3	8, 3	9, 5	3, 2	6, 2	9, 2
2	P2	8, 7	5, 7	2,10	3, 3	7, 7	2, 2	6, 4	11, 3	7, 5	2, 3	6, 2	7, 4
3	P3	13, 2	12, 0	2,10	4, 2	10, 4	3, 1	8, 4	9, 2	12, 2	2, 3	5, 3	9, 2
4	OMEGA-2	0, 3	0, 4	0,10	0, 2	0, 8	0, 1	0, 4	0, 0	0, 6	0, 3	0, 2	0, 3
5	CR.FR-2	0, 3	0, 4	0,10	0, 2	0, 8	0, 1	0, 4	0, 0	0, 6	0, 3	0, 2	0, 3
6	T*-2	0, 3	0, 4	0,10	0, 2	0, 8	0, 1	0, 4	0, 0	0, 6	0, 3	0, 2	0, 3
7	OMEGA-3	0, 3	0, 4	0,10	0, 2	0, 8	0, 1	0, 4	0, 0	0, 6	0, 3	0, 2	0, 3
8	CR.FR-3	0, 3	0, 4	0,10	0, 2	0, 8	0, 1	0, 4	0, 0	0, 6	0, 3	0, 2	0, 3
9	T*-3	0, 3	0, 4	0,10	0, 2	0, 8	0, 1	0, 4	0, 0	0, 6	0, 3	0, 2	0, 3
10	COMP1	0, 5	0, 3	0, 5	0, 2	0, 5	0, 3	0, 3	0, 2	0, 4	0, 1	0, 2	0, 1
11	COMP2	0, 3	0, 1	0, 5	0, 0	0, 1	0, 1	0, 1	0, 0	0, 1	0, 1	0, 0	0, 0
12	COMP3	0, 1	0, 1	0, 5	0, 1	0, 1	0, 0	0, 1	0, 0	0, 1	0, 1	0, 0	0, 0
13	LG1	4, 0	1, 0	1, 5	2, 0	2, 3	0, 0	1, 1	1, 0	2, 1	1, 1	1, 0	1, 0
14	LG2	4, 0	1, 0	1, 5	2, 0	2, 3	0, 0	1, 1	1, 0	2, 1	1, 1	1, 0	1, 0
15	LG3	4, 0	1, 0	1, 5	2, 0	2, 3	0, 0	1, 1	1, 0	2, 1	1, 1	1, 0	1, 0
16	LP1	14, 0	12, 0	9, 0	9, 0	5, 6	10, 0	11, 0	11, 0	11, 3	8, 0	13, 0	12, 0
17	LP2	14, 0	12, 0	8, 1	9, 0	5, 6	10, 0	11, 0	11, 0	14, 1	8, 0	13, 0	12, 0
18	LP3	14, 0	12, 0	9, 0	9, 0	6, 5	10, 0	11, 0	11, 0	13, 1	8, 0	13, 0	12, 0
19	LS1	12, 0	6, 3	8, 0	6, 2	4, 10	9, 1	12, 0	8, 0	5, 1	7, 0	8, 1	8, 0
20	LS2	12, 0	7, 2	8, 0	7, 1	5, 9	10, 0	11, 0	8, 0	7, 4	7, 0	8, 1	8, 0
21	LS3	12, 0	9, 0	8, 0	7, 1	8, 6	9, 1	12, 0	8, 0	7, 4	7, 0	8, 1	8, 0
22	LR1	14, 0	12, 0	8, 3	7, 6	3, 12	12, 0	11, 0	7, 1	5, 11	10, 0	11, 2	13, 1
23	LR2	14, 0	13, 0	7, 5	4, 4	0, 15	11, 1	6, 7	5, 3	3, 13	10, 0	10, 3	12, 2
24	LR3	14, 0	13, 0	9, 3	4, 6	7, 8	12, 0	7, 6	7, 1	7, 9	10, 0	12, 1	12, 2
25	LQ1	14, 0	15, 1	11, 1	6, 5	3, 12	13, 0	7, 6	11, 1	4, 11	13, 0	10, 1	13, 1
26	LQ2	14, 0	16, 1	11, 1	5, 6	0, 15	13, 0	6, 7	10, 2	3, 12	13, 0	11, 3	13, 1
27	LQ3	14, 0	15, 1	12, 0	5, 6	4, 11	13, 0	8, 5	10, 2	8, 7	13, 0	11, 3	14, 0

	EVENT :	47	48	49	50	53	55	56	57	58	59	60	61
1	P1	6, 8	6, 2	2,10	2,12	2,14	7, 3	2, 0	9, 1	9, 1	3, 4	7, 0	8, 4
2	P2	3,11	5, 3	0,12	0,14	0,16	7, 3	2, 0	2, 8	9, 1	4, 3	7, 0	9, 3
3	P3	1,13	5, 3	3, 9	1,13	0,16	10, 0	2, 0	6, 4	9, 1	5, 2	5, 2	9, 6
4	OMEGA-2	0,11	0, 4	3,12	0,13	0,16	0, 2	0, 0	0, 4	0, 0	0, 3	0, 0	0, 4
5	CR.FR-2	0,11	0, 4	0,12	0,13	0,16	0, 2	0, 0	0, 4	0, 0	0, 3	0, 0	0, 4
6	T*-2	0,11	0, 4	0,12	0,13	0,16	0, 2	0, 0	0, 4	0, 0	0, 3	0, 0	0, 4
7	OMEGA-3	0,11	0, 4	0,12	0,13	0,16	0, 2	0, 0	0, 4	0, 0	0, 3	0, 0	0, 4
8	CR.FR-3	0,11	0, 4	0,12	0,13	0,16	0, 2	0, 0	0, 4	0, 0	0, 3	0, 0	0, 4
9	T*-3	0,11	0, 4	0,12	0,13	0,16	0, 2	0, 0	0, 4	0, 0	0, 3	0, 0	0, 4
10	COMP1	0, 9	0, 1	0, 9	0, 9	0, 8	0, 4	0, 0	0, 3	0, 0	0, 0	0, 0	0, 3
11	COMP2	0, 8	0, 1	0, 5	0, 8	0, 5	0, 3	0, 0	0, 3	0, 0	0, 1	0, 0	0, 2
12	COMP3	0, 7	0, 1	0, 5	0, 5	0, 5	0, 3	0, 0	0, 3	0, 0	0, 1	0, 0	0, 2
13	LG1	0, 0	1, 0	1, 0	1, 0	1, 0	1, 0	0, 0	1, 0	0, 0	1, 1	0, 0	0, 2
14	LG2	0, 0	1, 0	1, 0	1, 0	1, 0	1, 0	0, 0	1, 0	0, 0	1, 1	0, 0	0, 2
15	LG3	0, 0	1, 0	1, 0	1, 0	1, 0	1, 0	0, 0	1, 0	0, 0	1, 1	0, 0	0, 2
16	LP1	11, 0	10, 0	3, 6	10, 1	11, 1	10, 0	10, 0	12, 0	13, 0	9, 2	14, 0	9, 2
17	LP2	11, 0	10, 0	3, 6	11, 1	12, 0	10, 0	10, 0	12, 0	13, 0	10, 1	14, 0	8, 2
18	LP3	11, 0	10, 0	5, 4	10, 1	12, 0	10, 0	10, 0	12, 0	13, 0	10, 1	14, 0	9, 2
19	LS1	12, 1	10, 0	3, 9	6, 6	8, 2	10, 0	10, 0	13, 0	13, 1	9, 0	11, 0	9, 1
20	LS2	12, 1	10, 0	4, 8	6, 6	9, 1	10, 0	10, 0	13, 0	13, 0	9, 0	11, 0	7, 3
21	LS3	11, 2	10, 0	4, 8	8, 4	9, 1	10, 0	10, 0	13, 0	13, 0	9, 0	11, 0	8, 2
22	LR1	8, 7	10, 0	6, 6	10, 2	7, 3	12, 0	11, 0	13, 0	10, 1	10, 3	12, 0	10, 5
23	LR2	9, 6	8, 2	5, 7	6, 6	6, 4	12, 0	8, 3	13, 0	9, 3	8, 5	12, 0	8, 4
24	LR3	13, 2	8, 2	6, 6	5, 7	6, 4	12, 0	7, 4	13, 0	12, 0	9, 5	12, 0	9, 3
25	LQ1	8, 5	12, 0	6, 5	7, 4	7, 2	10, 0	9, 2	13, 0	10, 1	8, 5	13, 0	11, 6
26	LQ2	7, 6	12, 0	5, 5	4, 7	5, 4	10, 0	9, 2	13, 0	9, 2	8, 5	12, 0	8, 6
27	LQ3	10, 3	12, 0	6, 4	5, 6	5, 4	10, 0	10, 1	13, 0	9, 2	8, 5	13, 0	12, 2

NUMBER OF (1) NOISE AND (2) SIGNAL MEASUREMENTS USED TO COMPUTE THE NETWORK ESTIMATES OF THE MAGNITUDES OF THE 27 PARAMETERS IN TABLE VI

	EVENT :	62	63	64	65	66	67	68	69	70	72	73	74
1	P1	11, 3	6, 6	10, 2	11, 1	7, 2	8, 3	9, 5	1, 0	9, 1	8, 2	6, 2	3, 0
2	P2	3, 11	1, 11	3, 9	10, 2	8, 1	3, 8	7, 7	1, 0	6, 4	4, 6	3, 5	2, 1
3	P3	4, 10	1, 11	6, 6	8, 4	6, 3	3, 8	11, 3	1, 0	7, 3	6, 4	2, 6	2, 1
4	OMEGA-2	0, 9	0, 11	0, 8	0, 2	0, 0	0, 7	0, 3	0, 0	0, 1	0, 5	0, 5	0, 1
5	CR.FR-2	0, 8	0, 11	0, 8	0, 2	0, 0	0, 7	0, 3	0, 0	0, 1	0, 5	0, 5	0, 1
6	T*-2	0, 8	0, 11	0, 8	0, 2	0, 0	0, 7	0, 3	0, 0	0, 1	0, 5	0, 5	0, 1
7	OMEGA-3	0, 8	0, 11	0, 8	0, 2	0, 0	0, 7	0, 3	0, 0	0, 1	0, 5	0, 5	0, 1
8	CR.FR-3	0, 8	0, 11	0, 8	0, 2	0, 0	0, 7	0, 3	0, 0	0, 1	0, 5	0, 5	0, 1
9	T*-3	0, 8	0, 11	0, 8	0, 2	0, 0	0, 7	0, 3	0, 0	0, 1	0, 5	0, 5	0, 1
10	COMP1	0, 6	0, 9	0, 3	0, 1	0, 2	0, 2	0, 4	0, 0	0, 3	0, 2	0, 2	0, 0
11	COMP2	0, 6	0, 9	0, 3	0, 1	0, 2	0, 1	0, 3	0, 0	0, 2	0, 1	0, 2	0, 0
12	COMP3	0, 6	0, 6	0, 3	0, 1	0, 1	0, 2	0, 0	0, 0	0, 1	0, 1	0, 2	0, 0
13	LG1	0, 0	1, 0	1, 0	1, 0	1, 0	1, 2	1, 1	1, 1	1, 1	1, 0	2, 0	1, 1
14	LG2	0, 0	1, 0	1, 0	1, 0	1, 0	1, 2	2, 0	1, 1	1, 1	1, 0	2, 0	1, 1
15	LG3	0, 0	1, 0	1, 0	1, 0	1, 0	1, 2	2, 0	1, 1	0, 2	1, 0	2, 0	1, 1
16	LP1	10, 1	14, 0	13, 0	15, 0	11, 0	8, 0	11, 0	7, 0	12, 0	9, 1	9, 4	8, 0
17	LP2	10, 1	14, 0	13, 0	15, 0	11, 0	8, 0	11, 0	7, 0	12, 0	9, 1	9, 4	8, 0
18	LP3	11, 0	14, 0	13, 0	15, 0	11, 0	8, 0	11, 0	7, 0	12, 0	10, 0	11, 2	8, 0
19	LS1	11, 0	12, 0	14, 0	15, 0	10, 0	8, 0	6, 4	6, 0	7, 0	9, 1	8, 4	6, 0
20	LS2	11, 0	12, 0	13, 1	15, 0	10, 0	8, 0	6, 4	6, 0	7, 0	9, 1	8, 4	6, 0
21	LS3	11, 0	12, 0	13, 1	15, 0	10, 0	8, 0	8, 2	6, 0	7, 0	9, 1	8, 4	6, 0
22	LR1	9, 3	13, 1	11, 2	16, 0	13, 1	9, 0	9, 4	8, 1	15, 0	9, 3	11, 3	9, 0
23	LR2	8, 4	12, 2	9, 4	16, 0	13, 1	9, 0	6, 7	8, 1	15, 0	11, 1	3, 11	9, 0
24	LR3	10, 2	12, 2	10, 3	16, 0	14, 0	9, 0	7, 6	8, 1	15, 0	11, 1	5, 9	9, 0
25	LQ1	10, 2	13, 0	12, 1	17, 0	15, 0	11, 0	8, 7	8, 1	14, 0	9, 4	7, 9	9, 0
26	LQ2	10, 2	13, 0	10, 3	17, 0	15, 0	11, 0	8, 7	8, 1	14, 0	9, 4	6, 10	9, 0
27	LQ3	10, 2	13, 0	12, 1	17, 0	15, 0	11, 0	9, 6	7, 2	14, 0	9, 4	7, 9	9, 0

	EVENT :	75	76	77	78	79	80	81	143	144	145	146	147
1	P1	7, 2	11, 0	2, 10	7, 1	5, 1	8, 1	1, 11	0, 13	1, 3	3, 8	5, 5	1, 11
2	P2	8, 1	11, 0	0, 12	8, 0	2, 4	4, 5	0, 12	0, 13	1, 3	1, 10	3, 7	0, 12
3	P3	7, 2	10, 1	0, 12	7, 1	3, 3	7, 2	0, 12	0, 13	2, 2	1, 10	5, 5	0, 12
4	OMEGA-2	0, 1	0, 0	0, 12	0, 0	0, 3	0, 3	0, 12	0, 13	0, 2	0, 10	0, 5	0, 12
5	CR.FR-2	0, 1	0, 0	0, 12	0, 0	0, 3	0, 3	0, 12	0, 13	0, 2	0, 10	0, 5	0, 12
6	T*-2	0, 1	0, 0	0, 12	0, 0	0, 3	0, 3	0, 12	0, 13	0, 2	0, 10	0, 5	0, 12
7	OMEGA-3	0, 1	0, 0	0, 12	0, 0	0, 3	0, 3	0, 12	0, 13	0, 2	0, 10	0, 5	0, 12
8	CR.FR-3	0, 1	0, 0	0, 12	0, 0	0, 3	0, 3	0, 12	0, 13	0, 2	0, 10	0, 5	0, 12
9	T*-3	0, 1	0, 0	0, 12	0, 0	0, 3	0, 3	0, 12	0, 13	0, 2	0, 10	0, 5	0, 12
10	COMP1	0, 1	0, 0	0, 8	0, 1	0, 1	0, 1	0, 5	0, 7	0, 2	0, 8	0, 1	0, 8
11	COMP2	0, 1	0, 0	0, 9	0, 0	0, 1	0, 1	0, 5	0, 7	0, 2	0, 8	0, 1	0, 7
12	COMP3	0, 0	0, 0	0, 9	0, 0	0, 0	0, 0	0, 5	0, 5	0, 1	0, 8	0, 1	0, 5
13	LG1	2, 0	1, 1	0, 0	1, 0	2, 0	0, 0	2, 0	1, 0	0, 0	1, 0	1, 0	1, 0
14	LG2	2, 0	1, 1	0, 0	1, 0	2, 0	0, 0	2, 0	1, 0	0, 0	1, 0	1, 0	1, 0
15	LG3	2, 0	1, 1	0, 0	1, 0	2, 0	0, 0	2, 0	1, 0	0, 0	1, 0	1, 0	1, 0
16	LP1	11, 0	12, 0	10, 3	7, 0	11, 0	8, 0	10, 1	1, 10	10, 0	12, 0	11, 0	10, 1
17	LP2	11, 0	12, 0	10, 3	7, 0	11, 0	8, 0	10, 1	1, 10	10, 0	12, 0	11, 0	10, 1
18	LP3	11, 0	12, 0	13, 0	7, 0	11, 0	8, 0	11, 0	2, 9	10, 0	12, 0	11, 0	9, 2
19	LS1	9, 0	10, 0	4, 6	7, 0	12, 0	7, 0	10, 2	4, 8	9, 0	11, 0	11, 1	8, 3
20	LS2	9, 0	10, 0	5, 5	7, 0	12, 0	7, 0	10, 2	3, 9	9, 0	11, 0	11, 1	8, 3
21	LS3	9, 0	10, 0	7, 3	7, 0	12, 0	7, 0	11, 1	3, 9	9, 0	11, 0	12, 0	9, 2
22	LR1	11, 0	12, 0	9, 4	10, 1	13, 0	8, 0	11, 1	2, 11	11, 0	12, 0	13, 0	8, 4
23	LR2	11, 0	11, 1	1, 12	10, 1	13, 0	8, 0	10, 2	1, 12	11, 0	12, 0	11, 2	10, 2
24	LR3	11, 0	12, 0	1, 12	10, 1	13, 0	8, 0	10, 2	4, 9	11, 0	12, 0	11, 2	10, 2
25	LQ1	12, 0	12, 1	4, 9	12, 1	14, 0	10, 0	12, 1	1, 11	11, 0	12, 0	10, 3	11, 1
26	LQ2	12, 0	12, 1	3, 10	12, 1	14, 0	10, 0	8, 5	1, 11	11, 0	12, 0	11, 0	10, 2
27	LQ3	12, 0	13, 0	3, 10	12, 1	14, 0	10, 0	10, 3	3, 9	11, 0	12, 0	11, 0	11, 1

NUMBER OF (1) NOISE AND (2) SIGNAL MEASUREMENTS USED TO COMPUTE THE NETWORK ESTIMATES OF THE MAGNITUDES OF THE 27 PARAMETERS IN TABLE VI

EVENT :	148	149	150	151	152	153	154	155	156	157	158	159
1 P1	2, 4	0,10	7, 3	4, 7	9, 3	9, 0	2, 9	8, 1	7, 1	3, 7	7, 1	9, 1
2 P2	1, 5	0,10	7, 3	2, 9	4, 8	7, 2	1,10	6, 3	3, 5	1, 9	2, 6	3, 1
3 P3	1, 5	1, 9	8, 2	4, 7	8, 4	8, 1	1,10	8, 1	4, 4	2, 8	6, 2	8, 2
4 OMEGA-2	0, 4	0,10	0, 1	0, 8	0, 0	0, 1	0, 9	0, 0	0, 3	0, 7	0, 2	0, 1
5 CR.FR-2	0, 4	0,10	0, 1	0, 8	0, 0	0, 1	0, 9	0, 0	0, 3	0, 7	0, 2	0, 1
6 T*-2	0, 4	0,10	0, 1	0, 8	0, 0	0, 1	0, 9	0, 0	0, 3	0, 7	0, 2	0, 1
7 OMEGA-3	0, 4	0,10	0, 1	0, 8	0, 0	0, 1	0, 9	0, 0	0, 3	0, 7	0, 2	0, 1
8 CR.FR-3	0, 4	0,10	0, 1	0, 8	0, 0	0, 1	0, 9	0, 0	0, 3	0, 7	0, 2	0, 1
9 T*-3	0, 4	0,10	0, 1	0, 8	0, 0	0, 1	0, 9	0, 0	0, 3	0, 7	0, 2	0, 1
10 COMP1	0, 0	0, 6	0, 3	0, 5	0, 2	0, 1	0, 8	0, 3	0, 2	0, 5	0, 1	0, 1
11 COMP2	0, 0	0, 6	0, 3	0, 5	0, 1	0, 0	0, 8	0, 0	0, 2	0, 4	0, 1	0, 1
12 COMP3	0, 0	0, 3	0, 0	0, 1	0, 0	1, 0	0, 7	1, 0	1, 3	1, 0	1, 0	1, 0
13 LG1	1, 0	0, 2	1, 0	2, 0	2, 0	1, 0	1, 0	1, 0	1, 0	1, 0	1, 0	2, 0
14 LG2	1, 0	2, 0	1, 0	2, 0	2, 0	1, 0	1, 0	1, 0	1, 0	1, 0	1, 0	2, 0
15 LG3	1, 0	2, 0	1, 0	2, 0	2, 0	1, 0	1, 0	1, 0	1, 0	1, 0	1, 0	2, 0
16 LP1	11, 0	7, 2	12, 0	11, 0	12, 1	13, 0	11, 0	9, 0	12, 0	11, 0	13, 0	12, 0
17 LP2	11, 0	7, 2	12, 0	11, 0	13, 0	13, 0	11, 0	9, 0	12, 0	11, 0	13, 0	12, 0
18 LP3	11, 0	7, 2	12, 0	11, 0	13, 0	13, 0	11, 0	9, 0	12, 0	11, 0	13, 0	12, 0
19 LS1	8, 0	4, 3	9, 0	6, 5	9, 0	8, 0	12, 0	5, 0	10, 0	11, 0	14, 0	11, 0
20 LS2	8, 0	5, 2	9, 0	6, 5	9, 2	10, 2	12, 0	5, 0	10, 0	12, 0	14, 0	11, 0
21 LS3	8, 0	5, 2	9, 0	7, 4	10, 1	8, 2	12, 0	5, 0	11, 0	12, 0	13, 0	12, 0
22 LR1	5, 2	3, 9	11, 0	6, 5	10, 3	9, 2	13, 0	10, 0	9, 3	10, 3	13, 0	12, 0
23 LR2	3, 4	2,10	9, 2	3, 8	8, 5	10, 1	13, 0	10, 0	10, 2	13, 0	15, 0	12, 0
24 LR3	4, 3	5, 7	10, 1	6, 5	8, 5	11, 0	13, 0	10, 0	10, 2	10, 3	13, 0	12, 0
25 LQ1	5, 2	4, 6	11, 1	6, 6	8, 5	11, 1	13, 0	8, 0	10, 2	10, 3	13, 0	12, 0
26 LQ2	4, 3	2, 8	11, 1	4, 8	8, 5	10, 2	13, 0	8, 0	8, 4	10, 3	13, 0	12, 0
27 LQ3	4, 3	3, 7	11, 1	5, 7	8, 5	12, 0	13, 0	8, 0	10, 2	12, 1	13, 0	12, 0

EVENT :	160	161	162	163	164	165	166	167	168	169	170	171
1 P1	11, 0	10, 3	4, 7	11, 1	3,12	11, 2	4,10	7, 3	6, 1	3,11	0,14	8, 6
2 P2	6, 5	8, 5	2, 9	3, 9	0,15	2,11	2,12	6, 4	5, 2	1,13	0,14	5, 9
3 P3	9, 2	9, 2	2, 9	4, 8	1,14	4, 9	8, 6	9, 1	7, 0	0,14	1,13	4,10
4 OMEGA-2	0, 2	0, 2	0, 8	0, 5	0,15	0, 9	0,10	0, 2	0, 2	0,12	0,14	0,10
5 CR.FR-2	0, 2	0, 2	0, 8	0, 5	0,15	0, 9	0,10	0, 2	0, 2	0,12	0,14	0,10
6 T*-2	0, 2	0, 2	0, 8	0, 5	0,15	0, 9	0,10	0, 2	0, 2	0,12	0,14	0,10
7 OMEGA-3	0, 2	0, 2	0, 8	0, 5	0,15	0, 9	0,10	0, 2	0, 2	0,12	0,14	0,10
8 CR.FR-3	0, 2	0, 2	0, 8	0, 5	0,15	0, 9	0,10	0, 2	0, 2	0,12	0,14	0,10
9 T*-3	0, 2	0, 2	0, 8	0, 5	0,12	0, 6	0, 9	0, 2	0, 2	0, 7	0, 8	0, 6
10 COMP1	0, 2	0, 1	0, 3	0, 2	0,11	0, 6	0, 3	0, 0	0, 0	1, 6	2, 8	1, 6
11 COMP2	0, 1	0, 1	0, 2	0, 2	0, 8	0, 6	0, 3	0, 0	0, 0	1, 5	2, 8	1, 6
12 COMP3	0, 0	1, 0	2, 0	1, 0	1, 0	1, 0	1, 0	1, 0	0, 0	1, 0	2, 0	1, 0
13 LG1	1, 0	1, 1	2, 0	1, 0	1, 0	1, 0	1, 0	1, 0	0, 0	1, 0	2, 0	1, 0
14 LG2	1, 0	1, 1	2, 0	1, 0	1, 0	1, 0	1, 0	1, 0	0, 0	1, 0	2, 0	1, 0
15 LG3	1, 0	1, 1	2, 0	1, 0	1, 0	1, 0	1, 0	1, 0	0, 0	1, 0	2, 0	1, 0
16 LP1	15, 0	10, 0	10, 0	10, 0	9, 5	11, 2	10, 0	8, 1	10, 0	12, 0	14, 0	14, 0
17 LP2	15, 0	10, 0	10, 0	10, 0	12, 2	11, 2	10, 0	8, 1	9, 0	13, 0	14, 0	14, 0
18 LP3	15, 0	10, 0	10, 0	10, 0	13, 1	13, 2	10, 0	8, 1	10, 0	12, 0	14, 0	14, 0
19 LS1	13, 0	7, 1	8, 0	8, 0	6, 6	10, 2	4, 7	5, 1	8, 0	7, 5	11, 0	11, 0
20 LS2	13, 0	7, 1	8, 0	8, 0	7, 5	11, 1	6, 5	5, 1	8, 0	8, 4	12, 0	12, 0
21 LS3	13, 0	7, 1	8, 0	8, 0	5, 7	10, 2	7, 4	5, 1	8, 0	8, 4	12, 0	12, 0
22 LR1	15, 0	10, 0	5, 2	9, 0	3,11	10, 2	3, 9	8, 2	11, 0	7, 5	14, 0	14, 0
23 LR2	15, 0	10, 1	2, 9	9, 0	2,12	6, 2	1,11	7, 3	11, 0	9, 4	14, 0	14, 0
24 LR3	15, 0	11, 0	4, 7	9, 0	6, 8	10, 2	3, 9	7, 3	12, 0	7, 5	14, 0	14, 0
25 LQ1	14, 0	11, 0	3, 8	12, 0	4, 9	8, 3	2,10	8, 2	9, 2	5, 4	14, 0	14, 0
26 LQ2	14, 0	12, 0	4, 7	12, 0	3,10	7, 4	1,11	7, 3	8, 3	5, 4	14, 0	14, 0
27 LQ3	14, 0	11, 1	5, 6	12, 0	6, 7	10, 1	2,10	8, 2	11, 0	7, 2	12, 0	14, 0

NUMBER OF (1) NOISE AND (2) SIGNAL MEASUREMENTS USED TO COMPUTE THE NETWORK ESTIMATES OF THE MAGNITUDES OF THE 27 PARAMETERS IN TABLE VI

	EVENT :	172	173	175	176	177	178	179	180	182	183	184	185
1	P1	10, 1	9, 1	3, 7	4, 2	7, 3	1, 5	4, 2	2, 4	8, 4	8, 4	6, 4	11, 0
2	P2	4, 7	7, 3	2, 8	4, 2	6, 4	0, 6	1, 5	3, 3	3, 9	2, 10	5, 5	6, 5
3	P3	9, 2	8, 2	1, 9	4, 2	6, 4	2, 4	2, 4	4, 2	5, 7	3, 9	6, 4	9, 2
4	OMEGA-2	0, 4	0, 2	0, 8	0, 2	0, 2	0, 6	0, 5	0, 3	0, 7	0, 9	0, 4	0, 2
5	CR.FR-2	0, 4	0, 2	0, 8	0, 2	0, 2	0, 6	0, 5	0, 3	0, 7	0, 9	0, 4	0, 2
6	T*-2	0, 4	0, 2	0, 8	0, 2	0, 2	0, 6	0, 5	0, 3	0, 7	0, 9	0, 4	0, 2
7	OMEGA-3	0, 4	0, 2	0, 8	0, 2	0, 2	0, 6	0, 5	0, 3	0, 7	0, 9	0, 4	0, 2
8	CR.FR-3	0, 4	0, 2	0, 8	0, 2	0, 2	0, 6	0, 5	0, 3	0, 7	0, 9	0, 4	0, 2
9	T*-3	0, 4	0, 2	0, 8	0, 2	0, 2	0, 6	0, 5	0, 3	0, 7	0, 9	0, 4	0, 2
10	COMP1	0, 4	0, 1	0, 7	0, 1	0, 2	0, 5	0, 2	0, 3	0, 5	0, 9	0, 3	0, 2
11	COMP2	0, 4	0, 1	0, 6	0, 1	0, 1	0, 5	0, 2	0, 3	0, 5	0, 9	0, 3	0, 2
12	COMP3	0, 1	0, 1	0, 1	0, 1	0, 1	0, 3	0, 2	0, 3	0, 5	0, 9	0, 3	0, 2
13	LG1	2, 0	3, 0	1, 0	1, 0	1, 1	1, 3	1, 2	1, 3	1, 5	1, 9	1, 3	2, 2
14	LG2	2, 0	2, 1	1, 0	1, 0	1, 1	1, 3	1, 2	1, 3	1, 5	1, 9	1, 3	2, 2
15	LG3	2, 0	2, 1	1, 0	1, 0	1, 1	1, 3	1, 2	1, 3	1, 5	1, 9	1, 3	2, 2
16	LP1	13, 0	11, 0	9, 2	14, 0	10, 2	1, 9	10, 2	12, 0	11, 2	14, 0	10, 1	9, 1
17	LP2	13, 0	11, 0	8, 3	14, 0	11, 1	2, 8	10, 1	12, 0	12, 1	14, 0	10, 1	8, 2
18	LP3	13, 0	11, 0	10, 1	14, 0	12, 1	2, 8	10, 1	12, 0	13, 1	14, 0	10, 1	10, 0
19	LS1	11, 0	8, 0	6, 0	12, 0	7, 0	1, 11	5, 3	11, 0	11, 2	13, 0	8, 2	8, 2
20	LS2	11, 0	8, 0	6, 0	12, 0	7, 0	0, 12	7, 1	11, 0	13, 0	13, 0	8, 2	8, 2
21	LS3	11, 0	8, 0	6, 0	12, 0	7, 0	1, 11	8, 1	11, 0	12, 1	13, 0	8, 2	10, 0
22	LR1	14, 1	12, 1	4, 0	13, 0	8, 2	2, 11	4, 0	14, 0	11, 1	11, 3	10, 0	6, 2
23	LR2	13, 2	12, 1	4, 8	13, 0	8, 2	0, 13	2, 6	14, 0	11, 1	11, 3	10, 0	6, 2
24	LR3	12, 3	12, 1	5, 7	13, 0	9, 1	6, 7	5, 5	14, 0	11, 1	13, 1	10, 0	6, 2
25	LQ1	10, 3	11, 1	5, 7	14, 0	11, 2	2, 11	5, 6	14, 0	14, 0	11, 2	9, 0	8, 2
26	LQ2	10, 3	10, 2	4, 8	14, 0	11, 2	1, 12	3, 8	14, 0	13, 1	10, 3	9, 0	7, 4
27	LQ3	11, 2	11, 1	6, 6	14, 0	12, 1	6, 7	4, 7	14, 0	13, 1	12, 1	9, 0	7, 5

	EVENT :	186	187	188	189	190	191	192	193	194	195	264	265
1	P1	2, 2	9, 0	9, 2	4, 7	5, 7	11, 1	8, 0	7, 2	9, 0	3, 9	0, 3	1, 4
2	P2	3, 1	7, 2	6, 5	3, 8	2, 10	7, 5	6, 2	5, 4	8, 1	2, 10	0, 3	0, 5
3	P3	4, 0	6, 3	8, 3	1, 10	5, 7	9, 3	7, 1	9, 2	9, 0	2, 9	0, 3	0, 5
4	OMEGA-2	0, 1	0, 2	0, 3	0, 10	0, 5	0, 3	0, 0	0, 1	0, 0	0, 9	0, 3	0, 5
5	CR.FR-2	0, 1	0, 2	0, 3	0, 10	0, 5	0, 3	0, 0	0, 1	0, 0	0, 9	0, 3	0, 5
6	T*-2	0, 1	0, 2	0, 3	0, 10	0, 5	0, 3	0, 0	0, 1	0, 0	0, 9	0, 3	0, 5
7	OMEGA-3	0, 1	0, 2	0, 3	0, 10	0, 5	0, 3	0, 0	0, 1	0, 0	0, 9	0, 3	0, 5
8	CR.FR-3	0, 1	0, 2	0, 3	0, 10	0, 5	0, 3	0, 0	0, 1	0, 0	0, 9	0, 3	0, 5
9	T*-3	0, 1	0, 2	0, 3	0, 10	0, 5	0, 2	0, 0	0, 1	0, 0	0, 9	0, 3	0, 5
10	COMP1	0, 1	0, 2	0, 3	0, 5	0, 5	0, 1	0, 0	0, 1	0, 0	0, 6	0, 1	0, 2
11	COMP2	0, 1	0, 1	0, 3	0, 5	0, 6	0, 1	0, 0	0, 1	0, 0	0, 6	0, 1	0, 2
12	COMP3	0, 1	0, 1	0, 1	1, 0	0, 2	0, 1	0, 0	0, 1	0, 0	0, 6	0, 1	0, 2
13	LG1	1, 0	2, 0	2, 0	1, 0	1, 2	1, 1	0, 0	2, 0	2, 0	2, 6	0, 1	2, 2
14	LG2	1, 0	2, 0	2, 0	1, 0	3, 0	1, 1	0, 0	2, 0	2, 0	2, 6	0, 1	2, 2
15	LG3	1, 0	2, 0	2, 0	1, 0	3, 0	1, 1	0, 0	2, 0	2, 0	2, 6	0, 1	2, 2
16	LP1	8, 1	9, 0	8, 0	11, 0	10, 0	9, 0	8, 0	11, 0	12, 0	8, 2	6, 1	6, 0
17	LP2	8, 1	9, 0	8, 0	11, 0	10, 0	9, 0	8, 0	11, 0	12, 0	8, 3	6, 1	6, 0
18	LP3	8, 1	9, 0	8, 0	11, 0	10, 0	9, 0	8, 0	10, 0	10, 0	8, 5	6, 1	6, 0
19	LS1	8, 1	9, 0	7, 0	9, 0	7, 0	8, 0	8, 0	10, 0	10, 0	6, 5	5, 1	6, 0
20	LS2	9, 1	9, 0	7, 0	9, 0	7, 0	8, 0	8, 0	10, 0	10, 0	6, 5	5, 1	6, 0
21	LS3	9, 0	9, 1	7, 0	9, 0	7, 0	8, 0	8, 0	10, 0	10, 0	6, 5	5, 1	6, 0
22	LR1	9, 2	9, 1	10, 2	13, 0	7, 6	11, 0	10, 0	9, 2	11, 0	7, 7	3, 2	7, 0
23	LR2	9, 2	7, 3	11, 1	13, 0	7, 6	11, 0	9, 1	7, 4	11, 0	7, 7	1, 4	7, 0
24	LR3	11, 0	10, 0	10, 2	13, 0	8, 5	11, 0	9, 1	8, 1	10, 0	6, 5	3, 2	7, 0
25	LQ1	10, 1	10, 1	10, 2	13, 0	8, 7	11, 0	10, 0	9, 1	10, 0	5, 10	3, 2	8, 0
26	LQ2	10, 1	9, 2	10, 2	13, 0	6, 7	11, 0	9, 1	10, 0	10, 0	8, 7	4, 3	8, 0
27	LQ3	11, 0	11, 0	10, 2	13, 0	8, 5	11, 0	9, 1	10, 0	10, 0	8, 7	4, 3	8, 0

NUMBER OF (1) NOISE AND (2) SIGNAL MEASUREMENTS USED TO COMPUTE THE NETWORK ESTIMATES OF THE MAGNITUDES OF THE 27 PARAMETERS IN TABLE VI

	EVENT :	266	267	268	269	270	271	272	273	274	276	277	278
1	P1	4, 9	1, 7	1, 9	0,14	1, 5	3,12	6, 1	0,12	1, 0	2, 0	4, 0	2, 2
2	P2	0,13	0, 8	0,10	0,14	0, 6	0,15	1, 6	0,12	0, 1	1, 1	1, 3	1, 3
3	P3	0,13	0, 8	0,10	1,13	0, 6	0,15	6, 1	1,11	0, 1	1, 1	2, 2	1, 3
4	OMEGA-2	0,13	0, 8	0,10	0,14	0, 6	0,15	0, 3	0,12	0, 1	0, 1	6, 1	0, 3
5	CR.FR-2	0,13	0, 8	0,10	0,14	0, 6	0,15	0, 3	0,12	0, 1	0, 1	0, 1	0, 3
6	T*-2	0,13	0, 8	0,10	0,14	0, 6	0,15	0, 3	0,12	0, 1	0, 1	0, 1	0, 3
7	OMEGA-3	0,13	0, 8	0,10	0,14	0, 6	0,15	0, 3	0,12	0, 1	0, 1	0, 1	0, 3
8	CR.FR-3	0,13	0, 8	0,10	0,14	0, 6	0,15	0, 3	0,12	0, 1	0, 1	0, 1	0, 3
9	T*-3	0,13	0, 8	0,10	0,14	0, 6	0,15	0, 3	0,11	0, 1	0, 1	0, 1	0, 3
10	COMP1	0, 8	0, 3	0, 6	0,10	0, 6	0,10	0, 4	0,11	0, 1	0, 1	0, 1	0, 1
11	COMP2	0, 8	0, 3	0, 6	0,10	0, 5	0,10	0, 4	0,11	0, 1	0, 1	0, 1	0, 1
12	COMP3	0, 8	0, 3	0, 6	0, 9	0, 5	0,10	0, 4	0,11	0, 1	0, 1	0, 1	0, 1
13	LG1	2, 0	1, 0	1, 0	1, 0	1, 0	2, 0	1, 0	1, 0	0, 0	0, 0	1, 0	1, 0
14	LG2	2, 0	1, 0	1, 0	0, 1	1, 0	2, 0	1, 0	1, 0	0, 0	0, 0	1, 0	1, 0
15	LG3	2, 0	1, 0	1, 0	1, 0	1, 0	2, 0	1, 0	1, 0	0, 0	0, 0	1, 0	1, 0
16	LP1	9, 0	9, 1	8, 1	11, 0	11, 0	9, 1	11, 0	10, 0	0, 0	0, 0	6, 0	6, 0
17	LP2	9, 0	9, 1	8, 1	11, 0	11, 0	10, 0	11, 0	10, 0	0, 0	0, 0	6, 0	6, 0
18	LP3	9, 0	10, 0	8, 1	11, 0	11, 0	10, 0	11, 0	10, 0	0, 0	0, 0	6, 0	6, 0
19	LS1	10, 0	6, 3	7, 2	11, 0	10, 1	7, 3	11, 0	12, 0	0, 0	0, 0	4, 0	5, 0
20	LS2	10, 0	6, 3	6, 3	12, 0	10, 1	8, 2	11, 0	11, 0	0, 0	0, 0	4, 0	5, 0
21	LS3	9, 1	6, 3	7, 2	12, 0	11, 0	8, 2	11, 0	12, 0	0, 0	0, 0	4, 0	5, 0
22	LR1	11, 0	7, 4	9, 3	11, 1	11, 0	12, 2	11, 0	14, 0	0, 0	1, 0	7, 0	7, 0
23	LR2	10, 1	5, 6	9, 3	9, 3	8, 3	7, 7	9, 4	14, 0	0, 0	1, 0	7, 0	7, 0
24	LR3	11, 0	6, 5	10, 2	8, 4	8, 3	7, 7	11, 2	14, 0	0, 0	1, 0	7, 0	7, 0
25	LQ1	10, 0	6, 5	11, 1	13, 0	12, 0	8, 4	12, 1	14, 0	0, 0	1, 0	8, 0	6, 0
26	LQ2	9, 1	5, 6	10, 2	11, 2	10, 2	6, 6	9, 4	13, 1	0, 0	2, 0	6, 1	6, 0
27	LQ3	10, 0	6, 5	11, 1	12, 1	9, 3	6, 6	12, 1	14, 0	0, 0	2, 0	5, 1	6, 0

APPENDIX III

Attenuation coefficient t* for each region-to-station path

a) ω^{-2} model

b) ω^{-3} model

T* FOR EACH REGION-TO-STATION PATH
ASSUMING FALL-OFF AS OMEGA-SQUARED

REGION 1 EVENT	ANMO	ANTO	ATAK	BFAK	BOCO	CHTO	CNAK	CTAO	GUMO	HNME	IR7	KAAO	KONO	KSRS
50	0.40			0.40			0.50	0.30			0.40	0.30		0.10
58														
64	0.20			0.50			0.50					0.20		
143	0.40		0.50	0.50		0.30	0.50	0.50			0.70	0.10		0.50
146				0.20			0.50							
148	0.30						0.60							
156				0.60										0.20
157	0.50			0.50		0.40								0.70
158														
165			0.10	0.50			0.60					0.10		
169	0.40		0.20	0.40			0.50	0.40				0.10		
171	0.40			0.60		0.30	0.60				0.10	0.20		
176											0.50	0.10		0.50
178	0.30					0.20								
180	0.10					0.10								0.40
182				0.50		0.20	0.90					0.20		
183			0.20	0.40		0.20								
186						0.40								
193														
194														
<T*>	0.333		0.250	0.464		0.262	0.578	0.400			0.425	0.162		0.400
SIGMA	0.122		0.173	0.112		0.106	0.130	0.100			0.250	0.074		0.219

REGION 2 EVENT	ANMO	ANTO	ATAK	BFAK	BOCO	CHTO	CNAK	CTAO	GUMO	HNME	IR7	KAAO	KONO	KSRS
36														0.40
47	0.40		0.20	0.40		0.30	0.30							
49	0.60					0.20		0.50		0.10	0.30	0.20		0.40
55				0.20										
56											0.20	0.30		
57				0.30										
60														
62				0.30			0.50							
144						0.40						0.20		
147	0.30		0.30	0.10		0.20	0.30				0.30	0.10		0.20
154				0.40			0.40				0.20	0.20		
164	0.40		0.60	0.30			0.40	0.40		0.50	0.40	0.20		0.40
<T*>	0.425		0.367	0.286		0.275	0.380	0.450		0.300	0.280	0.200		0.350
SIGMA	0.126		0.208	0.107		0.096	0.084	0.071		0.283	0.084	0.063		0.100

REGION 3 EVENT	ANMO	ANTO	ATAK	BFAK	BOCO	CHTO	CNAK	CTAO	GUMO	HNME	IR7	KAAO	KONO	KSRS
3				0.40			0.40				0.30	0.20		
18	0.40					0.20				0.20	0.20			0.30
37				0.70			0.40			0.20				
63	0.30			0.30			0.40				0.30	0.10		
269	0.80	0.30		0.40		0.30	0.30	0.40						0.80
<T*>	0.500	0.300		0.450		0.250	0.375	0.400		0.200	0.267	0.150		0.550
SIGMA	0.265	0.0		0.173		0.071	0.050	0.0		0.001	0.058	0.071		0.354

REGION 4 EVENT	ANMO	ANTO	ATAK	BFAK	BOCO	CHTO	CNAK	CTAO	GUMO	HNME	IR7	KAAO	KONO	KSRS
16	0.40									0.10		0.30		0.30
21	0.20		0.20	0.30			0.30			0.40	0.20	0.10		
65							0.20							
270	0.50	0.20				0.30								0.20
<T*>	0.367	0.200	0.200	0.300		0.300	0.250			0.250	0.200	0.200		0.250
SIGMA	0.153	0.0	0.0	0.0		0.0	0.071			0.212	0.0	0.141		0.071

T* FOR EACH REGION-TO-STATION PATH
ASSUMING FALL-OFF AS OMEGA-SQUARED

REGION 1 EVENT	LAO	MAIO	MAJO	NAO	NJAK	NWAO	RKON	SHIO	SNZO	TATO	TNAK	UCAK	ZOBO
											0.40	0.40	
50	0.50	0.30		0.80	0.80								
58											0.40	0.40	
64				0.30	0.80						0.40	0.50	
143	0.50				0.50						0.60	0.70	
146					0.60						0.40	0.40	
148											0.30		
156					0.10						0.20	0.40	
157					0.30								
158					0.40						0.40	0.60	
165	0.60			0.30	0.30						0.40	0.20	
169	0.40			0.10	0.20		0.20				0.20	0.70	
171	0.80				0.50								
176	0.30				0.30								
178		0.10											
180	0.80										0.50	0.90	
182					0.50						0.60	0.20	
183	0.30			0.20	0.30								
186												0.50	
193													
194													
<T*>	0.525	0.200		0.340	0.431		0.200				0.400	0.492	
SIGMA	0.198	0.141		0.270	0.214		0.0				0.128	0.207	

REGION 2 EVENT	LAO	MAIO	MAJO	NAO	NJAK	NWAO	RKON	SHIO	SNZO	TATO	TNAK	UCAK	ZOBO
36				0.60									
47	0.60				0.50		0.40				0.20	0.60	
49	0.60	0.40		0.20		0.30	0.10						
55					0.50								
56											0.20		
57													
60											0.40	0.40	
62	0.50		0.40	0.20	0.30								
144											0.20	0.20	
147	0.30			0.10							0.30	0.20	
154	0.20			0.30	0.50						0.30	0.30	
164	0.40	0.20		0.10	0.30								
<T*>	0.433	0.300	0.400	0.250	0.420	0.300	0.250				0.267	0.340	
SIGMA	0.163	0.141	0.0	0.187	0.110	0.0	0.212				0.082	0.167	

REGION 3 EVENT	LAO	MAIO	MAJO	NAO	NJAK	NWAO	RKON	SHIO	SNZO	TATO	TNAK	UCAK	ZOBO
											0.40		
3				0.60									
18							0.20						
37					0.30								
63	0.60	0.20	0.20		0.20						0.20	0.40	
269		0.30	0.20	0.10	0.50			0.20			0.40	0.40	
<T*>	0.600	0.250	0.200	0.350	0.333		0.200	0.200			0.333	0.400	
SIGMA	0.0	0.071	0.001	0.354	0.153		0.0	0.0			0.115	0.001	

REGION 4 EVENT	LAO	MAIO	MAJO	NAO	NJAK	NWAO	RKON	SHIO	SNZO	TATO	TNAK	UCAK	ZOBO
16				0.40			0.40						
21					0.30		0.20				0.20	0.30	
65				0.30				0.10					
270		0.20									0.200	0.300	
<T*>		0.200		0.350	0.300		0.300	0.100			0.0	0.0	
SIGMA		0.0		0.071	0.0		0.141	0.0					

T* FOR EACH REGION-TO-STATION PATH
ASSUMING FALL-OFF AS OMEGA-SQUARED

REGION 5 EVENT	ANMO	ANTO	ATAK	BFAK	BOCO	CHTO	CNAK	CTAO	GUMO	HNME	IR7	KAAO	KONO	KSRS
77			0.30	0.40		0.50	0.40				0.30	0.60		
145				0.30		0.20	0.30				0.10	0.10		0.10
160				0.30										0.50
<T*>			0.300	0.333		0.350	0.350				0.200	0.350		0.300
SIGMA			0.0	0.058		0.212	0.071				0.141	0.354		0.283

REGION 6 EVENT	ANMO	ANTO	ATAK	BFAK	BOCO	CHTO	CNAK	CTAO	GUMO	HNME	IR7	KAAO	KONO	KSRS
6											0.30			
25				0.30		0.30	0.40					0.20		
195											0.300	0.200		
<T*>				0.300		0.300	0.400				0.0	0.0		
SIGMA				0.0		0.0	0.0							

REGION 7 EVENT	ANMO	ANTO	ATAK	BFAK	BOCO	CHTO	CNAK	CTAO	GUMO	HNME	IR7	KAAO	KONO	KSRS
7				0.60			0.20				0.10			0.40
24							0.30				0.20	0.20		
27												0.10		
29											0.60			0.20
30			0.40	0.30		0.40	0.30							
31							0.90					0.20		
32						0.50	0.70					0.30		
34						0.50					0.40	0.30		
35				0.60		0.30	0.50					0.50		
39						0.40	1.00							
46				0.40			0.60					0.40		
68											0.10			
75														
78												0.30		
151				0.50			0.50							
159												0.20		1.00
166			0.80	0.60			0.40					0.10		
190				0.60			0.40					0.10		
191							0.60							
192														
<T*>			0.600	0.514		0.420	0.533				0.280	0.245		0.533
SIGMA			0.283	0.121		0.084	0.242				0.217	0.129		0.416

REGION 8 EVENT	ANMO	ANTO	ATAK	BFAK	BOCO	CHTO	CNAK	CTAO	GUMO	HNME	IR7	KAAO	KONO	KSRS
59											0.20	0.10		
66											0.10	0.20		
73														
74												0.10		0.70
149			0.40			0.20	0.30	0.30						
150				0.60										
153			0.60											0.40
170			0.40	0.40		0.40	0.50	0.30			0.60			
172														
173											0.50			
175				0.50			0.40				0.20			
185														
188				0.30										
272				0.40			0.10							
<T*>			0.467	0.440		0.300	0.325	0.300			0.320	0.133		0.550
SIGMA			0.115	0.114		0.141	0.171	0.001			0.217	0.058		0.212

T* FOR EACH REGION-TO-STATION PATH
ASSOMING FALL-OFF AS OMEGA-SQOARED

REGION 5 EVENT	LAO	MAIO	MAJO	NAO	NJAK	NWAO	RKON	SHIO	SNZO	TATO	TNAK	OCAK	ZOBO
77	0.50	0.40			0.40		0.20				0.20	0.40	
145	0.40				0.50						0.20	0.30	
160													
<T*>	0.450	0.400			0.450		0.200				0.200	0.350	
SIGMA	0.071	0.0			0.071		0.0				0.001	0.071	

REGION 6 EVENT	LAO	MAIO	MAJO	NAO	NJAK	NWAO	RKON	SHIO	SNZO	TATO	TNAK	UCAK	ZOBO
6													
25				0.50							0.60	0.40	
195	0.40	0.50			0.40								
<T*>	0.400	0.500		0.500	0.400						0.600	0.400	
SIGMA	0.0	0.0		0.0	0.0						0.0	0.0	

REGION 7 EVENT	LAO	MAIO	MAJO	NAO	NJAK	NWAO	RKON	SHIO	SNZO	TATO	TNAK	OCAK	ZOBO
7				0.20	0.80						0.40		
24	1.00												
27		0.30	0.40		0.30								
29				0.50	0.30		0.30				0.50	0.50	
30					0.50							0.60	
31		0.80											
32												0.50	
34		0.60			0.60							0.40	
35		0.50			0.80								
39				0.50									
46		0.20			0.50								
68													
75		0.50		0.70	0.60						0.60	0.40	
78				0.10									
151					0.90						0.50	0.70	
159	0.60	0.50		0.70								0.40	
166												0.20	
190													
191													
192													
<T*>	0.800	0.486	0.400	0.450	0.589		0.300				0.500	0.462	
SIGMA	0.283	0.195	0.0	0.251	0.215		0.0				0.082	0.151	

REGION 8 EVENT	LAO	MAIO	MAJO	NAO	NJAK	NWAO	RKON	SHIO	SNZO	TATO	TNAK	UCAK	ZOBO
59		0.10											
66													
73	0.50	0.10		0.30									
74		0.10									0.40	0.30	
149	0.40	0.10											
150													
153											0.40	0.50	
170	0.10	0.10		0.40	0.40		0.60					0.30	
172	0.60			0.20	0.50							0.60	
173		0.10									0.50	0.30	
175	0.60			0.10	0.30								
185		0.10											
188		0.10		0.30									
272					0.40								
<T*>	0.440	0.100		0.260	0.400		0.600				0.433	0.400	
SIGMA	0.207	0.000		0.114	0.082		0.0				0.058	0.141	

T* FOR EACH REGION-TO-STATION PATH
ASSUMING FALL-OFF AS OMEGA-SQUARED

REGION 9 EVENT	ANMO	ANTO	ATAK	BFAK	BOCO	CHTO	CNAK	CTAO	GUMO	HNME	IR7	KAAO	KONO	KSRS
14	0.10			0.10		0.30	0.10			0.20		0.10		
17				0.30			0.30					0.20		0.10
20	0.30					0.30		0.40		0.40	0.50	0.10		0.30
53	0.30		0.30	0.10			0.10	0.30			0.30	0.10		0.30
79														
81	0.30		0.20	0.10		0.30		0.40		0.30	0.40	0.20		0.30
152							0.40					0.20		
187				0.30			0.20							
189			0.20	0.30			0.20					0.10		
264														0.40
265	0.10							0.60						0.40
266			0.10	0.30		0.20	0.20	0.20				0.20		0.20
267	0.30		0.30	0.10				0.60				0.20		
268	0.30		0.30	0.40				0.40						0.20
271	0.10		0.10	0.30		0.30	0.20					0.10		0.30
276														
277														0.20
278														
<T*>	0.225		0.214	0.230		0.280	0.212	0.414		0.300	0.400	0.150		0.270
SIGMA	0.104		0.090	0.116		0.045	0.099	0.146		0.100	0.100	0.053		0.095

REGION 10 EVENT	ANMO	ANTO	ATAK	BFAK	BOCO	CHTO	CNAK	CTAO	GUMO	HNME	IR7	KAAO	KONO	KSRS
4														
9												0.10		
10														
23														
26												0.10		
28														
38											0.20			0.20
41											0.10			
45										0.10	0.20	0.10		
48				0.70							0.30	0.10		
67			0.40	0.30										
69														
70											0.20			
72														
76														
155												0.10		
161						0.20					0.30			0.20
179														
<T*>			0.400	0.500		0.200				0.100	0.217	0.100		0.200
SIGMA			0.0	0.283		0.0				0.0	0.075	0.000		0.001

REGION 11 EVENT	ANMO	ANTO	ATAK	BFAK	BOCO	CHTO	CNAK	CTAO	GUMO	HNME	IR7	KAAO	KONO	KSRS
61				0.10								0.20		
167							0.30					0.10		
<T*>				0.100			0.300					0.150		
SIGMA				0.0			0.0					0.071		

REGION 12 EVENT	ANMO	ANTO	ATAK	BFAK	BOCO	CHTO	CNAK	CTAO	GUMO	HNME	IR7	KAAO	KONO	KSRS
22	0.30										0.10	0.10		0.20
274														
<T*>	0.300										0.100	0.100		0.200
SIGMA	0.0										0.0	0.0		0.0

T* FOR EACH REGION-TO-STATION PATH
ASSUMING FALL-OFF AS OMEGA-SQUARED

REGION 9 EVENT	LAO	MAIO	MAJO	NAO	NJAK	NWAO	RKON	SHIO	SNZO	TATO	TNAK	UCAK	ZOBO
14	0.30	0.10	0.10		0.30		0.20				0.20		
17	0.40			0.10			0.30				0.20	0.30	
20							0.10			0.10			
53	0.30	0.10	0.30	0.10	0.10	0.20					0.30	0.10	
79	0.50						0.20					0.10	
81	0.30						0.20					0.40	
152		0.20											
187											0.10	0.20	
189	0.30	0.10		0.10	0.30								
264	0.50	0.20									0.20	0.20	
265	0.30			0.10							0.20		
266	0.30	0.10		0.10	0.30						0.20	0.30	
267	0.40	0.30									0.20	0.20	
268		0.10			0.10	0.30		0.30		0.10			
271		0.30		0.10	0.30	0.10							
276				0.10			0.10						
277							0.10						
278		0.20											
<T*>	0.360	0.170	0.200	0.100	0.233	0.200	0.171	0.300		0.100	0.211	0.225	
SIGMA	0.084	0.082	0.141	0.000	0.103	0.100	0.076	0.0		0.001	0.060	0.104	

REGION 10 EVENT	LAO	MAIO	MAJO	NAO	NJAK	NWAO	RKON	SHIO	SNZO	TATO	TNAK	UCAK	ZOBO
4		0.10											
9													
10													
23		0.10											
26		0.10											
28													
38		0.20									0.20		
41													
45													
48		0.10		0.60	0.30								
67													
69					0.20								
70				0.30	0.80						0.20	0.20	
72													
76												0.20	
155					0.20								
161		0.10											
179		0.10		0.20									
<T*>		0.114		0.367	0.375						0.200	0.200	
SIGMA		0.038		0.208	0.287						0.001	0.001	

REGION 11 EVENT	LAO	MAIO	MAJO	NAO	NJAK	NWAO	RKON	SHIO	SNZO	TATO	TNAK	UCAK	ZOBO
61	0.60	0.10											
167													
<T*>	0.600	0.100											
SIGMA	0.0	0.0											

REGION 12 EVENT	LAO	MAIO	MAJO	NAO	NJAK	NWAO	RKON	SHIO	SNZO	TATO	TNAK	UCAK	ZOBO
22							0.20						
274				0.10									
<T*>				0.100			0.200						
SIGMA				0.0			0.0						

T* FOR EACH REGION-TO-STATION PATH
ASSUMING FALL-OFF AS OMEGA-SQUARED

REGION 13 EVENT	ANMO	ANTO	ATAK	BFAK	BOCO	CHTO	CNAK	CTAO	GUMO	HNME	IR7	KAAO	KONO	KSRS
8							0.20				0.10	0.40		
80							0.60				0.20	0.30		
162							0.40					0.50		
163				0.20							0.10			
168											0.10			
177														
184														
<T*>				0.200			0.400				0.125	0.400		
SIGMA				0.0			0.200				0.050	0.100		

REGION 14 EVENT	ANMO	ANTO	ATAK	BFAK	BOCO	CHTO	CNAK	CTAO	GUMO	HNME	IR7	KAAO	KONO	KSRS
1	0.70		0.10	0.20		0.50	0.20					0.10		
19	0.30					0.30				0.30	0.10	0.10		0.50
33			0.30	0.50			0.20			0.40				
273	0.30			0.40		0.10	0.30					0.30		0.10
<T*>	0.433		0.200	0.367		0.300	0.233			0.350	0.100	0.167		0.300
SIGMA	0.231		0.141	0.153		0.200	0.058			0.071	0.0	0.115		0.293

REGION 13 EVENT	LAO	MAIO	MAJO	NAO	NJAK	NWAO	RKON	SHIO	SNZO	TATO	TWAK	UCAK	ZOBO
8													
80												0.60	
162	0.50	0.20		0.10	0.60							0.40	
163					0.20								
168	0.50												
177	0.40												
184	0.60	0.60		0.30	0.20								
<T*>	0.500	0.400		0.200	0.333							0.500	
SIGMA	0.082	0.283		0.141	0.231							0.141	

REGION 14 EVENT	LAO	MAIO	MAJO	NAO	NJAK	NWAO	RKON	SHIO	SNZO	TATO	TWAK	UCAK	ZOBO
1	0.50	0.40	0.30		0.10						0.70	0.10	
19	0.40		0.20				0.10			0.60			
33	0.50			0.10	0.50		0.20				0.30	0.20	
273		0.30	0.20	0.40	0.30						0.30	0.10	
<T*>	0.467	0.350	0.233	0.250	0.300		0.150			0.600	0.433	0.200	
SIGMA	0.058	0.071	0.058	0.212	0.200		0.071			0.0	0.231	0.100	

T* FOR EACH REGION-TO-STATION PATH
ASSUMING FALL-OFF AS OMEGA-CUBED

REGION	1													
EVENT	ANMO	ANTO	ATAK	BFAK	BOCO	CHTO	CNAK	CTAO	GUMO	HNME	IB7	KAAO	KONO	KSRS
50	0.30			0.30			0.30	0.10			0.20	0.30		0.10
58												0.10		
64	0.10			0.50			0.80							
143	0.20		0.30	0.30		0.10	0.20	0.30			0.40	0.10		0.40
146				0.10			0.50							
148	0.30						0.50							
156				0.60										0.10
157	0.40			0.30		0.40								0.60
158												0.10		
165			0.10	0.50			0.40					0.10		
169	0.40		0.20	0.40			0.40	0.40						
171	0.30			0.60		0.20	0.40				0.10	0.20		
176											0.20	0.10		0.20
178	0.30					0.10								
180	0.10					0.10								0.30
182				0.40		0.10	0.80					0.10		
183			0.10	0.30		0.10								
186						0.30								
193														
194														
<T*>	0.267		0.175	0.391		0.175	0.433	0.267			0.225	0.137		0.283
SIGMA	0.112		0.096	0.151		0.116	0.166	0.153			0.126	0.074		0.194

REGION	2													
EVENT	ANMO	ANTO	ATAK	BFAK	BOCO	CHTO	CNAK	CTAO	GUMO	HNME	IB7	KAAO	KONO	KSRS
36														0.30
47	0.20		0.10	0.20		0.20	0.20							
49	0.30					0.20		0.30		0.10	0.10	0.10		0.20
55				0.10										
56											0.10	0.20		
57				0.30										
60							0.50							
62				0.30								0.10		
144						0.30					0.30	0.10		0.10
147	0.10		0.20	0.10		0.20	0.10				0.10	0.10		
154				0.30			0.20				0.30	0.10		0.20
164	0.20		0.50	0.30			0.30	0.30		0.30	0.30	0.20		
<T*>	0.200		0.267	0.229		0.225	0.260	0.300		0.200	0.180	0.133		0.200
SIGMA	0.082		0.208	0.095		0.050	0.152	0.001		0.141	0.110	0.052		0.082

REGION	3													
EVENT	ANMO	ANTO	ATAK	BFAK	BOCO	CHTO	CNAK	CTAO	GUMO	HNME	IB7	KAAO	KONO	KSRS
3				0.20			0.30				0.10	0.20		
18	0.20					0.10				0.10	0.10			0.10
37				0.70			0.30			0.10				
63	0.20			0.30			0.20				0.10	0.10		
269	0.80	0.30		0.30		0.20	0.20	0.20						0.70
<T*>	0.400	0.300		0.375		0.150	0.250	0.200		0.100	0.100	0.150		0.400
SIGMA	0.346	0.0		0.222		0.071	0.058	0.0		0.001	0.001	0.071		0.424

REGION	4													
EVENT	ANMO	ANTO	ATAK	BFAK	BOCO	CHTO	CNAK	CTAO	GUMO	HNME	IB7	KAAO	KONO	KSRS
16	0.20						0.30			0.10		0.20		0.10
21	0.10		0.10	0.20			0.10			0.30	0.20	0.10		
65														0.10
270	0.40	0.20				0.30								
<T*>	0.233	0.200	0.100	0.200		0.300	0.200			0.200	0.200	0.150		0.100
SIGMA	0.153	0.0	0.0	0.0		0.0	0.141			0.141	0.0	0.071		0.001

T* FOR EACH REGION-TO-STATION PATH
ASSUMING FALL-OFF AS OMEGA-CUBED

REGION 1 EVENT	LAO	MAIO	MAJO	NAO	NJAK	NWAO	RKON	SHIO	SNZO	TATO	TNAK	UCAK	ZOBO
											0.20	0.30	
50	0.30	0.10		0.70	0.60								
58											0.40	0.10	
64				0.20	0.50						0.40	0.30	
143	0.40				0.30						0.60	0.50	
146					0.40						0.30	0.20	
148											0.20		
156					0.10						0.10	0.20	
157					0.20								
158					0.40						0.10	0.50	
165	0.60			0.10	0.20		0.10				0.40	0.20	
169	0.30			0.10	0.20						0.10	0.70	
171	0.80				0.30								
176	0.10				0.10								
178		0.10											
180	0.70										0.50	0.90	
182					0.40						0.30	0.10	
183	0.10			0.20	0.30								
186												0.20	
193													
194													
<T*>	0.412	0.100		0.260	0.308		0.100				0.300	0.350	
SIGMA	0.264	0.001		0.251	0.150		0.0				0.165	0.250	

REGION 2 EVENT	LAO	MAIO	MAJO	NAO	NJAK	NWAO	RKON	SHIO	SNZO	TATO	TNAK	UCAK	ZOBO
36				0.30			0.20				0.10	0.30	
47	0.50				0.30		0.10						
49	0.40	0.20		0.20		0.10							
55					0.50								
56											0.10		
57													
60											0.40	0.40	
62	0.40		0.30	0.10	0.10								
144											0.10	0.10	
147	0.10			0.10							0.20	0.20	
154	0.10			0.10	0.50						0.20	0.10	
184	0.30	0.10		0.10	0.30								
<T*>	0.300	0.150	0.300	0.150	0.340	0.100	0.150				0.183	0.220	
SIGMA	0.167	0.071	0.0	0.084	0.167	0.0	0.071				0.117	0.130	

REGION 3 EVENT	LAO	MAIO	MAJO	NAO	NJAK	NWAO	RKON	SHIO	SNZO	TATO	TNAK	UCAK	ZOBO
											0.20		
3				0.60									
18							0.20						
37					0.10								
63	0.60	0.10	0.20		0.10						0.10	0.40	
269		0.20	0.20	0.10	0.30			0.10			0.20	0.30	
<T*>	0.600	0.150	0.200	0.350	0.167		0.200	0.100			0.167	0.350	
SIGMA	0.0	0.071	0.001	0.354	0.115		0.0	0.0			0.058	0.071	

REGION 4 EVENT	LAO	MAIO	MAJO	NAO	NJAK	NWAO	RKON	SHIO	SNZO	TATO	TNAK	UCAK	ZOBO
16				0.40			0.40						
21					0.10		0.10				0.10	0.30	
65				0.30									
270		0.20						0.10					
<T*>		0.200		0.350	0.100		0.250	0.100			0.100	0.300	
SIGMA		0.0		0.071	0.0		0.212	0.0			0.0	0.0	

T* FOR EACH REGION-TO-STATION PATH
ASSUMING FALL-OFF AS OMEGA-CUBED

REGION 5 EVENT	ANMO	ANTO	ATAK	BFAK	BOCO	CHTO	CNAK	CTAO	GUMO	HNME	IR7	KAAO	KONO	KSRS
77			0.20	0.40		0.40	0.30				0.20	0.50		0.10
145				0.20		0.10	0.30				0.10	0.10		0.40
160				0.20										
											0.150	0.300		0.250
<T*>			0.200	0.267		0.250	0.300				0.071	0.283		0.212
SIGMA			0.0	0.115		0.212	0.001							

REGION 6 EVENT	ANMO	ANTO	ATAK	BFAK	BOCO	CHTO	CNAK	CTAO	GUMO	HNME	IR7	KAAO	KONO	KSRS
6											0.20	0.10		
25				0.20		0.10	0.20							
195											0.200	0.100		
				0.200		0.100	0.200				0.0	0.0		
<T*>				0.0		0.0	0.0							
SIGMA														

REGION 7 EVENT	ANMO	ANTO	ATAK	BFAK	BOCO	CHTO	CNAK	CTAO	GUMO	HNME	IR7	KAAO	KONO	KSRS
7				0.40			0.20				0.10			0.20
24							0.10				0.10	0.10		
27											0.30	0.10		0.20
29			0.20	0.20		0.20	0.20					0.10		
30						0.20	0.90					0.10		
31						0.20	0.70				0.10	0.10		
32				0.40		0.10	0.30					0.40		
34						0.20	1.00							
35				0.30			0.40				0.10	0.20		
39												0.20		
46				0.30			0.40					0.10		0.90
68				0.50			0.20					0.10		
75			0.60	0.40			0.30					0.10		
78							0.60							
151											0.140	0.145		0.433
159											0.089	0.093		0.404
166														
190														
191														
192														
<T*>			0.400	0.357		0.180	0.442							
SIGMA			0.283	0.098		0.045	0.294							

REGION 8 EVENT	ANMO	ANTO	ATAK	BFAK	BOCO	CHTO	CNAK	CTAO	GUMO	HNME	IR7	KAAO	KONO	KSRS
59											0.10	0.10		
66											0.10	0.10		
73												0.10		0.50
74			0.20			0.10	0.20	0.10						
149				0.30										0.20
150			0.30			0.30	0.30	0.20			0.30			
153			0.30	0.20										
170											0.20			
172				0.20			0.20				0.10			
173														
175				0.10			0.10							
185				0.40										
188											0.160	0.100		0.350
272											0.089	0.001		0.212
			0.267	0.240		0.200	0.200	0.150						
<T*>			0.058	0.114		0.141	0.082	0.071						
SIGMA														

T* FOR EACH REGION-TO-STATION PATH
ASSUMING FALL-OFF AS OMEGA-CUBED

REGION 5 EVENT	LAO	MAIO	MAJO	NAO	NJAK	NWAO	RKON	SHIO	SNZO	TATO	TWAK	UCAK	ZOBO
77	0.40	0.20			0.10		0.20				0.10	0.20	
145	0.20				0.20						0.10	0.30	
160													
<T*>	0.300	0.200			0.150		0.200				0.100	0.250	
SIGMA	0.141	0.0			0.071		0.0				0.001	0.071	

REGION 6 EVENT	LAO	MAIO	MAJO	NAO	NJAK	NWAO	RKON	SHIO	SNZO	TATO	TWAK	UCAK	ZOBO
6													
25				0.30									
195	0.30	0.50			0.30						0.40	0.30	
<T*>	0.300	0.500		0.300	0.300						0.400	0.300	
SIGMA	0.0	0.0		0.0	0.0						0.0	0.0	

REGION 7 EVENT	LAO	MAIO	MAJO	NAO	NJAK	NWAO	RKON	SHIO	SNZO	TATO	TWAK	UCAK	ZOBO
7				0.10	0.50						0.20		
24	1.00												
27		0.30	0.30		0.30								
29													
30				0.20	0.20		0.20				0.30	0.20	
31					0.30							0.40	
32		0.70											
34													
35		0.30			0.40							0.30	
39		0.20			0.80							0.30	
46				0.30									
68		0.10			0.30								
75													
78													
151		0.20		0.50	0.30						0.40	0.30	
159				0.10									
166	0.40	0.20			0.60						0.40	0.40	
190				0.60								0.30	
191												0.10	
192													
<T*>	0.700	0.286	0.300	0.300	0.411		0.200				0.325	0.287	
SIGMA	0.424	0.195	0.0	0.210	0.190		0.0				0.096	0.099	

REGION 8 EVENT	LAO	MAIO	MAJO	NAO	NJAK	NWAO	RKON	SHIO	SNZO	TATO	TWAK	UCAK	ZOBO
59		0.10											
66													
73	0.30	0.10		0.30									
74		0.10											
149	0.30	0.10									0.30	0.20	
150													
153													
170	0.10	0.10		0.20	0.20		0.40				0.20	0.20	
172	0.50			0.10	0.30							0.10	
173		0.10										0.30	
175	0.40			0.10	0.10						0.30	0.10	
185		0.10											
188		0.10		0.20									
272					0.20								
<T*>	0.320	0.100		0.180	0.200		0.400				0.267	0.180	
SIGMA	0.148	0.000		0.084	0.082		0.0				0.058	0.084	

T* FOR EACH REGION-TO-STATION PATH
ASSUMING FALL-OFF AS OMEGA-CUBED

REGION 9 EVENT	ANMO	ANTO	ATAK	BFAK	BOCO	CHTO	CNAK	CTAO	GUMO	HNME	IR7	KAAO	KONO	KSRS
14	0.10			0.10		0.30	0.10			0.10		0.10		
17				0.30			0.30					0.10		0.10
20	0.10					0.30		0.20		0.30	0.50	0.10		0.20
53	0.10		0.30	0.10			0.10	0.20			0.10	0.10		0.30
79												0.10		
81	0.10		0.20	0.10		0.30		0.20		0.20	0.40	0.10		0.20
152							0.30					0.10		
184				0.10			0.10							
187			0.10	0.20			0.10					0.10		0.40
189														0.40
264								0.50						0.20
265	0.10					0.10	0.10	0.10				0.10		
266			0.10	0.30				0.50				0.20		0.20
267	0.20		0.30	0.10				0.20						0.20
268	0.10		0.20	0.40								0.10		
271	0.10		0.10	0.20		0.30	0.20							
276														0.10
277														
278														
<T*>	0.112		0.186	0.190		0.260	0.162	0.271		0.200	0.333	0.110		0.230
SIGMA	0.035		0.090	0.110		0.089	0.092	0.160		0.100	0.208	0.032		0.106

REGION 10 EVENT	ANMO	ANTO	ATAK	BFAK	BOCO	CHTO	CNAK	CTAO	GUMO	HNME	IR7	KAAO	KONO	KSRS
4												0.10		
9														
10												0.10		
23														
26											0.10			0.10
28											0.10			
38										0.10	0.10	0.10		
41											0.20	0.10		
45				0.70										
48			0.30	0.10										
67											0.10			
69												0.10		
70														
72											0.10			0.10
76														
155						0.10					0.117	0.100		0.100
161										0.100	0.041	0.000		0.001
179			0.300	0.400		0.100				0.0				
<T*>			0.0	0.424		0.0								
SIGMA														

REGION 11 EVENT	ANMO	ANTO	ATAK	BFAK	BOCO	CHTO	CNAK	CTAO	GUMO	HNME	IR7	KAAO	KONO	KSRS
61				0.10			0.20					0.20		
167												0.10		
<T*>				0.100			0.200					0.150		
SIGMA				0.0			0.0					0.071		

REGION 12 EVENT	ANMO	ANTO	ATAK	BFAK	BOCO	CHTO	CNAK	CTAO	GUMO	HNME	IR7	KAAO	KONO	KSRS
22	0.10										0.10	0.10		0.10
274											0.100	0.100		0.100
<T*>	0.100										0.0	0.0		0.0
SIGMA	0.0													

T* FOR EACH REGION-TO-STATION PATH
ASSUMING FALL-OFF AS OMEGA-CUBED

REGION 9 EVENT	LAO	MAIO	MAJO	NAO	NJAK	NWAO	RKON	SHIO	SNZO	TATO	TNAK	UCAK	ZOBO
14	0.10	0.10	0.10		0.30		0.10				0.10		
17	0.30			0.10			0.20				0.20	0.30	
20							0.10			0.10			
53	0.20	0.10	0.30	0.10	0.10	0.10					0.10	0.10	
79	0.30						0.10					0.10	
81	0.20						0.20				0.10		
152		0.10										0.30	
187													
189	0.20	0.10		0.10	0.20						0.10	0.10	
264	0.30	0.10											
265	0.30			0.10									
266	0.20	0.10		0.10	0.10						0.10	0.20	
267	0.30	0.30									0.20		
268		0.10			0.10	0.20					0.20	0.30	
271		0.30		0.10	0.20	0.10		0.20		0.10	0.10	0.10	
276				0.10									
277							0.10						
278		0.20					0.10						
<T*>	0.240	0.150	0.200	0.100	0.167	0.133	0.129	0.200		0.100	0.133	0.187	
SIGMA	0.070	0.085	0.141	0.000	0.082	0.058	0.049	0.0		0.001	0.050	0.099	

REGION 10 EVENT	LAO	MAIO	MAJO	NAO	NJAK	NWAO	RKON	SHIO	SNZO	TATO	TNAK	UCAK	ZOBO
4		0.10											
9													
10													
23													
26		0.10											
28		0.10											
38													
41		0.10											
45											0.10		
48													
67		0.10		0.60	0.30								
69													
70					0.10								
72				0.10	0.80						0.10	0.10	
76													
155													
161		0.10			0.10							0.10	
179		0.10		0.10									
<T*>		0.100		0.267	0.325						0.100	0.100	
SIGMA		0.000		0.289	0.330						0.001	0.001	

REGION 11 EVENT	LAO	MAIO	MAJO	NAO	NJAK	NWAO	RKON	SHIO	SNZO	TATO	TNAK	UCAK	ZOBO
61	0.30	0.10											
167													
<T*>	0.300	0.100											
SIGMA	0.0	0.0											

REGION 12 EVENT	LAO	MAIO	MAJO	NAO	NJAK	NWAO	RKON	SHIO	SNZO	TATO	TNAK	UCAK	ZOBO
22							0.10						
274				0.10									
<T*>				0.100			0.100						
SIGMA				0.0			0.0						

T* FOR EACH REGION-TO-STATION PATH
ASSUMING FALL-OFF AS OMEGA-CUBED

REGION 13 EVENT	ANMO	ANTO	ATAK	BFAK	BOCO	CHTO	CNAK	CTAO	GUMO	HNME	IR7	KAAO	KONO	KSRS
8														
80							0.10				0.10	0.10		
162							0.50				0.10	0.10		
163				0.10			0.30					0.50		
168											0.10			
177											0.10			
184														
<T*>				0.100			0.300				0.100	0.233		
SIGMA				0.0			0.200				0.001	0.231		

REGION 14 EVENT	ANMO	ANTO	ATAK	BFAK	BOCO	CHTO	CNAK	CTAO	GUMO	HNME	IR7	KAAO	KONO	KSRS
1	0.70		0.10	0.10		0.30	0.10					0.10		
19	0.10					0.20				0.20	0.10	0.10		0.40
33			0.30	0.40			0.20			0.20				
273	0.10			0.20		0.10	0.10					0.20		0.10
<T*>	0.300		0.200	0.233		0.200	0.133			0.200	0.100	0.133		0.250
SIGMA	0.346		0.141	0.153		0.100	0.058			0.001	0.0	0.058		0.212

REGION 13 EVENT	LAO	MAIO	MAJO	NAO	NJAK	NWAO	RKON	SHIO	SNZO	TATO	TWAK	UCAK	ZOBO
8													
80													
162	0.30	0.10		0.10	0.40							0.40	
163					0.10							0.30	
168	0.30												
177	0.30												
184	0.30	0.60		0.30	0.20								
<T*>	0.300	0.350		0.200	0.233							0.350	
SIGMA	0.001	0.354		0.141	0.153							0.071	

REGION 14 EVENT	LAO	MAIO	MAJO	NAO	NJAK	NWAO	RKON	SHIO	SNZO	TATO	TWAK	UCAK	ZOBO
1	0.30	0.40	0.20		0.10						0.50	0.10	
19	0.30		0.10				0.10			0.60			
33	0.50			0.10	0.20		0.10				0.10	0.10	
273		0.10	0.20	0.20	0.20						0.20	0.20	
<T*>	0.367	0.250	0.167	0.150	0.167		0.100			0.600	0.267	0.133	
SIGMA	0.115	0.212	0.058	0.071	0.058		0.001			0.0	0.208	0.058	

APPENDIX IV

Discrimination variables calculated for each event

VALUES OF THE 20 DISCRIMINATION VARIABLES IN TABLE XIV

EVENT :	1	3	4	6	7	8	9	10	14	16	17	18
1	-1.023	-0.637	0.0	0.0	-0.933	0.0	1.223	0.064	-1.384	-1.352	-1.025	-1.443
2	-1.252	-0.424	-1.223	0.0	-0.921	-1.426	-1.146	-1.031	-1.735	-1.623	-1.822	-1.541
3	-0.757	0.192	0.0	0.0	-0.507	0.0	0.905	0.058	-1.642	-1.452	-1.399	-1.388
4	5.543	5.337	5.878	0.0	4.737	0.0	0.0	6.021	5.551	5.658	6.117	5.833
5	6.115	5.556	6.164	0.0	5.178	0.0	0.0	6.221	6.021	6.192	6.603	5.891
6	-0.557	-0.042	0.0	0.0	-0.263	-0.175	0.005	-0.020	-0.437	-0.639	-0.514	-0.553
7	-0.647	-0.182	0.0	0.0	0.018	0.0	-0.259	-0.515	-0.493	-0.273	-0.623	-0.615
8	-0.761	-0.335	0.0	0.0	-0.486	-0.916	-0.237	-0.599	-0.722	-0.406	-0.928	-0.624
9	0.0	1.392	0.910	0.0	0.543	0.0	1.635	0.0	-1.282	-0.402	-0.139	0.602
10	0.0	0.0	0.850	0.0	0.753	0.0	0.0	0.998	-0.542	-0.122	-0.289	0.0
11	1.143	2.352	1.640	0.0	1.733	0.0	2.975	1.878	0.338	0.648	0.771	0.0
12	0.0	1.802	0.980	4.140	0.613	0.0	0.0	0.0	-0.332	-0.232	0.181	0.0
13	0.0	2.012	1.290	0.0	0.923	0.0	0.0	0.0	0.028	-0.072	0.311	0.0
14	0.0	2.422	0.0	4.680	0.0	0.0	0.0	0.0	1.148	0.648	1.821	0.0
15	-3.351	-1.114	-1.719	1.060	-1.920	0.0	-0.534	-0.625	-3.315	-3.345	-3.428	0.0
16	-2.971	-0.174	-1.339	1.540	-1.570	-2.408	-0.194	-0.715	-3.575	-2.895	-3.256	0.0
17	-2.727	0.137	-1.030	1.500	-1.632	-2.066	-0.025	0.0	-3.372	-2.642	-2.934	-2.198
18	-3.240	-0.261	-1.872	1.330	-1.363	0.0	-0.084	-0.593	-3.412	-3.265	-3.285	0.0
19	-2.950	0.019	-1.602	1.810	-1.773	-2.370	-0.044	-1.233	-3.442	-3.042	-2.865	0.0
20	-2.580	0.109	-1.622	0.0	-1.601	0.0	-0.044	0.0	-3.282	-2.882	-2.825	0.0

EVENT :	19	20	21	22	23	24	25	26	27	28	29	30
1	-1.466	-1.414	-1.247	-0.961	0.0	0.503	-0.355	-0.146	-0.841	-0.517	-0.611	-0.987
2	-2.040	-2.409	-1.650	-2.238	-1.018	-1.252	-0.347	-0.601	-0.968	-1.814	-1.528	-1.544
3	-1.716	-2.006	-1.368	-1.702	0.0	0.159	0.472	0.291	-0.424	-1.141	-0.938	-0.785
4	6.119	6.632	5.649	5.693	0.0	6.324	5.464	5.896	5.740	6.669	3.527	5.528
5	6.684	7.029	5.990	5.961	0.0	0.0	5.588	6.011	5.853	6.863	4.791	5.940
6	-0.352	-0.470	-0.514	-0.840	-0.443	0.366	-0.274	0.0	-0.100	0.0	-0.160	0.195
7	-0.402	-0.454	-0.552	-0.923	-1.885	0.348	-0.125	0.0	-0.227	0.0	-0.311	0.094
8	-0.546	-0.559	-0.699	-1.021	0.0	0.131	-0.125	0.0	-0.733	0.0	-0.192	-0.160
9	-1.808	-1.726	-0.318	-0.412	0.0	0.0	0.0	0.0	0.836	-0.041	0.142	1.345
10	-1.298	-1.586	-0.218	-0.272	0.0	0.0	0.0	0.0	0.0	0.0	0.0	1.265
11	-0.598	-0.936	0.822	0.158	0.0	0.0	0.0	0.0	0.0	1.389	1.222	1.875
12	-1.408	-1.526	-0.398	-0.492	0.0	2.189	0.0	0.0	0.0	0.419	0.732	2.275
13	-0.978	-1.416	-0.118	-0.202	0.0	2.179	0.0	0.0	0.0	0.729	0.882	2.155
14	-0.728	-0.276	1.072	0.208	0.0	0.0	0.0	0.0	0.0	0.0	0.0	2.925
15	-4.573	-5.197	-2.975	-3.342	0.0	-0.313	0.367	0.0	-0.853	0.0	-1.735	-0.415
16	-3.813	-4.857	0.0	-3.082	0.0	-0.033	0.317	-0.008	-0.443	0.0	-1.475	-0.267
17	-3.383	-4.456	0.0	-3.245	0.0	-0.306	0.247	0.111	-1.064	0.0	-1.373	-0.480
18	-4.353	-4.824	-3.732	-3.335	0.0	0.069	0.397	-0.438	-0.486	-2.965	-1.407	-0.379
19	-4.033	-4.544	-3.582	-3.365	0.0	-0.051	0.457	-0.328	-0.566	-2.935	-1.587	-0.229
20	-3.773	-4.514	-3.352	-4.025	0.0	-0.371	0.497	0.092	-0.826	-2.815	-1.437	-0.509

VALUES OF THE 20 DISCRIMINATION VARIABLES IN TABLE XIV

EVENT :	31	32	33	34	35	36	37	38	39	41	45	46
1 :	-0.701	-0.524	-0.949	-0.508	-0.452	-0.232	-0.420	0.727	-0.772	-0.986	0.200	-0.079
2 :	0.117	-0.334	-1.360	-0.974	-0.643	-0.792	-0.805	0.0	0.167	-1.562	-1.438	-0.370
3 :	0.814	0.446	-0.946	-0.230	0.273	0.237	-0.022	1.095	0.768	-1.157	-0.127	0.664
4 :	5.967	5.753	5.706	4.752	5.099	5.625	5.334	0.0	5.616	5.155	4.028	5.376
5 :	5.953	5.928	5.675	4.614	4.960	5.670	5.517	0.0	5.945	5.349	5.104	5.211
6 :	-0.994	-0.716	-0.226	0.0	-0.031	-0.221	0.127	-0.337	-0.392	-0.021	-0.023	-0.617
7 :	-0.375	-0.316	-0.240	0.0	-0.104	-0.314	0.097	-0.346	-0.354	-0.291	0.069	-0.263
8 :	-0.052	-0.360	-0.637	0.0	-0.206	-0.034	-0.114	0.0	0.054	-0.492	0.0	-0.121
9 :	0.0	0.0	0.0	0.0	2.013	0.0	0.0	0.0	2.268	0.0	0.0	0.0
10 :	0.0	0.0	0.654	0.0	2.013	0.0	0.0	0.0	0.0	0.0	0.0	0.0
11 :	0.0	0.0	0.0	0.0	2.793	0.0	0.0	0.0	2.868	0.0	0.0	0.0
12 :	0.0	3.156	0.0	1.600	2.823	1.087	0.0	0.0	3.158	0.0	1.013	0.0
13 :	0.0	2.876	0.0	1.500	2.653	0.0	1.708	0.0	2.998	0.0	1.583	0.0
14 :	0.0	0.0	0.0	2.280	3.373	2.247	0.0	0.0	3.858	0.0	2.423	0.0
15 :	0.0	0.078	-1.798	-0.981	0.398	0.0	-0.805	0.194	1.123	0.0	-1.620	-0.208
16 :	0.0	0.0	-1.228	-0.701	0.567	-1.370	-0.175	1.144	1.343	0.0	-1.730	-0.218
17 :	0.0	0.0	-1.461	-0.420	0.428	0.0	0.078	0.835	1.303	0.0	-1.887	0.239
18 :	0.0	-0.060	-1.969	-0.606	0.553	0.0	-0.192	0.372	1.203	0.0	-1.384	-0.009
19 :	0.0	0.0	-1.949	-0.526	0.579	0.0	-0.082	0.862	1.333	0.0	-1.624	-0.069
20 :	0.0	0.160	0.0	-0.396	0.543	0.0	0.028	0.892	1.193	-3.039	-1.464	0.0

EVENT :	47	48	49	50	53	55	56	57	58	59	60	61
1 :	-0.627	-0.663	-0.697	-0.795	-1.347	-0.121	0.0	-1.162	0.651	-0.414	0.0	0.131
2 :	-1.512	-1.279	-1.603	-1.046	-2.262	-0.598	0.0	-0.450	-1.048	-1.364	0.0	-1.468
3 :	-0.773	-0.638	-0.789	-0.298	-1.849	0.445	0.0	-0.322	0.463	-0.523	0.0	-0.227
4 :	4.821	5.864	5.109	5.429	5.679	4.677	0.0	5.244	0.0	5.157	0.0	5.267
5 :	5.202	6.212	5.514	5.716	6.509	5.371	0.0	5.621	0.0	5.810	0.0	5.752
6 :	-0.484	-0.859	-0.380	-0.199	-0.385	-0.370	0.0	-0.115	-0.292	0.0	0.0	-0.018
7 :	-0.595	-1.129	-0.312	-0.253	-0.453	-0.283	0.0	-0.081	-1.054	0.0	0.109	-0.609
8 :	-0.546	0.0	-0.398	-0.556	-0.698	-0.504	0.0	-0.259	-0.731	0.0	0.0	0.0
9 :	0.0	0.0	1.031	0.662	-1.859	0.0	0.0	0.0	0.0	0.717	0.0	1.243
10 :	0.0	0.0	0.911	0.0	-1.579	0.0	0.0	0.0	0.0	0.487	0.0	1.663
11 :	0.0	0.0	1.591	1.472	-0.479	0.0	0.0	0.0	3.353	1.427	0.0	2.673
12 :	0.747	0.0	1.131	1.642	-1.089	0.0	0.0	0.0	2.753	0.0	0.0	1.503
13 :	0.887	0.0	1.111	1.582	-0.879	0.0	0.0	0.0	0.0	0.0	0.0	1.923
14 :	2.237	0.0	2.141	2.192	0.111	0.0	0.0	0.0	3.553	0.0	0.0	2.353
15 :	-0.759	0.0	-1.576	-1.563	-4.513	0.0	0.0	0.0	0.239	-1.733	0.0	-1.500
16 :	-0.709	-2.125	-1.226	-0.563	-4.213	0.0	-1.151	0.0	0.429	-1.469	0.0	-1.070
17 :	-1.339	-1.643	-1.524	-0.533	-3.989	0.0	-0.834	0.0	0.0	-1.388	0.0	-0.997
18 :	-0.479	0.0	-1.723	-0.733	-4.802	0.0	-1.384	0.0	0.019	-1.231	0.0	-1.534
19 :	-0.489	0.0	-1.513	-0.303	-4.302	0.0	-1.124	0.0	0.289	-1.311	-1.241	-1.024
20 :	-1.019	0.0	-1.723	-0.463	-4.192	0.0	-1.144	0.0	0.449	-1.121	0.0	-1.404

VALUES OF THE 20 DISCRIMINATION VARIABLES IN TABLE XIV

EVENT :	62	63	64	65	66	67	68	69	70	72	73	74
1	-1.173	-0.895	-0.774	0.043	0.642	-0.781	-0.312	0.0	-0.480	-0.690	-1.017	0.0
2	-0.978	-1.285	-0.659	-1.397	-1.338	-1.223	-0.309	0.0	-1.078	-1.066	-1.894	-1.344
3	-0.320	-0.801	-0.157	-0.440	0.165	-0.710	0.589	0.0	-0.428	-0.477	-1.473	0.0
4	5.605	5.098	5.129	4.688	0.0	5.822	4.571	0.0	6.294	5.017	5.368	6.000
5	5.032	5.637	5.430	5.542	0.0	6.108	4.587	0.0	5.599	5.491	5.993	6.200
6	-0.580	-0.671	-0.361	-0.104	0.171	-0.161	-0.507	0.0	-0.247	-0.240	-0.086	0.0
7	-0.454	-0.737	-0.281	-0.734	-0.539	0.296	-0.141	0.0	0.024	-0.683	-0.071	0.0
8	-0.464	-1.063	-0.446	-0.399	-0.595	0.046	0.0	0.0	0.0	-0.849	-0.100	0.0
9	0.810	0.0	0.0	0.0	0.0	0.0	0.0	0.0	0.0	0.643	-0.183	0.0
10	1.060	0.0	0.0	0.0	0.0	0.0	0.0	0.0	0.0	0.743	-0.073	0.0
11	0.0	0.0	0.0	0.0	0.0	0.0	0.0	0.0	0.0	0.0	0.487	0.0
12	0.0	0.0	0.0	0.0	0.0	0.0	2.489	0.0	0.0	0.663	0.057	0.0
13	0.0	0.0	1.413	0.0	0.0	0.0	2.649	0.0	0.0	0.993	0.167	0.0
14	0.0	0.0	2.533	0.0	0.0	0.0	3.329	0.0	0.0	2.063	0.977	0.0
15	-1.111	-2.822	-0.532	0.0	-1.216	0.0	0.138	0.0	0.0	-1.782	-3.248	0.0
16	-0.791	-2.452	-0.362	0.0	-1.276	0.0	0.568	0.0	0.0	-2.132	-2.318	0.0
17	-0.395	-2.246	-0.137	0.0	0.0	0.0	0.759	0.0	0.0	-1.727	-2.033	0.0
18	-1.005	0.0	-0.628	0.0	0.0	0.0	0.528	-2.942	0.0	-1.696	-2.454	0.0
19	-1.015	0.0	-0.348	0.0	0.0	0.0	0.598	-3.082	0.0	-1.766	-2.314	0.0
20	-0.595	0.0	-0.808	0.0	0.0	0.0	0.708	0.0	0.0	-1.516	-2.214	0.0

EVENT :	75	76	77	78	79	80	81	143	144	145	146	147
1	0.915	0.0	-1.033	0.459	-0.904	-0.224	-1.625	-0.855	-0.961	-1.095	-0.615	-1.236
2	-1.023	0.0	-1.356	0.0	-1.106	-0.274	-1.929	-1.481	-1.433	-1.461	-0.318	-2.414
3	0.728	0.0	-0.811	1.261	-0.747	0.622	-1.687	-0.663	-1.022	-1.052	0.391	-1.959
4	4.111	0.0	5.741	0.0	4.238	4.501	6.210	5.572	6.366	5.046	5.247	6.014
5	5.275	0.0	6.001	0.0	4.845	4.782	6.707	5.899	6.145	5.657	5.640	6.336
6	-0.784	0.0	-0.122	-0.423	0.032	-0.101	-0.424	-0.368	0.161	-0.699	-0.572	-0.677
7	-0.609	0.0	-0.277	0.0	-0.049	0.442	-0.494	-0.293	0.057	-0.729	-0.652	-0.712
8	0.0	0.0	-0.375	0.0	0.0	0.0	-0.653	-0.275	-0.845	-0.881	-0.602	-0.876
9	0.0	0.0	0.179	0.0	0.0	0.0	-1.417	1.069	0.0	0.0	0.0	-1.309
10	0.0	0.0	0.449	0.0	0.0	0.0	-1.367	0.999	0.0	0.0	0.0	-1.159
11	0.0	0.0	1.199	0.0	0.0	0.0	-0.337	1.939	0.0	0.0	0.0	-0.539
12	0.0	0.0	0.929	0.0	0.0	0.0	-1.227	1.319	0.0	0.0	1.321	-0.769
13	0.0	0.0	0.859	0.0	0.0	0.0	-0.957	1.209	0.0	0.0	1.721	-0.699
14	0.0	0.0	1.769	0.0	0.0	0.0	-0.537	2.329	0.0	0.0	0.0	-0.031
15	0.0	0.0	-2.399	0.993	0.0	0.0	-4.817	-1.341	0.0	0.0	0.0	-4.456
16	0.0	0.047	-1.359	0.813	0.0	0.0	-4.577	-1.081	0.0	0.0	-0.888	-4.428
17	0.0	0.0	-1.209	1.066	0.0	0.0	-4.115	-1.482	0.0	0.0	-0.379	-4.204
18	0.0	0.735	-1.636	1.089	0.0	0.0	-4.806	-1.316	0.0	0.0	-0.356	-4.827
19	0.0	0.165	-1.366	0.779	0.0	0.0	-4.356	-1.236	0.0	0.0	0.0	-4.517
20	0.0	0.0	-1.336	0.869	0.0	0.0	-4.356	-1.546	0.0	0.0	0.0	-4.627

VALUES OF THE 20 DISCRIMINATION VARIABLES IN TABLE XIV

EVENT :	148	149	150	151	152	153	154	155	156	157	158	159
1 :	-0.987	-1.015	0.045	-0.681	-0.639	0.0	-0.897	-0.303	-0.515	-0.872	-0.632	0.310
2 :	-1.102	-1.469	-0.620	-0.938	-0.391	-0.243	-1.328	-0.614	-0.624	-1.023	-0.070	-1.071
3 :	-0.628	-0.853	0.526	-0.149	0.212	0.0	-0.705	0.155	0.092	-0.474	0.534	0.202
4 :	0.0	5.347	4.978	5.043	4.255	6.310	5.386	0.0	4.388	5.649	6.056	6.098
5 :	5.738	5.870	4.596	5.370	4.765	5.504	5.794	0.0	5.219	5.837	6.298	7.057
6 :	0.0	-0.297	-0.130	-0.190	-0.399	0.0	-0.655	-0.235	-0.036	-0.599	0.0	0.0
7 :	0.0	-0.345	-0.340	-0.354	-0.200	0.0	-0.734	0.0	0.049	-0.711	-0.195	-2.044
8 :	0.0	-0.450	0.0	-0.473	-0.289	-0.794	-0.904	0.0	-0.703	-0.729	0.464	-1.396
9 :	0.0	-0.056	0.0	0.0	1.592	0.0	0.0	0.0	0.0	0.0	0.0	0.0
10 :	0.0	0.174	0.0	0.0	0.0	0.0	0.0	0.0	0.0	0.0	0.0	0.0
11 :	0.0	1.134	0.0	0.0	0.0	0.0	0.0	0.0	0.0	0.0	0.0	0.0
12 :	0.0	0.464	0.0	1.361	1.882	4.140	0.0	0.0	0.0	0.0	0.0	0.0
13 :	0.0	0.394	0.0	1.361	1.962	0.0	0.0	0.0	0.0	0.936	0.0	0.0
14 :	0.0	1.344	0.0	2.101	2.862	4.810	0.415	0.0	0.0	0.0	0.0	0.0
15 :	-1.755	-2.157	0.0	-1.297	-0.343	1.101	0.985	0.0	0.0	0.0	0.0	0.0
16 :	-1.335	-1.927	-0.572	-0.867	0.177	0.961	-2.926	0.0	-1.094	-1.881	-0.208	0.0
17 :	-1.203	-1.871	-0.689	-0.624	0.362	0.0	0.0	0.0	-0.434	-1.891	-0.178	0.0
18 :	-1.595	-1.903	-0.511	-0.879	0.128	0.888	0.0	0.0	-0.053	0.0	0.0	0.0
19 :	-1.546	-1.703	-0.711	-0.669	0.208	1.118	0.0	0.0	-0.331	-1.763	0.0	0.0
20 :	-1.296	-1.773	-0.881	-0.659	0.308	0.0	0.0	0.0	-0.211	-1.673	0.0	0.0
									-0.281	-1.413	0.0	0.0

EVENT :	160	161	162	163	164	165	166	167	168	169	170	171
1 :	0.0	-0.195	-0.713	-0.928	-1.231	-0.774	-0.633	-0.062	-0.088	-1.265	-0.845	-0.788
2 :	-0.243	-1.052	-1.044	-1.131	-1.328	-0.971	-0.700	0.073	-1.162	-1.630	-1.474	-1.066
3 :	0.0	-0.093	-0.298	-0.793	-0.863	-0.413	0.136	1.149	-0.068	-1.293	-0.662	-0.502
4 :	6.345	5.127	5.205	4.688	5.488	5.272	5.535	4.225	5.285	5.778	5.287	5.674
5 :	5.375	5.599	5.552	5.191	6.084	5.651	5.687	4.989	5.570	6.589	5.731	5.952
6 :	-0.840	-0.362	-0.027	-0.009	-0.310	-0.057	-0.113	0.0	0.0	-0.128	0.079	-0.760
7 :	-0.383	0.100	-0.135	-0.299	-0.147	0.044	-0.242	0.0	0.0	-0.081	-0.002	-0.817
8 :	0.0	0.0	0.0	0.0	-0.175	0.097	-0.604	0.0	0.0	-0.286	-0.156	-0.721
9 :	0.0	0.0	0.0	0.0	0.427	1.487	0.0	3.079	0.0	-0.263	1.264	0.0
10 :	0.0	0.0	0.0	0.0	0.347	1.387	0.0	3.279	1.452	0.0	1.354	0.0
11 :	0.0	0.0	0.0	0.0	0.547	0.0	0.0	4.329	0.0	0.767	1.774	0.0
12 :	0.0	2.197	0.0	0.0	0.697	1.557	2.186	3.189	0.0	0.307	1.794	0.988
13 :	0.0	2.147	0.0	0.0	0.747	1.247	2.286	3.759	0.0	0.277	1.744	0.0
14 :	0.0	2.687	0.0	0.0	2.037	2.657	3.066	5.039	0.0	1.137	2.534	0.0
15 :	0.0	-1.530	-1.053	0.0	-1.870	-1.398	-0.191	0.356	-1.764	-2.664	-1.119	0.0
16 :	0.0	-1.570	-0.593	0.0	-1.490	-0.398	0.059	0.586	-1.624	-2.994	-0.819	0.0
17 :	0.0	0.0	-0.468	0.0	-1.663	-0.433	0.106	0.954	0.0	-2.636	-0.801	0.0
18 :	0.0	-1.516	-0.764	0.0	-1.846	-0.932	0.216	0.513	-1.359	-2.689	-0.755	0.0
19 :	0.0	0.0	-0.734	0.0	-1.666	-0.662	0.306	0.913	-1.229	-2.589	-0.685	0.0
20 :	0.0	-1.716	-0.664	0.0	-1.786	-0.862	0.236	0.893	0.0	-2.579	-0.915	0.0

VALUES OF THE 20 DISCRIMINATION VARIABLES IN TABLE XIV

EVENT	172	173	175	176	177	178	179	180	182	183	184	185
1	-1.057	-0.826	-0.802	0.180	-0.025	-1.106	-1.094	-0.523	-0.923	-0.931	-0.070	0.0
2	-0.128	-0.348	-1.318	-0.922	-1.292	-1.360	-1.766	-0.882	-0.490	-1.294	-0.853	-0.316
3	0.053	-0.027	-0.642	0.374	-0.188	-0.907	-1.467	-0.108	-0.021	-0.918	0.195	0.0
4	5.026	4.749	5.016	4.348	5.643	5.001	5.326	5.076	6.107	4.783	5.688	4.477
5	5.148	5.154	5.222	4.171	6.164	5.627	5.501	5.916	6.327	5.302	6.165	5.122
6	0.065	-0.411	0.131	-1.919	-0.392	-0.257	0.271	0.034	-0.270	-0.546	-0.197	0.715
7	-0.041	-0.427	-0.051	-0.569	-0.333	-0.251	0.213	0.156	-0.094	-0.243	0.0	0.414
8	0.190	0.0	-0.234	-0.436	-0.208	-0.233	0.081	-0.300	-0.128	-0.414	0.0	0.0
9	0.0	0.0	0.228	0.0	1.232	1.393	-0.047	0.0	2.149	0.0	0.0	1.755
10	0.0	0.0	0.688	0.0	1.272	1.293	0.023	0.0	1.819	0.0	0.0	2.235
11	0.0	0.0	1.338	0.0	0.0	1.993	1.393	0.0	0.0	0.0	0.0	0.0
12	0.0	0.0	0.0	0.0	0.0	1.603	0.873	0.0	2.409	0.0	0.0	0.0
13	0.0	0.0	0.0	0.0	0.0	1.533	0.743	0.0	0.0	0.0	0.0	0.0
14	0.0	0.0	0.0	0.0	0.0	2.703	0.0	0.0	2.839	0.0	0.0	0.0
15	-0.471	-0.511	-1.705	0.0	-1.644	-0.791	-2.011	0.0	-1.003	-2.063	0.0	-0.074
16	-0.421	-0.711	-1.495	0.0	-1.594	-0.660	-1.481	0.0	-0.263	-1.933	0.0	0.506
17	-0.012	-0.332	-1.172	0.0	-1.583	-1.222	-1.602	0.0	-0.416	-1.888	0.0	0.625
18	-0.081	-0.401	-1.564	0.0	-1.459	-0.869	-1.939	0.0	0.0	-1.954	0.0	0.296
19	0.049	-0.111	-1.364	0.0	-1.459	-0.829	-1.529	0.0	-0.309	-1.724	0.0	0.486
20	0.149	0.029	-1.344	0.0	-1.509	-1.299	-1.559	0.0	-0.519	-1.794	0.0	0.706

EVENT	186	187	188	189	190	191	192	193	194	195	264	265
1	0.058	0.0	-0.491	-0.379	-0.574	-0.704	0.0	-0.392	0.0	-0.631	-1.008	-1.073
2	0.0	-0.860	-0.734	-1.790	-0.936	-0.327	-0.366	-0.599	-0.762	-0.762	-1.475	-2.058
3	-0.360	0.0	-0.130	-1.319	-0.177	0.106	0.0	0.145	0.0	-0.002	-1.031	-1.529
4	7.141	4.124	5.411	5.211	5.614	5.030	0.0	4.564	0.0	5.059	6.021	6.230
5	6.839	4.269	5.310	5.648	5.397	5.652	0.0	4.206	0.0	5.413	6.062	6.929
6	-0.825	-0.559	-0.035	-0.455	-0.122	0.212	0.417	-0.527	0.0	0.192	-0.418	0.136
7	-1.326	-0.519	-0.317	-0.585	-0.366	-0.149	0.0	-0.551	0.0	0.067	-0.618	0.015
8	-1.199	-0.017	-0.781	-0.827	-0.704	0.0	0.0	-0.859	0.0	-0.094	-0.670	-0.237
9	0.610	0.0	0.0	-0.439	0.0	0.0	0.0	0.0	0.0	1.178	0.0	-0.839
10	0.920	0.0	0.0	-0.089	0.0	0.0	0.0	0.0	0.0	0.973	0.0	-0.629
11	1.910	0.0	0.0	0.911	0.0	0.0	0.0	0.0	0.0	2.098	0.0	-0.109
12	1.230	0.0	0.0	0.031	0.0	0.0	0.0	0.0	0.0	1.828	0.508	-0.869
13	0.0	0.0	0.0	0.191	0.0	0.0	0.0	0.0	0.0	1.838	0.578	-0.329
14	0.0	0.0	0.0	0.0	0.0	0.0	0.0	0.0	0.0	2.768	0.0	0.751
15	-1.721	-0.877	-0.690	-3.086	-1.162	0.0	0.0	0.0	0.0	-0.796	-1.916	-3.836
16	-1.571	-0.517	-0.640	-3.056	-0.952	0.0	0.280	-0.064	0.0	-0.656	-1.266	-3.936
17	0.0	0.0	-0.315	-2.819	-0.777	0.0	0.525	-0.010	0.0	-0.512	-1.291	-3.376
18	-1.715	-0.925	-0.439	0.0	-0.946	0.0	0.0	-0.163	0.0	-0.470	-1.985	-3.768
19	-1.705	-0.765	-0.379	0.0	-0.656	0.0	0.319	0.0	0.0	-0.220	-1.465	-3.888
20	0.0	0.0	-0.199	-3.034	-0.756	0.0	0.329	0.0	0.0	-0.300	-1.325	-3.578

VALUES OF THE 20 DISCRIMINATION VARIABLES IN TABLE XIV

EVENT :	266	267	268	269	270	271	272	273	274	276	277	278
1 :	-1.221	-1.568	-1.288	-1.164	-1.166	-1.324	-0.742	-1.227	0.0	0.0	0.0	-1.231
2 :	-1.944	-2.256	-2.129	-1.454	-1.631	-2.245	0.102	-1.437	-2.060	-1.964	-1.644	-1.762
3 :	-1.657	-2.002	-1.707	-0.899	-1.247	-1.893	0.647	-0.366	-1.311	0.0	0.0	-1.366
4 :	5.638	6.543	5.941	5.970	5.261	5.937	4.714	5.053	5.166	4.609	6.064	4.875
5 :	6.098	7.192	6.532	6.352	6.060	6.525	5.293	5.614	6.156	6.005	6.494	5.798
6 :	-0.513	-0.444	-0.526	-0.469	-0.523	0.482	-0.907	-0.448	0.0	-1.676	-0.300	-0.912
7 :	-1.575	-0.446	-0.535	-0.528	-0.555	0.514	-0.570	-0.533	0.0	-1.179	0.0	-0.233
8 :	-0.646	-0.577	-0.653	-0.619	-0.668	0.287	-0.410	-0.660	0.0	0.0	0.0	-0.394
9 :	0.0	-2.432	-1.687	-0.176	-0.457	-1.993	0.0	-0.257	0.0	0.0	0.0	0.0
10 :	0.0	-2.152	-1.127	-0.176	-0.247	-1.313	0.0	0.013	0.0	0.0	0.0	0.0
11 :	1.203	-0.722	-0.297	0.684	0.773	-0.613	0.0	1.163	0.0	0.0	0.0	1.144
12 :	0.0	-1.482	-0.877	-0.396	-0.367	-1.123	0.0	-0.207	0.0	0.0	0.0	0.0
13 :	0.0	-1.532	-0.607	-0.236	-0.297	-1.093	0.0	-0.057	0.0	0.0	0.0	0.0
14 :	1.513	-0.302	0.103	0.044	0.753	-0.113	0.0	0.863	0.0	0.0	0.0	0.0
15 :	-2.787	-4.386	-4.166	-4.177	-3.316	-4.492	-0.009	-3.612	0.0	0.0	-2.200	-2.797
16 :	-2.807	-4.016	-4.056	-3.047	-2.916	-3.872	0.211	-3.362	0.0	0.0	-2.190	0.0
17 :	0.0	-3.808	-3.578	-2.836	-2.471	-3.524	0.127	-2.952	0.0	0.0	-2.555	-2.346
18 :	0.0	-4.514	-4.417	-3.682	-3.252	-4.213	-0.020	-3.507	0.0	0.0	-2.319	0.0
19 :	-2.771	-4.234	-4.197	-3.342	-3.272	-3.933	0.190	-3.707	0.0	0.0	-2.349	0.0
20 :	-2.491	-4.204	-4.107	-3.302	-2.742	-3.913	0.0	-3.087	0.0	0.0	-2.789	0.0